Kidney diseases and Endothelium: RAGE (receptor for advanced glycation end products): from inflammation to aging

Marie Frimat

Centre Hospitalier Régional Universitaire de Lille

FACULTE DE MEDECINE HENRI WAREMBOURG

Université de Lille

Université de Lille

HABILITATION A DIRIGER DES RECHERCHES

Ecole Doctorale BIOLOGIE SANTE Lille

Maladies rénales et Endothélium
« RAGE (receptor for advanced glycation end products): de l'inflammation au vieillissement »

Présentée et soutenue publiquement par

Marie Frimat

Le 9 février 2021

Devant un jury composé de :

Monsieur le Professeur Marc HAZZAN *MD, PhD, Pr en Néphrologie, Université de Lille*	Président du jury
Madame le Professeur Fatouma TOURE *MD, PhD, Pr en Néphrologie, Université de Limoges*	Rapporteur externe
Monsieur le Professeur Emmanuel MORELON *MD, PhD, Pr en Néphrologie, Université de Lyon*	Rapporteur externe
Monsieur le Professeur David LAUNAY *MD, PhD, Pr en Médecine interne, Université de Lille*	Rapporteur interne
Madame le Professeur Sophie SUSEN *MD, PhD, Pr en Biologie Hémostase, Université de Lille*	Examinatrice
Madame le Docteur Véronique FREMEAUX-BACCHI *MD, PhD, Dr en Immunologie, HEGP, Paris*	Examinatrice
Monsieur le Professeur Éric BOULANGER *MD, PhD, Pr en Gériatrie, Université de Lille*	Garant

Remerciements

Cette Habilitation à Diriger les Recherches est l'occasion de faire le bilan de mes activités et m'offre l'opportunité de remercier les nombreuses personnes qui me permettent aujourd'hui de présenter ces travaux et perspectives.

Je souhaiterais remercier le Pr Hazzan et le Pr Noel, qui par leur soutien m'ont permis et me permettent encore maintenant de mener de front mes projets de recherche et mes activités médicales au sein du service de Néphrologie du CHU de Lille. Merci également à l'ensemble des médecins du service pour leur confiance, sans laquelle ces travaux ne pourraient aboutir.

Je remercie le Dr Véronique Frémeaux-Bacchi pour m'avoir chaleureusement accueillie il y a quelques années avec le Dr Lise Halbwachs-Mecarelli dans le monde de la recherche et transmis « le virus ». Merci à tous les membres des équipes de recherche des unités INSERM U845 au sein de l'hôpital Necker puis de l'unité U872 au Centre de Recherche des Cordeliers pour leurs conseils et leurs aides. J'ai eu la chance d'y faire de belles rencontres, parmi lesquelles je tiens à remercier tout particulièrement le Dr Lubka Roumenina dont l'enthousiasme, la rigueur et les qualités pédagogiques continuent de constituer un exemple.

Un grand merci au Pr Eric Boulanger pour m'avoir accueillie en 2014 au sein de son groupe de recherche, pour la confiance et l'autonomie qu'il m'a accordée. Nous étions alors peu nombreux et je remercie en particulier le Dr Maité Daroux pour son soutien à l'époque. Je souhaite remercier l'ensemble des membres de notre équipe qui ne cesse depuis de grandir de nouvelles compétences et d'idées. En particulier, dans notre groupe « inflammation », merci au Pr Steve Lancel pour son enthousiasme et sa rigueur, au Pr Marc Lambert et au Dr Cécile Yelnik pour notre belle collaboration autour du SAPL, au Pr Raphael Favory et au Pr Sébastien Préau pour nos échanges sur RAGE et la microcirculation. Merci également à toutes les personnes aidantes des unités INSERM U995 puis plus récemment U1167 que j'ai pu être amenée à solliciter au fil des dernières années.

Un grand nombre des travaux et projets présentés ici sont le fruit de rencontres et collaborations. C'est aussi l'occasion de leur exprimer mes remerciements pour ces échanges fructueux. Merci notamment à nos amis du service d'Anatomopathologie Rénale à Lille, et en particulier au Dr Viviane Gnemmi et au Dr Jean-Baptiste Gibier ainsi qu'à l'ensemble des membres du groupe rein-endothélium.

Je terminerai en remerciant l'ensemble des étudiants qui en souhaitant travailler avec moi et en acceptant d'y consacrer parfois beaucoup de temps ont permis de faire avancer tous ces projets. Merci ainsi à Olivia, Anne, Valentine, Juliette, Cécile L., Marie, Mehdi, Amandine, Cécile Y. et Timothée !

« I find that a great part of the information I have was acquired by looking up something and finding something else on the way. » - Franklin P. Adams

« The most exciting phrase to hear in science, the one that heralds new discoveries, is not "Eureka" but "That's funny..." » - Isaac Asimov

Sommaire

Curriculum Vitae

Marie FRIMAT, 39 ans (30.01.1981)
Pacsée, 3 enfants (Thibault 5ans, Adelaïde & Guilhem 2ans)

Adresse Professionnelle
Service de Néphrologie
Hôpital Huriez, CHRU de Lille
Bd Michel Polonovski - 59037 Lille Cedex
Téléphone : 03 20 44 40 34
marie.frimat@univ-lille.fr

N° Ordre : 59/21262
RPPS : 10100194090

TITRES ET FONCTION

- ***Titres hospitaliers et universitaires :***
  Au sein du Service de Néphrologie, CHU Lille, Université de Lille
  - MCU-PH 2017 -
  - Praticien Hospitalo-Universitaire 2013-2017
  - Chef de Clinique des Universités- Assistant Hospitalier 2010-2013
  - Interne des Hôpitaux 2005-2010

- ***Diplômes universitaires***
  - Certificat de bonnes pratiques cliniques (formation ClinEssForm, CHU Lille) 11.2017
  - Thèse d'Université (Université Paris Descartes, Paris VI) 10.2013
  - D.E.S de Néphrologie (Faculté de Médecine Warembourg, Université Lille 2) 2010
  - Doctorat en Médecine (Faculté de Médecine Warembourg, Université Lille 2) 2009
  - Master 2 (Université Pierre et Marie Curie, Paris V) 2009
  - Diplôme Universitaire : Techniques d'Epuration Extra Rénale (Université Strasbourg 1) 2008
  - Diplôme Universitaire : Antibiothérapie clinique (Université Lille 2) 2007
  - Diplôme Interuniversitaire : Toxicologie médicale (Université Lille 2) 2006

- ***Fonctions***
  - Membre du CNU, sous-section 52-03, collège B 2019 -
  - Membre du groupe de travail Rein-Endothelium (French Renal ENDothelial Society) 2016 -
  - Responsable de la Commission « Recherche et Développement » du réseau Nephronor 2014 -
  - Responsable des RCP Néphrologie-Maladies rares (réunion régionale mensuelle) 2014 -
  - Responsable de l'Unité Fonctionnelle Hémodialyse chronique, CHU Lille 2014 -
  - Membre du conseil de Faculté, collège B (Faculté de Médecine, Université de Lille) 2013-2017
  - Membre de la Société francophone de Néphrologie, Dialyse et Transplantation 2013 -
  - Membre de l'Association des Néphrologues du Nord-Pas-de-Calais 2008 -

ACTIVITE DE RECHERCHE

Parcours Recherche

- Master 1 « Biologie Santé » (EDBSL, Université Lille) 2005
  > 2002 : MSBM de Biochimie Métabolique et Régulation
  > 2003 : MSBM de Physiopathologie des maladies transmissibles

- Master 2 « Biologie intégrative et Physiologie » (UPMC, Paris V) 2009
  > Laboratoire d'accueil : INSERM U845 (Pr Friedlander), Equipe "Mécanismes et stratégies thérapeutiques des néphropathies chroniques" (Dr Terzi), Hôpital Necker ;
  > Travail de Recherche : « Activation du complément par les cellules endothéliales humaines ». Direction : Dr Halbwachs-Mecarelli

- Thèse d'Université « Physiologie et physiopathologie » (Université Paris Descartes) 10.2013
  > Ecole Doctorale : Gc2id
  > Laboratoire d'accueil : INSERM U872 (Pr Fridman), Equipe « Complément et maladie » (Dr Fremeaux-Bacchi), Centre de Recherche des Cordeliers ;
  > Travail de recherche : « Lésions endothéliales liées à un défaut de contrôle du complément : de la génétique du complément au syndrome hémolytique et urémique » Direction : Dr Fremeaux-Bacchi et Dr Halbwachs-Mecarelli

Unités d'appartenance :

Université de Lille, équipe du Pr Boulanger : *Glycation, from inflammation to aging*
Au sein des unités :

- INSERM U995/LIRIC, dirigé par le Pr DESRUMAUX 2015 - 2019
- INSERM UMR1167, dirigé par le Pr AMOUYEL 2020 -

Responsabilités propres au sein de l'équipe :

- Animation entre 2015 et 2017 du groupe Rein-Vaisseaux de l'équipe
- Thématiques : endothélium, hème, RAGE (receptor for AGEs), vieillissement vasculaire et rénal
- Développement de projets autour de deux axes principaux :
  - Axe 1 : Implication du RAGE dans le vieillissement rénal et vasculaire accéléré
  - Axe 2 : Implication du RAGE dans l'activation endothéliale complément/hème-dépendante
- Développement de collaborations :
  - Locale : Groupe Rein (Pr Glowacki, Dr Cauffiez) de l'Equipe EA4483 ; Service d'Anatomo-pathologie du CHRU (Pr MC Coppin, Dr V Gnemmi, Dr JB Gibier) ;
  - Nationale : Equipe « complément et maladie » (Dr Roumenina, Dr Véronique Frémeaux-Bacchi) au CRC (Paris) ; Equipes de recherche du groupe Rein-Endothelium ;
  - Internationale: Pr Ann Mary Schmidt (New York University); Pr Satchell (Bristol University).

PRIX ET BOURSES

- Subvention Recherche par la SFNDT (18 K€) 10.2020
- Obtention d'un financement M2, Faculté de Médecine de Lille (année recherche) 2019
- Subvention Recherche par l'AIRG (15 K€) 12.2018
- Bourse « Master 2 Recherche » Société de Néphrologie 2015 (34 k€) 2016
- Obtention d'un financement M2, Faculté de Médecine de Lille (année recherche) 2015
- Subvention Recherche par la Société de Néphrologie (20K€) 10.2014
- Travel award au 24th International Complement Workshop 10.2012
- Titulaire d'une bourse de thèse (AIRG) 10.2010
- Prix au World Congress of Nephrology (ERA-EDTA) 05.2009

Indices bibliométriques

- 40 publications dont 10 en (co)premier/(co)dernier auteur (IF> 3)
- 29 articles originaux dont 6 (+1 en révision) en (co)premier/(co)dernier auteur (IF> 3)
- Score Sigaps : 504 points
- 972 citations, h-index : 13 (sampra)

Répartition par catégorie et par année

Période : 2012 - 2020								
Année	**Total**	**A**	**B**	**C**	**D**	**E**	**NC**	**Score**
2012	2	1	0	0	0	1	0	30
2013	1	1	0	0	0	0	0	32
2014	3	1	1	1	0	0	0	18
2015	1	1	0	0	0	0	0	8
2016	5	3	0	1	1	0	0	67
2017	5	2	1	1	0	1	0	74
2018	5	2	0	2	0	1	0	70
2019	12	4	6	1	0	1	0	128
2020	6	2	2	1	1	0	0	77
Total	**40**	**17**	**10**	**7**	**2**	**4**	**0**	**504**

Répartition par catégorie et par position

Période : 2012 - 2020							
Position	**Total**	**A**	**B**	**C**	**D**	**E**	**NC**
1	6	3	3	0	0	0	0
2	7	2	0	1	0	4	0
3	2	1	0	1	0	0	0
Inv	4	2	1	1	0	0	0
k	16	8	3	3	2	0	0
ADA	3	0	2	1	0	0	0
DA	2	0	2	0	0	0	0
Total	**40**	**16**	**11**	**7**	**2**	**4**	**0**

Principales publications

1. *The receptor for advanced glycation end products is a sensor for cell-free heme. May O, Yatime L, Merle N, Delguste F, Howsam M, Daugan M, Billamboz M, Ghinet A, Lancel S, Dimitrov JD, Boulanger E, Roumenina L*, **Frimat M***. In revision in FEBS Journal (IF: 4.8)*
2. Complement system: a driver of the acute kidney injury in rhabdomyolysis. I Boudhabhay[#], V Poillerat[#], A Grunenwald, C Torset, J Leon, M Daugan, F Lucibello, Kl El Karoui, A Ydee, S Chauvet, P Girardie, S Sacks, M Rabant, P de Lonlay, C Rambaud, V Gnemmi, V Fremeaux-Bacchi, **M Frimat** and LT. Roumenina. Kidney Int. 2020 Oct 30:S0085-2538(20)31244-8. doi: 10.1016/j.kint.2020.09.033. *(IF: 8.4)*
3. The use of highly individualized complement blockade revolutionized the posttransplant clinical outcomes and renal epidemiology of atypical HUS. Zuber J, **Frimat M**, Caillard S, Kamar N, Gatault P, (…), Rondeau E, Le Quintrec M, Frémeaux Bacchi V. J Am Soc Nephrol. 2019 Oct 1. pii: ASN.2019040331. (IF : 8.6)
4. Knock out of receptor for advanced glycation end-products attenuates age-related renal lesions. T Teissier, V Quersin, V Gnemmi, M Daroux, M Howsam, F Delguste, C Lemoine, C Fradin, AM Schmidt, C Cauffiez, T Brousseau, F Glowacki, FJ Tessier, E Boulanger and **M Frimat**. Aging Cell. 2019 Apr;18(2):e12850. doi: 10.1111/acel.12850. Epub 2019 Feb 22. (IF :7.6)
5. Heme Drives Susceptibility of Glomerular Endothelium to Complement Overactivation Due to Inefficient Upregulation of Heme Oxygenase-1. May O, Merle NS, Grunenwald A, Gnemmi V, Leon J, Payet C, Robe-Rybkine T, Paule R, Delguste F, Satchell SC, Mathieson PW, Hazzan M, Boulanger E, Dimitrov JD, Fremeaux-Bacchi V, **Frimat M***, Roumenina LT*. Front Immunol. 2018 Dec 20;9:3008. (IF: 6.4)
6. Renal Cortical Necrosis in Postpartum Hemorrhage: A Case Series. **Frimat M**, Decambron M, Lebas C, Moktefi A, Lemaitre L, Gnemmi V, Sautenet B, Glowacki F, Subtil D, Jourdain M, Rigouzzo A, Brocheriou I, Halimi JM, Rondeau E, Noel C, Provôt F, Hertig A. Am J Kidney Dis. 2016 Jan 16. pii: S0272-6386(15)01496-1. (IF:6.3)
7. Complement activation by heme as a secondary hit for atypical hemolytic uremic syndrome. **Frimat M**., F. Tabarin, J. D. Dimitrov, C. Poitou, L. Halbwachs-Mecarelli, V. Fremeaux-Bacchi, and L. T. Roumenina. Blood 2013; 122:282-292. (IF:9.8)
8. A prevalent C3 mutation in aHUS patients causes a direct C3 convertase gain of function. Roumenina, L. T*, **M. Frimat***, E. C. Miller, F. Provot, M. A. Dragon-Durey, P. Bordereau, S. Bigot, C. Hue, S. Satchell, P. Mathieson, C. Mousson, C. Noel, C. Sautes-Fridman, L. Halbwachs-Mecarelli, J. P. Atkinson, A. Lionet, and V. Fremeaux-Bacchi. Blood 2012; 119:4182-4191. (IF:9.1)

Exposé des travaux de recherche

Depuis mon Master 2, mes projets de recherche se sont inscrits plus particulièrement dans la thématique « maladies rénales et endothélium » à travers des modèles de pathologies aussi bien aiguës (microangiopathies thrombotiques, vascularites, atteintes réno-vasculaires de la grossesse) que chroniques, l'insuffisance rénale avancée constituant, en soi, un modèle d'accélération de vieillissement vasculaire.

Entre 2010 et 2013, j'ai eu l'opportunité de travailler dans le cadre de ma thèse d'Université au sein des équipes des Dr Halbwachs-Mecarelli (Inserm U845 - Hôpital Necker, Paris) et Dr Frémeaux-Bacchi (Inserm U872 - CRC, Paris), en collaboration avec le service de Néphrologie de Lille, sur un projet centré sur le syndrome hémolytique et urémique atypique. Ce projet a regroupé deux aspects complémentaires, l'un clinique (caractérisation phénotypique des patients atteints de SHUa et porteurs de la mutation R161W) et l'autre fondamental (étude des mécanismes lésionnels endothéliales complément-dépendants).

J'ai rejoint en 2014 l'équipe du Pr Boulanger, au sein de l'unité INSERM U995, en vue d'étudier les conséquences rénales et vasculaires des produits de glycation avancée (AGEs) et les effets de l'activation de leur principal récepteur, le RAGE (receptor for advanced glycation end products). Mon objectif, au sein de cette équipe a été de développer des projets conjuguant à la fois les thématiques du laboratoire et mes compétences relatives aux maladies rénales, au complément et à l'endothélium. Dans ce cadre, se sont dessinés deux axes de recherche :

- Axe 1 : Vieillissement rénal accéléré par la glycation alimentaire : Implication de RAGE
- Axe 2 : Etude de l'implication du RAGE dans l'activation endothéliale complément-dépendante dans des modèles d'agression aiguë (syndrome hémolytique et urémique, syndrome des anti-phospholipides) ou chronique (vieillissement accéléré rénal et vasculaire).

En parallèle, je poursuis depuis 2010 mon activité clinique au sein du service de Néphrologie, Dialyse et Transplantation du Pr Hazzan au CHU de Lille où j'ai pu participer ou conduire plusieurs travaux de recherche clinique touchant aux pathologies vasculaires en néphrologie.

Les principaux résultats issus de ces travaux sont détaillés ci-dessous et les publications en rapport sont présentés en fin de manuscrit.

Travaux de thèse d'Université

Lésions endothéliales liées à un défaut de contrôle du complément : de la génétique du complément au syndrome hémolytique et urémique

Background : L'identification fréquente de mutations des protéines régulatrices du complément suggère que les lésions endothéliales dans le syndrome hémolytique et urémique atypique (SHUa) résultent d'une activation incontrôlée de la voie alterne du complément. Les mutations, en soi, ne constituent cependant que des facteurs de susceptibilité et les mécanismes menant de l'anomalie de régulation du complément au développement de lésions de microangiopathie thrombotique rénale restent mal compris.

L'objectif de ce projet était d'étudier certains mécanismes de l'activation du complément à la surface des cellules endothéliales dans le SHUa et les conséquences de cette activation pour l'endothélium. Dans ce but, nous nous sommes initialement focalisés sur la mutation $C3_{R139W}$, identifié en 2012 chez 4% des patients de la cohorte française de SHUa, dont nous avons réalisé la caractérisation phénotypique et fonctionnelle et qui a constitué un modèle d'étude des conséquences d'un complément dérégulé sur l'endothélium. Dans la deuxième partie de ce travail et en vue de préciser les liens entre anomalie du complément et activation des cellules endothéliales, nous nous sommes intéressés au rôle de l'hémolyse, l'un des dénominateurs communs du SHU.

1ère partie : Etude centrée sur la mutation $C3_{R139W}$: Caractérisation fonctionnelle et caractéristiques phénotypiques des SHUa associés

La mutation $C3_{R139W}$ est hétérozygote, portée par l'exon 4 du *C3*, caractérisée par la substitution en position 481 d'une cytosine par une thymine (**figure 1**). Cette substitution conduit au remplacement d'un résidu arginine par un résidu tryptophane, en position 139 de la protéine C3 mature (absence du peptide signal de 22 résidus), au sein de son deuxième domaine macroglobuline (MG2). L'intérêt porté à cette mutation est lié à sa prévalence puisqu'elle avait été identifiée, de façon sporadique, chez 14 patients-SHUa (alors 4% de la cohorte française des SHUa et 50% des patients avec mutation du C3). Communément, les SHUa sont rattachés à une mutation ponctuelle rare concernant l'une des protéines activatrices ou régulatrices du complément et le petit nombre de patients partageant la même mutation complique l'analyse de leurs conséquences propres et des facteurs additionnels influençant la pénétrance et l'expression de la pathologie. Ainsi, les objectifs de ce travail étaient de réaliser la caractérisation phénotypique des SHUa présentés par ces patients, de déterminer d'éventuels facteurs susceptibles d'influencer l'expression de la pathologie et d'étudier les caractéristiques fonctionnelles de ce C3 muté ainsi que ses conséquences sur l'endothélium.

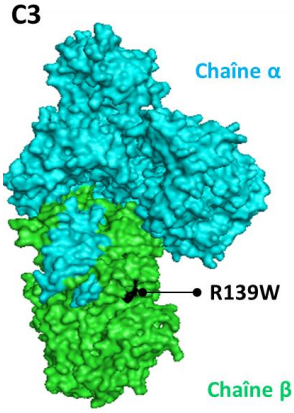

Figure 1: Mapping of R139W on the surface of C3 using Pymol software

Résultats

La mutation $C3_{R139W}$ a donc été identifiée chez 14 patients ainsi que chez 11 des 19 apparentés sains chez qui une étude génétique a pu être réalisée. La présence de polymorphismes de susceptibilité au SHUa, dans les gènes du FH (FH gtgt) ou de MCP (MCP ggaac), était significativement plus fréquente chez les patients qu'au sein d'une population témoin ou que parmi les apparentés sains porteurs de la mutation. Ces résultats ont conforté le caractère multigénique du SHUa et l'influence des polymorphismes à risque dans sa pénétrance.

L'étude de l'expression phénotypique des SHU a révélé une distribution hétérogène, l'âge de survenue de la pathologie variant entre 8 mois et 72 ans (médiane : 22 ans). Elle a confirmé une apparente susceptibilité du sexe féminin à l'âge adulte (8/9 patients adultes) ainsi que la fréquente identification de facteurs déclenchant (10/14). L'évolution fonctionnelle rénale était souvent sévère, puisque six patients évoluaient vers l'insuffisance rénale chronique terminale dans la première année et il persistait, dans les autres cas, une insuffisance rénale chronique séquellaire. Par ailleurs, sur les 7 transplantations rénales réalisées, 4 étaient marquées par une récidive de SHUa, conduisant dans tous les cas, à une perte fonctionnelle du greffon. Nous avons identifié une fréquence non négligeable d'événements neurologiques (5/14) et cardiologiques (8/14), appuyant l'intérêt d'évaluer initialement et de surveiller la fonction cardiaque chez les patients (dosage des troponines, échocardiographie). Enfin, le taux plasmatique de C3 était abaissé en phase aigüe du SHU chez 6/9 patients ainsi qu'en dehors de tout épisode chez 5/8 patients, alors qu'il était constamment normal chez les apparentés sains (8/8).

L'étude des conséquences endothéliales de la mutation $C3_{R139W}$, en termes d'activation du complément et d'acquisition d'un phénotype pro thrombotique, a été réalisée, à partir de sérum de patients, sur deux modèles cellulaires endothéliaux (HUVECs et cellules endothéliales glomérulaires humaines issues d'une lignée immortalisée, GEnC). Sur cellules natives, il n'existait pas, en cytométrie de flux, de différence significative du dépôt membranaire de C3 entre sérums-contrôles et sérums-patients. A l'inverse, nous avons montré, sous l'effet d'une pré-activation endothéliale par des cytokines inflammatoires, une augmentation de ce dépôt et ce de façon significativement plus marquée avec les sérums-patients et ceux des apparentés sains porteurs de la mutation qu'avec les sérums-contrôles (**figure 2**). Dans ces mêmes conditions d'activation endothéliale, nous avons mis en évidence une élévation des taux de C3a, C5a et C5b-9 soluble libérés lors de l'incubation des cellules endothéliales en présence de sérums porteurs de la mutation ainsi qu'une augmentation de l'expression membranaire de facteur tissulaire. Comme dans le cas du dépôt de C3, nous n'avons pas observé, pour ces paramètres, de différence significative entre témoins et patients en l'absence de pré-activation cellulaire. Ces résultats ont renforcé l'hypothèse selon laquelle

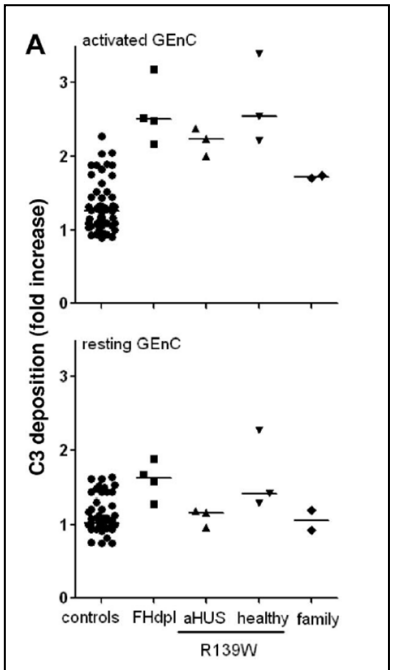

Figure 2: Complement activation on glomerular endothelial cells, incubated with sera from R139W aHUS patients and their healthy relatives.

le SHU serait provoqué par l'amplification par un complément mal régulé, d'un événement lésionnel initial touchant les cellules endothéliales (théorie des hits multiples). Ils sont, par ailleurs, concordants avec les données cliniques, qui suggèrent que l'expression de la pathologie chez les sujets porteurs de la mutation $C3_{R139W}$, requiert des facteurs additifs (facteurs déclenchants : 10/14 ; polymorphismes à risque : 7/14). Par ailleurs, nous avons montré, sur cellules activées, qu'en cas d'inhibition du FH, par addition d'anticorps bloquants lors de l'étape d'incubation avec le sérum de patient, le dépôt de C3 était supérieur qu'en cas d'inhibition de MCP (anticorps bloquant), suggérant que la mutation $C3_{R139W}$ soit majoritairement régulée par le FH. Pour appuyer cette hypothèse, nous avons établi que l'addition de FH purifié au sérum de patient s'accompagnait d'une diminution dose-dépendante du dépôt membranaire de C3.

La caractérisation fonctionnelle de la mutation $C3_{R139W}$ a été réalisée à partir de protéines recombinantes. Cette mutation est localisée à proximité des sites de fixation du FH, de MCP et du FB. La liaison de ces trois protéines avec le $C3_{R139W}$ recombinant a été étudiée par ELISA et SPR (surface plasmon resonnance). En premier lieu, nous avons observé une diminution de la liaison de MCP avec le $C3_{R139W}$, tandis que l'interaction avec le FH était, elle, comparable à celle de la protéine témoin. Ceci est concordant avec les données précédemment décrites, qui suggèrent un rôle particulièrement important du FH chez les patients porteurs de la mutation $C3_{R139W}$. D'autre part, nous avons mis en évidence une augmentation nette de la liaison de la protéine $C3_{R139W}$ avec le FB, qui s'est avérée associée à la formation d'une C3 convertase plus efficace (analyse par SPR).
Nous avons ainsi démontré que la mutation $C3_{R139W}$ modifiait les caractéristiques fonctionnelles de la protéine C3, induisant un gain de fonction, à la fois, direct par augmentation de l'affinité avec le FB, et indirect par réduction de l'interaction avec la MCP.

Conclusions : ce travail a identifié la mutation $C3_{R139W}$ comme un facteur de susceptibilité au SHUa, caractérisé ses conséquences fonctionnelles à type de gain de fonction direct et indirect et mis en avant l'importance des facteurs additionnels dans sa pénétrance et expression. Cliniquement, il a souligné l'importance de l'évaluation et de la surveillance cardiologique au cours du SHUa.

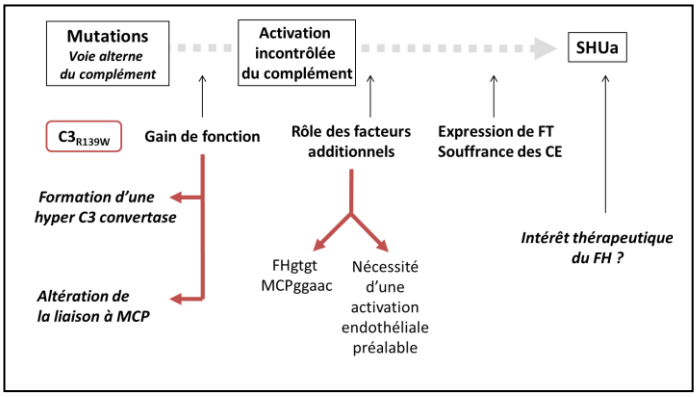

2ème partie : Etude de l'activation du complément par l'hème et implication dans le SHUa

Dans la deuxième partie des travaux et en vue de préciser les liens entre anomalie du complément et activation des cellules endothéliales, nous nous sommes intéressés au rôle de l'hémolyse. En effet, indépendamment de la nature du facteur déclenchant initial, l'hémolyse constitue un dénominateur commun des SHU, ses dérivés ont un fort pouvoir pro-inflammatoire et leur capacité à activer la voie alterne du complément en phase fluide avait été récemment rapporté. Nous avons ainsi évoqué l'hypothèse que l'hème puisse intervenir en deuxième ligne pour induire, via notamment une activation du complément, une amplification des processus pro-thrombotiques, susceptible de majorer les lésions de MAT et donc d'aggraver l'expression clinique du SHU.

Résultats

Nous avons confirmé que l'hème induisait une activation du complément en phase fluide, en mettant en évidence une augmentation dose-dépendante des taux de C3a, C5a et C5b-9 soluble, mesurés par ELISA, dans du sérum témoin exposé à des doses croissantes d'hème. Cette augmentation persistait en cas d'inhibition de la voie classique, mais n'était plus observée en sérum déplété en FB, signe d'une activation voie alterne-dépendante.

Nous avons démontré une activation du complément sous l'effet de l'hème à la surface des cellules endothéliales (HUVEC et GEnC). En effet, une augmentation dose-dépendante du dépôt membranaire de C3 était observée (**figure 1**) et persistait après lavage des cellules entre les étapes d'exposition à l'hème et d'incubation avec le sérum, permettant d'éliminer un dépôt uniquement secondaire à une activation du complément en phase fluide par l'hème. Cette activation du complément à la surface des cellules était également dépendante de la voie alterne et s'accompagnait de la formation de complexes d'attaque membranaires, traduisant la mise en œuvre de la voie terminale commune. Nous avons, par ailleurs, précisé la nature du C3 lié aux cellules et ainsi montré que l'hème induisait à la fois une fixation covalente de C3b et iC3b mais également une fixation de C3 non clivé, comme le suggère la liaison membranaire de l'anti-C3a. Notre hypothèse est que ce C3 non clivé corresponde à du C3(H_2O)-like, rappelant ici ce qui a été décrit à la surface des plaquettes activées ou des biomatériaux.

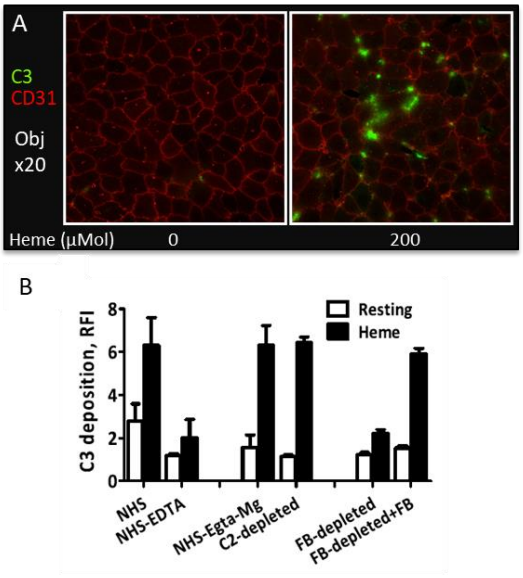

Figure 1: Study by A) immunofluorescence and B) flow cytometry of C3 deposits on heme-treated endothelial cells.

Dans le but de se rapprocher des conditions pathologiques du SHUa, le dépôt de C3 à la surface des cellules était étudié en présence de sérum de patients ayant présentés un SHUa et porteurs d'une mutation connue (FH ou C3). Les résultats étaient comparés à ceux de 30 sérums témoins. Ces expériences ont montré, sur cellules natives, un dépôt de C3 faible mais significativement supérieur en présence de sérums pathologiques, différence exacerbée en cas d'exposition préalable des cellules à l'hème. Des résultats similaires étaient observés en conditions artificielles de dysrégulation du

complément, mimant différentes conditions de susceptibilité au SHUa (FB recombinant porteur d'une mutation gain de fonction ; sérums déplétés en FH ou en FI ; anticorps anti-FH bloquant la région N- ou C-terminale).

Ce travail a permis d'identifier trois mécanismes par lesquels l'hème est susceptible d'activer la VA du complément en phase fluide et/ou à la surface des cellules endothéliales :

1- Nous avons démontré, par SPR, que l'hème interagissait fortement et de façon dose-dépendante avec le C3 immobilisé (C3(H_2O)-like). Cette interaction est apparue majoritairement dépendante du fragment C3a. Les sites de liaison potentielle de l'hème au C3 ont été déterminés par docking moléculaire et localisés principalement dans le domaine ANA ou à proximité du pont thioester dans le domaine TED (**figure 2**). Nous avons émis l'hypothèse que le groupement redox de l'hème pourrait favoriser l'hydrolyse du pont thioester et ainsi la transition du C3 natif vers sa forme hydrolysée. Le C3 hydrolysé est capable de former une C3 convertase alterne, ce qui pourrait expliquer l'activation du complément notamment en phase fluide. D'autre part, une augmentation des interactions homophiliques du C3, sous l'effet de l'hème, était suggérée en spectroscopie d'absorption et confirmée par SPR et chromatographie d'exclusion stérique. Ceci serait susceptible de favoriser la formation de C5 convertases. De façon cohérente, nous avons observé en SPR à la surface de chip recouverts de C3, la formation de C3/C5 convertases de plus en plus efficace sous l'effet de doses croissantes d'hème. L'hème peut donc induire la formation d'hyper C3/C5 convertases, renforçant ainsi l'activation du complément.

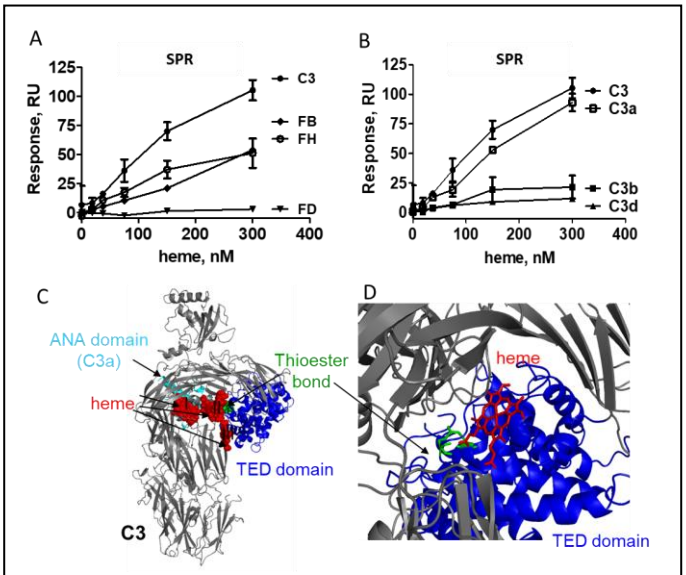

Figure 2: Binding of heme to C3. (A) SPR analysis of the binding of different concentration of heme to AP proteins and (B) to C3 fragments. (C) Molecular docking of heme to C3 and (D) zoom to the II cluster with the top score heme molecule visualized in ball-and-stick in red. The distance between the thioester bond (green) and heme is less than 10Å.

2- Nous avons établi que l'hème induisait une diminution de l'expression membranaire de MCP et de DAF à la surface des cellules endothéliales (HUVEC), ce qui est susceptible de réduire les capacités de régulation du complément à la surface de ces cellules. Parallèlement, nous avons observé, sous l'effet de ce stimulus, l'apparition d'un dépôt de FH à la surface des cellules traitées, sans que l'hème ne semble induire d'altération de ses propriétés de régulation membranaire. Le FH pourrait ainsi compenser, à la façon de ce qui est observé à la surface des cellules apoptotiques, la baisse d'expression membranaire de MCP et de DAF, rendant compte de son rôle particulièrement important dans ces conditions d'activation, et par projection dans les pathologies hémolytiques. Il est ici intéressant de rappeler que les dysfonctions du FH sont les principales anomalies rapportées actuellement dans le SHUa.

3- Enfin, nous avons montré que l'exposition des cellules endothéliales à l'hème déclenchait une mobilisation de leurs corps de Weibel-Palade, préalable à la libération de FvW et de P-selectine. La P-

selectine membranaire est capable de lier le C3b et de servir de plateforme à la formation d'une C3 convertase alterne, participant ainsi à activer la voie alterne du complément. D'autre part, la libération de multimères de THPM du FvW par les corps de Weibel-Palade endothéliaux constitue un autre mécanisme par lequel l'hémolyse peut induire l'acquisition d'un phénotype endothélial prothrombotique, susceptible d'amplifier les lésions de MAT.

Conclusions : Nous avons ainsi montré que l'hème libre activait la voie alterne du complément dans le sérum et à la surface des cellules endothéliales, cela de façon exacerbée en cas de dysrégulation sous-jacente du complément, et identifié plusieurs des mécanismes en cause (formation d'hyper C3/C5 convertase, baisse des capacité régulatoires, mobilisation des corps de Weibel Palade). Par ces travaux, nous avons précisé les liens entre activation du complément et acquisition d'un phénotype endothélial pro-thrombotique dans le SHUa et identifié l'hème comme un acteur de l'amplification des lésions endothéliales complément-dépendantes.

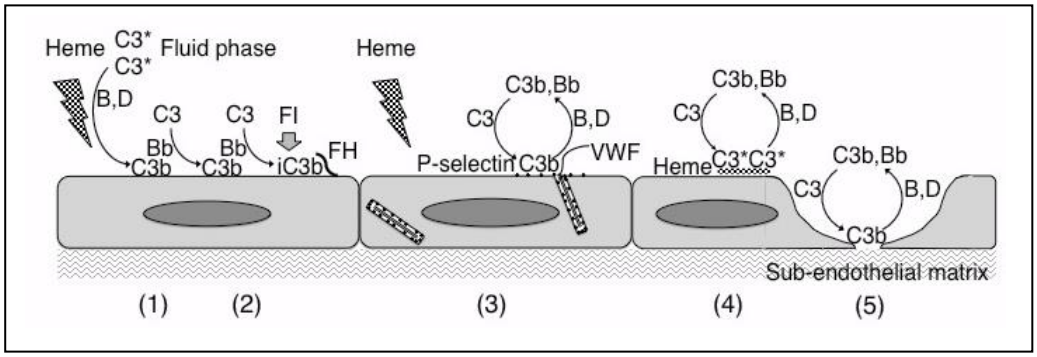

Valorisation

Manuscrits :

- A prevalent C3 mutation in aHUS patients causes a direct C3 convertase gain of function. Roumenina, L. T*, **M. Frimat***, E. C. Miller, F. Provot, M. A. Dragon-Durey, P. Bordereau, S. Bigot, C. Hue, S. Satchell, P. Mathieson, C. Mousson, C. Noel, C. Sautes-Fridman, L. Halbwachs-Mecarelli, J. P. Atkinson, A. Lionet, and V. Fremeaux-Bacchi. Blood 2012; 119:4182-4191. (IF: 9,1).

- Complement activation by heme as a secondary hit for atypical hemolytic uremic syndrome. **Frimat M**., F. Tabarin, J. D. Dimitrov, C. Poitou, L. Halbwachs-Mecarelli, V. Fremeaux-Bacchi, and L. T. Roumenina. Blood 2013; 122:282-292. (IF: 9,8)

Communications orales *en congrès nationaux et internationaux : 3*
Communications affichées *en congrès nationaux et internationaux : 7*

Prix et Bourses **:**

- **24th International Complement Workshop, 2013:** Travel award pour le travail: "Free heme transforms endothelial cells into alternative pathway activators. Implications for the Hemolytic and Uremic Syndrome".
- **Congrès de la Société Française de Néphrologie, 2010** : Bourse de thèse pour le projet : "Lésions endothéliales liées à un défaut de contrôle du complément : de la génétique du complément au SHU."
- **World Congress of Nephrology, 2009 :** Prix des meilleurs résultats pour un sujet soumis par un médecin de moins de 40 ans, pour le travail : “R161W complement C3 mutation predispose to atypical hemolytic uremic relapse after kidney transplantation.”

Travaux Postdoctoraux

Axe 1 : Implication de RAGE dans le vieillissement rénal et vasculaire accéléré

Le débit de filtration glomérulaire (DFG) diminue avec l'âge (Glassock et al 2017), rendant compte d'une vulnérabilité des personnes âgées à l'insuffisance rénale chronique (IRC). La prévalence de l'IRC était ainsi supérieure à 30% dans une cohorte européenne de patients âgés de plus de 70 ans (Ebert et al. 2016). Etant donné le vieillissement attendu de la population, une augmentation de l'incidence de l'IRC parait inévitable. Cependant, plus d'un tiers des personnes ne présentent aucune altération de leur DFG avec l'âge (Bolignano et al. 2014), suggérant que l'insuffisance rénale liée à l'âge soit conditionnée. Le genre, l'origine ethnique, les facteurs génétiques et les comorbidités sont connus pour influencer la fonction rénale, mais il paraît prioritaire d'identifier de nouveaux facteurs dans le but de freiner la progression de l'IRC et de ses conséquences.

Les produits de glycation avancée ou AGEs (advanced glycation end products) forment un groupe hétérogène de molécules résultant de la liaison irréversible d'une protéine et d'un sucre. Ils sont issus soit d'une formation endogène (en cas d'hyperglycémie, de stress oxydatif, mais également au cours du vieillissement), soit de l'alimentation avec une ingestion quotidienne de Nε-carboxyméthyllysine (CML, l'AGE le plus étudié) observée jusqu'à 252 µg/kg de poids corporel dans une population européenne (Tessier and Birlouez-Aragon 2012). Leur rôle dans la maladie rénale chronique est évoqué *via* notamment l'activation de leur principal récepteur, le RAGE, dont les propriétés pro-inflammatoires et pro-oxydantes participeraient à accélérer le vieillissement et ce même en l'absence d'autres conditions pathologiques (Stinghen et al. 2016; Frimat et al. 2017). L'impact de l'exposition chronique aux AGE alimentaires sur le vieillissement demeure toutefois peu étudié. Compte tenu de l'accumulation préférentielle de la CML dans les reins sous l'effet d'un régime enrichi (Li et al. 2015; Tessier et al. 2016) et des études reliant les AGE alimentaires et les lésions rénales (Feng et al. 2007; Zheng et al. 2002), **nous avons émis l'hypothèse que les reins pourraient être des organes cibles du vieillissement accéléré par les interactions AGEs-RAGE.** Dans le but d'étudier cette hypothèse, des souris mâles C57Bl/6, Wild-type (WT) ou RAGE$^{-/-}$, ont reçu durant 18 mois une alimentation témoin ou enrichie en CML.

<u>Résultats</u>

Accumulation rénale de CML sous l'effet d'un régime enrichi

Nous avons observé en immunohistochimie un marquage rénal diffus de la CML plus prononcé chez les souris WT et RAGE$^{-/-}$ soumises au régime enrichi en CML comparativement aux souris exposées au régime contrôle. Ce marquage prédominait au sein des tubes proximaux. Cette accumulation rénale de CML - indépendante du RAGE - sous l'effet d'un régime enrichi a été confirmée en LC-MS/MS, avec mise en évidence non seulement d'une plus forte concentration de CML libre (issues possiblement de l'alimentation), mais également de CML liée aux protéines laissant suggérer un processus de

néoformation d'AGEs endogènes sous l'effet d'un stress oxydatif.

Absence d'effet significatif d'un régime enrichi en CML sur le vieillissement rénal

Aucune des souris WT ou RAGE$^{-/-}$ ne devenait diabétique, dyslipidémique ou obèse sous l'influence d'un régime enrichi en CML. Le poids rénal, la créatinine et l'urée plasmatique n'étaient pas statistiquement différents entre les groupes témoins et les groupes CML, que ce soit chez les souris WT ou RAGE$^{-/-}$. L'expression de *Kim-1* et *Ngal* n'était pas affectée par le régime riche en CML, tout comme les lésions de hyalinose artériolaire, atrophie tubulaire ou fibrose. Seule une aggravation de la sclérose glomérulaire (GS) était observée sous l'influence de l'alimentation riche en CML chez les souris WT (seuls 6,5 % des glomérules ne présentaient aucun signe de sclérose chez les souris WT-CML contre 31, 61 et 67 % chez les souris WT-contrôles, RAGE$^{-/-}$-contrôles et RAGE$^{-/-}$-CML). Ces différences n'étaient toutefois pas significatives et afin d'analyser l'impact de l'invalidation du RAGE sur le vieillissement rénal, nous avons concentré nos analyses sur les différences entre souris WT et RAGE$^{-/-}$, indépendamment de leur alimentation.

Atténuation des lésions rénales associées au vieillissement chez les souris RAGE-KO

Le pourcentage médian de vaisseaux présentant des dépôts hyalins était plus élevé chez les souris WT que chez les souris RAGE$^{-/-}$ (24 % vs 12 %, respectivement, p <0,001). Atrophie tubulaire et fibrose interstitielle étaient également plus présentes chez les souris WT comparativement aux souris RAGE$^{-/-}$. La fibrose était identifiée dans l'interstitium rénal de toutes les souris WT, tandis qu'elle restait légère ou absente chez les souris RAGE$^{-/-}$. L'expression de *Ngal*, plus spécifiquement associée aux lésions tubulo-interstitielles (Rysz et al. 2017) était significativement plus élevée chez les souris WT (∼15.5 ±6.6) que chez les souris RAGE$^{-/-}$ (∼6.4 ±5.6, p<0.05). Enfin, le score médian de glomérulosclérose (GS), calculé sur évaluation histologique de la densité de glomérules scléreux (60 glomérules/souris) était plus élevé chez les souris WT (49 A.U.) que RAGE$^{-/-}$ (10 A.U., p <0,001), **figure 1**. Seuls 13% des glomérules n'avaient aucun signe de sclérose chez les souris WT contre 63% chez les RAGE$^{-/-}$ (p <0,001).

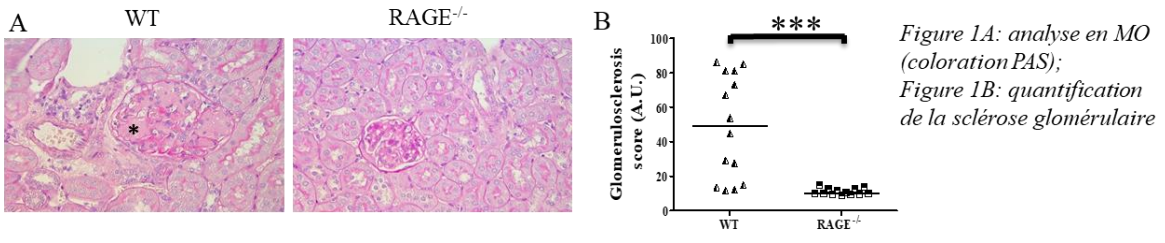

Figure 1A: analyse en MO (coloration PAS); Figure 1B: quantification de la sclérose glomérulaire

Absence d'amylose sénile chez les souris RAGE-KO

L'aspect nodulaire de la GS faisait suspecter des dépôts amyloïdes confirmés par la coloration du Rouge Congo et l'identification de fibrilles de 5-10 nm par microscopie électronique. Huit des 14 souris WT (57 %) étaient amyloïdes contre 1 des 13 souris RAGE$^{-/-}$ (8 %). Le typage de ces dépôts révélaient une amylose à ApoA-II (AApoA-II) associée au vieillissement chez la souris (Kitagawa et al. 2003), **figure 2A**. Les souris WT avaient un score médian AApoA-II significativement plus élevé que les souris RAGE$^{-/-}$ qui

n'avaient pas ou très peu de dépôts (2,5 ±1,3 *vs* 1,1 ±0,2 A.U., respectivement : p <0,01). L'intensité de la GS était corrélée au score AApoA-II (r=0,92, p <0,0001), **figure 2B**.

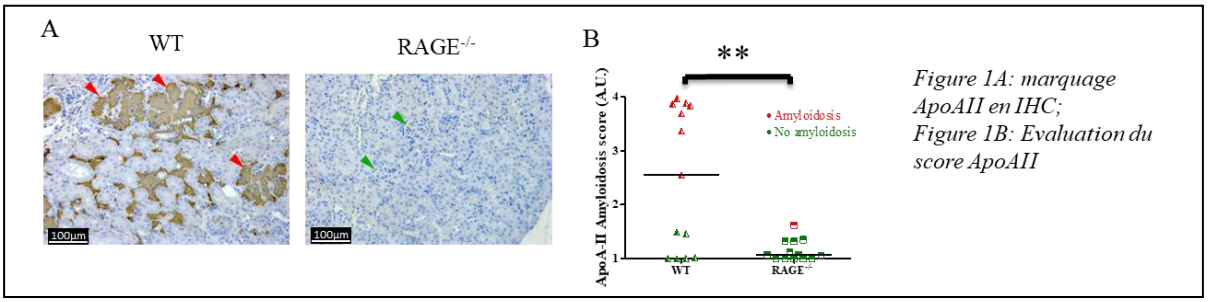

Figure 1A: marquage ApoAII en IHC;
Figure 1B: Evaluation du score ApoAII

Atténuation des margeurs de l'inflammation et du stress oxydatif chez souris RAGE-KO

Par rapport à des souris WT âgées de 3 mois, les taux d'ARNm d'Il-*6*, *Tnf-α* et *Vcam-1* augmentaient significativement chez les souris WT de 20 mois, tandis que l'augmentation était moindre et non significative chez les souris âgées RAGE$^{-/-}$, suggérant un profil similaire entre les jeunes souris WT et les souris âgées RAGE$^{-/-}$. De même, l'expression de *Sod2*, gène antioxydant, était significativement plus faible chez les souris WT de 20 mois que chez les jeunes souris WT (p <0,01) et les souris âgées RAGE$^{-/-}$ (p<0,05). De façon intéressante, SIRT1, associé à la longévité et connu pour diminuer avec l'âge était plus élevée chez les souris RAGE$^{-/-}$ que chez les souris WT (p=0,056), tandis que l'activation de la voie Akt étaient moindre chez les souris âgées RAGE$^{-/-}$ que chez les souris WT (p<0,05).

Conclusions : Nous avons ainsi observé des taux plus élevés de CML dans les reins des souris WT et RAGE$^{-/-}$. Le régime riche en CML n'a pas eu d'impact significatif sur les paramètres rénaux étudiés, où seule une tendance à l'aggravation de la sclérose glomérulaire était détectée. Indépendamment du régime, les souris RAGE$^{-/-}$ étaient significativement protégées contre les lésions de néphrosclérose et d'amylose sénile, en faveur d'un effet protecteur de la suppression de RAGE vis-à-vis du vieillissement rénal. Cela pourrait être dû à une réduction de l'inflammation et du stress oxydatif chez les souris RAGE$^{-/-}$, positionnant RAGE comme un récepteur essentiel du vieillissement associé à l'inflammation ou inflammaging.

Encadrements

Master2 :

- **Valentine Quersin** (Interne Néphrologie) — 2014-2015
  Encadrement 100%
  Financement : Année recherche.
  EDBSL, Université de Lille. « **Modifications fonctionnelles, structurelles et moléculaires rénales induites par les produits de la glycation alimentaire** »
  Note : 16/20

- **Cécile Lemoine** (Interne Néphrologie) — 2015-2016
  Encadrement 100%
  Financement : bourse de la Société française de Néphrologie.
  M2 Biologie du vieillissement, Université Paris Diderot. « **Effets des produits de glycation avancée sur le vieillissement endothélial rénal** »
  Note : 15/20

Financements

- **2014** : Financement d'un Master2 par Année Recherche (Faculté de Médecine, Lille) ;
- **2015** : Allocation Recherche de la Société de Néphrologie 2015 pour un Master 2, 34 k€ ;
- **2016** : Partenaire dans le cadre d'un financement industriel (VF BioSciences) pour le projet « Vieillissement rénal accéléré par la glycation alimentaire : Implication de RAGE » (180 k€/3years) - porteur : Pr Boulanger.

Valorisation

Manuscrits :

- Is RAGE the receptor for inflammaging? **Frimat M**., Teissier T., Boulanger E. Aging (Albany NY). 2019 Sep8;11(17):6620-6621. (IF : 5,2)
- Knock out of receptor for advanced glycation end-products attenuates age-related renal lesions. T Teissier, V Quersin, V Gnemmi, M Daroux, M Howsam, F Delguste, C Lemoine, C Fradin, AM Schmidt, C Cauffiez, T Brousseau, F Glowacki, FJ Tessier, E Boulanger and **M Frimat**. Aging Cell. 2019;18:e12850.
- Kidney, heart, and brain: three organs targeted by aging and glycation. **Frimat M**, Daroux M, Litke R, Nevière R, Tessier F, Boulanger E. Clin Sci (Lond). 2017 Jun 1;131(11):1069-1092

Communications orales *en congrès nationaux et internationaux : 2*
Communications affichées *en congrès nationaux et internationaux : 2*

***Axe 2 : Etude de l'implication du RAGE dans l'activation endothéliale complément/heme-dépendante**, à travers deux modèles : le syndrome hémolytique et urémique (SHU) et le syndrome catastrophique des anti-phospholipides (SAPL).*

L'hémolyse intravasculaire est un processus pathologique rencontré dans différentes maladies, telles que certaines anomalies du globule rouge (drépanocytose, déficit en G6PD) ou les microangiopathies thrombotiques (SHU). La libération massive d'hémoglobine libre et de ses dérivés s'accompagne de réactions pro-inflammatoires et pro-oxydatives majeures. L'hème, en particulier, induit une activation de la voie alterne du complément dont nous avons déjà étudié l'impact comme « second hit » dans la physiopathologie du SHU atypique, microangiopathie thrombotique de tropisme rénale associée à un défaut de régulation du complément. La répétition d'épisodes hémolytiques conduit par ailleurs à un vieillissement vasculaire accéléré.

Les effets cellulaires de l'hème sont notamment médiés par sa liaison au TLR4 (Toll like receptor 4), son seul récepteur membranaire actuellement connu. Cependant, les interactions TLR4-hème ne suffisent pas à expliquer tous les effets pro-inflammatoires rattachés à l'hème. De façon intéressante, RAGE et TLR4 présentent plusieurs caractéristiques communes (ligands, voie de signalisation) et tous deux sont considérés comme des PPRs (Pattern recognition receptors). De plus, il a été rapporté que le C3a, anaphylatoxine issue du clivage du C3, constituait un ligand de haute affinité pour RAGE. Les effets du C3a ne sont cependant décrits que pour sa liaison au C3aR (C3a receptor) tandis que les conséquences endothéliales induites par la liaison RAGE/C3a restent inconnues. **Nous avons ainsi émis l'hypothèse que le RAGE puisse constituer l'un des liens unissant les acteurs hème-complément-activation endothéliale.**

L'objectif de ce projet était donc de préciser la place du RAGE dans le développement d'endothélites aiguës hème/complément-dépendantes, telles que le SHU atypique et le syndrome catastrophique des anti-phospholipides que nous avons choisi d'étudier plus spécifiquement du fait d'un accès privilégié aux données et échantillons de patients ayant présentés et/ou suivis pour ces pathologies.

Résultats

Caractérisation de la liaison RAGE-hème : RAGE est un récepteur de l'hème

Etude d'interaction : Deux formes de RAGE ont été utilisées pour l'étude de son interaction avec l'hème: une protéine d'origine commerciale (hRAGE-Fc, R&D Systems) ainsi qu'une protéine recombinante du domaine extracellulaire de RAGE, le VC1C2 (collaboration avec le Dr L. Yatime, UMR 5235, Université de Montpellier), et les domaines purifiés VC1, V et C2. Nous avons utilisé comme contrôle la protéine IgG1 Fc (R&D Systems). La BSA glyquée avec de la CML était utilisée comme ligand contrôle du RAGE.

Dans un premier temps, nous avons étudié l'interaction hème-RAGE en spectrométrie d'absorbance (collaboration avec le Dr J. Dimitrov, UMR_S 1138, Centre de Recherche des Cordeliers) et retrouvé des arguments pour l'existence d'une liaison. Ces résultats étaient corroborés par une chromatographie d'exclusion stérique réalisée dans le cadre de notre collaboration avec le Dr Yatime. Dans un deuxième temps, nous avons procéder à une étude d'interaction en SPR, qui confirmait une liaison dose-dépendante hème-hRAGE avec une affinité de l'ordre du micromolaire (**figure 1**), alors que l'hème ne liait pas la protéine contrôle IgG1-Fc. L'utilisation de domaines purifiés de RAGE (VC1C2, VC1, V et C2) nous a permis de mettre en évidence que le site de liaison de l'hème se situait sur le domaine V. Afin de caractériser plus en détail cette liaison, l'utilisation de différentes protoporphyrines (Zinc(II)PP, Manganèse(III)PP, Cobalt(III)PP, Magnésium(II)PP) et des molécules contenant du Fer (Fer(III)phtalocyanine, ferroine) nous a permis de mettre en évidence que le RAGE semblait interagir avec les molécules contenant du Fer et d'autres métaux de transition.

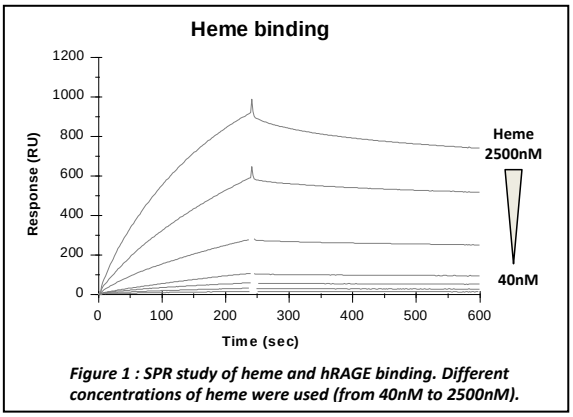

Figure 1 : SPR study of heme and hRAGE binding. Different concentrations of heme were used (from 40nM to 2500nM).

<u>*Etude sur modèle murin*</u> : Des souris C57BL/6 invalidées ou non pour RAGE ont été traitées à J0 par injection intrapéritonéale (IP) d'hème (100µmol/kg) ou par PBS. A J1, les souris étaient sacrifiées et différents organes récupérés (reins, cœur, poumons, rate). L'expression de *RAGE* était étudiée en RTq-PCR, ainsi que l'expression de marqueurs de l'inflammation au niveau pulmonaire (*TNFα*, *IL1β*, *IL6*, *facteur tissulaire*), organe exprimant le plus fortement RAGE.

L'injection IP d'hème induisait chez les souris WT une augmentation de l'expression de *RAGE*, mesurée en RTq-PCR, dans les reins, le cœur et la rate. En revanche, dans les poumons, organes exprimant le plus fortement *RAGE* en condition homéostatique, le niveau d'expression restait stable. Compte tenu de ces résultats, le tissu pulmonaire était ciblé pour l'analyse des effets pro-inflammatoires de l'hème et leurs comparaisons entre souris WT et RAGE$^{-/-}$. Chez les souris WT, l'injection d'hème comparativement au PBS, induisait une augmentation de l'expression de *TF,* d'*IL1β* et de *TNFα* de respectivement ~4.5, ~2.5, ~2. Leur expression basale après injection de PBS n'était pas différente chez les souris RAGE$^{-/-}$ par rapport aux souris WT. Le traitement par l'hème induisait chez les souris RAGE$^{-/-}$ une augmentation moindre de l'expression d'*IL1β, TNFα* et *TF* (**figure 2**).

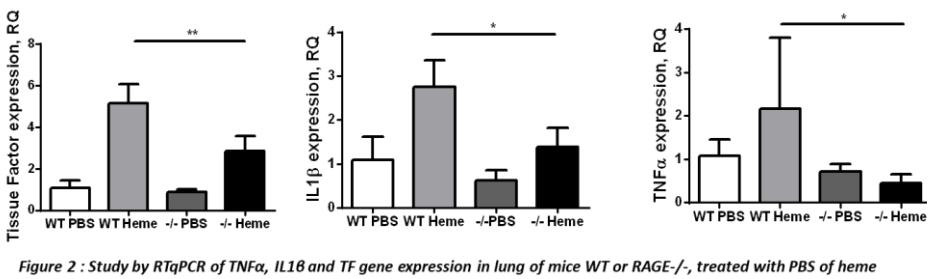

Figure 2 : Study by RTqPCR of TNFα, IL1β and TF gene expression in lung of mice WT or RAGE-/-, treated with PBS of heme (100µmol/kg). n=3-5 per groups.

Pour comprendre les mécanismes de l'effet protecteur de l'invalidation du RAGE, nous avons choisi d'étudier deux voies de signalisation activées par l'hème et le RAGE : ERK1/2 et Akt. Le rapport phospho-ERK: ERK-total était faiblement modifié par l'injection d'hème chez les souris WT (~1,5 augmentation du nombre de plis), alors qu'il diminuait chez les souris RAGE$^{-/-}$. Après traitement par l'hème, le rapport phospho-ERK : ERK-total chez les souris RAGE$^{-/-}$ était en effet ~0,5 fois inférieure à celui des souris WT. Des résultats similaires étaient observés avec la voie Akt. Chez les souris WT traitées à l'hème, le rapport phospho-Akt : Akt-total augmentait d'environ 1,1 fois par rapport aux souris contrôle, alors que le traitement à l'hème induisait une diminution significative du rapport phospho-Akt : Akt-total chez les souris RAGE$^{-/-}$ (~0,29 fois).

Conclusions : Nous avons découvert que le RAGE était un récepteur de l'hème, et identifié que le site de liaison se trouvait sur le domaine V. A l'aide d'un modèle murin invalidé pour le RAGE et traité +/- par l'hème, nous avons mis en évidence que i) l'invalidation de RAGE avait un effet protecteur en cas d'exposition à l'hème, marqué par une diminution de l'expression de gènes de l'inflammation (IL1β, TNFα) et du facteur tissulaire au niveau pulmonaire, organe exprimant le plus fortement RAGE, ii) l'hème activait la phosphorylation des voies ERK1/2 et Akt via le RAGE.

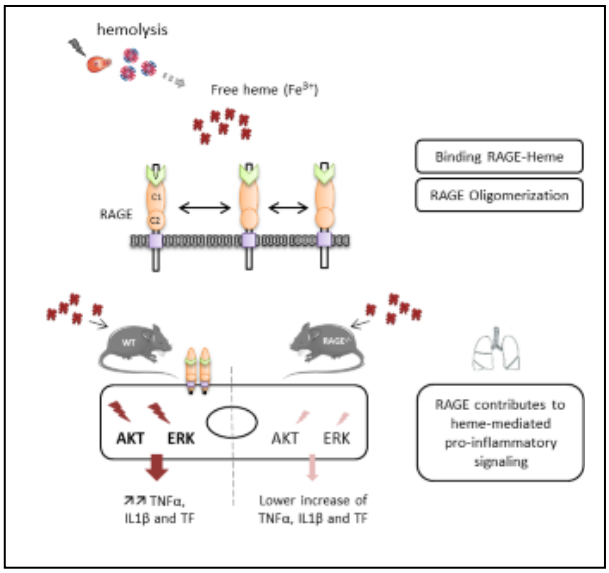

II- Autres résultats

- Modulation de l'expression génique et membranaire du RAGE sous l'influence de l'hème avec augmentation significativement plus importante sur les cellules endothéliales glomérulaires comparativement aux HUVEC et aux HMEC, rendant compte d'un rôle possible de RAGE dans le tropisme d'organe de certaines maladies vasculaires.
- Mise en évidence d'une liaison RAGE-aPL, dans certaines conditions, avec une affinité supérieure à celle des contrôles (RAGE-IgG témoins). Mise au point d'un modèle murin de dysfonction endothéliale induite par les aPL. Dans ce modèle, nous avons observé une diminution des marqueurs de dysfonction endothéliale (analyse fonctionnelle de la vaso-relaxation artérielle endothélium-dépendante) chez la souris RAGE$^{-/-}$, ce qui pourrait suggérer une implication de ce récepteur dans la physiopathologie du SAPL.

Encadrements

Ce projet a été initié dans le cadre d'**une thèse d'Université (EDBSL, Lille) réalisé entre 2015 et 2018 par le Dr Olivia May**, alors CCA dans le service de Néphrologie du CHU de Lille. Olivia a pu dégager plusieurs mécanismes susceptibles de participer au tropisme endothélial glomérulaire du SHU et a travaillé sur la liaison RAGE-hème (points I- des résultats cités ci-dessus).

Concernant le modèle du SAPL, nous disposons de données préliminaires (point II- des résultats cités ci-dessus) que nous avons prévu de développer à travers une **thèse d'Université conduite par le Dr Cécile Yelnik** (MCU-PH, Thérapeutique), projet qui sera développé dans les perspectives (détails, p.38).

Financements

- **2018** : Allocation de recherche par l'AIRG (Association pour l'information et la recherche sur les maladies rénales génétiques), 20 k€ ;
- **2015** : Allocation de recherche de la Société de Néphrologie « « Etude des conséquences endothéliales de l'interaction C3a/RAGE : Implication du RAGE dans l'acquisition du phénotype endothélial prothrombotique complément-dépendant », 20 k€.

Valorisation

Manuscrits :

- The receptor for advanced glycation end products is a sensor for cell-free heme. May O, Yatime L, Merle N, Delguste F, Howsam M, Daugan M, Billamboz M, Ghinet A, Lancel S, Dimitrov JD, Boulanger E, Roumenina L*, Frimat M*. in revision in FEBS (IF: 4,8)
- Hemolysis Derived Products Toxicity and Endothelium: Model of the Second Hit. **Frimat M**, Boudhabhay I, Roumenina LT. Toxins. 2019 Nov 13;11(11). pii: E660. doi: 10.3390/toxins11110660. Review. (IF: 3,3)
- Endothelium structure and function in kidney health and disease. Jourde-Chiche N, Fakhouri F, Dou L, Belien J, Burtey S, **Frimat M**, Jarrot P, Kaplanski G, Le Quintrec M, Pernin V, Rigothier C, Sallée M, Frémeaux-Bacchi V, Guerrot D and Roumenina L. Nat Rev Nephrol. 2019 Feb;15(2):87-108. doi: 10.1038/s41581-018-0098-z (IF :14.1)
- Heme Drives Susceptibility of Glomerular Endothelium to Complement Overactivation Due to Inefficient Upregulation of Heme Oxygenase-1. May O, Merle NS, Grunenwald A, Gnemmi V, Leon J, Payet C, Robe-Rybkine T, Paule R, Delguste F, Satchell SC, Mathieson PW, Hazzan M, Boulanger E, Dimitrov JD, Fremeaux-Bacchi V, **Frimat M***, Roumenina LT*. Front Immunol. 2018 Dec 20;9:3008 (IF: 6,4).
- Characterization of Renal Injury and Inflammation in an Experimental Model of Intravascular Hemolysis. Merle NS, Grunenwald A, Figueres ML, (…), Chauvet S, Daugan M, Knockaert S, Robe-Rybkine T, Noe R, May O, **Frimat M**, Brinkman N, Gentinetta T, Miescher S, Houillier P, Legros V, Gonnet F, Blanc-Brude OP, Rabant M, Daniel R, Dimitrov JD, Roumenina LT. Front Immunol. 2018 Mar 1;9:179. doi: 10.3389/fimmu.2018.00179. eCollection 2018.
- Endothelial cells: source, barrier and target of defensive mediators. Roumenina L, Rayes J, **Frimat M** and Fremeaux-Bacchi V. Immunol Rev. 2016 Nov;274(1):307-329 (IF: 10,2)

Communications orales *en congrès nationaux et internationaux : 5*
Communications affichées *en congrès nationaux et internationaux : 2*

Recherche clinique

Parallèlement à ces projets conduits au sein du laboratoire, j'ai pu participer à plusieurs travaux de recherche clinique ciblant plus particulièrement des pathologies avec atteintes microvasculaires rénales.

Pathologies vasculo-rénales au cours de la grossesse

Nous avons réalisé plusieurs travaux ciblant la grossesse et le post-partum. En effet, la grossesse, même normale, conduit à de nombreuses adaptations endothéliales (présence d'une endothéliose glomérulaire, activation du complément, élévation des taux plasmatiques de FvW, augmentation de la capacité à générer de la thrombine) et ces modifications participent à augmenter l'expression de certaines pathologies vasculaires en particulier en cas de facteurs de susceptibilité sous-jacents.

1- En 2015, nous avons rapporté une série de 18 patientes ayant présenté une **nécrose corticale rénale du post-partum**, tandis même que cette complication obstétricale avait pratiquement disparu dans les pays à haut revenu. Toutes les patientes avaient présenté une hémorragie du post-partum sévère. Une instabilité hémodynamique et une coagulation intravasculaire disséminée étaient identifiées chez 5 et 11 patients, respectivement. Six mois après l'accouchement, 8 patientes restaient dépendantes de la dialyse et aucune n'avait retrouvé une fonction rénale normale. La durée d'exposition à l'acide tranexamique, un inhibiteur de la fibrinolyse, était significativement plus longue chez les femmes dont le taux de filtration glomérulaire estimé restait inférieur à 15 ml/min (7,1±4,8 heures contre 2,9±2,4 heures, p=0,03).

Ce travail à but descriptif a également eu pour volonté de souligner les effets endothéliaux d'un cumul d'agression (hypovolémie sévère due à une hémorragie massive, utilisation concomitante de concentrés de fibrinogène, CIVD et coagulopathie complexe liée à la grossesse), circonstances dans lesquelles l'inhibition prolongée de la fibrinolyse pourrait avoir été délétère. Outre de souligner le caractère multifactoriel (théorie des hits multiples) de ces nécroses corticales rénales, ce travail a plaidé en faveur d'une utilisation sous forme de bolus de l'acide tranexamique en particulier dans ces situations cliniques où l'insuffisance rénale est fréquente (modalités de prescription proposées dans l'essai WOMAN : *Lancet. 2017 May 27;389(10084):2105-2116. doi: 10.1016/S0140-6736(17)30638-4*.).

Valorisation: "Renal Cortical Necrosis in Postpartum Hemorrhage: A Case Series. ***Frimat M****, Decambron M, Lebas C, Moktefi A, Lemaitre L, Gnemmi V, Sautenet B, Glowacki F, Subtil D, Jourdain M, Rigouzzo A, Brocheriou I, Halimi JM, Rondeau E, Noel C, Provôt F, Hertig A. Am J Kidney Dis. 2016 Jan 16. pii: S0272-6386(15)01496-1. (IF :6,3)"*

2- Nous avons également caractérisé dans le cadre d'un travail rétrospectif et monocentrique notre population de **patientes greffées rénales présentant une ou plusieurs grossesses évolutives au**

cours de leur suivi. Les grossesses en transplantation rénale sont plus risquées, en particulier en termes d'évènements vasculo-rénales (prééclampsie ≈ 37%, RR ≈ 7 par rapport à une population générale américaine). Elles sont ainsi encadrées de recommandations, parmi lesquelles l'adaptation des posologies d'anticalcineurines (ACN) à leurs résiduels sériques qui diminuent per-partum sans preuve cependant d'une baisse d'efficacité thérapeutique. Nous avons étudié les caractéristiques et le devenir de 34 grossesses au cours desquelles les posologies d'ACN n'ont pas été modifiées. Nous avons confirmé dans ce contexte une diminution des tacrolémies et ciclosporinémies résiduelles moyennes de 48 et 55% (nadir : 30 semaines d'aménorrhée, SA). Aucun rejet aigu n'était observé per-partum. Une allo-immunisation anti-HLA était identifiée chez 6 patientes (23%) à 1 an et 15 (55%) à 4 ans, de type Donor Specific Antigen dans respectivement 1 et 3 cas. Huit patientes (30%) avaient une dysfonction du greffon à 2 ans, rattachée à un processus immunologique, à une toxicité des ACN ou sans cause identifiée chez respectivement 2, 2 et 4 d'entre elles. Hypertension artérielle gravidique et pré-éclampsie survenaient chez 13 (38%) et 6 (18%) des patientes. Le poids de naissance moyen était de 2447 grammes (500-3650) et le terme moyen de 35.6 (±3.7) SA. Une prématurité et une hypotrophie étaient rapportées dans 44% et 46% des cas.

Ce travail suggère que l'absence de majoration per-partum de la posologie des ACN n'est pas pourvoyeuse de rejet aigu ou de dysfonction chronique du greffon, et le taux de complications vasculo-rénales apparait plus bas que dans la littérature. Nous souhaiterions maintenant comparer notre population à celle de patientes greffées rénales avec grossesses évolutives chez qui les posologies d'ACN n'ont pas été modifiées.

Valorisation en cours: « Renal and obstetrical outcomes of pregnancy in kidney transplant under calcineurin inhibitors. R. Lenain, J. Perche, F. Glowacki, P. Subtil, F. Provot, P. Deruelle, C. Samaille, M. Hazzan, ***M. Frimat*** *»*

3- Par ailleurs, dans la continuité de ces travaux, je suis **référente pour le CHU de Lille du registre CRISTEL** (registre franco-belge) qui a pour but de recueillir de façon sécurisée les données relatives aux grossesses (planifiées, non planifiées, aboutissant ou n'aboutissant pas) survenant chez des patientes transplantées d'un organe solide.

Microangiopathies Thrombotiques

Le CHU de Lille est centre de compétence des microangiopathies thrombotiques (MAT) sous la tutelle locale du Dr François Provôt. Dans ce contexte, notre service est particulièrement sensibilisé à ces pathologies.

1- En 2017, j'ai participé à un travail, conduit par le Pr Julien Zuber (Hôpital Necker, AP-HP), évaluant **l'impact d'une prophylaxie par eculizumab en transplantation rénale**. En effet, le syndrome

hémolytique et urémique atypique (SHUa) est depuis longtemps associé à des taux élevés de récidive post-transplantation et de perte du greffon. Fin 2011, l'utilisation d'une prophylaxie hautement individualisée basée sur le blocage du complément pour prévenir les récidives du SHUa après transplantation a été recommandée à l'échelle nationale. Notre objectif était d'évaluer l'impact de cette stratégie sur le pronostic des transplantations rénales. Pour ce faire, une étude multicentrique a été menée à partir du registre national des SHUa. Tous les patients adultes atteints de SHUa ayant bénéficié d'une analyse du complément et d'une transplantation rénale depuis le 1er janvier 2007 étaient inscrits. Au total, 126 transplantations rénales réalisées chez 116 patients ont été inclus et 43 (34%) ont été marquée par une récidive de SHUa. 52 transplantations rénales, dont 39 à haut risque de récidive, ont été réalisées sous couverture d'une prophylaxie par l'eculizumab. Cette stratégie thérapeutique a été indépendamment associée à un risque moins élevé de récidive (HR=0,06 ; p<0,0001) et à une survie plus longue des greffons (HR=0,195 ; p=0,04).
Cette étude soutient ainsi l'utilisation de la prophylaxie par eculizumab sur la base d'une stratification du risque en pré-greffe. Il est intéressant de noter qu'en parallèle de la mise en œuvre de cette stratégie, la proportion de greffes a fortement augmenté chez les patients en insuffisance ranale chronique terminale liée à un SHUa, de 46,2 à 72,3 % entre 2012 et 2016.

*Valorisation: "The use of highly individualized complement blockade revolutionized the posttransplant clinical outcomes and renal epidemiology of atypical HUS. Zuber J, **Frimat M**, Caillard S, Kamar N, Gatault P, (…), Rondeau E, Le Quintrec M, Frémeaux Bacchi V. J Am Soc Nephrol. 2019 Oct 1. pii: ASN.2019040331. (IF : 8, 6)"*

2- Nous poursuivons avec le Dr Viviane Gnemmi (anatomopathologie, CHU Lille) un travail de **corrélation anatomo-clinique ciblant l'activation du complément dans les MAT sur rein natif**. Brièvement, si de nombreuses causes peuvent être à l'origine de MAT rénales, l'identification d'anomalies de la régulation du complément souligne le rôle central de ce système. En l'absence d'études spécifiques, l'analyse d'immunomarquages témoignant de l'activation du complément sur la biopsie rénale n'est que rarement incluse dans la démarche diagnostique et thérapeutique. Les résultats d'un travail préliminaire réalisé au CHU de Rouen (données non publiées) démontrent que des dépôts artériolo-glomérulaires de C4d et C5b-9 sont fréquents lors des MAT, et les différences observées pourraient témoigner des mécanismes physiopathologiques en jeu, variables selon l'étiologie sous-jacente. L'objectif de ce travail est d'étudier, sur une large cohorte de patients atteints de MAT sur rein natif, la présence de témoins histologiques de l'activation du complément par ses différentes voies, et d'analyser ces dépôts en fonction de la présentation anatomo-clinique et de l'étiologie retenue. Il s'agit d'une étude multicentrique (Lille, Rouen, Tenon), rétrospective, incluant les patients diagnostiqués avec une MAT sur rein natif entre 2005 et 2018 avec une réserve tissulaire paraffinée disponible. Les données clinico-biologiques ont été recueillies au temps de la biopsie rénale et jusqu'au dernier suivi disponible. En plus de l'étude en microscopie optique, des immunomarquages anti C3, C4, C1q, C4d et C5b-9 ont été réalisés. Une analyse semi-quantitative des lésions élémentaires

histologiques, de l'intensité et de la disposition des dépôts a été réalisée de manière centralisée en aveugle par rapport aux données cliniques.

Nous espérons ainsi apporter un éclairage sur l'intérêt potentiel de l'étude de l'activation du complément sur la biopsie rénale pour orienter le bilan diagnostique et la thérapeutique des MAT sur rein natif.

Ces travaux ont pu être réalisés grâce aux étudiants activement impliqués dans ces différents projets (cf. activités d'encadrement, p.28) et avec l'aide de différentes collaborations développées ces dernières années parmi lesquelles les plus actives sont avec :

1- **Le service d'anatomopathologie rénale du CHU de Lille** (Dr V Gnemmi, Dr JB Gibier, Pr MC Coppin). Les données issues des biopsies rénales de nos patients constituent souvent un point de départ ou de d'enrichissement de nos travaux de recherche clinique ou fondamentale et à ce titre, les échanges avec nos collègues en anatomopathologie rénale sont très fréquents ;

2- **L'équipe « complément et maladies »** (INSERM UMR872) avec les Dr Roumenina et Dr Véronique Frémeaux-Bacchi au Centre de Recherche des Cordeliers. Dans les suites de ma thèse d'Université, nous avons continué de travailler en étroite collaboration. Actuellement, nos champs de recherche communs ciblent plus spécifiquement l'hème dans le cadre d'un projet développé dans les perspectives (détails, p.38) ;

3- **L'équipe « Fibrose, senescence et cancer »** (CNRS - UMR-S 1277 Inserm) avec les Pr Glowacki et Dr Cauffiez à Lille. Cette collaboration s'est développée dans le cadre du projet relatif à l'implication de RAGE dans le vieillissement rénal ;

4- **Le groupe de travail national Rein-Endothelium** (French Renal ENDothelial Society). Depuis 2016, nous avons développé, en collaboration avec plusieurs équipes travaillant sur l'endothélium et les maladies rénales, un réseau national de chercheurs (Bordeaux, Lille, Marseille, Montpellier, Nantes, Paris, Rouen) ayant pour thématiques communes la cellule endothéliale agressée ou activée par différents agents (complément, immunité, hème, anomalies génétiques, toxines urémiques, etc.) au cours de maladies rénales (MAT, maladie rénale chronique, maladies de système, etc.). Nos différentes équipes ont développé des approches méthodologiques variées, et l'intérêt de ce groupe est notamment de les mettre en commun et de croiser nos thématiques.

Activité d'encadrement

Activités d'encadrement au sein de l'équipe de recherche

Mes activités d'encadrement au sein de l'équipe du Pr Boulanger (U995 puis U1167) s'inscrivent dans le cadre des projets, déjà détaillés précédemment, étudiant l'implication de RAGE dans le vieillissement rénal et vasculaire accéléré (axe 1) ou dans l'activation endothéliale complément/heme-dépendante (axe 2).

Depuis novembre 2014, j'ai ainsi encadré **deux étudiants en Master 1**, **trois étudiants en Masters 2** (+ 1 co-encadrement dans la filière STAPS), et j'ai participé ou participe actuellement à **l'encadrement de deux thèses d'Université** (dont l'une soutenue en octobre 2018).

Projets et étudiants encadrés :

Axe 1 : Implication de RAGE dans le vieillissement rénal et vasculaire accéléré

Master2

- **Valentine Quersin** (Interne Néphrologie) Encadrement 100% Financement : Année recherche. EDBSL, Université de Lille. « **Modifications fonctionnelles, structurelles et moléculaires rénales induites par les produits de la glycation alimentaire** » Note : 16/20	2014-2015
- **Cécile Lemoine** (Interne Néphrologie) Encadrement 100% Financement : bourse de la Société française de Néphrologie. M2 Biologie du vieillissement, Université Paris Diderot. « **Effets des produits de glycation avancée sur le vieillissement endothélial rénal** » Note : 15/20	2015-2016

Axe 2: Implication du RAGE dans l'activation endothéliale complément/heme-dépendante

Master 1

- **Cécile Lemoine** (Interne Néphrologie) Encadrement 100% EDBSL, Université de Lille. « **Blocage du RAGE endothélial au cours du SAPL** ».	07-2015
- **Marie Gilbert** (Interne Néphrologie) Encadrement 100% EDBSL, Université de Lille. « **Implication du RAGE dans l'activation du complément et l'acquisition d'un phénotype endothélial prothrombotique induits par hémolyse** »	07-2016

Master2

- **Timothée Laboux** (Interne Néphrologie) — 2019-2020
  Encadrement 50% (co-encadrement avec le Dr MAANAOUI, CCA Néphrologie)
  Financement : Année recherche.
  EDBSL, Université de Lille. « **Rôle des glycosaminoglycanes du glycocalyx endothélial glomérulaire dans la physiopathologie du syndrome hémolytique et urémique atypique** »
  Note : 16/20

Thèse d'Université

- **Olivia May** (CCA Néphrologie) — 2015-2018
  Encadrement 50%
  Codirection : Pr Boulanger, U995 Lille et Dr Roumenina, U872 CRC Paris.
  EDBSL, Université de Lille « **Etude du tropisme rénal du syndrome hémolytique et urémique atypique : susceptibilité endothéliale glomérulaire à l'hème et découverte de RAGE comme un nouveau récepteur de l'hème** ».
  Soutenue le 30 octobre 2018

- **Cécile Yelnik** (MCU-PH, medecine interne) — 2019-2022
  Encadrement : 50%, codirection avec le Pr Lambert
  EDBSL, Université de Lille « **Syndrome des anti-phospholipides : Etude des déterminants de ses variants phénotypiques** »

Activités d'encadrement au sein du service de Néphrologie, CHU Lille

En parallèle de mes activités au sein de l'équipe de recherche, je participe à l'encadrement pédagogique des internes et étudiants en formation dans le service de Néphrologie à travers différents projets.

1. Depuis 2014, j'ai encadré **2 internes pour leur thèse d'exercice et 5 pour leur mémoire de DES de Néphrologie** :

Encadrements de Thèses de Médecine et de Mémoires de DES de spécialité:

- **Olivia May** : « Analyse des propriétés de protection contre l'activation du complément et de thrombo-résistance de l'endothélium rénal » — 10.2014
- **Juliette Perche** : « Evolution des grossesses menées sous anticalcineurines en transplantation rénale » — 01.2016
- **Anne-Sophie Vasseur :** « Sténose de l'artère du greffon : à propos de 24 cas » — 03.2016
- **Anne Grunenwald** : « Etude de l'activation du complément sur cellules endothéliales en conditions hémolytiques » — 03.2016
- **Valentine Quersin** : « Conséquences rénales d'une alimentation riche en produits de la glycation avancée (AGEs) et implication du RAGE » — 10.2016
- **Cécile Lemoine** : « Influence des produits issus de la glycation avancée sur le vieillissement endothélial glomérulaire » — 06.2017
- **Mehdi Maanaoui :** « Caractérisation de la matrice rénale décellularisée en vue d'une recellularisation par cellules IPS » — 10.2017

2. D'autre part, nous avons accueilli pour la première fois cette année une étudiante, Marie Thuaudet, inscrite dans le parcours « APAS, Activité Physique Adaptée et Santé ». **Je l'ai encadré pour son stage pratique de Master 2 autour d'un projet sur l'activité physique chez les patients pris en charge en hémodialyse chronique intermittente.**

Projet : Les bénéfices de l'activité physique (AP) en dialyse sont maintenant bien connus. Plusieurs méta-analyses (Mansueto Gomes Neto, 2018 ; Nada Salhab, 2019 ; Chung, 2016) rapportent que l'exercice intra-dialytique 30 minutes 2 à 3 fois par semaine pendant au moins ≥ 8 semaines améliore la condition physique, les capacités fonctionnelles et la qualité de vie. Les exercices aérobies sont le plus souvent pratiqués sur des ergocycles adaptés, dont le coût d'achat peut constituer une limite à la mise en place de tels programmes dans les centres de dialyse. Or, des exercices de renforcement musculaire peuvent aussi être effectués *via* des contractions concentriques et excentriques à l'aide d'haltères, de bandes élastiques épaisses, de sangles de chevilles lestées ou avec l'intervenant qui exerce une force opposée au mouvement.

Ce projet avait pour but de comparer rétrospectivement deux modalités d'entrainement intra-dialytique, l'une associant pédalage sur ergocycle et renforcement musculaire (population UDM SANTELYS), et l'autre proposant uniquement du renforcement musculaire (population UDM et Centre lourd, CHR). Les capacités fonctionnelles, la fragilité, la qualité de vie ont été évaluée dans les deux semaines précédant l'initiation du programme d'APA (02/2020, S-2->S0). Il était prévu que les patients inclus soient réévalués au terme de 8 semaines d'APA (05/2020, S9->10).

A

Variables	Groupe 1 Santélys (n = 77)	Groupe 2 CHR (n = 19)
TDM6 (mètres)	187,6 ± 150,8	240,1 ± 109,6
Score SF-12 physique	35 ± 11,1	32,8 ± 8,2
Score SF-12 mental	40,7 ± 8,9	43,2± 11,3
Score HAD anxiété	8 ± 3,4	8,2 ± 3,8
Score HAD dépression	7,6 ± 4	6,3 ± 4,4
Score estime de soi Rosenberg	28,8 ± 4,7	32,3 ± 5,3
Score Niveau AP	16,7 ± 7,2	11 ± 8,9

Figure 1: Résultats issus du travail de M2 (STAPS) de Marie THUAUDET

A) Caractéristiques des deux populations (modalités d'entrainement différentes)

B) Evaluation de la satisfaction des patients par auto-questionnaire

B

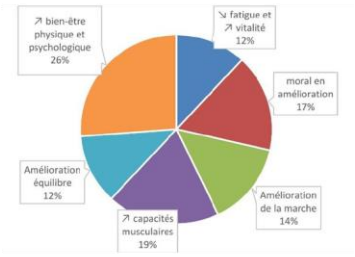

Malheureusement le contexte sanitaire n'a pas permis la finalisation de ce projet. Le mémoire a été soutenu avec les données de caractérisation initiale des deux populations associées à une évaluation du ressenti du patient à mi-programme par auto-questionnaire (**figure 1**).

Ce travail n'a pas pu aboutir dans sa forme prévue mais il est à l'origine d'une collaboration avec la Faculté des Sciences et des Sports (Dr DAUSSIN, MCU) et l'association SANTELYS et d'un travail actuel sur un projet d'évaluation de l'APA dans la population MRC que nous espérons pouvoir concrétiser dans le cadre d'une thèse d'Université en cotutelle STAPS-Néphrologie (candidate : Marie THUAUDET).

3. Enfin, dans le cadre des stages réalisés en anatomopathologie ouvert aux internes de Néphrologie depuis 2016 (1/an), **nous nous efforçons d'élaborer avec le Dr Viviane GNEMMI (MCU-PH, service d'anatomopathologie) des projets spécifiques de néphro-pathologie pour chacun des internes passant sur ce terrain de stage.**

Interne	Projet	Valorisation
Anne Grunenwald (2016)	Mise au point du marquage HO-1 et Thrombomoduline sur biopsies rénales 10.2014	*Données utilisées dans : May O, Merle NS, Grunenwald A, (…) Gnemmi V, (…), **Frimat M***, Roumenina LT*. Front Immunol. 2018 Dec 20;9:3008. (IF: 6,4)*
Elise Bouderlique (2017)	Relecture des biopsies rénales de patients avec lésions de MAT	*Travail collaboratif avec le Pr FRANCOIS (CHU Rouen) et le Pr BUOB (APHP, Tenon) manuscrit en préparation*
Nicolas Wayolle (2018)	Relecture des biopsies rénales des patientes avec vascularites à ANCA	*Données utilisées dans : Bitton L, Vandenbussche C, Wayolle N, (…), **Frimat M**, (…), Gnemmi V.J Nephrol. 2020 Jan 8. (IF : 2,7)*
Amandine Ydée (2019)	Mise au point du marquage JM403 (Glycocalyx) sur biopsies rénales	*Travaux complémentaires en cours (M2 Recherche, Timothée Laboux)*

Perspectives de recherche

Objectifs principaux

Mes perspectives de recherche restent centrées sur la thématique « maladies rénales et endothélium ». S'agissant d'une thématique large, mes projets continueront de cibler plus particulièrement les microangiopathies thrombotiques, le syndrome des anti-phopholipides et les vasculopathies liées à l'insuffisance rénale chronique, profitant dans les trois cas d'un accès privilégié à des données ou échantillons issus de cohortes de patients déjà constituées. Nous poursuivrons l'étude, dans ces modèles, des mécanismes d'activation endothéliale et d'accélération du vieillissement vasculaire et rénal en ciblant notamment le rôle du RAGE dans ces processus.

Cet objectif est en adéquation avec la restructuration de notre équipe de recherche issue de la récente révision quinquennale. En effet, depuis janvier 2020, l'équipe du Pr Boulanger a rejoint l'unité INSERM U1167 dirigé par le Pr Amouyel sur un projet général dédié au vieillissement et à ses mécanismes et au sein duquel le RAGE tient une place centrale. Les objectifs annoncés de notre équipe, qui s'enrichissent à l'occasion de cette restructuration de membres spécialisés dans l'étude de la dysfonction mitochondriale et dans le drug design, se structurent autour des 3 axes suivants :

1- To dissect the metabolic impact of glycation on aging and its influence on inflammaging
2- To study RAGE-Ligand axis in chronic and acute inflammation
3- To develop drug discovery approaches to counteract RAGE activation induced inflammaging

Mes perspectives de recherche actuelles s'inscrivent plus spécifiquement dans l'axe 2. J'interviendrai de façon plus indirecte dans les axes 1 et 3 que je vais donc peu détailler.

Brièvement, **l'axe 1** cible plus particulièrement les AGEs et nous bénéficions dans l'équipe de l'expertise du Pr Tessier et du Dr Howsam pour analyser le processus de glycation. Les AGEs ont tenu un rôle prépondérant dans mon approche initiale à mon arrivée dans le laboratoire (*impact des AGEs dans le vieillissement rénal*). Cependant, les travaux conduits en parallèle ont mis en avant l'intérêt d'autres ligands de RAGE susceptibles de favoriser le vieillissement médié par l'inflammation. Parmi eux, certains tel que l'hème, s'appliquent plus facilement à des modèles d'inflammation aigue et à l'étude, dans un second temps, des conséquences vasculaires à moyen et long terme de ces processus aigus.

Ainsi, la place consacrée aux AGEs dans mes projets s'est significativement réduite si ce n'est à travers nos échanges intergroupes et la collaboration prévue autour de la cohorte INTEGRA. Il s'agit d'une cohorte qui se développe actuellement au sein du CHU de Lille dans le cadre d'un FHU, projet auquel je prends part pour la composante néphrologique. Cette cohorte se compose de patients présentant un diabète, une obésité ou un syndrome métabolique avec à l'inclusion un interrogatoire détaillé, des prélèvements sériques, plasmatiques, urinaires ainsi que de phanères (ongles et cheveux). Ce dernier aspect nous intéresse tout particulièrement puisqu'en parallèle de la mise en place de ce FHU, le Pr Tessier et le Dr Howsam ont pu mettre au point une méthode de quantification des AGEs dans les ongles à partir de populations de sujets sains ou hémodialysés chroniques plus ou moins diabétiques. Un projet s'inscrivant dans le cadre d'une étude ancillaire et ayant pour but de corréler au sein de cette cohorte INTEGRA le niveau de glycation des ongles avec le devenir rénal est en cours d'élaboration.

Concernant l'axe 3, notre équipe s'est donc enrichie d'experts en chimie analytique et « Drug design » qui travaillent d'ores et déjà, sous la tutelle des Drs Alina Guinet et Christophe Furman au développement de molécules antagonistes de RAGE. Nous prévoyons de tester ces molécules et d'étudier ainsi l'impact d'une inhibition pharmacologique de RAGE sur nos différents modèles cellulaires et murins.

Axe 2- To study RAGE-Ligand axis in chronic and acute inflammation

Il s'agit de l'axe de travail sur lequel je souhaite concentrer mes projets au sein d'un groupe maintenant conduit par Steve Lancel (MCU) et comprenant, en plus des étudiants en M2 et en thèse, Chantal Fradin (MCU), le Pr Marc Lambert (PU-PH, Medecine interne), le Pr Raphael Favory (PU-PH, Réanimation) et le Pr Sébastien Preau (PU-PH Réanimation).

Cet axe de recherche est ou sera notamment alimenté *via* 4 projets que je vais détailler ci-dessous et qui auront, à divers degrés, pour but de répondre aux questions suivantes :

- *Quels paramètres modulent la liaison de RAGE à ses ligands et avec quelles conséquences fonctionnelles ?*

  Le RAGE tend à être reconnu aujourd'hui comme un PRR (Pattern recognition receptor) à travers sa capacité à lier différents PAMPs (pathogen associated molecular pattern) et DAMPs (danger associated molecular pattern). Nous souhaitons étudier les rapports de RAGE avec les autres récepteurs de l'immunité innée et en particulier les TLRs et définir dans quelles mesures ces interactions potentielles modulent l'impact en aval sur la signalisation intracellulaire et leurs conséquences proinflammatoires.

- *RAGE est-il un acteur de l'hétérogénéité d'expression phénotypique de certaines pathologies (MAT, SAPL, choc septique, vieillissement vasculaire)?*

  Dans le cadre de travaux conduits sur les MAT, nous avons identifié le système du complément et de l'heme-oxygenase comme des acteurs du tropisme endothélial rénal du syndrome hémolytique et urémique. Nous suspectons que RAGE puisse également être impliqué dans cette susceptibilité d'atteinte de certains lits vasculaires et souhaitons l'étudier dans différentes pathologies d'expression variable.

- *L'inhibition de RAGE constitue-t-elle une cible thérapeutique potentielle dans des modèles d'agression endothéliale aigue ?*

  Prenant en compte l'absence de spécificité connue de la signalisation intracellulaire de RAGE, nous étudierons si l'inhibition pharmacologique de ce récepteur s'accompagnera d'une diminution des marqueurs inflammatoires ou si elle sera compensée par l'action d'autres récepteurs.

A travers ces différentes questions, nous espérons améliorer la compréhension des mécanismes impliquant RAGE dans l'activation endothéliale et, conduisant à travers des processus inflammatoires et oxydatifs à un vieillissement vasculaire et rénal prématuré.

Projet 1- Caractérisation des processus de reconnaissance endothéliaux de l'hème et de ses mécanismes effecteurs

Background : L'hème libéré en cas d'hémolyse intravasculaire constitue, comme nous l'avons vu, une alarmine proinflammatoire dont la détection par l'endothélium reste encore mal caractérisée. Son seul récepteur membranaire endothélial connu est le TLR4, cependant des données préliminaires montrent, dans un modèle d'induction d'hémolyse intravasculaire, que l'atteinte rénale ainsi que l'expression d'une série de gènes liés à l'inflammation et l'activation endothéliale ne sont pas modifiés chez des souris TLR4$^{-/-}$, soulignant l'implication potentielle d'autres récepteurs d'hème, notamment au niveau rénal.

Nous travaillons en collaboration avec le Dr Lubka Roumenina (CRC, Paris) et le Dr Laure Yatime (Montpelier). Au sein de nos équipes, ont été identifiés deux nouveaux récepteurs membranaires de l'hème, en plus du TLR4. **Notre objectif** est de disséquer les mécanismes moléculaires de la reconnaissance de l'hème par ses différents récepteurs membranaires et d'étudier les interactions entre leurs voies de signalisation et le profil de réponse cellulaire induit (protecteur ou inflammatoire). Ce projet se décompose ainsi en 4 axes :

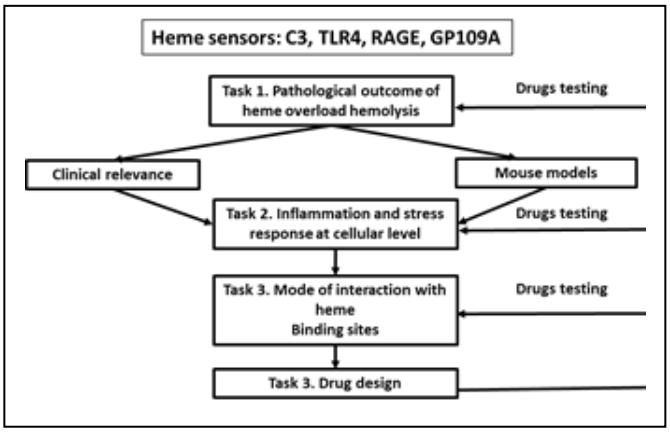

(1) identifier le rôle de chaque récepteur de l'hème (membranaire et plasmatique) sur les conséquences délétères de la surcharge en hème *in vivo*; (2) caractériser l'implication fonctionnelle de chaque récepteur dans l'inflammation et la réponse au stress au niveau cellulaire; (3) étudier le mode d'interaction de l'hème avec ses récepteurs du complément et de la membrane cellulaire ; (4) concevoir et évaluer l'efficacité thérapeutique de molécules ciblant ces récepteurs.

Dans le cadre de ce projet collaboratif, notre rôle à Lille est de caractériser **les interactions entre l'hème et le RAGE**.

Travaux en cours et résultats préliminaires :

<u>Partie 1</u> : Poursuite de la caractérisation de RAGE en tant que récepteur de l'hème

Nous avons montré que l'hème se liait au RAGE et induisait son oligomérisation (*article en révision*). Parrallèllement à ces travaux, nous avons étudié le complément en tant que système effecteur susceptible d'être impliqué par cette liaison hème-RAGE. En effet, il a été rapporté que le C3a, anaphylatoxine issue du clivage du C3, constituait un ligand de haute affinité pour ce récepteur (Ruan

et al, 2010). Cette interaction directe n'était cependant clairement décrite qu'en ELISA. En SPR, l'interaction RAGE-C3a n'était présentée qu'en présence d'oligonucléotides de type CpGA (oligonucléotides de cytosine-guanine non méthylé riche en ADN A). Nos premiers résultats obtenus dans le cadre du travail de thèse d'Olivia n'ont pas confirmé de liaison directe entre le RAGE immobilisé (hRAGE) et le C3a ou le C1q, autre protéine du complément décrite pour lier RAGE, et ce même à forte concentrations. Aucune liaison n'était non plus mise en évidence avec d'autres protéines du complément ou avec leurs formes désarginées (C3b, C3a désarginé, C5a, C5a désarginé), tandis qu'il était bien observé dans les mêmes conditions une interaction RAGE-CML (contrôle positif, **figure 1**).

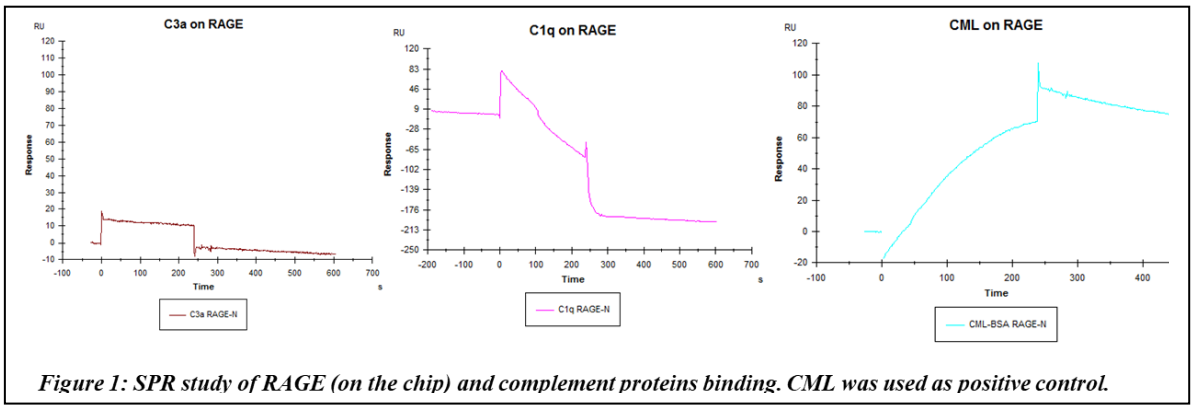

Figure 1: SPR study of RAGE (on the chip) and complement proteins binding. CML was used as positive control.

Par homologie avec les travaux de Ruan *et al* où la présence de CpGA était nécessaire à l'interaction RAGE-C3a et ayant préalablement montré que l'hème liait la fraction C3a de la protéine C3 (Frimat *et al*, 2013), nous avons émis l'hypothèse que l'hème puisse potentialiser une liaison RAGE-C3a. Nous avons confirmé cette hypothèse en montant qu'après liaison d'hème sur le RAGE immobilisé, plusieurs protéines du complément, en particulier le C1q, le C3a et sa forme désarginée liaient le complexe RAGE-hème avec une forte affinité. Le C5a et sa forme désarginée liaient le complexe RAGE-hème avec une affinité moindre tandis qu'il n'y avait pas de liaison entre ce complexe et le C3b, résultat en faveur d'une spécificité des liaisons précédentes (**figure 2A**). De façon intéressante, l'étude des interactions TLR4-hème-protéines du complément en SPR dans les mêmes conditions, montraient des liaisons de plus faible affinité (**figure 2B**).

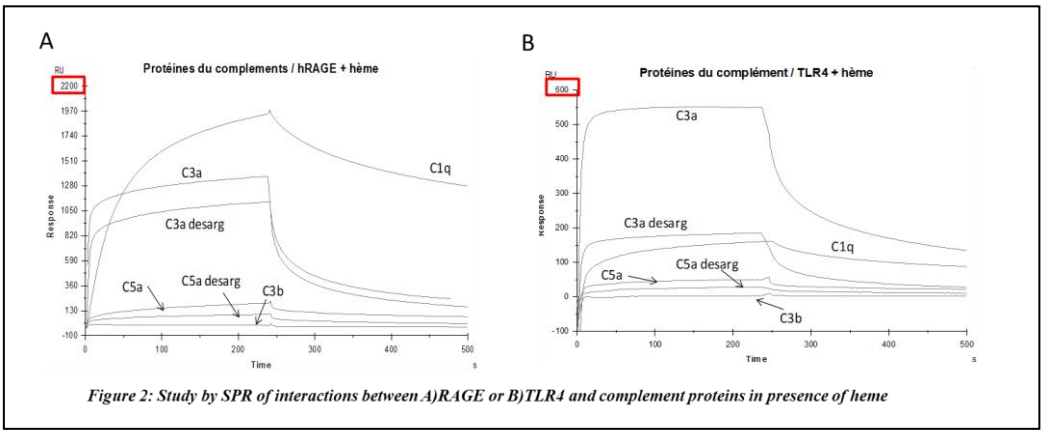

Figure 2: Study by SPR of interactions between A)RAGE or B)TLR4 and complement proteins in presence of heme

Nous avons étudié plus spécifiquement la liaison du C3a à RAGE et TLR4 et pu confirmer le caractère dose-dépendant de ces liaisons en présence d'hème. A concentration de C3a égale, la liaison de cette protéine à RAGE paraissait plus affine qu'à TLR4 (**figure 3**).

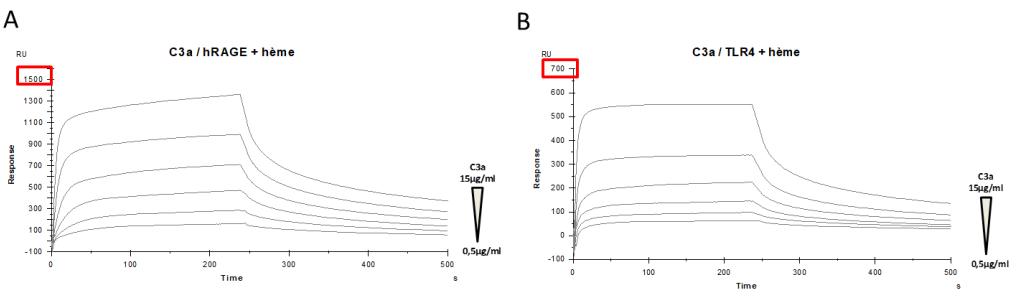

Figure 3: SPR study of C3a and A)RAGE or B)TLR4 binding. Different concentrations of C3a were used.

<u>Conclusions</u> : Nos travaux confirment une interaction entre RAGE et plusieurs protéines du complément, en particulier C1q et C3a, dans des conditions cependant spécifiques puisque la présence d'hème est nécessaire. Ainsi RAGE pourrait constituer un lien possible entre dérégulation de la voie alterne du complément et survenue d'une souffrance endothéliale observée dans le SHUa.

De façon intéressante, les liaisons de ces protéines envers RAGE paraissaient plus affines qu'envers TLR4. Cela ne présage cependant pas de plus fortes conséquences fonctionnelles et des travaux complémentaires sont nécessaires pour préciser les rapports entre ces deux récepteurs et les protéines du complément en particulier en condition hémolytique.

<u>Partie 2</u>. Étude fonctionnelle de la signalisation induite par l'interaction hème-RAGE

Nous travaillons actuellement à la mise au point d'un modèle cellulaire invalidé pour le RAGE. Il n'a pas été possible de le réaliser par siRNA. Nous avons pour objectif d'isoler des cellules endothéliales rénales (*Marelli-Berg et al., Journal of Immunological Methods, 2000*) de souris WT, RAGE $^{-/-}$ (disponible dans notre animalerie) et TLR4$^{-/-}$ (disponible dans l'équipe du Dr Roumenina). Ces cellules seront stimulées avec différentes doses d'hème et les voies de signalisation seront évaluées par un système de criblage haut débit Proteome Profiler (RandD systems) permettant l'évaluation simultanée de la phosphorylation de 43 protéines kinases différentes. Cette comparaison nous permettra d'identifier les voies de signalisation qui découlent directement de TLR4 et celles qui peuvent être attribuées à d'autres récepteurs (dont RAGE). Par le profil de phosphorylation des kinases et phosphoprotéines, nous serons capables de déduire la nature de ces récepteurs (système Cystoscope, ClueGo).

Pour valider ces observations *in vivo*, nous injecterons de l'hème en intrapéritonéal ou induirons une hémolyse chez des souris WT et RAGE$^{-/-}$. La présence des récepteurs de l'hème (TLR4 et RAGE),

l'expression de l'HO-1, l'activation du complément sera évaluée dans les différents organes de ces souris. Nous analyserons le phénotype des cellules endothéliales rénales et des macrophages spléniques par le même panel d'étude que pour l'étude *in vitro*. Nous avons obtenu l'autorisation pour la conduite de ces expérimentations (APAFiS #15214).

Partie 3. Pertinence clinique du RAGE comme récepteur de l'hème

Le rein est un organe particulièrement touché au cours des maladies hémolytiques. Dans le but d'identifier chez l'homme un rôle potentiel du RAGE en situation d'hémolyse, nous avons pour objectif : 1- de comparer le marquage de RAGE en immunofluorescence ou immunohistochimie entre du tissu rénal sain (rein sain péri-tumoral ou biopsies de greffons dites «normales/peu modifiées ») et des biopsies rénales réalisées en situation d'hémolyse aigue et pathologique (MAT en particulier SHU, drépanocytose) ou situation d'hémolyse chronique et stable (patients porteurs d'une valve mécanique). Nous corrèlerons les résultats à la gravité clinico-biologique (marqueurs d'hémolyse biologique, phénotype clinique) ; 2- de réaliser une extraction d'ARNm à partir de biopsies rénales et d'analyser l'expression des gènes du complément et des protéines identifiées comme dépendantes de la cascade d'activation découlant de l'interaction RAGE-hème dans les expérimentations précédentes.

Ce projet qui cible en premier lieu l'hème - ses récepteurs et mécanismes effecteurs - est l'occasion de préciser le rôle de RAGE dans une situation d'agression vasculaire aigue qu'est l'hémolyse et d'étudier l'impact d'interactions potentielles avec d'autres récepteurs tels que TLR4 (modulation d'activité ?).

Projet 2- Syndrome des anti-phospholipides : Etude des déterminants de ses variants phénotypiques

Ce projet est actuellement conduit par le Dr Cécile Yelnik dans le cadre d'une thèse d'Université (2019-2022) que je co-encadre avec le Pr Lambert.

Background : Le syndrome des anti-phospholipides (SAPL) est une maladie auto-immune caractérisée par l'association de manifestations cliniques thrombotiques, pouvant toucher tous les territoires vasculaires (artère, veine, circulation placentaire et microcirculation), avec des marqueurs immunologiques spécifiques : les anticorps anti-phospholipides (aPL). Trois marqueurs sont actuellement reconnus dans les critères internationaux du SAPL : l'anticoagulant circulant lupique (LA), les anticorps anti-cardiolipine (aCL) et les anticorps anti-bêta2 Glycoprotéine I (ab2GPI)) (Miyakis 2006). Les manifestations cliniques observées au cours du SAPL sont très hétérogènes et de gravité variable, allant de la thrombose veineuse profonde distale à des tableaux catastrophiques (CAPS) d'activation diffuse de la coagulation avec thromboses multiples artérielles, veineuses et microcirculatoires mettant en jeu le pronostic vital. Le traitement actuel repose principalement sur une anticoagulation efficace prolongée chez l'ensemble des patients. Il apparait que les aPL, marqueurs biologiques spécifiques du SAPL, ne permettent pas d'expliquer à eux seuls les mécanismes à l'origine de cette diversité clinique. Ainsi, les marqueurs physiopathologiques permettant d'expliquer l'atteinte préférentiellement veineuse, artérielle, placentaire ou microcirculatoire chez un patient donné ne sont pas connus, alors que ceux-ci pourraient permettre d'identifier de nouvelles cibles thérapeutiques afin d'adapter la prise en charge au profil du patient.
L'apparition d'une dysfonction endothéliale est une des étapes clé de la physiopathologie du SAPL. Plusieurs récepteurs, comme l'apoER2 ont été impliqués dans l'interaction entre les aPL et la surface cellulaire, mais il apparait que cette interaction est complexe et qu'elle met en jeu plusieurs récepteurs et ligands qui ne sont pas encore complètement identifiés. Nous émettons l'hypothèse que le récepteur RAGE, à travers une interaction avec les aPL, pourrait avoir un rôle significatif dans la physiopathologie du SAPL et plus particulièrement dans ses tableaux microvasculaires disséminés (CAPS).

L'objectif principal de ce projet est donc de déterminer les mécanismes à l'origine de la grande variabilité phénotypique observée chez les patients atteints d'un SAPL, que nous étudierons par l'intermédiaire de deux approches complémentaires :

- Partie 1 **:** Une analyse en clusters à partir des données cliniques et biologiques issues d'une large cohorte de patients SAPL, dont l'objectif est d'identifier et caractériser s'il existe des profils de patients clinico-biologiques homogènes ;
- Partie 2 : Une étude des déterminants physiopathologiques à l'origine de la dysfonction endothéliale induite par les aPL, ciblant plus particulièrement le système du complément et un récepteur endothélial - le récepteur aux produits de glycation avancés (RAGE) - tous deux récemment impliqués comme acteur dans cette maladie.

Travaux en cours et résultats préliminaires :

<u>Partie 1</u> : Caractérisation d'une cohorte de patients SAPL et recherche d'une corrélation entre phénotype clinique et profil biologique.

Les patients SAPL sont recrutés à partir d'une base de données informatisée lilloise. Les autorisations réglementaires à la constitution de cette cohorte (CPP, CNIL) ont été obtenues par Cécile en Février 2020 (N° : CPP2020-03-024a / 2020-A00239-30 / 20.02.19.62511). Outre le recueil de données cliniques, il a été mis en place des séro- et plasmathèque constitués d'échantillons de patients SAPL suivis en consultation (hors évènement aigu thrombotique). A ce jour, 270 patients sont inclus dans la base et environ la moitié d'entre eux a un prélèvement en biobanque disponible pour les expérimentations.

Notre objectif est d'évaluer le profil cytokinique *(Kit commerciaux, ThermoFisher)* des patients, leur niveau d'activation du complément (C5b9 soluble, C3a et C5a, *Kit commerciaux, InVitrogen*) et du système RAGE (RAGE soluble, sRAGE et esRAGE). Les données seront ensuite analysées en cluster avec l'aide du département de biostatistique du CHU de Lille (Pr Duhamel, Dr Elodie Drumez).

Valorisation

Yelnik CM, Miranda S, Mékinian A, Lazaro E, Quéméneur T, Provot F, Frimat M, Morell-Dubois S, Le Guern V, Hachulla E, Costedoat-Chalumeau N, Lambert M Refractory Catastrophic Antiphospholipid Syndrome patients respond inconsistently to Eculizumab. Blood 2020. IF 16.562

<u>Partie 2</u> : Implication du RAGE dans l'acquisition du phénotype prothrombotique du SAPL

Cette 2ème partie du projet se développera autour de 3 approches, l'une en biologie moléculaire visant à préciser les interactions entre RAGE et les aPL, la 2nde et la 3ème en biologie cellulaire et animale dans le cadre de l'étude *in vitro* et *in vivo* des conséquences fonctionnelles de la liaison RAGE-aPL.

<u>*Biologie moléculaire*</u> : nous disposons de données préliminaires en SPR montrant, dans certaines conditions, une liaison RAGE-APL dont l'affinité est supérieure à celle des contrôles (**figure 1**). Nous prévoyons de compléter cette analyse en augmentant le nombre d'échantillons testés et de la vérifier par thermophorèse, technique maitrisée par Christophe FURMAN qui a rejoint l'équipe en janvier 2020.

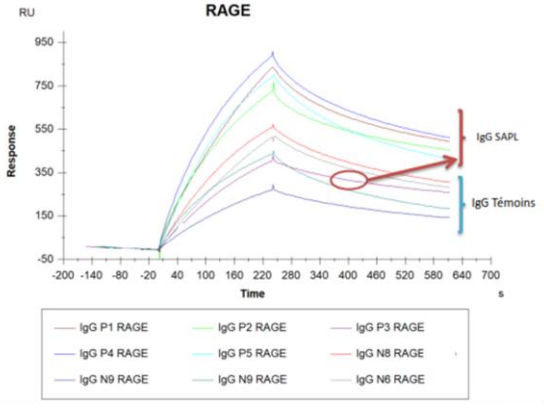

Figure 1: Etude en SPR de l'affinité de liaison entre RAGE et des IgG-aPL (n=5) ou IgG-contrôles (donneurs sains, n=4)

Modèles cellulaires : Nous prévoyons de travailler avec différentes cellules endothéliales, à savoir HUVECs en tant que modèle veineux macrovasculaire (cellules issues de veines de cordons ombilicaux isolées en routine dans le laboratoire), HMEC et GnEC en tant que modèles microvasculaires (lignées de cellules microvasculaires issues des capillaires du derme et des glomérules respectivement, disponibles au laboratoire), et des cellules d'origine artérielle qui seront achetées dans le commerce. La mise au point de notre modèle sera en premier lieu réalisé sur des HUVEC.

Nos cellules seront exposées à des aPL +/- de l'hème en conditions natives ou après exposition à des inhibiteurs de RAGE (incubation 16h) de façon à déterminer si les effets proinflammatoires et prothrombotiques potentiellement observés sont influencés par RAGE. Nous espérons pouvoir compléter cette analyse sur un modèle cellulaire invalidé pour RAGE, en cours de mise au point au laboratoire. Différents marqueurs seront étudiés (molécules d'adhérences, marqueurs membranaires d'activation du complément et de la coagulation, état d'apoptose/nécrose) après détachement des cellules.

Modèles murins : cette étape sera réalisée +/- parallèle de l'étape 2 en fonction de la disponibilité des souris RAGE KO. Cécile a pu mettre au point au laboratoire lors de son Master 2 un modèle murin de dysfonction endothéliale induite par les aPL. Brièvement, des souris C57BL/6 WT ou RAGE$^{-/-}$ âgées de 12 à 36 semaines étaient traitées à J0 par une injection intrapéritonéale de solution d'IgG-aPL ou -contrôle préalablement isolés (6 mg dans un volume de 400 µL de solution, dose déterminée à partir des résultats préliminaires de mise au point du modèle lors du M2). Dans ces conditions étaient observées une diminution des marqueurs de dysfonction endothéliale (analyse fonctionnelle de la vaso-relaxation artérielle endothélium-dépendante) chez la souris RAGE$^{-/-}$, suggérant une possible implication de ce récepteur dans la physiopathologie du SAPL (**figure 2**, *résultats non publiés*).

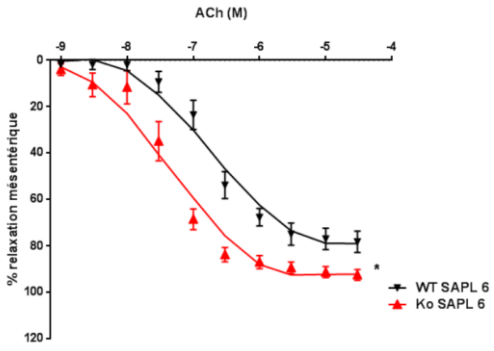

Figure 2: Comparaison de l'effet de l'injection d'immunoglobulines contenant des anticorps antiphospholipides sur la vasorelaxation mésentérique chez les souris RAGE déficientes par rapport aux souris sauvages. n=6 souris par groupe. Pourcentage de relaxation de l'anneau aortique pré-contracté à la phényléphrine à des concentrations croissantes d'acétylcholine. Analyse statistique réalisée à partir du calcul des aires sous les courbes de relaxation. *p<0.05; **p<0.01; ***p<0.001, test de Mann-Whitney.

Afin de se rapprocher d'un modèle de CAPS, cette injection sera, selon les groupes, suivie d'une injection intrapéritonéale de PBS (contrôle) ou de phénylhydrazine (PHZ), stimulus visant à mimer l'hémolyse par lyse des globules rouges. A J1 de l'injection de PHZ, les souris seront sacrifiées après anesthésie générale par voie intrapéritonéale. Il s'agit là aussi d'un modèle murin d'hémolyse validé et que nous avons pu reproduire au laboratoire durant la thèse d'Université d'Olivia May. Nous avons obtenu l'autorisation pour la conduite de ces expérimentations animales (APAFiS #15214).

Nous étudierons dans les tissus prélevés l'expression génique et protéique de cytokines proinflammatoires (TNFa, IL1b, IL6, IL12) et chémokines notamment impliquées dans l'activation macrophagique (MCP-1, MMP1) ; de marqueurs de stress oxydant (eNOS, SOD, HO1); de marqueurs de coagulation (Facteur tissulaire, Thrombomoduline) ; de RAGE et de C3. Nous étudierons en immunohistochimie ou en immunofluorescence selon les tissus, l'expression de RAGE pour rechercher une modulation de son expression chez les souris WT sous l'effet d'une exposition aux aPL +/- aux produits issus de l'hémolyse. Nous étudierons également des marqueurs d'activation du complément (C3c, C5b9) à la membrane.

Ce projet a pour objectif de mieux préciser les molécules et voies de signalisations responsables des différentes manifestations cliniques du SAPL. Le modèle murin permettra en particulier l'étude de l'atteinte microvasculaire encore mal connue. Nos résultats pourraient permettre de proposer une prise en charge personnalisée ciblée des patients SAPL en fonction de leur phénotype clinique, en priorité chez les patients réfractaires au traitement anticoagulant ou cas de mise en cause du pronostic vital. Ainsi, la présence de clusters de patients dans lesquelles une surexpression du TNFalpha ou de l'IL-6 seraient observés inciterait à proposer un traitement ciblé sur ces molécules. Si nous confirmons l'implication du RAGE, nos résultats permettraient d'offrir une nouvelle approche thérapeutique pour les patients SAPL réfractaires.

Projet 3- Rôle des glycosaminoglycanes du glycocalyx endothélial glomérulaire dans la physiopathologie du syndrome hémolytique et urémique atypique.

Ce projet s'inscrit dans la continuité de travaux cliniques conduits dans le service autour des microangiopathies thrombotiques (détails, p.26). Les données présentées ci-dessous sont issus du travail de Master 2 réalisé en 2020 par Timothée Laboux, interne de Néphrologie.

Background : Je rappelle l'identification fréquente, chez plus de 50% des patients, de mutations des protéines régulant le complément dans le SHUa. Cependant, leurs pénétrance et expression variables démontrent qu'elles ne sont qu'un facteur de susceptibilité, suggérant l'intervention d'autres mécanismes. Parmi les acteurs encore peu caractérisés mais susceptibles de moduler la réponse au complément à la surface de l'endothélium figure le glycocalyx. Recouvrant les cellules endothéliales, cette structure riche en glycosaminoglycanes (GAGs) participe en effet à lier le facteur H, principal régulateur de la voie alterne du complément, par l'intermédiaire en particulier des héparanes-sulfates (HS), principal composant du glycocalyx endothélial. Ce projet a ainsi pour **objectif** de préciser le rôle du glycocalyx dans la genèse du SHUa, à travers deux approches : 1- la caractérisation des HS rénaux au sein de notre cohorte de patients MAT ayant bénéficié d'une biopsie rénale ; 2- mise au point d'un modèle cellulaire endothélial *in vitro* dans lequel les HS ont été dégradés par méthode enzymatique (héparinases) avec étude dans ces conditions de marqueurs d'activation du complément et de RAGE.

Travaux en cours et résultats préliminaires :

<u>Partie 1</u> : Caractérisation des héparanes-sulfates sur des biopsies rénales de patients-MAT

Notre équipe a observé que le SHU était associé à une diminution de la densité des HS du glycocalyx endothélial glomérulaire et artériolaire rénal sur un travail pilote.

Brièvement, les biopsies rénales congelées de 8 patients suivis pour un SHU atypique ont été étudiées (notées « patients-SHU ») et comparées à 4 biopsies de patients présentant une microangiopathie thrombotique (MAT) d'autre nature que le SHU (notées « patients-MAT ») ainsi qu'à 4 biopsies témoins de rein sain péri-tumoral (RSPT) (recueillies sur pièces d'exérèse de néphrectomie, référées comme « patients-RSPT »). Le marquage des HS du glycocalyx endothélial glomérulaire et artériolaire a été mis au point en IF avec l'anticorps anti-HS Jm403 (370730, Amsbio). Ce marquage a été contrôlé dans d'autres néphropathies (GEM, LGM) avec des résultats cohérents avec la

Fig.1: Marquage des Héparanes-Sulfates de l'endothélium glomérulaire

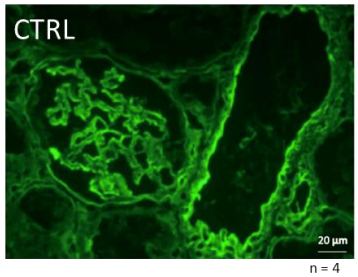

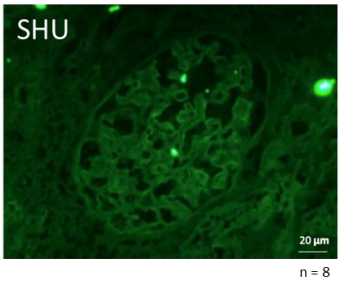

	ANTICORPS ANTI-HS		
	0-1+	2+	3+
Patients-SHU (n =8)	5	2	1
Patients-MAT (n = 4)	0	1	3
Patients-RSPT (n = 4)	0	0	4

	0-1+	2+	3+
SHU Perls + (n =4)	3	1	0
SHU Perls - (n = 2)	1	1	0

littérature. Une lecture semi-quantitative (0 à 3+), en aveugle, par deux opérateurs indépendants dont un anatomopathologiste (Dr JB Gibier, CHU Lille), était réalisée.

Le SHU était associé à une diminution de la densité des HS endothéliales dans 7 cas sur 8. Ainsi, 5 des 8 patients-SHU présentaient un marquage des HS absent ou faible (0-1+), 2 présentaient un marquage modéré (2+) et 1 seulement conservait un marquage comparable au contrôle (3+). A l'inverse, le marquage des HS était préservé dans les groupes témoins : les 4 patients-RSPT présentaient tous un marquage intense à 3+, et 3 patients-MAT sur 4 présentaient un marquage intense à 3+ (le dernier présentant un marquage modéré à 2+) (**figure 1**). La coloration de Perls marquant les ions ferriques Fe^{3+} servait à mettre en évidence dans le tissu la présence d'hème, produit de dégradation de l'hémoglobine libéré dans la circulation en cas d'hémolyse. Sans surprise, le Perls était plus souvent positif chez les patients SHU récemment hémolytiques (4/6) tandis qu'il était négatif chez les 4 patients MAT. Le marquage des HS était effacé chez 3 patients SHU-Perls+ contre 1 chez les patients SHU-Perls. Dans la limite d'un échantillon de petite taille, nous nous sommes interrogés sur l'implication de l'hémolyse et de l'hème dans la dégradation des HS observée dans le SHU.

Dans le but de vérifier ces données préliminaires, nous avons identifié à partir de la base de données d'anatomopathologie 55 patients avec un diagnostic histologique de MAT et pris en charge en néphrologie à Lille entre 2010 et 2020. Le classement des patients entre le groupe SHU et le groupe MAT non SHU est en cours selon des critères préétablis par deux néphrologues (T.Laboux/ M. Frimat) de façon indépendante. En parallèle, le marquage des HS d'échantillons biopsiques de ces 55 patients et l'évaluation semi-quantitative de leur densité a été réalisé, à l'aveugle, par deux opérateurs indépendants (T.Laboux/V.Gnemmi, anatomopathologie rénale, CHU Lille).

<u>Partie 2 :</u> Impact de la dégradation du glycocalyx sur l'activation du complément dans un modèle cellulaire endothélial in vitro

Prenant en compte les liens décrits du glycocalyx avec le système du complément et nos données préliminaires montrant une moindre densité des HS endothéliales chez les patients-SHU hémolytiques, nous avons émis l'hypothèse que l'altération du glycocalyx endothélial rénal serait impliquée dans l'activation locale de la voie alterne du complément, favorisant ainsi les poussées de SHUa. Cette hypothèse a été étudié dans le cadre du M2 de Timothée Laboux qui a mis au point un modèle de dégradation enzymatique des HS du glycocalyx de cellules endothéliales (HUVEC). Il a ensuite étudié : i/ l'effet de la dégradation du glycocalyx sur la capacité de la cellule endothéliale à activer localement le complément ; ii/ l'impact d'une exposition courte à l'hème sur le glycocalyx endothélial, avec pour hypothèse que l'hème puisse être responsable de la diminution de la densité des HS observée dans nos travaux préliminaires ; iii/ l'impact d'une exposition prolongée à l'hème sur l'expression génique des enzymes impliquées dans la biosynthèse des HS dans le cadre d'une collaboration avec le Pr Fabrice Allain, expert en glycobiologie (Université Lille).

Brièvement, ce travail a révélé, en conditions *in vitro*, qu'un endothélium dont les HS avaient été préalablement dégradées constituait une surface propice à l'activation locale du complément. En effet, une augmentation dose-dépendante du dépôt de C3b était observée en IF et CMF après traitement par héparinases (**figure 2**).

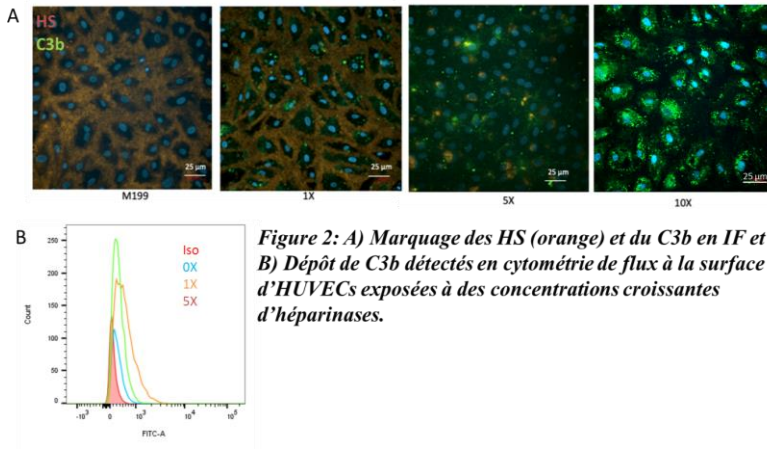

Figure 2: A) Marquage des HS (orange) et du C3b en IF et B) Dépôt de C3b détectés en cytométrie de flux à la surface d'HUVECs exposées à des concentrations croissantes d'héparinases.

Après exposition de courte durée à l'hème (30 min), nous avons observé une diminution dose-dépendante du marquage des HS, suggérant un impact de cette molécule sur l'intégrité du glycocalyx. L'étude des mécanismes en cause sont en cours. De façon intéressante, une exposition prolongée à l'hème (16h) a induit des modifications transcriptionnelles dose-dépendantes des enzymes impliquées dans la biosynthèse des HS, marquées par une diminution d'expression de la C5-Epimérase et une augmentation de celles de la 6-OST1 et de la 3-OST1, rendant compte d'un profil transcriptomique des enzymes de biosynthèse des HS devenu de type antithrombine sous l'effet de l'hème. Cet effet dual de l'hème a déjà été décrit, notamment à travers l'induction de l'expression d'hème-oxygenase 1 capable d'effets anti-inflammatoires et anti-oxydants. Nous émettons l'hypothèse que l'acquisition d'un profil antithrombine sous l'effet de l'hème ne soit pas homogène au sein des différents endothéliums et prévoyons ainsi de les comparer (collaboration Pr Allain). L'absence de survenue d'un tel profil à la surface de l'endothélium glomérulaire notamment, pourrait participer à expliquer la susceptibilité rénale observé dans le SHU.

Nous espérons ainsi que l'amélioration des connaissances des facteurs de susceptibilité et de la physiopathologie du SHUa permettent d'envisager d'éventuelles stratégies préventives et de nouvelles options thérapeutiques (modulation pharmacologique du glycocalyx).

Projet 4- Evaluation fonctionnelle de la microcirculation dans nos modèles d'étude

Background : Bien que l'atteinte microcirculatoire soit admise comme un élément physiopathologique majeur au cours de l'inflammation aigüe, son évaluation fonctionnelle reste anecdotique en dehors du sepsis, contexte dans lequel elle a été le plus étudié. Il a ainsi été décrit dans le choc septique, une baisse globale de la densité des capillaires, une réduction du nombre de capillaires perfusés et une hétérogénéité des zones de perfusion. Cette évaluation de la microcirculation a notamment été réalisée par imagerie sublinguale. Il s'agit d'une technique d'imagerie optique du contenu microvasculaire utilisée en recherche clinique depuis environ 15 ans qui permet la visualisation des anomalies de flux dans les microvaisseaux de diamètre inférieur à 100 microns au niveau sublingual. Dans le sepsis, l'altération de la microcirculation ainsi monitorée a été corrélée à un plus mauvais pronostic de survie des patients et a permis de démontrer l'absence de concordance systématique entre l'état de la macro- et la microcirculation. Dans le domaine de la néphrologie, il existe peu de travaux. Il a été décrit une altération de la microcirculation sublinguale chez les hémodialysés chroniques comparativement à des volontaires sains. Cette altération était moindre chez des patients transplantés rénaux (Yeh et al. 2017). L'ultrafiltration per dialytique a été identifié comme un facteur d'altération de la microcirculation sublinguale indépendamment des paramètres d'évaluation macrocirculatoire (Meinders et al. 2015; Veenstra et al. 2017). L'impact de cette altération reste cependant mal défini. Parmi les mécanismes impliqués et également évaluable par les outils d'imagerie sublinguale, figure l'altération du glycocalyx mise en évidence dans une population de patients hémodialysés chroniques (Vlahu et al. 2012). Hors contexte septique, ce type d'évaluation de la microcirculation rénale dans des situations d'agression aigue (vascularite, MAT, etc..) n'a pas été réalisée.

L'objectif est d'appliquer à nos modèles d'étude cette méthodologie d'évaluation de l'endothélium dans le but de coupler deux approches complémentaires, l'une fonctionnelle visant à « imager » *in vivo* les anomalies de la microcirculation chez l'homme et l'autre visant à mesurer des biomarqueurs de l'atteinte de la cellule endothéliale directement dans le sang circulant ou *in vitro* à la surface de cellules endothéliales exposées à du sérum de patients. La mise en place de ce projet profitera de l'expérience du Pr Favory, membre du groupe inflammation de notre équipe de recherche, qui a été formé à la technique d'imagerie sublinguale ainsi que d'un accès facilité à plusieurs populations de patients.

Parmi les populations d'intérêt identifiées figurent :

1- **Les patients pris en charge pour une calciphylaxie** :

Ce projet s'inscrirait dans le cadre d'un projet ancillaire rattaché à un PHRC national porté par le Dr Arnaud LIONET, PH dans notre service, dans lequel je suis intervenue en tant que conseiller scientifique et dont le financement a été validé fin 2019.

La calciphylaxie est une maladie rare qui provoque des lésions cutanées ischémiques douloureuses rattachées à des calcifications microvasculaires associées à une thrombose du derme et du tissu adipeux sous-cutané. L'insuffisance rénale terminale (IRCT) et l'obésité sont deux facteurs de risque

identifiés et son pronostic est sombre (mortalité à 1 an : 40- 80 %). Les anomalies du métabolisme phosphocalcique sont mises en avant dans la physiopathologie de la calciphylaxie. Cependant, l'hétérogénéité des présentations cliniques, l'absence dans plus de 30% des cas de calcifications lésionnelles, les effets partiels des traitements visant cet aspect conduisent à envisager d'autres acteurs physiopathologiques parmi lesquelles la dysfonction endothéliale et microcirculatoire. L'objectif de ce PHRC est d'évaluer l'efficacité de la rheophérèse en traitement adjuvant de la calciphylaxie du patient en hémodialyse chronique *via* une étude prospective randomisée en simple aveugle. Notre hypothèse est que cette technique d'aphérèse, en éliminant un spectre défini de protéines de haut poids moléculaire, et notamment des facteurs impliqués dans l'inflammation vasculaire et la thrombose (fibrinogène ou le LDL-cholestérol) améliore l'état microcirculatoire (viscosité, glycocalyx, activation endothéliale).

Dans le cadre d'un projet ancillaire, nous prévoyons d'évaluer par imagerie sublinguale l'impact de la technique sur l'état de la microcirculation (caractéristiques de perfusion, glycocalyx). Par ailleurs, la constitution d'une séro- et plasmathèque est prévue et nous permettra d'évaluer le rôle de certains acteurs impliqués dans l'inflammation vasculaire parmi lesquelles le RAGE, dont l'accumulation dans le tissu adipeux des patients obèses est bien décrit (Hurtado Del Pozo et al. 2019). Dans le cas de la mise en évidence d'un effet RAGE-dépendant, nous préciserons les mécanismes moléculaires en cause en ciblant plus spécifiquement la voie AKT-mTOR que nous avons déjà identifiée comme étant influencée par l'invalidation de RAGE dans nos différents modèles (hémolyse, vieillissement vasculaire).

Ce projet pourrait donc permettre l'identification d'autres cibles thérapeutiques dans la calciphylaxie et améliorer la compréhension de ces mécanismes physiopathologiques.

2- **Les patients pris en charge pour une microangiopathie thrombotique** :

Cette approche complémentaire nous permettra d'enrichir de données *in vivo* fonctionnelles nos résultats actuels. Nous envisageons de comparer, à une population témoin appariée pour l'âge et le niveau de fonction rénale, des patients pris en charge pour un SHU au moment de l'épisode aigu et en dehors, dans le cadre de leur suivi en consultation.

Les résultats issus de ce travail pourraient amener des arguments supplémentaires à l'intérêt d'une modulation pharmacologique du glycocalyx.

Liste des publications

Indices bibliométriques

- 40 publications dont 37 depuis la thèse d'Université
- 29 articles originaux dont 6 (+1 en révision) en (co)premier/(co)dernier auteur (IF> 3)
  dont 5 en second ou avant-dernier auteur (dont 4 avec IF>3)
- Score Sigaps : 504 points
- 972 citations, h-index : 13 (sampra)

Publications scientifiques originales

1. *The receptor for advanced glycation end products is a sensor for cell-free heme. May O, Yatime L, Merle N, Delguste F, Howsam M, Daugan M, Billamboz M, Ghinet A, Lancel S, Dimitrov JD, Boulanger E, Roumenina L*, **Frimat M***. In revision in FEBS Journal (IF: 4.8)*
2. Complement system: a driver of the acute kidney injury in rhabdomyolysis. I Boudhabhay[#], V Poillerat[#], A Grunenwald, C Torset, J Leon, M Daugan, F Lucibello, Kl El Karoui, A Ydee, S Chauvet, P Girardie, S Sacks, M Rabant, P de Lonlay, C Rambaud, V Gnemmi, V Fremeaux-Bacchi, **M Frimat**, LT. Roumenina. Kidney Int. 2020 Oct 30:S0085-2538(20)31244-8. doi: 10.1016/j.kint.2020.09.033. *(IF: 8.4)*
3. Refractory Catastrophic Antiphospholipid Syndrome patients respond inconsistently to Eculizumab. CM Yelnik, S Miranda, A Mékinian, E Lazaro, T Quéméneur, F Provot, **M Frimat**, S Morell-Dubois, V Le Guern, E Hachulla, N Costedoat-Chalumeau, M Lambert. 2020 Jul 28;blood.2020007499. doi: 10.1182/blood.2020007499. (IF: 16,6)
4. A simple score to predict early death after kidney transplantation. J Bamoulid, **M Frimat**, C Courivaud, T Crepin, E Gaiffe, M Hazzan, D Ducloux. Eur J Clin Invest. 2020 Jun 13;e13312. doi: 10.1111/eci.13312. Online ahead of print. (IF: 3,1)
5. Prognostic significance of the renal resistive index in the primary prevention of type II diabetes. Delsart P, Vambergue A, Ninni S, Machuron F, Lelievre B, Ledieu G, Fontaine P, Merlen E, **Frimat M**, Glowacki F, Montaigne D, Mounier-Vehier C. J Clin Hypertens (Greenwich). 2020 Feb;22(2):223-230. doi: 10.1111/jch.13819. Epub 2020 Jan 31. (IF: 2, 6)
6. Tubulointerstitial damage and interstitial immune cell phenotypes are useful predictors for renal survival and relapse in antineutrophil cytoplasmic antibody-associated vasculitis. Bitton L, Vandenbussche C, Wayolle N, Gibier JB, Cordonnier C, Verine J, Humez S, Bataille P, Lenain R, Ramdane N, Azar R, Mac Namara E, Hatron PY, Maurage CA, Perrais M, **Frimat M**, Vanhille P, Glowacki F, Buob D, Copin MC, Quéméneur T, Gnemmi V.J Nephrol. 2020 Jan 8. doi: 10.1007/s40620-019-00695-y. [Epub ahead of print]. (IF: 2,7)
7. The use of highly individualized complement blockade revolutionized the posttransplant clinical outcomes and renal epidemiology of atypical HUS The use of highly individualized complement blockade revolutionized the posttransplant clinical outcomes and renal epidemiology of atypical HUS. Zuber J, **Frimat M**, Caillard S, Kamar N, Gatault P, (…), Rondeau E, Le Quintrec M, Frémeaux Bacchi V. J Am Soc Nephrol. 2019 Oct 1. pii: ASN.2019040331. (IF: 8, 6)
8. Ten-Year Outcome of Islet Alone or Islet After Kidney Transplantation in Type 1 Diabetes: A Prospective Parallel-Arm Cohort Study. Vantyghem MC, Chetboun M, Gmyr V, Jannin A, Espiard S, Le Mapihan K, Raverdy V, Delalleau N, Machuron F, Hubert T, **Frimat M**, Van Belle E, Hazzan M, Pigny P, Noel C, Caiazzo R, Kerr-Conte J, Pattou F. Diabetes Care. 2019 Nov;42(11):2042-2049. doi: 10.2337/dc19-0401. (IF : 13, 4)
9. Caveolin-1 rs4730751 single-nucleotide polymorphism may not influence kidney transplant allograft survival. Maanaoui M, Lenain R, Hamroun A, Van der Hauwaert C, Lopez B, Gibier JB, **Frimat M**, Savary G,

Hennart B, Larrue R, Pottier N, Broly F, Provôt F, Hazzan M, Glowacki F, Cauffiez C. Sci Rep. 2019 Oct 29;9(1):15541. doi: 10.1038/s41598-019-52079-8. (IF: 4,1)

10. Hypercalcemia is common during Pneumocystis pneumonia in kidney transplant recipients. Hamroun A, Lenain R, Bui Nguyen L, Chamley P, Loridant S, Neugebauer Y, Lionet A, **Frimat M,** Hazzan M. Sci Rep. 2019 Aug 29;9(1):12508. doi: 10.1038/s41598-019-49036-w. (IF: 4,1)
11. Adverse events associated with currently used medical treatments for cystinuria and treatment goals: results from a series of 442 patients in France. Prot-Bertoye C, Lebbah S, Daudon M, Tostivint I, Jais JP, Lillo-Le Louët A, Pontoizeau C, Cochat P, Bataille P, Bridoux F, Brignon P, Choquenet C, Combe C, Conort P, Decramer S, Doré B, Dussol B, Essig M, **Frimat M**, Gaunez N, Joly D, Le Toquin-Bernard S, Méjean A, Meria P, Morin D, N'Guyen HV, Normand M, Pietak M, Ronco P, Saussine C, Tsimaratos M, Friedlander G, Traxer O, Knebelmann B, Courbebaisse M; French Cystinuria Group. BJU Int. 2019 Nov;124(5):849-861. doi: 10.1111/bju.14721. Epub 2019 Mar 25. (IF :4.7)
12. The prognostic impact of cirrhosis on patients receiving maintenance haemodialysis. Artru F, Louvet A, Glowacki F, Bellati S, **Frimat M,** Gomis S, Castel H, Barthelon J, Lassailly G, Dharancy S, Noel C, Hazzan M, Mathurin P. Aliment Pharmacol Ther. 2019 Jul;50(1):75-83. doi: 10.1111/apt.15279. Epub 2019 May 14. (IF : 7, 4)
13. Indications for islet or pancreatic transplantation: Statement of the TREPID working group on behalf of the Société francophone du diabète (SFD), Société francaise d'endocrinologie (SFE), Société francophone de transplantation (SFT) and Société française de néphrologie - dialyse - transplantation (SFNDT). Wojtusciszyn A, Branchereau J, Esposito L, Badet L, Buron F, Chetboun M, Kessler L, Morelon E, Berney T, Pattou F, Benhamou PY, Vantyghem MC; TREPID group. Diabetes Metab. 2019 Jun;45(3):224-237. doi: 10.1016/j.diabet.2018.07.006. Epub 2018 Sep 14. (IF :3.7)
14. Knock out of receptor for advanced glycation end-products attenuates age-related renal lesions. T Teissier, V Quersin, V Gnemmi, M Daroux, M Howsam, F Delguste, C Lemoine, C Fradin, AM Schmidt, C Cauffiez, T Brousseau, F Glowacki, FJ Tessier, E Boulanger and **M Frimat**. Aging Cell. 2019 Apr;18(2):e12850. doi: 10.1111/acel.12850. Epub 2019 Feb 22 (IF :7.6)
15. Heme Drives Susceptibility of Glomerular Endothelium to Complement Overactivation Due to Inefficient Upregulation of Heme Oxygenase-1. May O, Merle NS, Grunenwald A, Gnemmi V, Leon J, Payet C, Robe-Rybkine T, Paule R, Delguste F, Satchell SC, Mathieson PW, Hazzan M, Boulanger E, Dimitrov JD, Fremeaux-Bacchi V, **Frimat M***, Roumenina LT*. Front Immunol. 2018 Dec 20;9:3008 (IF: 6,4)
16. Intravascular hemolysis activates complement via cell-free heme and heme-loaded microvesicles. Merle NS, Grunenwald A, Rajaratnam H, Gnemmi V, **Frimat M**, Figueres ML, Knockaert S, Bouzekri S, Charue D, Noe R, Robe-Rybkine T, Le-Hoang M, Brinkman N, Gentinetta T, Edler M, Petrillo S, Tolosano E, Miescher S, Le Jeune S, Houillier P, Chauvet S, Rabant M, Dimitrov JD, Fremeaux-Bacchi V, Blanc-Brude OP, Roumenina LT. JCI Insight. 2018 Jun 21;3(12). pii: 96910. doi: 10.1172/jci.insight.96910. eCollection 2018 Jun 21**.** (IF: 6)
17. Long-term efficacy of remission-maintenance regimens for ANCA-associated vasculitides. Terrier B, Pagnoux C, Perrodeau É, Karras A, Khouatra C, Aumaître O, Cohen P, Decaux O, Desmurs-Clavel H, Maurier F, Gobert P, Quémeneur T, Blanchard-Delaunay C, Bonnotte B, Carron PL, Daugas E, Ducret M, Godmer P, Hamidou M, Lidove O, Limal N, Puéchal X, Mouthon L, Ravaud P, Guillevin L; French Vasculitis Study Group. Ann Rheum Dis. 2018 Aug;77(8):1150-1156. doi: 10.1136/annrheumdis-2017-212768. Epub 2018 May 3. (IF: 12,3)
18. Characterization of Renal Injury and Inflammation in an Experimental Model of Intravascular Hemolysis. Merle NS, Grunenwald A, Figueres ML, (…), **Frimat M**, Gentinetta T, Miescher S, Houillier P, Legros V, Gonnet F, Blanc-Brude OP, Rabant M, Daniel R, Dimitrov JD, Roumenina LT. Front Immunol. 2018 Mar 1;9:179. doi: 10.3389/fimmu.2018.00179. eCollection 2018. (IF: 6,4)
19. Anti-factor-B and anti-C3 autoantibodies in infection-related glomerulonephritis. Marinozzi MC, Roumenina L, Chauvet S, Hertig A, Bertrand D, Olagne J, **Frimat M**, Ulinski T, Deschênes G, Burtey S, Moulin B, Legendre

C, Frémeaux-Bacchi V, Le Quintrec M. J Am Soc Nephrol. 2017 Jan 17. pii: ASN.2016030343. doi: 10.1681/ASN.2016030343. (IF: 9,1)

20. Collapsing glomerulopathy is common in the setting of thrombotic microangiopathy of the native kidney. Buob D, Decambron M, Gnemmi V, **Frimat M**, Hoffmann M, Azar R, Gheerbrant JD, Guincestre T, Noël C, Copin MC, Glowacki F. Kidney Int. 2016 Sep 17. (IF: 8,6)

21. Long-term outcome after early cyclosporine withdrawal in kidney transplantation: ten years after. Tabibzadeh N, Glowacki F, **Frimat M**, Elsermans V, Provôt F, Lionet A, Gnemmi V, Hertig A, Noël C, Hazzan M. Clin Transplant. 2016 Sep 13. doi: 10.1111/ctr.12843. (IF: 1,8)

22. Renal Cortical Necrosis in Postpartum Hemorrhage: A Case Series. **Frimat M**, Decambron M, Lebas C, Moktefi A, Lemaitre L, Gnemmi V, Sautenet B, Glowacki F, Subtil D, Jourdain M, Rigouzzo A, Brocheriou I, Halimi JM, Rondeau E, Noel C, Provôt F, Hertig A. Am J Kidney Dis. 2016 Jan 16. pii: S0272-6386(15)01496-1. doi: 10.1053/j.ajkd.2015.11.022. (IF: 6,3)

23. Donor ABCB1 genetic polymorphisms influence epithelial-to-mesenchyme transition in tacrolimus-treated kidney recipients. Bloch J, Hazzan M, Van der Hauwaert C, Buob D, Savary G, Hertig A, Gnemmi V, **Frimat M**, Perrais M, Copin MC, Broly F, Noël C, Pottier N, Cauffiez C, Glowacki F. Pharmacogenomics. 2014 Dec;15(16):2011-24. doi: 10.2217/pgs.14.146. (IF: 3,2)

24. Loss of DGKε induces endothelial cell activation and death independently of complement activation. Bruneau S, Néel M, Roumenina LT**, Frimat M**, Laurent L, Frémeaux-Bacchi V, Fakhouri F. Blood. 2015 Feb 5;125(6):1038-46. doi: 10.1182/blood-2014-06-579953. Epub 2014 Dec 10. (IF:10,45)

25. Rituximab versus azathioprine for maintenance in ANCA-associated vasculitis. Guillevin L, Pagnoux C, Karras A, Khouatra C, and al; French Vasculitis Study Group. N Engl J Med. 2014 Nov 6;371(19):1771-80. doi: 10.1056/NEJMoa1404231. (IF: 55,9)

26. Mapping end-stage renal disease (ESRD): spatial variations on small area level in northern France, and association with deprivation. Occelli F, Deram A, Génin M, Noël C, Cuny D, Glowacki F; Néphronor Network. PLoS One. 2014 Nov 3;9(11):e110132. doi: 10.1371/journal.pone.0110132. (IF: 3,2)

27. Complement activation by heme as a secondary hit for atypical hemolytic uremic syndrome. **Frimat, M**., F. Tabarin, J. D. Dimitrov, C. Poitou, L. Halbwachs-Mecarelli, V. Fremeaux-Bacchi, and L. T. Roumenina. Blood 2013; 122:282-292. (IF: 9,8)

28. A prevalent C3 mutation in aHUS patients causes a direct C3 convertase gain of function. Roumenina, L. T*, **M. Frimat*,** E. C. Miller, M. A. Dragon-Durey, P. Bordereau, S. Bigot, S. Satchell, C. Mousson, C. Noel, C. Sautes-Fridman, L. Halbwachs-Mecarelli, J. P. Atkinson, A. Lionet, and V. Fremeaux-Bacchi. * LTR and MF contributed equally to this study. Blood 2012; 119:4182-4191. (IF: 9,1)

29. [Renal malakoplakia: an underestimate cause of renal failure]. Daroux M, **Frimat M,** Mirault T, Fleury D, Lemaitre V, Noel LH, Vanhille P. Nephrol Ther. 2012 Apr;7(2):111-6. (IF: 0,45)

Editorial sur invitation

1. Is RAGE the receptor for inflammaging? **Frimat M.**, Teissier T., Boulanger E. Aging (Albany NY). 2019 Sep 8;11(17):6620-6621. (IF: 5,2)

Lettres à l'éditeur et cas cliniques

1. A challenging case of pneumo-renal syndrome. Hamroun A, Fages V, Julien B, Lenain R, Frimat M. J Nephrol. 2020 Oct 24. doi: 10.1007/s40620-020-00889-9.
2. [Vancomycin poisoning successfully treated with intermittent hemodialysis: A case report]. Zaworski J, **Frimat M**, Duval M, Saint-Jacques C, Bouderlique É, Glowacki F, Noël C, Hazzan M, Provôt F. Nephrol Ther. 2018 Apr;14(2):112-116. doi: 10.1016/j.nephro.2017.10.004. Epub 2017 Dec 30. (IF: 0,45)
3. Glomerulonephritis and granulomatous vasculitis in kidney as a complication of the use of BRAF and MEK inhibitors in the treatment of metastatic melanoma: A case report. Maanaoui M, Saint-Jacques C, Gnemmi V, **Frimat M**, Lionet A, Hazzan M, Noël C, Provot F. Medicine (Baltimore). 2017 Jun;96(25):e7196. doi: 10.1097/MD.0000000000007196. (IF: 2,0)
4. In reply to "Prolonged administration of tranexamic acid to treat postpartum hemorrhage should be discouraged until further evidence is available". **Frimat M**, Provôt F, Hertig A. Am J Kidney Dis. 2017 Jan;69(1):160-161. doi: 10.1053/j.ajkd.2016.10.011. (IF: 6,3)
5. FDG PET/CT allowing detection and follow-up of tumor cell transplantation. Jaillard A, Baillet C, Béron A, Tabibzadeh N, Scherpereel A, **Frimat M**, Perbet R, Gnemmi V, Noël C, Huglo D. Ann Nucl Med. 2016 Apr;30(3):250-4. doi: 10.1007/s12149-015-1051-x. Epub 2015 Dec 17

Revues et publications didactiques

1. Heme oxygenase 1: a defensive mediator in kidney diseases. Grunenwald A, Roumenina LT and **Frimat M**. Int J Mol Sci. *In revision* (IF: 4.6)
2. Hemolysis Derived Products Toxicity and Endothelium: Model of the Second Hit. **Frimat M**, Boudhabhay I, Roumenina LT. Toxins (Basel). 2019 Nov 13;11(11). pii: E660. doi: 10.3390/toxins11110660. (IF: 3,3)
3. Endothelium structure and function in kidney health and disease. Jourde-Chiche N, Fakhouri F, Dou L, Belien J, Burtey S, **Frimat M**, Jarrot P, Kaplanski G, Le Quintrec M, Pernin V, Rigothier C, Sallée M, Frémeaux-Bacchi V, Guerrot D and Roumenina L. Nat Rev Nephrol. 2019 Feb;15(2):87-108. doi: 10.1038/s41581-018-0098-z (IF :14.1)
4. [New scores in renal transplantation: How can we use them?]. Hazzan M, **Frimat M**, Glowacki F, Lionet A, Provot F, Noël C. Nephrol Ther. 2017 Apr;13 Suppl 1:S131-S136. doi: 10.1016/j.nephro.2017.01.005. (IF: 0,5)
5. Kidney, heart, and brain: three organs targeted by aging and glycation. **Frimat M**, Daroux M, Litke R, Nevière R, Tessier F, Boulanger E. Clinical Science. Clin Sci (Lond). 2017 Jun 1;131(11):1069-1092 (IF: 5,6)
6. Endothelial cells: source, barrier and target of defensive mediators. Roumenina L, Rayes J, **Frimat M** and Fremeaux-Bacchi V. Immunol Rev. 2016 Nov;274(1):307-329 (IF: 10,2)
7. Prise en charge de l'insuffisance rénale chronique de l'octogénaire. Glowacki F, Moranne O, **Frimat M,** Beuscart JB, Boulanger E. (Revue du Praticien-Medecine générale, manuscrit produit sur demande de l'éditeur).

Tirés à part des manuscrits les plus significatifs

1. *The receptor for advanced glycation end products is a sensor for cell-free heme. May O, Yatime L, Merle N, Delguste F, Howsam M, Daugan M, Billamboz M, Ghinet A, Lancel S, Dimitrov JD, Boulanger E, Roumenina L*, **Frimat M***. In revision in FEBS Journal (IF: 4.8)*
2. Complement system: a driver of the acute kidney injury in rhabdomyolysis. I Boudhabhay[#], V Poillerat[#], A Grunenwald, C Torset, J Leon, M Daugan, F Lucibello, Kl El Karoui, A Ydee, S Chauvet, P Girardie, S Sacks, M Rabant, P de Lonlay, C Rambaud, V Gnemmi, V Fremeaux-Bacchi, **M Frimat** and LT. Roumenina. Kidney Int. 2020 Oct 30:S0085-2538(20)31244-8. doi: 10.1016/j.kint.2020.09.033. (IF: 8.4)
3. Knock out of receptor for advanced glycation end-products attenuates age-related renal lesions. T Teissier, V Quersin, V Gnemmi, M Daroux, M Howsam, F Delguste, C Lemoine, C Fradin, AM Schmidt, C Cauffiez, T Brousseau, F Glowacki, FJ Tessier, E Boulanger and **M Frimat**. Aging Cell. 2019 Apr;18(2):e12850. doi: 10.1111/acel.12850. Epub 2019 Feb 22. (IF :7.6)
4. Heme Drives Susceptibility of Glomerular Endothelium to Complement Overactivation Due to Inefficient Upregulation of Heme Oxygenase-1. May O, Merle NS, Grunenwald A, Gnemmi V, Leon J, Payet C, Robe-Rybkine T, Paule R, Delguste F, Satchell SC, Mathieson PW, Hazzan M, Boulanger E, Dimitrov JD, Fremeaux-Bacchi V, **Frimat M***, Roumenina LT*. Front Immunol. 2018 Dec 20;9:3008. (IF: 6.4)
5. Renal Cortical Necrosis in Postpartum Hemorrhage: A Case Series. **Frimat M**, Decambron M, Lebas C, Moktefi A, Lemaitre L, Gnemmi V, Sautenet B, Glowacki F, Subtil D, Jourdain M, Rigouzzo A, Brocheriou I, Halimi JM, Rondeau E, Noel C, Provôt F, Hertig A. Am J Kidney Dis. 2016 Jan 16. pii: S0272-6386(15)01496-1. (IF:6.3)
6. Complement activation by heme as a secondary hit for atypical hemolytic uremic syndrome. **Frimat M**., F. Tabarin, J. D. Dimitrov, C. Poitou, L. Halbwachs-Mecarelli, V. Fremeaux-Bacchi, and L. T. Roumenina. Blood 2013; 122:282-292. (IF:9.8)
7. A prevalent C3 mutation in aHUS patients causes a direct C3 convertase gain of function. Roumenina, L. T*, **M. Frimat***, E. C. Miller, F. Provot, M. A. Dragon-Durey, P. Bordereau, S. Bigot, C. Hue, S. Satchell, P. Mathieson, C. Mousson, C. Noel, C. Sautes-Fridman, L. Halbwachs-Mecarelli, J. P. Atkinson, A. Lionet, and V. Fremeaux-Bacchi. Blood 2012; 119:4182-4191. (IF:9.1)

Color: Fig 1-6

The receptor for advanced glycation end products is a sensor for cell-free heme

Olivia May[1,2,3], Laure Yatime[4], Nicolas S. Merle[3], Florian Delguste[1], Mike Howsam[1], Marie V. Daugan[3], Charles Paul-Constant[1], MurielBillamboz[1,5], Alina Ghinet[1,5,6], Steve Lancel[1], Jordan D. Dimitrov[3,7,8], Eric Boulanger[1], Lubka T. Roumenina[3,7,8 ¶,*] & Marie Frimat[1,2¶,*]

[1] Univ. Lille, Inserm, Institut Pasteur de Lille, U1167 - RID-AGE, F-59000 Lille, France

[2] Univ. Lille, CHU Lille, Nephrology Department, F-59000, Lille, France

[3] INSERM, UMR_S 1138, Centre de Recherche des Cordeliers, F-75006, Paris, France

[4] LPHI, UMR 5235, University of Montpellier, CNRS, INSERM, F-34095, Montpellier, France

[5] Yncréa Hauts-de-France, Ecole des Hautes Etudes d'Ingénieur, UCLille, Health & Environment Department, Team Sustainable Chemistry, Laboratoire de Chimie Durable et Santé, 13 Rue de Toul, 59000, Lille, France

[6] 'Alexandru Ioan Cuza' University of Iasi, Faculty of Chemistry, Bd. Carol I nr. 11, 700506 Iasi, Romania

This article has been accepted for publication and undergone full peer review but has not been through the copyediting, typesetting, pagination and proofreading process, which may lead to differences between this version and the Version of Record. Please cite this article as doi: 10.1111/febs.15667

[7] Sorbonne Universités, UPMC Univ Paris 06, F-75006, Paris, France

[8] Université Paris Descartes, Sorbonne Paris Cité, F-75006, Paris, France

¶ *These authors contributed equally to this work.*

***Corresponding authors**

Dr. Marie Frimat, MD, PhD. U1167 - RID-AGE.

Nephrology Department, CHU Lille, 2 avenue Oscar Lambret, F-59000 Lille, France

Phone: 33-3-20-44-40-34/ Fax: 33-3-20-44-60-34,

E-mail: marie.frimat@chru-lille.fr

Lubka T. Roumenina, Ph.D. INSERM UMRS 1138, Centre de Recherche des Cordeliers, 15 rue de l'Ecole de Medecine, 75006 Paris, France

Phone: 33-1-44-27-90-96/ Fax: 33-1-40-51-04-20,

E-mail: lubka.roumenina@sorbonne-universite.fr

Running title: Free heme binds to RAGE

Abbreviations:

AGE: Advanced glycation end products

CML: Carboxymethyllysine

CoPPIX or Co(III)PP: Cobalt protoporphyrin IX chloride

DAMP: Damage-associated molecular pattern

Fe(III)pht: Fe(III) phthalocyanine chloride

Hb: Hemoglobin

HMGB-1: High mobility group box-1 protein

HPIX: Hematoporphyrin IX

MAPK: Mitogen-activated protein kinase

MgPPIX or Mg(II)PP: Magnesium protoporphyrin IX

MnPPIX or Mn(III)PP: Manganese protoporphyrin IX chloride

NADPH: Nicotinamide adenine dinucleotide phosphate

NF-κB: Nuclear factor kappa B

NHS: *N*-hydroxysuccinimide

PAMPs: Pathogen-associated molecular patterns

RAGE: Receptor for advanced glycation end-products

SEC: Size exclusion chromatography

SPR: Surface plasmon resonance

TLR4: Toll-like receptor 4

TF: Tissue factor

Key words: heme, protein interaction, iron, receptor for advanced glycation end products, receptor oligomerization.

Conflicts of Interest: The authors declare no conflict of interest

Abstract

Heme's interaction with toll-like receptor 4 (TLR4) does not fully explain the pro-inflammatory properties of this hemoglobin-derived molecule during intravascular hemolysis. The receptor for advanced glycation end-products (RAGE) shares many features with TLR4 such as common ligands and pro-inflammatory, -thrombotic and -oxidative signaling pathways, prompting us to study its involvement as a heme sensor.

Stable RAGE-heme complexes with micromolar affinity were detected as heme-mediated RAGE oligomerization. The heme binding site was located in the V domain of RAGE. This interaction was Fe^{3+}-dependent and competitive with carboxymethyllysine, another RAGE ligand. We confirmed a strong basal gene expression of RAGE in mouse lungs. After intraperitoneal heme injection, pulmonary TNFα, IL1β and tissue factor gene expression levels increased in WT mice but were significantly lower in their $RAGE^{-/-}$ littermates. This may be related to the lower activation of ERK1/2 and Akt observed in the lungs of heme-treated, $RAGE^{-/-}$ mice.

Overall, heme binds to RAGE with micromolar affinity and could promote pro-inflammatory and pro-thrombotic signaling *in vivo*, suggesting that this interaction could be implicated in heme overload conditions.

Introduction

Heme is an iron-containing complex involved in fundamental cellular functions, notably as a gas transporter in red blood cells where it is an essential component of hemoglobin (Hb). The heme prosthetic group retains the 4 pyrrole rings linked by a -CH group of its precursor protoporphyrin IX, with the addition, in its center, of an iron ion in a reduced Fe(II) or oxidized Fe(III) state [1]. Given the catalytic properties of the iron atom, and to limit oxidation processes, heme is strictly compartmentalized inside cells but can accumulate in blood during massive intravascular hemolysis when scavenging detoxification systems are overwhelmed. Free heme triggers vascular dysfunction, pro-inflammatory and pro-thrombotic effects by inducing nitric oxide scavenging and production of reactive oxygen species (together with Hb), and also by activating the complement and coagulation systems [2,3]. Moreover, heme acts as a damage-associated molecular pattern (DAMP) binding to toll-like receptor 4 (TLR4). *Via* TLR4, it mediates inflammatory processes such as the synthesis of pro-inflammatory cytokines, monocyte/macrophage activation, and mobilization of Weibel Palade bodies from endothelial cells [4–6]. The deleterious properties of free heme are not, however, fully explained by its interaction with TLR4, raising questions about the implication of other receptor(s) [7,8].

RAGE is a multi-ligand membrane receptor and member of the immunoglobulin (Ig) superfamily. It consists of three Ig-like domains, one variable (V) and two constant (C1 and C2) in the extracellular part, a single-pass transmembrane helix and a short cytosolic tail [9]. Like TLR4, RAGE plays a major role in immunity, especially through its binding to DAMPs and PAMPs (pathogen-associated molecular patterns). High mobility group box-1 protein (HMGB-1), S100A8/A9 heterodimer, S100A12 and bacterial lipopolysaccharides are common ligands of both TLR4 and RAGE. Both of these receptors promote the activation of major pro-inflammatory and pro-oxidative signalling pathways such as nuclear factor kappa B (NF-κB), mitogen-activated protein kinase (MAPK) or nicotinamide adenine dinucleotide phosphate (NADPH) oxidase [10,11]. Moreover, a synergistic cooperation between RAGE and TLR4 has been proposed as amplifying the inflammatory response in different endothelial cell or murine models [12,13].

Considering the common characteristics between RAGE and TLR4, and studies linking heme with other ligands of RAGE [14], we hypothesized that this receptor could interact with heme. Here

we characterized the binding of heme to RAGE, identified its binding domain and studied the effects of exposure to heme in a RAGE-KO mouse model.

Results

RAGE is a heme receptor

To test whether heme interacts with human RAGE (hRAGE), we analyzed the binding between heme and hRAGE-Fc using UV-visible absorbance spectroscopy. The spectra of the hRAGE-heme complex showed a concentration-dependent increase in the molar extinction coefficient at the so-called Soret band (~400 nm) in the presence of RAGE, without any shift in the maxima (**Figure 1A**). This did not reach saturation point, even at an 8-fold molar excess of heme, suggesting that heme induces RAGE oligomerization.

To further characterize the hRAGE-heme interaction and to possibly determine the stoichiometry of the complex, we performed size exclusion chromatography (SEC) experiments on a Superdex 75 Increase column. Incubation of hRAGE VC1C2 (corresponding to the domain from residues Ala23 to Pro323 with a predicted molecular weight of 33 kDa) with a 10-fold molar excess of heme led to the formation of a novel species eluting much earlier on the SEC column (7.6 mL) than the VC1C2 domain alone (9.6 mL) (**Figure 1B**, left side, dark blue and green curves, respectively). The novel species contained both the VC1C2 domain (as evaluated by SDS-PAGE analysis of the corresponding fractions, **Figure 1B**, right side), and the heme molecule (as assessed by UV absorption at 404 nm of the corresponding fractions, **Figure 1B**, red curve), whereas no absorption at 404 nm was observed for the same fractions in the chromatograms corresponding to either VC1C2 alone or heme alone (**Figure 1B**, cyan and dotted brown curves, respectively). As this novel species eluted quite early, almost in the void volume of the column, the experiment was repeated on a Superose 6 Increase column which enables separation of much higher molecular weight species. Again, on this column, incubation of VC1C2 with a 20-fold molar excess of heme led to the formation of higher molecular weight species which contained both hRAGE and the heme molecule (**Figure 1C**, left side, dark blue curve). The peak corresponding to the complex is quite broad with a shoulder on the leading edge, suggesting that the complex is large and heterogeneous, *i.e.* a mix of oligomers of various sizes is probably formed upon binding of heme to RAGE. Incubation of VC1C2 with lower concentrations of heme

(1- to 10-fold molar excess of heme; **Figure 1C**) led to the formation of intermediate species of lower molecular weight (dark arrow heads), indicating that RAGE molecules progressively cluster upon heme binding until all of the free RAGE has been consumed. For each VC1C2 / heme mixture analyzed by SEC, we also plotted the molar ratio of heme : VC1C2 in each peak fraction, by measuring the molar concentrations of both RAGE and heme from their absorbance at 280 and 404 nm, respectively (**Figure 1C,** right side). For all complexes thus isolated, an average of two to three molecules of heme were bound to VC1C2. Heme may also possibly bind to monomeric RAGE, although a large fraction of monomeric VC1C2 remains in the apo- form. In any case, the width of the SEC peaks indicates that RAGE : heme complexes are highly heterogeneous and probably exhibit various stoichiometries. These data must therefore be interpreted with caution and are not presented here as a reflection of the real stoichiometry of these complexes. The SEC experiments were repeated with shorter fragments of the RAGE extracellular domain. However, massive precipitation was observed in the samples upon incubation of heme with either the VC1 (residues Ala23 to Glu231) or V (residues Ala23 to Tyr118) domains suggesting that heme induces an uncontrolled aggregation of the RAGE fragments and formation of large, oligomeric species that are no longer soluble.

To provide an independent proof for the interaction of heme and hemozoin (a dark-brown heme crystal produced by the intraerythrocytic parasite Plasmodium which causes malaria) with RAGE, both were immobilized on a gelatin-coated surface and probed with biotinylated hRAGE ectodomain (fragment corresponding to residues Ala23 to Ala345 fused to a C-terminal biotinylated AviTag sequence). Strong and dose-dependent interactions were observed in both cases (**Figure 2A**). The interaction of heme and RAGE was further studied by surface plasmon resonance (SPR). Heme bound in a concentration-dependent manner to immobilized hRAGE-Fc (Kd= 7.57×10^{-5} M), but not to the Fc fragment alone (**Figure 2B**, left panel). This result was confirmed using home-made, recombinant tag-free hRAGE VC1C2, to which heme bound with even higher affinity (Kd= 6.78×10^{-6} M). This binding was detected even at the very low heme concentration of 40nM (**Figure 2B**, right panel).

Taken together, our results suggest that RAGE binds heme and that this interaction induces receptor oligomerization.

The V domain of RAGE is the binding site for heme

To localize the heme-binding domain of RAGE, we used recombinant fragments VC1, C2 (residues Pro232 to Pro323) and V and tested their interaction with heme by SPR (**Figure 3A**). The C1 domain could not be tested alone because its binding was not stable. We observed that heme bound directly to both VC1 and V but not C2, meaning that the binding site was on the V domain. We tested carboxymethyllysine-modified Bovine Serum Albumin (CML-BSA) in the same conditions and confirmed that CML binds to the V domain [15] (**Figure 3B**).

To validate that the V domain contains the heme binding site, we performed an absorbance spectroscopy assay with heme and the recombinant V (**Figure 3C**) and C2 (**Figure 3D**) domains. Concentration-dependent increases in the molar extinction coefficient at the Soret band were detected for the V domain but not for C2, confirming the results obtained by SPR. Again, the interaction showed no saturation even at high heme : V domain ratios, suggesting oligomer formation as observed for the full-length RAGE ectodomain.

RAGE interacts with molecules containing transition metals

To understand the role played by the different structural elements of heme (the pyrrolic structure and the iron ion), we examined RAGE's interaction with hematoporphyrin IX (HPIX, heme without iron), other iron-carrying molecules, and porphyrins containing different transition metals.

HPIX bound to hRAGE and the V domain-containing constructs (**Figure 4A**), but with lower affinity compared with heme (RU ~10 fold lower). The binding of hRAGE VC1C2 to HPIX was also evaluated with SEC. As shown in **Figure 1C** (gray curve), no complexes similar to those formed by VC1C2 and heme were detected upon incubation of VC1C2 with a 10-fold molar excess of HPIX. A small amount of aggregated protein was detected in the void volume (fractions 14-15 of the gray curve) probably due to partial precipitation of HPIX upon mixing in the aqueous SEC buffer, the precipitated HPIX compound being also present in the void volume (**Figure 4B**, magenta curve). In any case, most of the VC1C2 protein remained in the monomeric form (peak eluting at 17.5 mL) and uncomplexed (no UV absorption at 600 nm detected in the fractions around 17.5 mL for the VC1C2:HPIX mix). Thus, no stable complex seems to have been formed between RAGE and HPIX on the SEC column.

In a novel finding, we observed that Fe(III)-phtalocyanine binds directly to RAGE (**Figure 4C**). A similar result, but with much lower intensity, was observed for ferroin, namely 1,10-Phenanthroline iron(II) sulfate complex. Moreover, protoporphyrins with transition metal ions other than Fe (Mn(III)PP, Co(III)PP) also bound to RAGE, albeit with a lower affinity than heme. *A contrario*, Mg(II)PP, bearing a divalent cation but lacking a transition metal ion, did not interact with RAGE (**Figure 4D**).

Heme perturbs the interaction of RAGE with its classical carboxymethyllysine ligand

To find out whether exposure to heme alters the capacity of RAGE to bind to carboxymethyllysine (CML), its classical ligand, we performed a competition assay by SPR. After immobilization of hRAGE, heme or buffer was injected. Then, without regeneration, CML-BSA or control-BSA was introduced to the system. After heme injection, the binding between CML and RAGE was no longer detected (**Figure 4E**).

RAGE contributes to heme-mediated pro-inflammatory and pro-thrombotic signaling in the lungs of mice

As the expression of RAGE is described as being highest in the lungs (**Figure 5A-B**), we analyzed RAGE signaling pathways in this organ in WT and *RAGE*$^{-/-}$ mice, injected or not with heme (100µmol/kg) and sacrificed one day after treatment. We confirmed a strong basal expression of both the RAGE gene and protein in lungs (data not shown), that was not modified by heme (**Figure 5C**). Exposure to heme was confirmed by expression of HO-1, a heme-induced enzyme, which served as a positive control (**Figure 5D**), measurement of the exact amount of injected heme reaching the lungs *vs.* the high level of endogenous heme being technically impossible.

In WT mice, heme injection induced increased expression of several inflammation mediators, as compared to PBS injection, respectively ~2.5, ~2 and ~21.9-fold increases for *IL1β*, *TNFα* and *IL6* (**Figure 5F**). The basal expression of these inflammation mediators after PBS injection was not different in *RAGE*$^{-/-}$ compared with WT mice. After heme treatment however, *IL1β* increased ~2.2-fold less in *RAGE*$^{-/-}$ mice than in WT mice (p=0.02). *TNFα* did not increase in *RAGE*$^{-/-}$ mice treated with heme: gene expression was 0.63-fold that of PBS-treated *RAGE*$^{-/-}$ mice. For *IL6*, no differences were observed between heme-treated WT and *RAGE*$^{-/-}$ mice. The pro-thrombotic

phenotype was assessed by *tissue factor* (TF) expression. In WT mice, injection of heme was associated with a ~4.5-fold increase in TF expression, while only a ~3.3-fold increase was observed in *RAGE*$^{-/-}$ mice **(Figure 5E)**.

Heme activates signaling pathways via RAGE, leading to phosphorylation of ERK 1/2 and AKT

To understand the mechanisms of the protective effect of RAGE invalidation, we studied two pathways activated by heme and RAGE: ERK1/2 and Akt [16–18]. The ratio of phospho-ERK : ERK-total was weakly modified by the injection of heme in WT mice (~1.5 fold-increase), whereas it decreased in heme-treated *RAGE*$^{-/-}$ mice compared with control *RAGE*$^{-/-}$ mice. After heme treatment, the phospho-ERK : ERK-total ratio in *RAGE*$^{-/-}$ mice was indeed ~0.5 fold lower than in WT mice (**Figure 6A**). Similar results were observed with the Akt pathway. In heme-treated WT mice, the phospho-Akt : Akt-total ratio increased ~1.1-fold compared to control mice, whereas the heme treatment induced a significant decrease of the ratio of phospho-Akt : Akt-total in *RAGE*$^{-/-}$ mice (~0.29-fold, **Figure 6B**).

Discussion

Here we provide the first evidence that heme is a ligand of RAGE and binds within the V domain. This interaction resulted in formation of RAGE oligomers and perturbed the binding of the classical RAGE ligand (CML) that interacts within the V domain of RAGE. *In vivo*, RAGE deficiency appears to attenuate the pro-inflammatory and pro-thrombotic phenotype induced by administration of heme.

Heme is a known ligand of TLR4 and we hypothesized that it is also a ligand of RAGE. Biosensor analyses revealed that heme binds to RAGE with apparent micromolar affinity and that the heme binding site is localized within the V domain, known to serve as a binding platform for many ligands of RAGE [19]. Taken together, SEC experiments and SPR results suggest that while the protoporphyrin core of heme can interact weakly and transiently with RAGE, probably through hydrophobic contacts with apolar residues on the surface of the receptor, the strength of the interaction resides mainly in the chelation of the central iron ion [20,21]. Indeed, we found that two other Fe-containing molecules (Fer(III)-phtalocyanine and ferroin) both bound to RAGE in

SPR, as did protoporphyrins containing other transition metals (Mn(III)PP, Co(III)PP), while a porphyrin lacking a transition metal ion (Mg(II)PP) did not. In addition, the oxidation state of the central ion appeared to influence the strength of the binding: ferroin, which has an oxidation state of 2^+ and not 3^+, bound to RAGE but with much lower affinity than heme or Iron(III)-phthalocyanine. These findings suggest that characteristics of the central metal ion in the porphyrins play an important role in the interaction of heme with RAGE.

Our assay revealed competition between heme and CML, the most-studied ligand of RAGE among the advanced glycation end products (AGE), which also binds to the V domain with an affinity of Kd~100 μM [15,22]. The binding sites of CML and heme must therefore overlap, at least partially, on the RAGE surface and the reports that CML binding to RAGE engenders pro-inflammatory and pro-fibrotic signaling suggests there may also be negative consequences to heme overload due to hemolysis, rhabdomyolysis, atherosclerosis, etc. Further studies are needed to identify whether heme shares the same signaling pathway as AGEs and what the physiological consequences of this competition could be. It has already been shown that heme does not share the same signaling pathway as LPS upon binding to TLR4 [8,23–25].

The spectral data obtained here indicate that binding of heme to the V domain of RAGE is not accompanied by changes in the molecular environment. The absence of shifts in the absorbance maxima suggests that heme likely binds to the surface of the protein. The fact that the binding of heme to RAGE and its V domain was not saturable, along with the detection of oligomers by SEC, suggest that this surface-exposed heme stimulates homophilic interactions, as previously observed for C3 [26]. RAGE is known to form oligomers on the cell surface, potentiated by S100B and AGEs among others, and oligomerization is a key element for signal transduction [15,27]. Part of RAGE oligomerization occurs via dimerization of the V domain, which serves as an initial clustering point for RAGE molecules, even in the absence of ligands, and this could be amplified by association of other domains of RAGE to which ligands are bound, as suggested for S100B or S100A6 [28,29]. Heme is a very hydrophobic molecule with a tendency to form aggregates, and heme dimers and higher-order oligomers could thus also serve as bridges between two or more RAGE molecules. Moreover, we observed that heme aggregates in the form of hemozoin also interacted with RAGE *in vitro*. Taken together, our data suggest that heme acts in a similar

manner to other RAGE ligands: it binds to the V domain, induces RAGE clustering and subsequent signal transduction, and potentially triggers pro-inflammatory and pro-coagulant cell responses.

Both TNFα and IL1β are known inflammatory mediators, released from macrophages after stimulation by heme [24,30]. We tested the contribution of RAGE to heme-mediated inflammation in the lungs, and confirmed previous findings that this organ has a very strong basal RAGE expression, especially in alveolar type I cells [31,32]. Although the small sample sizes necessitate caution in interpreting our results, our *in vivo* experiments show that heme induced TNFα and IL1β expression and that this induction was smaller in RAGE knock-out mice. Therefore, RAGE signaling could contribute to local inflammation in the lungs, possibly in concert with TLR4. Heme also activates the coagulation cascade [3]. Indeed, heme has been shown to trigger tissue factor expression and coagulation activation on macrophages and perivascular cells in the lungs of heme-injected mice and heme-exposed human leucocytes *ex vivo* [33,34]. These processes are TLR4-dependent [35]. We again found upregulation of tissue factor in the lungs of WT mice injected with heme in our study. This effect was attenuated in RAGE deficient mice, suggesting a role for RAGE in combination with TLR4. Our observation of decreased levels of phosphorylated ERK and AKT in heme-exposed $RAGE^{-/-}$ mice could indicate a role for RAGE invalidation in limiting hemolysis-induced inflammation. Taken together, these findings confirm our hypothesis that RAGE has a potentially important role in heme sensing in a complex environment, and add weight to the theory of a pro-inflammatory RAGE-TLR4 loop that has been suggested in different disease models [36–39]. Testing in single- and double-knockout $RAGE^{-/-}$ and $TLR4^{-/-}$ cell lines or mice is now needed to understand the distinct role of each receptor in heme-induced signaling.

In summary, although the effects of free heme are well documented, the molecular sensors of this small molecule on the cell surface and in plasma remain largely unknown, with only TLR4 described as a membrane receptor. Reducing the inflammatory response and tissue injury in pathologies associated with heme release requires a better understanding of how cell-free heme is detected. In a novel finding, we here report that heme is a ligand for RAGE, binding to the V domain and inducing RAGE oligomerization. *In vivo* stimulation of RAGE by heme can result in a pro-inflammatory and pro-coagulant phenotype in the lungs. This supports the classification of RAGE as a pattern recognition receptor, as well as propositions that it plays a pathologic role

beyond those already described for it in diabetes mellitus. These findings also underline the potential importance of the RAGE-heme interaction in hemolytic diseases and raise the possibility of it being a therapeutic target to reduce hemolysis-mediated tissue injury.

Materials and Methods

Reagents

The Fe^{3+} form of heme [hemin (ferriprotoporphyrin IX), designated as heme (Frontier Scientific or Sigma-Aldrich)], Manganese protoporphyrin IX chloride (MnPPIX or Mn(III)PP, Frontier Scientific), Cobalt protoporphyrin IX chloride (CoPPIX or Co(III)PP, Frontier Scientific) and Magnesium protoporphyrin IX (MgPPIX or Mg(II)PP, Frontier Scientific) were dissolved to 10 mM in 50mM NaOH and 145mM NaCl. Hematoporphyrin IX (HPIX, Sigma-Aldrich) was dissolved to 5 mM in 50mM NaOH and 145mM NaCl. Fe(III) phthalocyanine chloride (Fe(III)pht, Sigma-Aldrich) and 1,10-Phenanthroline iron(II) sulfate complex (designated as ferroin, Sigma Aldrich) were dissolved to 10mM in H_2O. Reagents were stored in the dark and further diluted in appropriate vehicle solvent just before use.

Carboxymethyllysine-modified Bovine Serum Albumin (CML-BSA) and non-glycated BSA (control-BSA) were obtained as previously described [40]. After glycation (16h, 37°C), 37–40% of the lysine moieties were found to be modified, 80–99% of which (on a molar basis) had been modified to CML. The control-BSA was prepared under the same conditions but glyoxylic acid was omitted.

Recombinant human RAGE proteins

Different recombinant forms of the extracellular domain of the human RAGE receptor (hRAGE) were used. A fully glycosylated version of the protein (residues Gln24 to Ala344), produced in the mouse myeloma cell line NS0 as a fusion with the Fc fragment of human IgG1, was purchased from R&D Systems. This form, denoted hRAGE-Fc, was reconstituted at 100 µg/mL in sterile PBS. Recombinant Human IgG1 Fc, expressed in the same mouse cell line and reconstituted at 100µg/mL in sterile PBS, was used as a control protein (R&D Systems). Unglycosylated and shorter versions of hRAGE extracellular domain, devoid of fusion protein, were also expressed

recombinantly in bacteria as previously described [9]: the VC1C2 domain (residues Ala23 to Pro323), the VC1 fragment (residues Ala23 to Glu231) and the isolated V (residues Ala23 to Tyr118) and C2 (residues Pro232 to Pro323) domains. Briefly, all proteins were expressed in *E.coli* Shuffle T7 Express cells (New England Biolabs) with a cleavable N-terminal polyhistidine (His_6) tag. The proteins were then purified by two-step affinity chromatography on a Nickel column with removal of the His_6-tag by cleavage with TEV protease between the two chromatographic steps. The proteins were further purified using either cation exchange chromatography (V, VC1 and VC1C2 domains) or size exclusion chromatography (C2 domain). All proteins were finally transferred into a buffer containing 20mM Tris-HCl pH 7.5 and 200mM NaCl, then flash-frozen in liquid nitrogen and stored at -80ºC until use. Biotinylated hRAGE ectodomain (residues Ala23 to Ala345 followed by C-ter AviTag) was expressed recombinantly in bacteria and purified using the same protocol as for hRAGE VC1C2. The central Lys residue on the C-ter AviTag was then biotinylated *in vitro* using home-made recombinant Bir A ligase, at a molar ratio of 1 : 20 as compared to hRAGE ectodomain, in the presence of 2 mM D-biotin and 5 mM ATP/ $MgCl_2$. Biotinylation was performed at 18ºC for 60 hours. The sample was further purified using cation exchange chromatography to separate biotinylated RAGE from unreacted sample and D-biotin. The biotinylation level of the sample was assessed with HABA reagent (Pierce Biotin Quantitation Kit).

Spectrophotometry absorbance

UV-visible spectroscopic assays for the binding of heme to RAGE protein (hRAGE-Fc from R&D systems and domains V and C2 alone) were performed in PBS, pH 7.4, with a UNICAM Helios b, UV-visible spectrophotometer, as previously described [26,41,42]. A stock solution of heme (10mM), dissolved in 50mM NaOH and 145mM NaCl, was added to the buffer (at concentrations of 0 to 8µM) containing separate RAGE proteins (1µM). After heme addition, the samples were homogenized. The absorption spectra of the solutions were then recorded in the wavelength range from 350 to 650 nm. The absorption spectra of RAGE proteins alone in the range 350–650 nm were also recorded and were found to be similar to the background absorbance of the buffer alone. For titration of the binding of heme to RAGE proteins, aliquots from a heme stock solution were added to 1µM solution of hRAGE and domains and to reference cuvette containing PBS

only. After each addition, samples in the two cuvettes were homogenized at 25°C. Then, differences in absorption spectra were recorded. The RAGE proteins - heme binding curves were built by plotting the difference in absorbance (*A*heme-RAGE protein – *A*heme) at 390 nm *versus* molar concentrations of heme.

Size exclusion chromatography

Size exclusion chromatography (SEC) experiments to assess the formation of stable complexes between RAGE and heme were performed at 18ºC on either a 24mL Superdex 75 Increase column or on a 24 mL Superose 6 Increase column (GE Healthcare Life Sciences) connected to an Äkta Purifier system (GE Healthcare Life Sciences), and both equilibrated in a buffer containing 20mM Tris-HCl pH 8.0, 200mM NaCl (SEC buffer). 400µg of hRAGE VC1C2, VC1 or V domains were incubated for 2h at room temperature in SEC buffer either alone or in the presence of a molar excess of heme (1 to 20-fold excess) or of HPIX (10-fold molar excess). Elution on the SEC column was performed in SEC buffer at a flow rate of 0.5 mL/min and fractions of 0.5 mL were collected during the entire elution. UV absorbance was monitored at 280, 404 and 600 nm. The mean values of the UV absorbance measured at 280 and 404 nm were collected for each peak fraction of the chromatograms. Molar concentrations for both VC1C2 and heme were derived from these values using a molar extinction coefficient at 280 nm of 39 335 $M^{-1}.cm^{-1}$ for VC1C2, and a molar extinction coefficient at 404 nm of 170 000 $M^{-1}.cm^{-1}$ for heme. For each VC1C2 : heme mix analyzed by SEC, the average heme : VC1C2 molar ratio in each peak fraction was then reported as a histogram.

ELISA for the Interaction of biotinylated RAGE with hemin and hemozoin

To test the interaction of hemin (Fronter Scientific) and hemozoin (InvivoGen) with RAGE, an ELISA approach was applied as previously described [43]. Briefly, plates were coated with 0.25% gelatin (diluted in PBS) and incubated for 1 h at room temperature. Further, hemin or hemozoin were immobilized on gelatin. To this end, hemin was diluted in 1:1 (DMSO:water) to 1mM and hemozoin was diluted to 100 µg/ml in PBS. Solutions thus obtained were applied at 50 µl/well on two different gelatin-coated plates and 25 µl/well of an aqueous 60 mM EDC solution was added for cross-linking. After incubation for 2 h at room temperature, in the dark with regular shaking

of the plates, they were washed 3x with distilled water, followed by incubation with 100 µl/well of 1 M ethanolamine-HCl (pH 8) for 5 min. After 3x washes, the plates were blocked with 0.25% Tween 20 in PBS for 1 h at room temperature. Plates were washed again and incubated with different concentrations of recombinant, C-terminally biotinylated hRAGE ectodomain in PBS, containing 0.05% Tween 20 (T-PBS) for 1 h at room temperature. After 5 washes with T-PBS, the plates were incubated for 30 min at RT with streptavidin-HRP diluted 200x in T-PBS. Following 5 washes, the signal was developed with OPD Sigma Fast substrate system. The reaction was stopped with 2M HCl and the absorbance measured at 492 nm.

Surface plasmon resonance (SPR)

hRAGE-Fc, IgG1 Fc, VC1C2, V, VC1 and C2 domain proteins were immobilized on a CM5 Biacore sensor chip surface by amine coupling (Biacore) in buffer containing 10mM HEPES (pH 7.4), 150mM NaCl, 3mM EDTA and 0,005% Tween 20. Briefly, the CM5 Biacore chip was activated for 7 minutes using 0.1M *N*-hydroxysuccinimide (NHS) and 0.4M (*N*-(3-dimethylaminopropyl)-*N'*-ethylcarbodiimide (EDC) mixed at 1:1 (v/v) ratio. hRAGE (hRAGE-Fc or VC1C2) (10µg/mL in 10mM sodium acetate [pH 5.5]), IgG1 Fc (10µg/mL in 10mM sodium acetate [pH 5]), V (30µg/mL in 10mM sodium acetate [pH 5.5]), VC1 (15µg/mL in 10mM sodium acetate [pH 5.5]), and C2 (15µg/mL in 10mM sodium acetate [pH 3]) domains were directly captured through amine coupling, and deactivated with 1M ethanolamine-HCl. The coupling density of the surface for each of the proteins was: hRAGE (6000 response units [Ru]), Fc (3500 Ru), V (4000 Ru), VC1 (3000 Ru) and C2 (2000 Ru) domains. The activated/deactivated surface was used as the blank control. Real-time biomolecular interaction between porphyrins (heme, MnPPIX, CoPPIX, MgPPIX and HPIX), iron-containing molecules (Fe(III)-phtalocyanine and ferroin (Fe(II)), CML-BSA, control-BSA and different hRAGE protein fragments were performed at 25°C, pH 7.2 - 7.4. A series of 7 cascade dilutions of heme from 2500 to 40nM were injected for 5 min at a flow rate of 10µL/min. All surfaces were completely regenerated by a 30s pulse of a solution of 0.5M imidazole after heme binding or 1M NaCl and 50mM NaOH after other binding of other molecules. Data were processed using the blank surface as reference and buffer injections as background.

Evaluation was carried out using BIAevaluation Software (GE Healthcare). The response curves were obtained by subtraction of the signals over the reference surface from the binding response to RAGE immobilized surface, by fit of sensorgrams. Affinity was determined by kinetic analysis.

RAGE expression plot

Mouse transcriptomic data - RNASeq data from the GEO GSE74747 study was used to examine *Ager* gene expression (Transcript per million) in 9 different mouse tissues.

Human transcriptomic data - GTEx data was used to access to *Ager* gene expression (Transcript per million) in different human tissues. The Genotype-Tissue Expression (GTEx) Project was supported by the Common Fund of the Office of the Director of the National Institutes of Health, and by NCI, NHGRI, NHLBI, NIDA, NIMH, and NINDS. The data used for the analyses described in this manuscript were obtained from the GTEx Portal on 01/04/2020 [44].

Animal experimentation

All experiments were conducted in accordance with the recommendations for the care and use of laboratory animals of the French Ministry of Agriculture and with the approval of Ethics Committee for animal experimentation (Lille, France, APAFiS #15214). Seven to 10 month old WT (Janvier Laboratories, Le Genest-St-Isle, France) and $RAGE^{-/-}$ (from Pr. A.M. Schmidt, New York University) C57Bl/6 littermate mice (4-5group) were treated with intraperitoneal injection of 300µL of PBS or freshly prepared heme (100µmol/kg corresponding to 67.5µg/g body weight) at day 0, using a protocol adapted from our previous study [45]. At day 1, mice were culled, and lungs were recovered and conserved in RNAlater (Thermo fisher) for RNA extraction, or frozen in dry ice for western blot assays.

RTqPCR. RNA extraction from lungs was performed with TRIzol™ Reagent from Invitrogen™ (Thermo Fisher Scientific). Quality and quantity of RNA were measured by Nanodrop. RNA integrity was considered acceptable if absorbance ratio A260/280 was > 1.8 and ratio A260/230 in 1.8 and 2.2 ranges. After standard retrotranscription, amplification of cDNA was performed with the following probes: RAGE - Mm01134785_g1, IL1 - Mm434228_m1, IL6 - Mm446190_m1, TNFα - Mm00443258_m1 and Tissue Factor - Mm0438855_m1. Data were analyzed by QuantStudio™ software. The mean cycle threshold (CT) values for both the target

and internal control (*ppia*) were determined for each sample. The fold change in the target gene, normalized to *ppia* and relative to the expression of untreated condition, was calculated as $2^{-\Delta\Delta CT}$.

Western Blot. Lungs were lysed in RadioImmunoPrecipitation Assay (RIPA) buffer and 25µg were deposited on Bolt™ 4-12% pre-casted acrylamide gels (Bis-Tris Plus Gels, 15-well, Invitrogen™ Thermo Fisher Scientific). After 7 minutes transfer by "Trans-Blot Turbo" on the PVDF membrane, membranes were saturated with BSA 5% for one hour at room temperature. Then, primary antibodies were incubated overnight at 4°C: anti-ERK1/2 (Cell Signaling 4695S, dilution 1/1000), anti-phosphoERK1/2 (Cell Signaling 4376S, dilution 1/1000), anti-Akt (R&D MAB2055, dilution 1/2500), anti-phosphoAkt (R&D AF887, dilution 1/500). Anti-GAPDH antibody (Santa Cruz sc32233, dilution 1/500) was incubated during 1h30 at room temperature the day after. After washing, the secondary antibodies used, incubated 1h30 at room temperature, were either anti-Rabbit HRP (Cell Signaling HRP 7074S, dilution 1/5000) for ERK, phosphoERK and phospoAkt, or anti-Mouse HRP (Cell Signaling 7076, dilution 1/5000) for Akt and GAPDH. WB were revealed by chemiluminescence (ECL BioRad Clarity).

Statistics

Statistical analysis was performed with GraphPad software. Data are presented as mean and standard deviation (SD). A Mann-Whitney test was used for comparisons. A *p*-value <0.05 was considered as significant.

Author contributions

OM, LR and MF conceived and designed the study. OM and JD performed spectrophotometry absorbance and SPR experiments. LY designed and performed SEC experiments. RAGE expression plot was performed by MD. Synthesis and characterization of compounds were performed by LY, AG and MB. EB provided $RAGE^{-/-}$ mice. Animal studies were performed by OM, CPC, FD and SL. The manuscript was written by OM, LR and MF with input from all other authors. All authors discussed the data and approved the submission. MH provided English proofreading assistance.

Acknowledgments

This work was supported by grants from Fondation du Rein under the aegis of the French Medical Research Foundation AMGEN 2014 FdR-SdN / FRM to MF, Agence Nationale de la Recherche ANR JCJC - INFLACOMP 2015-2018 ANR-15-CE15-0001 to LTR and INSERM. We are grateful to the DHURE (University of Lille, experimental research department) for their support with the animal experimentation. We thank Amélie Pau, Solenne Dezitter and Chantal Fradin for their practical assistance. We are grateful to Véronique Fremeaux-Bacchi, Dominique Guerrot, Marc Hazzan and Fatouma Touré for the fruitful discussions.

References

1 Kumar S & Bandyopadhyay U (2005) Free heme toxicity and its detoxification systems in human. *Toxicol Lett* **157**, 175–188.

2 Frimat M, Boudhabhay I & Roumenina LT (2019) Hemolysis Derived Products Toxicity and Endothelium: Model of the Second Hit. *Toxins* **11**, 660.

3 Roumenina LT, Rayes J, Lacroix-Desmazes S & Dimitrov JD (2016) Heme: Modulator of Plasma Systems in Hemolytic Diseases. *Trends Mol Med* **22**, 200–213.

4 Figueiredo RT, Fernandez PL, Mourao-Sa DS, Porto BN, Dutra FF, Alves LS, Oliveira MF, Oliveira PL, Graça-Souza AV & Bozza MT (2007) Characterization of heme as activator of Toll-like receptor 4. *J Biol Chem* **282**, 20221–20229.

5 Belcher JD, Chen C, Nguyen J, Milbauer L, Abdulla F, Alayash AI, Smith A, Nath KA, Hebbel RP & Vercellotti GM (2014) Heme triggers TLR4 signaling leading to endothelial cell activation and vaso-occlusion in murine sickle cell disease. *Blood* **123**, 377–390.

6 Belcher JD, Zhang P, Nguyen J, Kiser ZM, Nath KA, Hu J, Trent JO & Vercellotti GM (2020) Identification of a Heme Activation Site on the MD-2/TLR4 Complex. *Front Immunol* **11**.

7 Merle NS, Paule R, Leon J, Daugan M, Robe-Rybkine T, Poillerat V, Torset C, Frémeaux-Bacchi V, Dimitrov JD & Roumenina LT (2019) P-selectin drives complement attack on endothelium during intravascular hemolysis in TLR-4/heme-dependent manner. *Proc Natl Acad Sci USA* **116**, 6280–6285.

8 Prestes EB, Alves LS, Rodrigues DAS, Dutra FF, Fernandez PL, Paiva CN, Kagan JC & Bozza MT (2020) Mitochondrial Reactive Oxygen Species Participate in Signaling Triggered by Heme in Macrophages and upon Hemolysis. *The Journal of Immunology*.

9 Yatime L & Andersen GR (2013) Structural insights into the oligomerization mode of the human receptor for advanced glycation end-products. *FEBS J* **280**, 6556–6568.

10 Teissier T & Boulanger É (2019) The receptor for advanced glycation end-products (RAGE) is an important pattern recognition receptor (PRR) for inflammaging. *Biogerontology* **20**, 279–301.

11 Chang ZL (2010) Important aspects of Toll-like receptors, ligands and their signaling pathways. *Inflamm Res* **59**, 791–808.

12 Yamamoto Y, Harashima A, Saito H, Tsuneyama K, Munesue S, Motoyoshi S, Han D, Watanabe T, Asano M, Takasawa S, Okamoto H, Shimura S, Karasawa T, Yonekura H & Yamamoto H (2011) Septic shock is associated with receptor for advanced glycation end products ligation of LPS. *J Immunol* **186**, 3248–3257.

13 Lv B, Wang H, Tang Y, Fan Z, Xiao X & Chen F (2009) High-mobility group box 1 protein induces tissue factor expression in vascular endothelial cells via activation of NF-kappaB and Egr-1. *Thromb Haemost* **102**, 352–359.

14 Flemmig J, Zámocký M & Alia A (2018) Amyloid β and free heme: bloody new insights into the pathogenesis of Alzheimer's disease. *Neural Regen Res* **13**, 1170.

15 Xie J, Reverdatto S, Frolov A, Hoffmann R, Burz DS & Shekhtman A (2008) Structural basis for pattern recognition by the receptor for advanced glycation end products (RAGE). *J Biol Chem* **283**, 27255–27269.

16 Wang J-Y, Lee Y-T, Chang P-F & Chau L-Y (2009) Hemin promotes proliferation and differentiation of endothelial progenitor cells via activation of AKT and ERK. *J Cell Physiol* **219**, 617–625.

17 Ishihara K, Tsutsumi K, Kawane S, Nakajima M & Kasaoka T (2003) The receptor for advanced glycation end-products (RAGE) directly binds to ERK by a D-domain-like docking site. *FEBS Lett* **550**, 107–113.

18 Qin Q, Niu J, Wang Z, Xu W, Qiao Z & Gu Y (2013) Heparanase induced by advanced glycation end products (AGEs) promotes macrophage migration involving RAGE and PI3K/AKT pathway. *Cardiovasc Diabetol* **12**, 37.

19 Bongarzone S, Savickas V, Luzi F & Gee AD (2017) Targeting the Receptor for Advanced Glycation Endproducts (RAGE): A Medicinal Chemistry Perspective. *J Med Chem* **60**, 7213–7232.

20 Schneider S, Marles-Wright J, Sharp KH & Paoli M (2007) Diversity and conservation of interactions for binding heme in b-type heme proteins. *Nat Prod Rep* **24**, 621–630.

21 Li T, Bonkovsky HL & Guo J (2011) Structural analysis of heme proteins: implications for design and prediction. *BMC Struct Biol* **11**, 13.

22 Syed A, Zhu Q & Smith EA (2016) Ligand binding affinity and changes in the lateral diffusion of receptor for advanced glycation endproducts (RAGE). *Biochim Biophys Acta* **1858**, 3141–3149.

23 Porto BN, Alves LS, Fernández PL, Dutra TP, Figueiredo RT, Graça-Souza AV & Bozza MT (2007) Heme induces neutrophil migration and reactive oxygen species generation through signaling pathways characteristic of chemotactic receptors. *J Biol Chem* **282**, 24430–24436.

24 Fortes GB, Alves LS, de Oliveira R, Dutra FF, Rodrigues D, Fernandez PL, Souto-Padron T, De Rosa MJ, Kelliher M, Golenbock D, Chan FKM & Bozza MT (2012) Heme induces programmed necrosis on macrophages through autocrine TNF and ROS production. *Blood* **119**, 2368–2375.

25 Fernandez PL, Dutra FF, Alves L, Figueiredo RT, Mourão-Sa D, Fortes GB, Bergstrand S, Lönn D, Cevallos RR, Pereira RMS, Lopes UG, Travassos LH, Paiva CN & Bozza MT (2010) Heme Amplifies the Innate Immune Response to Microbial Molecules through Spleen Tyrosine Kinase (Syk)-dependent Reactive Oxygen Species Generation. *J Biol Chem* **285**, 32844–32851.

26 Frimat M, Tabarin F, Dimitrov JD, Poitou C, Halbwachs-Mecarelli L, Fremeaux-Bacchi V & Roumenina LT (2013) Complement activation by heme as a secondary hit for atypical hemolytic uremic syndrome. *Blood* **122**, 282–292.

27 Zong H, Madden A, Ward M, Mooney MH, Elliott CT & Stitt AW (2010) Homodimerization is essential for the receptor for advanced glycation end products (RAGE)-mediated signal transduction. *J Biol Chem* **285**, 23137–23146.

28 Xue J, Manigrasso M, Scalabrin M, Rai V, Reverdatto S, Burz DS, Fabris D, Schmidt AM & Shekhtman A (2016) Change in the Molecular Dimension of a RAGE-Ligand Complex Triggers RAGE Signaling. *Structure* **24**, 1509–1522.

29 Yatime L, Betzer C, Jensen RK, Mortensen S, Jensen PH & Andersen GR (2016) The Structure of the RAGE:S100A6 Complex Reveals a Unique Mode of Homodimerization for S100 Proteins. *Structure* **24**, 2043–2052.

30 Dutra FF, Alves LS, Rodrigues D, Fernandez PL, de Oliveira RB, Golenbock DT, Zamboni DS & Bozza MT (2014) Hemolysis-induced lethality involves inflammasome activation by heme. *Proc Natl Acad Sci USA* **111**, E4110-4118.

31 Brett J, Schmidt AM, Yan SD, Zou YS, Weidman E, Pinsky D, Nowygrod R, Neeper M, Przysiecki C & Shaw A (1993) Survey of the distribution of a newly characterized receptor for advanced glycation end products in tissues. *Am J Pathol* **143**, 1699–1712.

32 Dahlin K, Mager EM, Allen L, Tigue Z, Goodglick L, Wadehra M & Dobbs L (2004) Identification of Genes Differentially Expressed in Rat Alveolar Type I Cells. *Am J Respir Cell Mol Biol* **31**, 309–316.

33 Sparkenbaugh EM, Chantrathammachart P, Wang S, Jonas W, Kirchhofer D, Gailani D, Gruber A, Kasthuri R, Key NS, Mackman N & Pawlinski R (2015) Excess of heme induces tissue factor-dependent activation of coagulation in mice. *Haematologica* **100**, 308–314.

34 de Souza GR, Hounkpe BW, Fiusa MML, Colella MP, Annichino-Bizzacchi JM, Traina F, Costa FF & De Paula EV (2017) Tissue factor-dependent coagulation activation by heme: A thromboelastometry study. *PLoS ONE* **12**, e0176505.

35 Rehani T, Mathson K, Belcher JD & Vercellotti GM (2013) Heme Potently Stimulates Tissue Factor Expression By Peripheral Blood Monocytes: A Novel Mechanism For Thrombosis In Intravascular Hemolytic Diseases. *Blood* **122**, 2215–2215.

36 Kovačić M, Mitrović-Ajtić O, Beleslin-Čokić B, Djikić D, Subotički T, Diklić M, Leković D, Gotić M, Mossuz P & Čokić VP (2018) TLR4 and RAGE conversely mediate pro-inflammatory

S100A8/9-mediated inhibition of proliferation-linked signaling in myeloproliferative neoplasms. *Cell Oncol (Dordr)*.

37 Salem A, Almahmoudi R, Vehviläinen M & Salo T (2018) Role of the high mobility group box 1 signalling axes via the receptor for advanced glycation end-products and toll-like receptor-4 in the immunopathology of oral lichen planus: a potential drug target? *Eur J Oral Sci* **126**, 244–248.

38 Nielsen TB, Pantapalangkoor P, Yan J, Luna BM, Dekitani K, Bruhn K, Tan B, Junus J, Bonomo RA, Schmidt AM, Everson M, Duncanson F, Doherty TM, Lin L & Spellberg B (2017) Diabetes Exacerbates Infection via Hyperinflammation by Signaling through TLR4 and RAGE. *mBio* **8**.

39 Wang C, Wang H, Chang D-Y, Hao J, Zhao M-H & Chen M (2015) High mobility group box 1 contributes to anti-neutrophil cytoplasmic antibody-induced neutrophils activation through receptor for advanced glycation end products (RAGE) and Toll-like receptor 4. *Arthritis Res Ther* **17**, 64.

40 Grossin N, Auger F, Niquet-Leridon C, Durieux N, Montaigne D, Schmidt AM, Susen S, Jacolot P, Beuscart J-B, Tessier FJ & Boulanger E (2015) Dietary CML-enriched protein induces functional arterial aging in a RAGE-dependent manner in mice. *Mol Nutr Food Res* **59**, 927–938.

41 Roumenina LT, Radanova M, Atanasov BP, Popov KT, Kaveri SV, Lacroix-Desmazes S, Frémeaux-Bacchi V & Dimitrov JD (2011) Heme interacts with c1q and inhibits the classical complement pathway. *J Biol Chem* **286**, 16459–16469.

42 Dimitrov JD, Roumenina LT, Doltchinkova VR, Mihaylova NM, Lacroix-Desmazes S, Kaveri SV & Vassilev TL (2007) Antibodies Use Heme as a Cofactor to Extend Their Pathogen Elimination Activity and to Acquire New Effector Functions. *J Biol Chem* **282**, 26696–26706.

43 Bozinovic N, Noé R, Kanyavuz A, Lecerf M & Dimitrov JD (2020) Method for identification of heme-binding proteins and quantification of their interactions. *Anal Biochem* **607**, 113865.

44 Lonsdale J, Thomas J, Salvatore M, Phillips R, Lo E, Shad S, Hasz R, Walters G, Garcia F, Young N, Foster B, Moser M, Karasik E, Gillard B, Ramsey K, Sullivan S, Bridge J, Magazine H,

Syron J, Fleming J, Siminoff L, Traino H, Mosavel M, Barker L, Jewell S, Rohrer D, Maxim D, Filkins D, Harbach P, Cortadillo E, Berghuis B, Turner L, Hudson E, Feenstra K, Sobin L, Robb J, Branton P, Korzeniewski G, Shive C, Tabor D, Qi L, Groch K, Nampally S, Buia S, Zimmerman A, Smith A, Burges R, Robinson K, Valentino K, Bradbury D, Cosentino M, Diaz-Mayoral N, Kennedy M, Engel T, Williams P, Erickson K, Ardlie K, Winckler W, Getz G, DeLuca D, MacArthur D, Kellis M, Thomson A, Young T, Gelfand E, Donovan M, Meng Y, Grant G, Mash D, Marcus Y, Basile M, Liu J, Zhu J, Tu Z, Cox NJ, Nicolae DL, Gamazon ER, Im HK, Konkashbaev A, Pritchard J, Stevens M, Flutre T, Wen X, Dermitzakis ET, Lappalainen T, Guigo R, Monlong J, Sammeth M, Koller D, Battle A, Mostafavi S, McCarthy M, Rivas M, Maller J, Rusyn I, Nobel A, Wright F, Shabalin A, Feolo M, Sharopova N, Sturcke A, Paschal J, Anderson JM, Wilder EL, Derr LK, Green ED, Struewing JP, Temple G, Volpi S, Boyer JT, Thomson EJ, Guyer MS, Ng C, Abdallah A, Colantuoni D, Insel TR, Koester SE, Little AR, Bender PK, Lehner T, Yao Y, Compton CC, Vaught JB, Sawyer S, Lockhart NC, Demchok J & Moore HF (2013) The Genotype-Tissue Expression (GTEx) project. *Nat Genet* **45**, 580–585.

45 Merle NS, Grunenwald A, Figueres M-L, Chauvet S, Daugan M, Knockaert S, Robe-Rybkine T, Noe R, May O, Frimat M, Brinkman N, Gentinetta T, Miescher S, Houillier P, Legros V, Gonnet F, Blanc-Brude OP, Rabant M, Daniel R, Dimitrov JD & Roumenina LT (2018) Characterization of Renal Injury and Inflammation in an Experimental Model of Intravascular Hemolysis. *Front Immunol* **9**, 179.

Figure legends

Fig 1. RAGE is a heme receptor. (A) Absorbance spectrophotometry of heme binding to hRAGE. The molar ratio of heme:RAGE varies from 0.5 to 8. **(B left)** SEC analysis of the binding of heme to hRAGE on a 24 mL Superdex 75 Increase column (GE Healthcare Life Sciences). The samples injected on the SEC column for the different chromatograms are as follow: VC1C2 alone (green and cyan curves), 1:10 VC1C2:heme mix (dark blue and red curves), heme alone (orange and brown dotted curves). All mixes were incubated for 2 hours at room temperature before injection. The chromatograms display the absorbance at either 280 or 404 nm, as indicated on the figure. **(B right)** SDS-PAGE analysis of the peak fractions observed for the different chromatograms. The fractions analyzed and the corresponding chromatogram at 280 nm are indicated above the corresponding lane on the gel. H and R correspond to control samples containing only the heme or hRAGE VC1C2 in SEC buffer, respectively. **(C left)** SEC analysis of the binding of heme and HPIX to hRAGE on a 24 mL Superose 6 Increase column (GE Healthcare Life Sciences). All mixes were incubated 2 hours at room temperature in SEC buffer before injection on the column. The samples injected on the Superose 6 Increase column for the different chromatograms are as follow: VC1C2 alone (green curve), 1:20 VC1C2:heme mix (dark blue curve), 1:10 VC1C2:heme mix (cyan curve), 1:5 VC1C2:heme mix (orange curve), 1:2 VC1C2:heme mix (magenta curve), 1:1 VC1C2:heme mix (red curve), 1:10 VC1C2:HPIX mix (gray curve). All chromatograms display the absorbance at 280 nm during elution of the injected samples. Black arrow heads indicated the different RAGE:heme complexes separated on the column. (**C right**) Plot of the average heme to RAGE molar ratio measured in each peak fraction of the various chromatograms recorded for the different VC1C2:heme mixes analyzed by SEC.

Fig 2. Heme bind to RAGE in a concentration-dependent manner. **(A)** ELISA study of Interaction between hemin (red curve) or hemozoin (black curve) and RAGE. **(B)** SPR study of heme and hRAGE binding. hRAGE was used as bait protein. Left: SPR study of heme, hRAGE-Fc and IgG1-Fc binding; Right: different concentrations of heme were used as prey protein (from 40nM to 2500nM).

Fig 3. The V domain of RAGE is the binding site for heme. (A) SPR study of heme (2.5µM) and RAGE proteins binding. **(B)** SPR study of CML (400ng/mL) binding to RAGE proteins. **(C)**

Absorbance spectrophotometry of heme binding to V domain. The ratio of heme:RAGE varies from 0.5 to 8. **(D)** Absorbance spectrophotometry of heme binding to C2 domain. The ratio of heme:RAGE varies from 0.3 to 2.4.

Fig 4. RAGE interacts with molecules containing transition metals. (A) SPR study of HPIX (hemoporphyrin, 30µM) and RAGE proteins binding. **(B)** SEC analysis of the binding of HPIX to hRAGE on a 24 mL Superose 6 Increase column. The samples injected on the SEC column for the different chromatograms are as follow: VC1C2 alone (green and dotted cyan curves), 1:10 VC1C2:HPIX mix (gray and magenta curves), HPIX alone (orange and brown curves). All mixes were incubated for 2 hours at room temperature before injection. The chromatograms display the absorbance at either 280 or 600 nm, as indicated on the figure. **(C-D)** SPR study of iron molecules (heme, iron(III)pht and ferroin, 10µM) and porphyrin (heme, Mn(III), Co(III), Mg(II), 10µM), and hRAGE binding. **(E)** SPR study of CML (400ng/mL) was us as prey protein, on hRAGE +/- pre-exposure to 2.5µM of heme.

Fig 5. RAGE contributes to heme-mediated pro-inflammatory and pro-thrombotic signaling in the lungs of mice. C57Bl/6 littermate mice (4-5group) were treated with PBS or heme at day 0 before sacrifice at day 1. **(A)** Violin plot representing the gene expression of human *AGER* expressed in TPM in 54 non-diseased tissue sites across nearly 1000 individuals. The tissues are median sorted. **(B)** Comparison of the RAGE expression (AGER gene) in different organs of adult male C57BL/6 mouse, analysed by RNAseq (GEO accession number: GSE74747). **(C)** Study by RTqPCR of RAGE gene expression in lungs of mice WT, treated with heme (100µmol/kg corresponding to 67.5µg/g body weight) or PBS. n=5 per groups. **(D)** Study by RTqPCR of HO-1 gene expression in lungs of mice WT or $RAGE^{-/-}$, treated with PBS of heme (100µmol/kg). n=5 per groups. **(D-E)** Study by RTqPCR of *TF, TNFα, IL1β* and *IL6* gene expression in lung of mice WT or $RAGE^{-/-}$, treated with PBS of heme (100µmol/kg). n=5 per groups. Data are presented as mean and standard deviation (SD). Mann-Whitney test was used for comparisons.

Fig 6. Heme activates signaling pathways via RAGE, leading to phosphorylation of ERK 1/2 and AKT. (A) ERK1/2 and **(B)** Akt pathways studied by Western Blot on lung lysates of mice WT (n=4)

or RAGE$^{-/-}$(n=3), treated with PBS or heme (100µmol/kg). Molecular weight (MW) is represented on the left of WB. Histograms under each WB represent quantification of phosphorylated protein/total protein ratio; expression divided by control condition (PBS). Control gene used was *GAPDH*. Data are presented as mean and standard deviation (SD).

Fig. 1

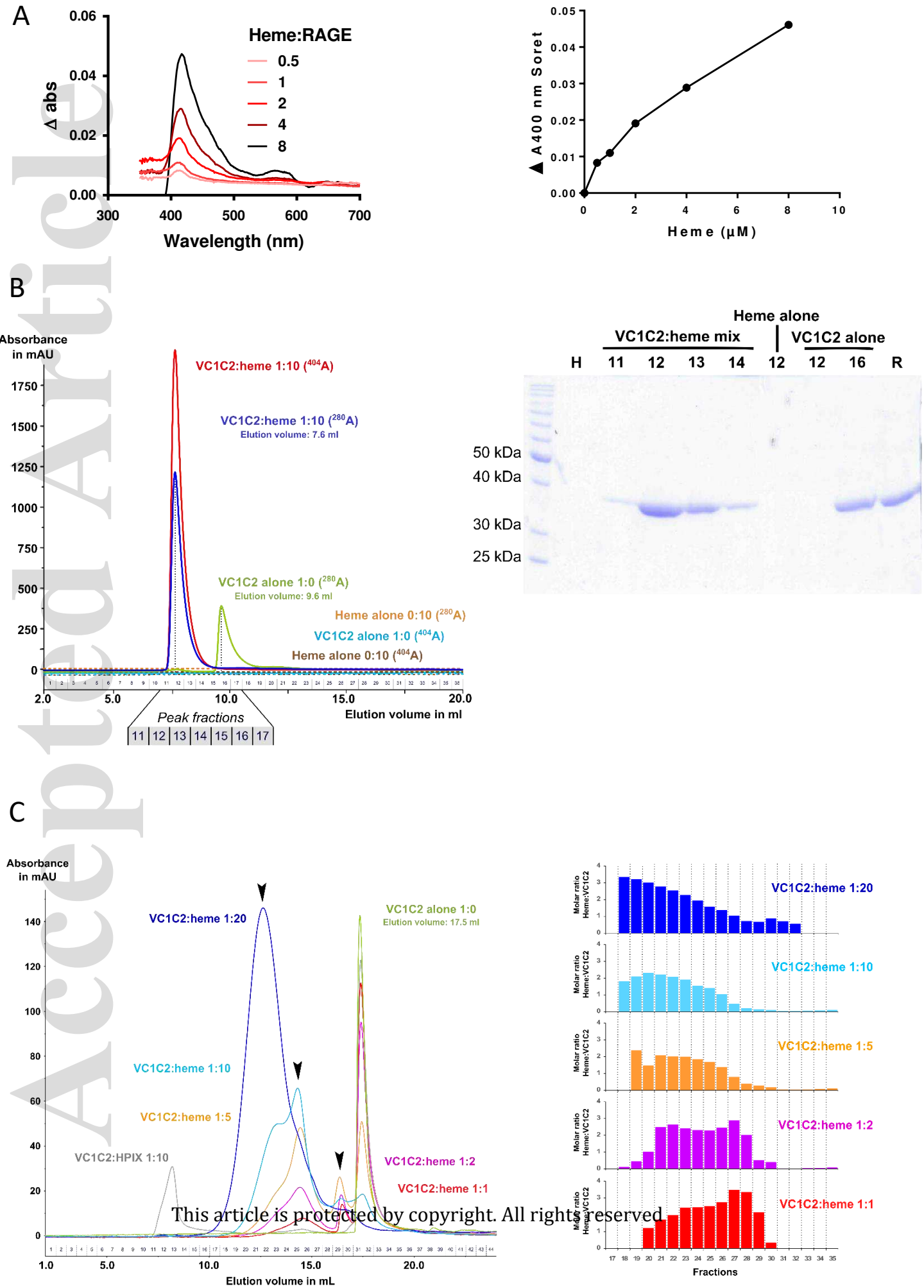

Fig. 2

A

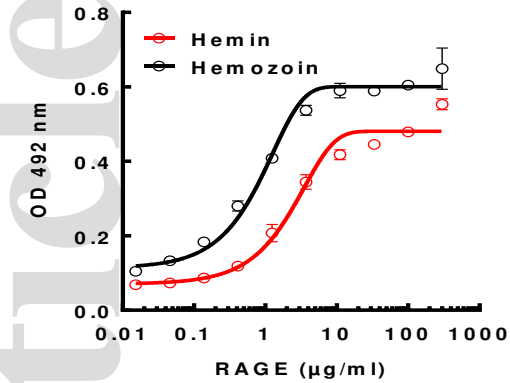

B

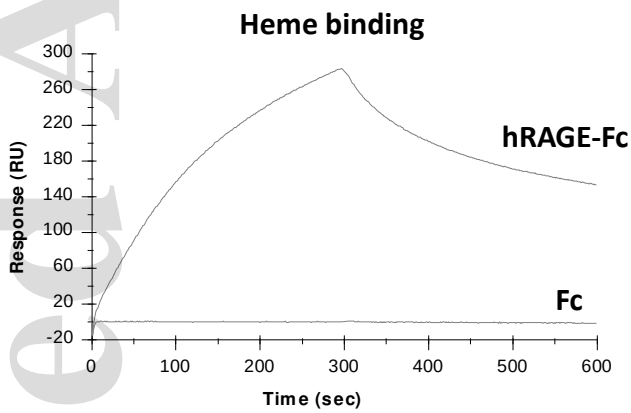

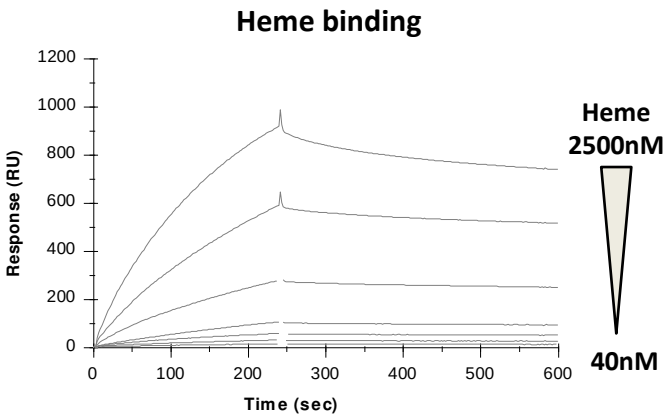

Fig. 3

febs_15667_f3.pdf

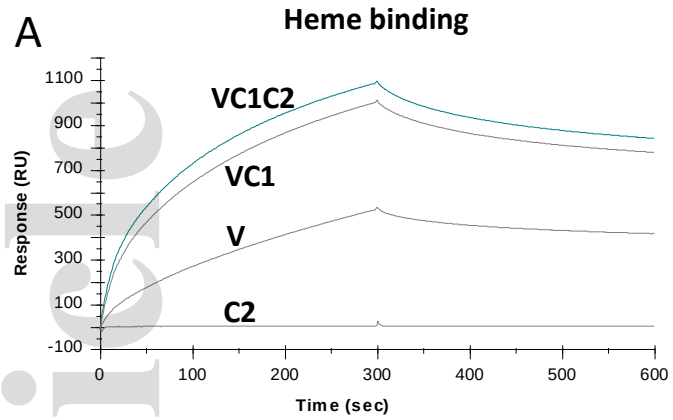

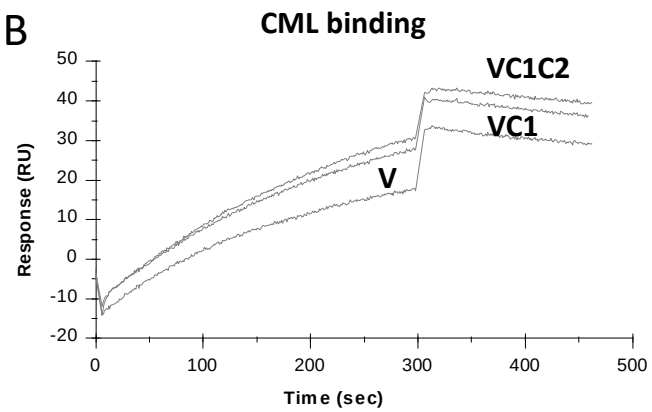

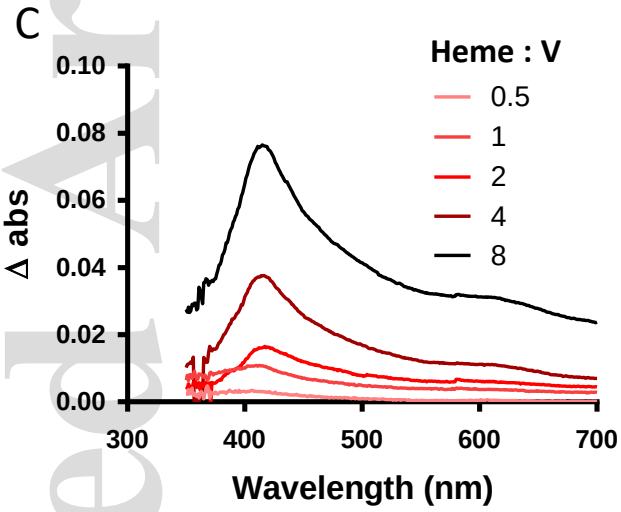

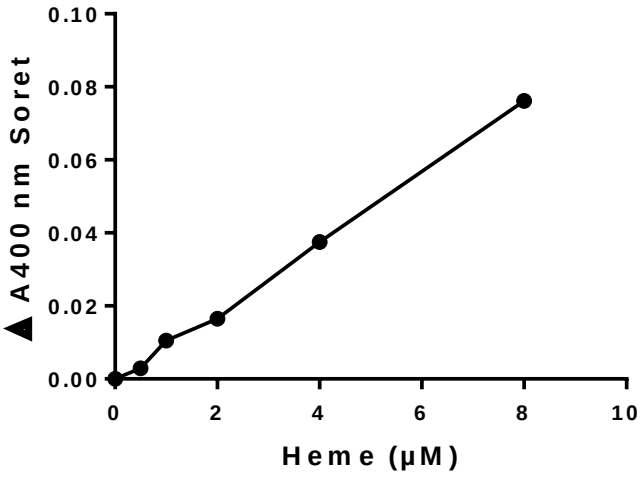

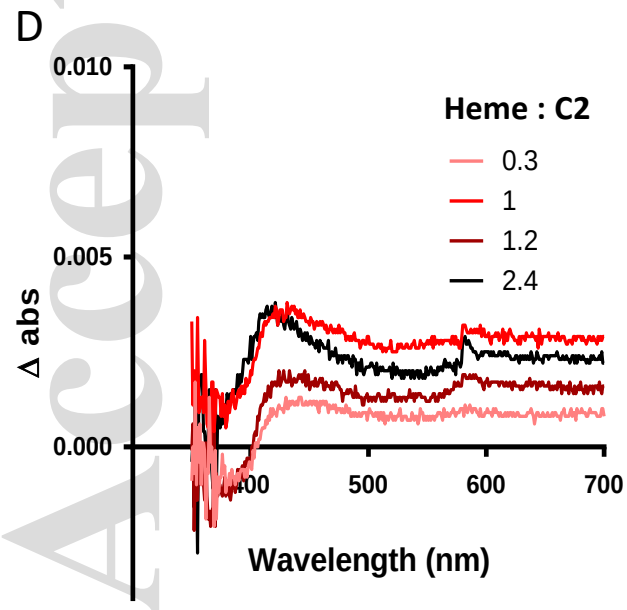

Fig. 4

febs_15667_f4.pdf

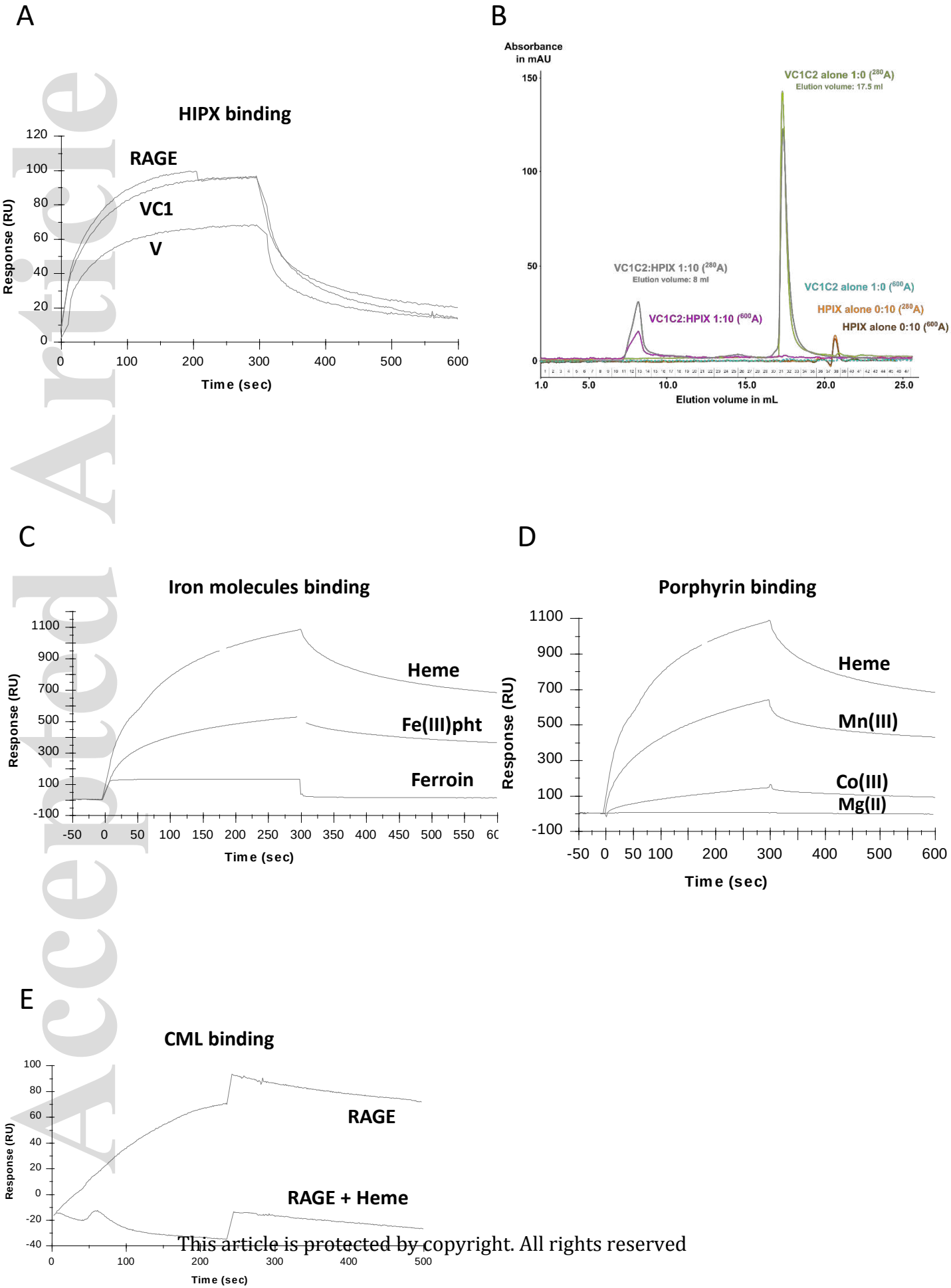

Fig. 5

A

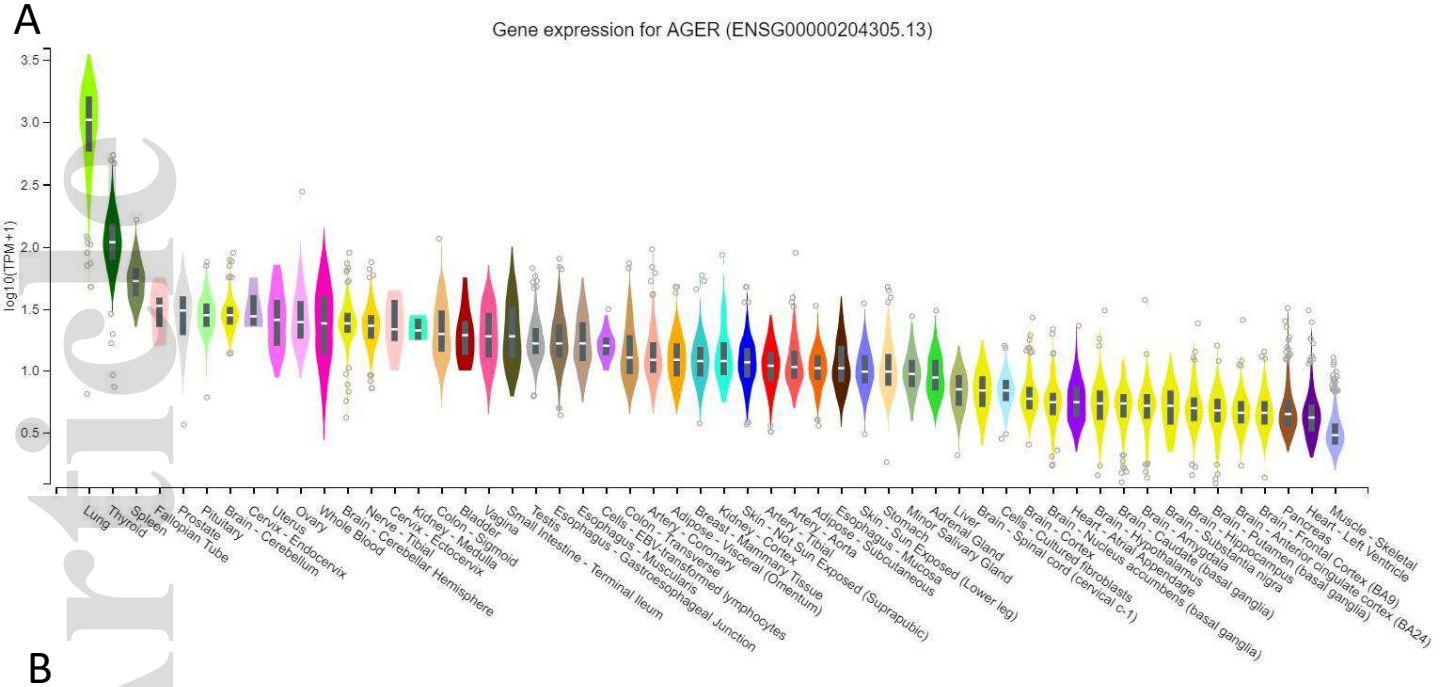

B

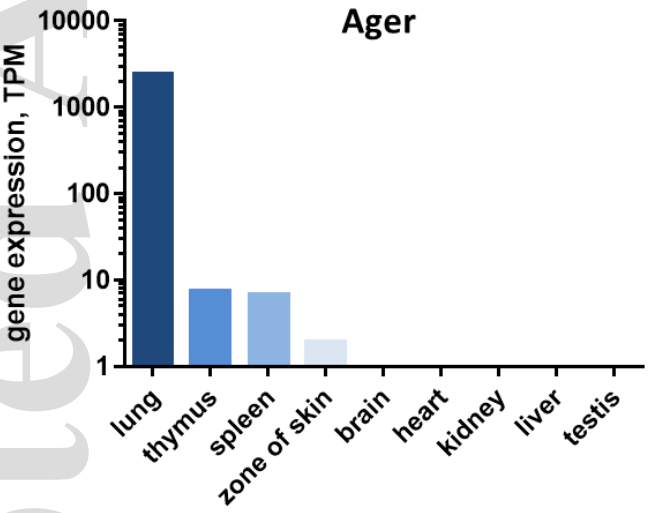

C

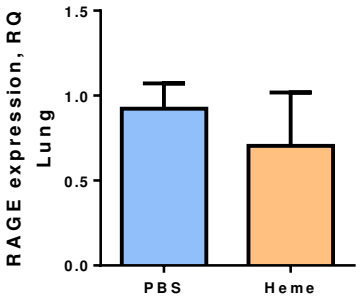

D

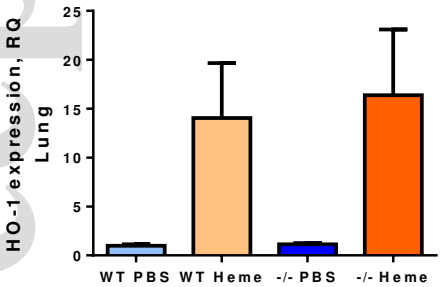

E

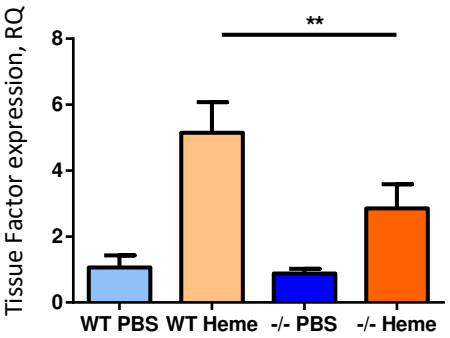

F

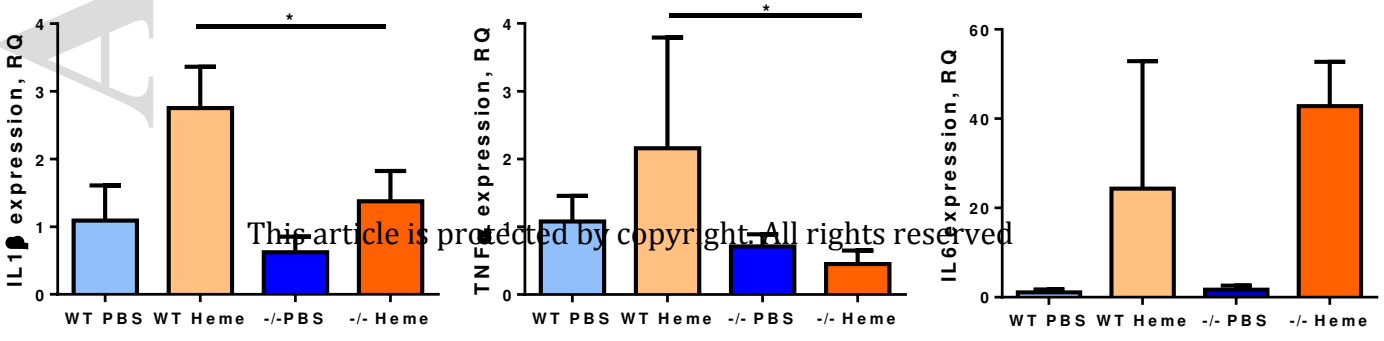

Fig. 6

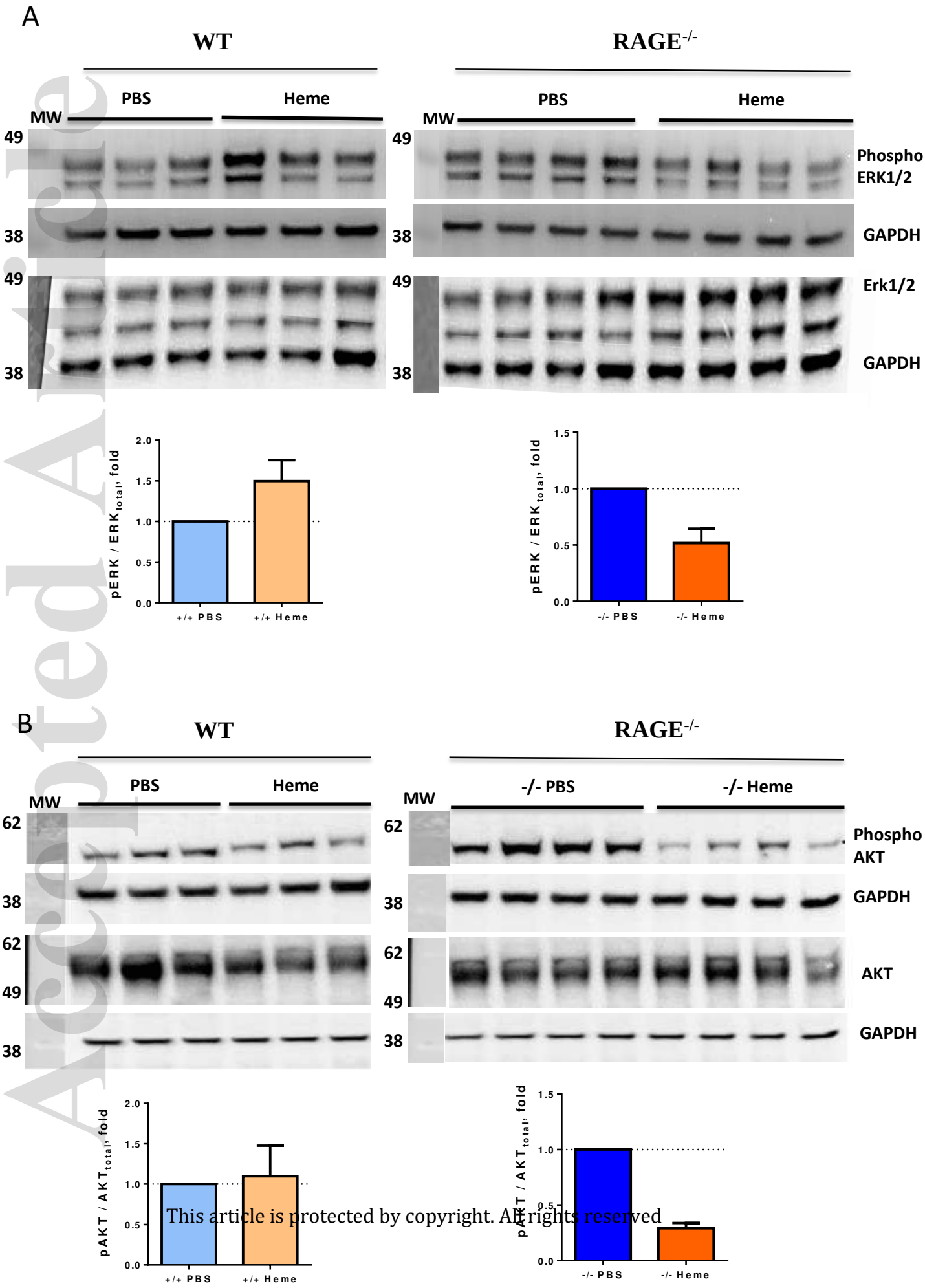

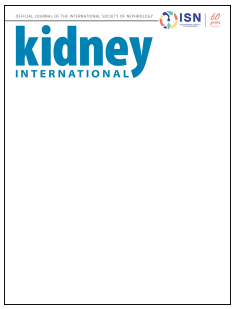

Complement activation is a crucial driver of acute kidney injury in rhabdomyolysis

Idris Boudhabhay, Victoria Poillerat, Anne Grunenwald, Carine Torset, Juliette Leon, Marie V. Daugan, Francesca Lucibello, Khalil El Karoui, Amandine Ydee, Sophie Chauvet, Patrick Girardie, Steven Sacks, Conrad A. Farrar, Peter Garred, Romain Berthaud, Moglie Le Quintrec, Marion Rabant, Pascale de Lonlay, Caroline Rambaud, Viviane Gnemmi, Veronique Fremeaux-Bacchi, Marie Frimat, Lubka T. Roumenina

PII: S0085-2538(20)31244-8

DOI: https://doi.org/10.1016/j.kint.2020.09.033

Reference: KINT 2352

To appear in: *Kidney International*

Received Date: 7 May 2020

Revised Date: 1 September 2020

Accepted Date: 25 September 2020

Please cite this article as: Boudhabhay I, Poillerat V, Grunenwald A, Torset C, Leon J, Daugan MV, Lucibello F, El Karoui K, Ydee A, Chauvet S, Girardie P, Sacks S, Farrar CA, Garred P, Berthaud R, Le Quintrec M, Rabant M, de Lonlay P, Rambaud C, Gnemmi V, Fremeaux-Bacchi V, Frimat M, Roumenina LT, Complement activation is a crucial driver of acute kidney injury in rhabdomyolysis, *Kidney International* (2020), doi: https://doi.org/10.1016/j.kint.2020.09.033.

Complement activation is a crucial driver of acute kidney injury in rhabdomyolysis

10 human RIAKI biopsies

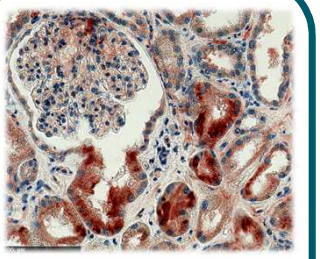

Tubular C3d deposit

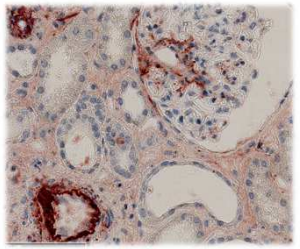

Vascular C5b-9 deposits

Glycerol induced rhabdomyolysis RIAKI mouse model

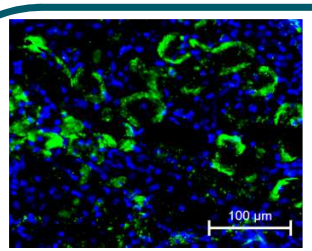

Tubular C3b/iC3b deposits

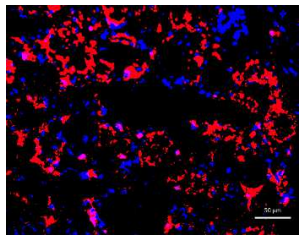

C5aR1 on tubular and interstitial cells

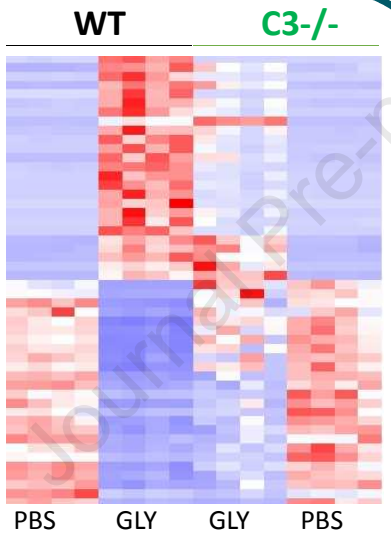

C3 knockout reverses RIAKI transcriptomic signature

C3-/-

+ Hemopexin

WT

Kidney Protection

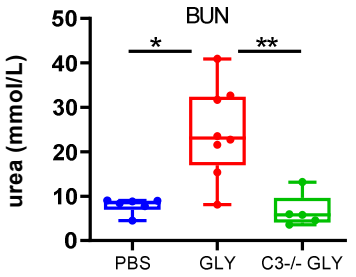

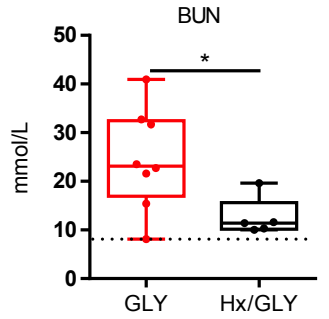

CONCLUSION: Complement system is activated in rhabdomyolysis induced acute kidney injury (RIAKI).

Complement blocking and heme scavenging are promising therapeutic strategies.

kidney INTERNATIONAL
OFFICIAL JOURNAL OF THE INTERNATIONAL SOCIETY OF NEPHROLOGY

Boudhabhay, 2020

[QUERY TO AUTHOR: title and abstract rewritten by Editorial Office – not subject to change]

Complement activation is a crucial driver of acute kidney injury in rhabdomyolysis

Idris Boudhabhay[1#], Victoria Poillerat[1#], Anne Grunenwald[1#], Carine Torset[1], Juliette Leon[1], Marie V. Daugan[1], Francesca Lucibello[2], Khalil El Karoui[3], Amandine Ydee[4], Sophie Chauvet[1,5], Patrick Girardie[6], Steven Sacks[7], Conrad A. Farrar[7], Peter Garred[8], Romain Berthaud[9], Moglie Le Quintrec[10], Marion Rabant[11], Pascale de Lonlay[12], Caroline Rambaud[13], Viviane Gnemmi[4], Veronique Fremeaux-Bacchi[1,14], Marie Frimat[15,16], Lubka T. Roumenina[1,*]

[1]Centre de Recherche des Cordeliers, INSERM, Sorbonne Université, Université de Paris, F-75006 Paris, France.

[2]INSERM U932, PSL University, Institut Curie, Paris, 75005, France.

[3]Service de néphrologie et transplantation rénale, Hôpital Henri Mondor, Assistance Publique-Hôpitaux de Paris, Créteil, Paris, France.

[4]Pathology Department, Lille University Hospital (CHU), Pathology Institute, Inserm UMR-S1172 Lille, JPARC-Jean-Pierre Aubert Research Center, Team 'Mucins, Epithelial Differentiation and Carcinogenesis", Lille University, CHU Lille, Lille, France.

[5]Department of Nephrology, Georges Pompidou European Hospital, Paris, France.

[6]Intensive care department, Université de Lille, CHU Lille, 59000, Lille, France.

[7]MRC Centre for Transplantation, Peter Gorer Department of Immunobiology, School of Immunology & Microbial Sciences, King's College London, London, UK.

[8]Laboratory of Molecular Medicine, Dept. of Clinical Immunology, University of Copenhagen, Copenhagen, Denmark.

[9]Department of Pediatric Nephrology, Necker Hospital, Assistance Publique - Hôpitaux de Paris (AP-HP), Paris, France.

[10]Department of Nephrology and Kidney Transplantation, CHU de Montpellier, Montpellier, France.

[11]Department of Pathology, Necker Hospital, Assistance Publique - Hôpitaux de Paris (AP-HP), Paris, France.

[12]Reference Centre for Metabolic Diseases, Necker-Enfants Malades Hospital, Imagine Institute, Université Paris-Descartes, APHP, Paris, France.

[13]APHP, Service Médecine Légale, Hôpital Raymond Poincaré, Garches, France.

[14]Assistance Publique-Hôpitaux de Paris, Laboratory of Immunology, Hôpital Européen Georges Pompidou, Paris, France.

[15]Univ. Lille, U995-LIRIC-Lille Inflammation Research International Center, F-59000 Lille, France.

[16] Lille University Hospital CHU, Department of Nephrology, F-59000 Lille, France.

[#] these authors contributed equally to the study

* Correspondence to: Lubka T. Roumenina, Ph.D.

Cordeliers Research Center, INSERM UMRS 1138;

15 rue de l'Ecole de Medecine; 75006 Paris, France

Phone: 33-1-44-27-90-96/ Fax: 33-1-40-51-04-20.

e-mail: lubka.roumenina@sorbonne-universite.fr

Running title: Complement in RIAKI

Abstract:

Rhabdomyolysis is a life-threatening condition caused by skeletal muscle damage with acute kidney injury being the main complication dramatically worsening the prognosis. Specific treatment for rhabdomyolysis-induced acute kidney injury is lacking and the mechanisms of the injury are unclear. To clarify this, we studied intra-kidney complement activation (C3d and C5b-9 deposits) in tubules and vessels of patients and mice with rhabdomyolysis-induced acute kidney injury. The lectin complement pathway was found to be activated in the kidney; likely via an abnormal pattern of Fut2-dependent cell fucosylation, recognized by the pattern recognition molecule collectin-11 and this proceeded in a C4-independent, bypass manner. Concomitantly, myoglobin-derived heme activated the alternative pathway. Complement deposition and acute kidney injury were attenuated by pre-treatment with the heme scavenger hemopexin. This indicates that complement was activated in a unique double-trigger mechanism, via the alternative and lectin pathways. The direct pathological role of complement was demonstrated by the preservation of kidney function in C3 knockout mice after the induction of rhabdomyolysis. The transcriptomic signature for rhabdomyolysis-induced acute kidney injury included a strong inflammatory and apoptotic component, which were C3/complement-dependent, as they were normalized in C3 knockout mice. The intra-kidney macrophage population expressed a complement-sensitive phenotype, overexpressing CD11b and C5aR1. Thus, our results demonstrate a direct pathological role of heme and complement in rhabdomyolysis-induced acute kidney injury. Hence, heme scavenging and complement inhibition represent promising therapeutic strategies.

Key words: C3 deposition/ complement/ heme/ hemopexin/ lectin pathway/ rhabdomyolysis-induced acute kidney injury/

Translational Statement

Rhabdomyolysis induced acute kidney injury (RIAKI), which is the main complication of this life-threatening condition is associated with a poor prognosis, mainly due to the lack of specific treatments. Until recently, understanding of its physiopathology didn't include any role for complement activation. We provide here new evidences for complement system activation in human kidney biopsies with rhabdomyolysis. We discovered that complement system activation is mainly induced by both the lectin and the alternative pathways in a mouse model of RIAKI, attenuated by pre-treatment with heme-scavenger, hemopexin. Finally, we demonstrate a direct causal role of the complement system, showing that mice lacking C3 are protected from RIAKI. Actual RIAKI treatment is limited to volume expansion, forced diuresis and renal replacement therapy. Therefore, heme scavenging and complement inhibition represent promising therapeutic strategies for these critically ill patients opening a new field in rhabdomyolysis treatment, to be explored in the future.

Introduction

Rhabdomyolysis is a life-threatening condition caused by skeletal muscle injury and subsequent release of breakdown products into the circulation. The causes are multiple, but dominated by trauma ("crush syndrome"), muscle hypoxia, genetic defects, medication or drug abuse.[1] Acute kidney injury (AKI) is the major complication of rhabdomyolysis, seen in up to 50% of the patients.[2, 3] Rhabdomyolysis-induced AKI (RIAKI) occurs in adults, due to trauma or intoxication, and in children due to inherited muscle disorders. There is no specific treatment for RIAKI and patients' management is mostly symptomatic. Myoglobin and its oxygen-carrying moiety heme play a key role in RIAKI through: (i) renal vasoconstriction;[4] (ii) direct injury of proximal tubular cells through oxidative stress, lipid peroxidation,[5] and macrophage activation;[6-8] (iii) myoglobin precipitation with uromodulin, forming pigmented casts in distal tubules. RIAKI was considered complement-independent, since no C3c-positive staining was detected in the renal biopsies in the few published case reports. Nevertheless, complement may be implicated in RIAKI, since C3 depletion improved renal function in a rat model.[9] Complement is an essential effector of innate immunity.[10] However, complement overactivation is implicated in diseases affecting kidneys and/or associated with heme release.[11, 12] Indeed, cell-free heme activates the alternative pathway.[13] Moreover, complement is pathogenic in ischemia-reperfusion injury (I/R).[14-17]

Here, we demonstrate that complement is activated in RIAKI in mice and patients and describe the mechanisms, by which it contributes to the AKI.

Results

Complement activation in kidneys of RIAKI patients

Ten biopsies of RIAKI patients were collected. The main features of patients (RIAKI 1-RIAKI 10) are summarized in **Table 1.** Kidney biopsies revealed a typical pattern of RIAKI, characterized by acute tubular necrosis (ATN) associated with tubular casts (**Fig. 1A**). C3c staining was negative in the tubules in 8/10 RIAKI patients, and in 2 controls: a patient with AKI (Cr=420 µmol/L) caused by ATN without rhabdomyolysis and in an allograft kidney biopsy from a patient 2 days post-transplantation, used as example of I/R (**Fig. 1B**). Nevertheless, C3d staining, regardless of rhabdomyolysis etiology, revealed a strong cytoplasmic and granular staining within the tubular cells. C3d staining was tested in 4 patients with ATN. With the exception of one patient with hypovolemia-associated ATN, C3d staining was positive in ATN induced by ischemic causes especially in I/R but negative in other causes such Cisplatin toxicity (**Fig. 1C**). Vascular C5b-9 staining was detected in big vessels and on arterioles (**Fig S1A,B**) in 6 tested biopsies. We found evidence for localization of C5b-9 staining together with C3d in 3/6 cases (**Fig S1C**), although not in all vessels, as described in graft rejection.[18]

Systemic markers of complement activation were analyzed in the plasma of 13 patients with rhabdomyolysis (P1-P13) (**Table S1**). No patient had auto-immune disease. One patient (P2) had chronic kidney disease related to Bardet Biedl syndrome and type 2 diabetes mellitus was present in three patients (P2, P6 and P11). Soluble C5b-9 (sC5b-9) was increased in only 2 patients one of which, P2, developed septic shock early after admission which could explain this result. P7 also had inflammatory syndrome, but not so severe. In P12 the sC5b-9 was borderline. Plasma P13 corresponds to the patient with biopsy RIAKI 9.

Validation of the RIAKI mouse model

We studied the implication of complement in RIAKI using a mouse model in C57BL/6 mice (**Fig. S2A**). Immediately after glycerol injection (GLY), all mice presented with lameness of the injected limb (**Fig. S2B**). Rhabdomyolysis biomarkers, CK and ASAT, were elevated in GLY vs PBS mice ($p=0.0042$ and $p<0.0001$ respectively) (**Fig. S2C**). A dark discoloration of the urine of GLY mice at 6h was indicative of necrotic tubules and myoglobinuria (**Fig. S2D**). AKI was evident by the increase in both blood urea nitrogen (BUN) (**Fig. S2E**) and creatinine (Cr) ($p<0,0001$ and $p=0,0006$ respectively). Likewise, proteinuria increased in GLY mice ($p=0,02$), mainly composed of albumin (60kDa band) (**Fig. S2F**). Tubular damage/injury

markers Lcn2 (Lipocalin 2, the mouse ortholog of human NGAL) and Havcr1 (KIM-1), and endothelial activation markers P-Selectin (p<0,0001), E-Selectin (p<0,0001), ICAM-1 (p<0,0001) and VCAM-1 (p<0,0001), (**Fig. S2G**) were upregulated in GLY mice. Lcn2/NGAL staining was intense on tubular cells of GLY mice (**Fig. S2H**). Likewise, VCAM-1 staining appeared positive in peri-tubular capillaries (**Fig. S2I**).

Complement activation occurs in the kidney and correlates with RIAKI in mice

Histopathological examination of GLY mice kidneys revealed the same lesions as in humans, with ATN and tubular casts (**Fig. 2A**). Staining with anti-C3b/iC3b antibody revealed the expected weak signal in PBS mice, on the tubular basement membrane and Bowman's capsule.[16] However, after glycerol injection, this staining increased dramatically in the tubular lumen and inside the cytoplasm of tubular cells and at the basolateral pole (**Fig. 2B, C**). No significant difference was found between CD31 staining in PBS, Glycerol and Cisplatin injected mice. The antibody does not recognize intact C3, indicating activation of complement in RIAKI. Conversely, cisplatin-injected mice did not show an increase in tubular C3b/iC3b deposits. Quantification of the staining revealed a linear correlation with AKI markers, assessed by BUN (r^2=0.64; p<0,0001) and by plasma creatinine (r^2=0,69; p<0,0001) in GLY mice (**Fig. 2D**).

Complement activation occurs locally in the kidney

We used a C3 western blot of plasma and urine to investigate complement system activation (**Fig. S3A**). In plasma, C3 western blot of GLY mice was similar to PBS mice, with no sign of C3 cleavage (**Fig. S3B** left), whereas in urine C3b (recognized by α' band) appeared at 2 hours following GLY injection and more markedly at 24 hours after GLY injection (right). The same pattern was observed in all 3 tested patients with RIAKI (R1:CK= 88 000 ui/L; Cr=141µmol/L, R2: CK=10000ui/L; Cr=1615µmol/L; R3: CK=17126ui/L; Cr=903µmol/L), with no cleavage in plasma but in urine (**Fig. S3C**). The urine R2 corresponds to biopsy RIAKI5. Moreover, among 12 tested patients with RIAKI, C3 was decreased for only one case (**Table S1**).

Systemic C3 mainly contributes to complement activation in the kidney

Further, we tested if plasma and/or local C3 was involved in RIAKI. C3 kidney mRNA was upregulated in GLY mice compared to PBS (p<0.0001), indicating renal production

during RIAKI (**Fig. S4A**). Moreover, C3d-staining in human and mouse kidneys appeared cytoplasmic and co-localized with LAMP1, indicative of intracellular C3, at least in part with lysosomal localization (**Fig. S4B, S4C**). To evaluate the role of systemic C3 in RIAKI, we injected glycerol in HepatoFH-/- mice, which have a low concentration of plasma C3 at steady state because of systemic FH deficiency and subsequent C3 consumption (**Fig. S4D)**.[19] C3 kidney mRNA expression was similar in hepatoFH-/- GLY mice compared to WT-GLY mice (p=0.8), indicating persistent renal production. However, hepatoFH-/- GLY mice tended to be protected from RIAKI (**Fig. S4E**), with less tubular injury assessed by Lcn2 expression (**Fig. S4F**), and with less C3-deposits in their kidneys (**Fig. S4G)**. Likewise, WT mice injected with cobra venom factor (CVF) prior to glycerol, displayed persistent plasma C3 consumption, 24h post-injection (**Fig. S4H)**, and nearly no C3b/iC3b deposits within the kidneys in comparison to mice injected with PBS prior to glycerol (**Fig. S4I).**

The complement system is over-activated through a C4-bypass pathway

In vitro, a dose-dependent increase in C3 activation fragments was observed on renal proximal tubular epithelial cells (RPTEC), incubated with increasing dose of myoglobin and serum (**Fig. 3A** left). No C4 deposits were detected (**Fig. 3A** right). Moreover, C4 was negative in 9 RIAKI biopsies tested (**Fig. 3B)**. C1q staining was mostly negative in tubules of 6/8 RIAKI patients. However, 2 patients had a granular staining in scarce tubules (RIAKI 1 and 7), 1 had focal and segmental deposits in glomeruli (RIAKI 4) and 2 had positive staining of peritubular capillaries (RIAKI 8 and 9) **(Fig. S5A**). C1s staining was positive in vessels and capillaries including glomerular ones with very weak tubular staining in 2/2 RIAKI patients. **(Fig. S5B**). In mice, Glycerol injection induced an increased glomerular C1q staining (**Fig. S5C**). Gene expression revealed a decreased C1s1 expression of -0.54 log2 fold-change (p=0.02) without significant difference for C1r (-0.38 log2 fold-change (p=0.19)). Furthermore, glycerol injection in C4-/- mice revealed no protection from RIAKI (**Fig. 3C**) and even enhanced vascular aggression (up-regulation of P-Selectin (p<0,001), E-Selectin (p<0,001), VCAM-1 (p<0,001), and ICAM-1 (p<0,001) (**Fig. 3D**). Tubular injury markers, Lcn2 and Havcr1 were not different in C4-/- GLY mice, compared to WT-GLY but significantly upregulated compared to WT-PBS (Lcn2: p=0,02 Havcr1: p=0,04) (**Fig. 3E**). Finally, C3b/iC3b staining revealed intense tubular deposits in C4-/- mice, similar to WT-GLY mice, suggesting that complement activation is independent from C4 in this model (**Fig. 3F).**

A C4 by-pass lectin pathway operates in ischemic kidneys through collectin-11/L-fucose interaction.[20] Collectin-11 (CL-11) staining increased in mouse RIAKI kidney tubules. Moreover, CL-11 and C3b/iC3b showed partial colocalization, indicating that complement was largely deposited at the site of CL-11 binding (**Fig. 3G**). Human renal biopsies, including those of RIAKI patients, showed CL-11 overexpression on tubular cells, suggesting that this protein is readily available in the kidney (**Fig. S6A).** CL-11 staining was positive mainly on proximal tubules identified by their auto-fluorescent brush border. **(Fig. S6B)**

Complement dysregulation contributes to C3 deposits

Complement receptor 1–related protein y (Crry) is the only complement regulator on mouse tubular epithelial cells.[16] Staining of Crry revealed a linear repartition at the basolateral pole of tubular cells in PBS mice, but decreased and lost polarity in GLY mice. This could amplify complement activation and explain the basolateral localization of C3 deposits (**Fig. S7A**). Complement Factor H (FH) is a plasma regulator, which can bind to the cell membrane to control alternative pathway. Cfh gene expression was downregulated in GLY kidneys (**Fig. S7B**). Kidney tissue from a patient with idiopathic nephrotic syndrome caused by minimal change disease was FH-low/negative whereas liver sections, a biopsy from a patient with lupus nephritis and a biopsy from a patient with ATN without rhabdomyolysis were positive (**Fig. S7C**). In human RIAKI tissue sections, FH staining was positive in a small portion of the proximal tubules, showing an intracellular granular pattern. Compared to C3d-staining, only a few of the C3d-positive tubules appeared FH-positive (**Fig. S7D**).

Heme overload promotes complement activation.

Numerous C3 deposits did not colocalize with CL-11. Therefore, alternative pathway could be triggered independently. As cell-free heme is a well-known alternative pathway activator in hemolysis, we studied if myoglobin-released free heme, reflected by HO-1 up-regulation in GLY mice (**Fig. 4A**), contribute to complement activation and kidney injury. In vitro, incubation of renal proximal tubular epithelial cells (RPTEC) with oxidized heme and serum, increased C3 deposits (**Fig. 4B)**. In vivo, we evaluated the contribution of heme by a preventive injection of its natural scavenger, hemopexin. The injected hemopexin dose was the maximal well-tolerated in heme-overload.[21] The induction of rhabdomyolysis was efficient since CK and ASAT were not different in GLY mice +/- hemopexin. However, renal function (BUN) improved in hemopexin injected mice (p=0,01) (**Fig. 4C**). No change in tubular injury markers was observed, but vascular injury markers were markedly

decreased (P-selectin: p=0,0095; E-Selectin: p=0,014; VCAM-1: p=0,03 ICAM-1: p=0,06) **(Fig. 4D-E)**. Finally, C3 deposits significantly decreased (p=0,02) (**Fig. 4F-G)** whereas renal C3 gene expression was not different from GLY mice (p=0,5; not shown).

Tubular cell and macrophage C5aR1 is upregulated in mouse RIAKI

Renal C3aR1 mRNA expression in GLY-injected mice was not different from PBS mice (p=0,89) (**Fig. 5A**). However, C5aR1 mRNA was markedly upregulated in GLY mice (p<0,0001) (**Fig. 5A**). Strong staining for C5aR1 was detected in the tubules of GLY mice and in interstitial cells (**Fig. 5B**). To identify those cells, C5aR1 was measured on myeloid populations from kidneys by flow cytometry. Eight hours after glycerol injection, there was an increase in macrophage and neutrophil infiltration within GLY kidney compared to PBS (p=0,0152 and p=0,0022 respectively) (**Fig. 5C**). At 24 hours, there was no quantitative difference in neutrophil and macrophage infiltration, as described.[22] No difference was detected for C5aR1 expression on neutrophils in both groups (p=0,18), but in GLY mice both M1 (CCL2, TNFα) and M2 (Arginase 1) markers were co-expressed (**Fig. S8**). Indeed, intrarenal macrophages showed phenotypic alteration. Expression of C5aR1 was not different among macrophages expressing class II HLA ($CD45^+Ly6G^-CD68^+IAb^+$; p=0,55) and their proportion did not differ between PBS and GLY mice. However, $CD45^+Ly6G^-CD68^+IAb^-C5aR1^+$ macrophages increased in GLY mice (p=0,02) mostly because of the emergence of a peculiar sub-population of $CD45^+Ly6G^-CD68^+IAb^-C5aR1^+CD11b^{hi}$ cells (**Fig. 5D**). CD11b/CD18 is a receptor for C3b/iC3b. Interestingly, immunofluorescence on frozen kidneys revealed a close relationship between $CD11b^+$ cells and C3b/iC3b deposits (**Fig. 5E)**.

C3-/- mice are protected from RIAKI

To explore the causal link between complement and RIAKI, we injected glycerol in C3-/- mice. C3-/- GLY mice presented the same lameness of the injected limb and increase in CK and ASAT, compared to PBS WT mice (p=0,03 and p=0,0043 respectively) reaching the same level as WT-GLY mice (p=0,2 and p=0,5 for CK and ASAT). In addition, HO-1 was equally upregulated in WT-GLY and C3-/- GLY mice (**Fig. S9A**). However, BUN was significantly lower in C3-/- GLY compared to WT-GLY mice (p=0,002) (**Fig. 6A**), disrupting the correlation between kidney injury and muscle injury (**Fig. 6B**). In addition, C3-/- GLY mice kidneys displayed very light ATN and rare tubular casts (not shown) following hematoxylin/eosin staining. Even sensitive markers of tubular injury such as

Lcn2 and Havcr1 were reduced in C3-/- mice, (p=0.001 and p=0.0005 respectively) (**Fig. S9B**), as well as endothelial activation markers (P-Selectin: p=0,001; E-selectin: p=0.01; ICAM-1: p=0;0005; VCAM: p=0,0005) (**Fig. S9C**).

RIAKI in mice is associated with a pro-inflammatory and apoptotic transcriptomic signature.

Bulk RNA sequencing analysis on kidneys from PBS versus GLY mice revealed 2056 significantly upregulated genes, 1786 significantly downregulated genes and 16683 genes without significant difference (difference was considered significant when p<0,05 and fold change at least superior to 2) (**Fig. 6C**). Analysis of the 25 most up-regulated and the 25 most down-regulated genes, allowed definition of a rhabdomyolysis transcriptomic signature (**Fig.6D**). Interestingly, one of the most upregulated genes was Fucosyltransferase 2 (Fut2) enzyme, responsible for tagging stressed cells with fucosyl residues, recognized by the lectin pathway.[23] Performing gene ontology on all significantly upregulated genes showed the most up-regulated pathways involved the inflammatory response (cytokine and chemokines such as Cxcl1, Cxcl2, Cxcl3, Cxcl5, Cxcl14, Cxcl17, Ccl2, Ccl3, Ccl4, Ccl7, Ccl9, Ccl11, Ccl12, Ccl17, Ccl20, Il6, Il11, Il24, TNFα, members of the IL1 family, etc), and the cell response to inflammatory processes (response to biotic stimulus such as Glutathione S-transferase A-1 gene, protein phosphorylation and regulation of intracellular transduction), as well as apoptosis (e.g Trib1 and Myc). Classical tubular injury markers Lcn2 (NGAL) and Havcr1 (Kim1) were dramatically upregulated. The most downregulated pathways affected renal metabolism (drug metabolic processing, small molecule processing and lipid metabolism), and intracellular transports (ion transport and trans-membrane transport such as SLC34a3 coding for Sodium-dependant phosphate transport protein 2C and SLC12A1 gene, coding for the $Na^+/K^+/2Cl^-$ cotransporter).

C3 deficiency attenuates the RIAKI signature in mice

C3-/- mice injected with PBS presented a transcriptomic profile very close to the PBS WT mice. Strikingly, C3-/- mice injected with glycerol (C3-/- GLY) lost the majority of the RIAKI signature, compared to the WT-GLY mice (**Fig. 6E)**. Indeed, inflammatory pathways were drastically less upregulated than in WT-GLY mice and, cellular metabolism or ion transport were less affected. Lcn2 and Havcr1 were significantly reduced in C3-/- mice, confirming the data from the RTqPCR (**Fig. 6E**, **Fig. S9B**). Comparison of RIAKI

signature genes between WT and C3-/- PBS (WT/C3-/- PBS), or glycerol (WT/C3-/- GLY) allowed us to classify them into 3 groups: 1) genes, which are completely normalized in the C3-/- GLY mice (p-value WT-GLY vs C3-/-GLY<0.05 and p-value C3-/- PBS vs WT-GLY>0.05); 2) genes which are partially normalized in the C3-/- GLY mice (p-value 'WT-GLY vs C3-/-GLY'<0.05 and p-value 'C3-/- PBS vs WT-GLY'<0.05); 3) genes which are not affected by C3 deficiency (p-value 'WT-GLY vs C3-/-GLY'>0.05 and p-value 'C3-/- PBS vs WT-GLY'>0.05). The completely normalized genes included Fut2 among the upregulated and a set of down-regulated genes, involved in pathways related to potassium ion transport and protein dephosphorylation. Partial correction by C3 deficiency was achieved for upregulated genes involved in the cellular response to cytokines (such as: Ccl12, Cxcl1, Fgb, Lcn2, Socs3, Sox9, Spp1, Timp1) and apoptosis (the same set except Cxcl1 but including Fgg and Sfn). Among them Ccl12, Fgb, Lcn2 and Sox9 belong to the cellular response to IL-1 pathway. The set of downregulated genes, attenuated in C3-/- mice, were not enriched in any particular pathway. A set of genes, including such involved in the cellular response to hypoxia (Eif4ebp1 and Myc) were not affected by C3 deficiency.

Discussion

In addition to myoglobin casts and acute tubular necrosis which are common histology features for rhabdomyolysis,[24] complement deposits occurred in kidneys of mice and patients with RIAKI, independent of the rhabdomyolysis cause. Complement activation occurred intrarenally most likely by the lectin pathway via a C4-bypassing mechanism, and by the alternative pathway via heme. Intrarenal macrophages in RIAKI became particularly sensitive to complement, overexpressing C5aR and CD11b. C3-/- mice were protected from kidney injury, demonstrating a direct pathophysiological link and placing complement as a potential therapeutic target in RIAKI.

We discovered C3d-deposits in the kidneys of patients with RIAKI, regardless of the cause of rhabdomyolysis, demonstrating that complement activation is a consequence of a common factor, present during muscle injury. C3d staining was negative in most of the tested ATN without rhabdomyolysis biopsies, suggesting that complement activation is not a consequence of all tubular injuries. Interestingly, C3c staining was negative/weak in RIAKI biopsies. This can be explained by the rapid cleavage of iC3b to C3c then to C3d, since all biopsies were performed more than 24 hours after the initiation of rhabdomyolysis.[25] In lupus nephropathy (LN) C3c vs C3d staining allows the

differentiation between active and not-active LN.[26] Noteworthy, C3c but not C3d-immunostaining is performed as routine work-up on kidney biopsies and might explain why C3-deposits have not been described until now in RIAKI.

Furthermore, we detected massive C3-deposits in the mouse model. C3 cleavage or consumption did not occur in plasma from the patients or mice. Thus, complement activation occurs locally within the kidney, and we detected C3 fragments in urine of patients and mice. This intrarenal complement activation could be due to the local overexpression of C3, as described in lupus nephritis[27] and in graft rejection,[28, 29] and/or mediated by the systemic C3 as in I/R[30] or hemolysis-induced renal injury.[12] Since glycerol-injected mice with plasma C3 consumption (FHhepato-/- and CVF-treated mice) were protected from complement activation, the major role was played by the systemic C3.

Complement could be activated in RIAKI by different pathways. In rat RIAKI, enhanced C1q staining in tubules was detected[9], whereas here C1q was mainly negative in RIAKI biopsies and enhanced only in some glomeruli in the mouse model. Renal fibrosis models revealed increased expression of C1q, C1r, and C1s and classical pathway activation in the interstitial compartment.[31, 32] We detected a decrease of C1s and C1r expression at 24h. Nevertheless, we cannot exclude an involvement of the classical pathway in RIAKI, potentially later in time, with the progression of the fibrotic process as previously suggested.[32] However, C4-/- mice were not protected from RIAKI and C3 deposits, suggesting that classical pathway and C4 have a minor role in RIAKI's complement activation. The alternative pathway is responsible, at least in part, for the observed deposits. Indeed, heme binds C3, activates the alternative pathway[13] and it induced complement activation on primary tubular cells. This process could be mediated also by properdin.[33, 34] Moreover, the injection of heme-scavenger hemopexin, which can be filtered through the glomerular basement membrane, partially improved kidney function and vascular aggression, as described.[7] Hemopexin decreased C3-deposits, showing a direct role of heme in the intrarenal complement activation.

Conventional lectin pathway proceeds through C4,[35] but a C4-bypass pathway was found in post-ischemic tissue, where CL-11 binds abnormally fucosylating cells and its associated protease MASP-2 cleaves directly C3 to C3b and C3a.[36, 37] Fucosyltransferase 2 (Fut2) is the enzyme which fucosylates epithelium in case of enhanced inflammation.[23] In RIAKI, we detected CL-11 staining, partially colocalizing with C3b/iC3b and Fut2 was one of the most up-regulated genes in the transcriptomic signature. Moreover, Fut2 is strongly dependent on complement, as it was completely normalized in the C3-/- mice,

suggesting that complement activation, potentially triggered by heme, creates an environment that promotes a vicious cycle of further lectin pathway activation. The RIAKI is therefore a particular situation, where both the alternative and the lectin pathways may be triggered in the kidney and the alternative pathway is not a mere amplification loop. Moreover, the reduced regulatory capacity of the stressed tubular cells in RIAKI that we found amplifies the complement activation.

To better understand the molecular mechanisms of RIAKI and the role of complement, we defined a "RIAKI transcriptomic signature" in the mouse model. A clear signature of apoptosis was detected, consistent with the tubular injury. If there was no evidence for increase of TNF alpha expression in kidney,[38] a strong pro-inflammatory signature was observed with a high involvement of genes for response to cytokines and cytokine production. This is concordant with the hypothesis that tubular injury observed in rhabdomyolysis is an inflammatory disease,[38-40] involving infiltrating immune cells, especially macrophages in glycerol induced RIAKI.[6, 39, 41, 42] Myoglobin was shown to modulate the phenotype of the macrophages.[8] Additionally, myoglobin-activated tubular cells in culture express Ccl2 and Ccl7, potent macrophages-recruiting factors.[6] Indeed, significant upregulation of these and other chemokines and cytokines were detected, which could explain the enhanced infiltration of macrophages and neutrophils. Markers of both M1 and M2 macrophages were detected as described.[6]

We identified a RIAKI-associated sub-population of macrophages, negative for HLA-II but expressing strongly C5aR1 and CD11b. This population will be highly susceptible to complement overactivation, being responsive to contact with C3b/iC3b as well as with C5a. Macrophage CD11b/CD18 engagement by direct contact with heme-activated platelets triggered macrophage extracellular trap formation and kidney injury.[7] C3b/iC3b is a ligand of CD11b/CD18 and since we detected CD11b+ cells in close contact with C3b/iC3b deposits on affected proximal tubules in situ, we hypothesize that macrophage activation and kidney damage could be mediated due to this direct contact. Moreover, the overexpression of C5aR1 on tubular cells, together with its increase on macrophages could contribute to the AKI, as described in renal I/R injury[43, 44] and hemolysis.[12] Evaluation of C5a in urine of human and murine RIAKI could be a potential future biomarker, as urine C5a has been associated with AKI.[45] Interestingly, we found no tubular C5b-9 deposits in mice or in humans, contrary to previous report in rat RIAKI. [9] This might reflect an efficient regulation of C5b-9 at this site, likely due to CD59 overexpression [9]. A low

sensitivity of the C5b-9 staining cannot be excluded, despite the clear detection of C5b-9 in blood vessels.

To provide direct proof that complement is a mediator of injury in RIAKI, we induced RIAKI in C3-/- mice. C3-/- mice have already been described as protected in a model of mechanical ischemia/reperfusion.[15] Remarkably, C3-/- mice were also protected from RIAKI, and mostly lost the RIAKI transcriptomic signature, demonstrating the pathogenic role of C3 and/or downstream complement activation in this model. In particular, the cellular response to cytokines and apoptosis pathways appeared to be C3-dependent. Renal tubular injury and dysfunction were markedly attenuated in glycerol-injected mice, deficient in interleukin (IL)-1β or NLRP3 inflammasome.[22] Indeed, the cellular response to the IL1 pathway genes were attenuated in C3-/- mice. Complement overactivation and C5b-9 induce macrophages to release IL-1β,[46, 47] providing a potential mechanistic link between complement and the IL-1/cytokine response pathway. C3-/- mice were also protected from fibrosis and peritubular rarefaction in a model of unilateral ureteral obstruction and authors proposed that macrophages polarization could be involved with C3a induced M1 macrophages responsible in vitro for angiogenesis suppression.[48] Therefore, complement C3 and/or downstream components are directly pathogenic for tubular cells and act in cooperation with macrophages to promote renal injury. However, specific cell types where inflammatory and apoptotic pathways are activated cannot be defined by the bulk RNA sequencing approach. Finally, C5b-9 deposits were detected in vessels of patients, suggesting that endothelial activation could contribute to the vascular aggression in RIAKI. Consistent with this hypothesis, the vascular aggression observed in the mouse model was attenuated in the C3-/- injected with glycerol.

These results suggest a benefit for complement inhibition in RIAKI. C3b is the central protein of the complement cascade, allowing its own amplification through C3 convertase formation. C3-/- mice protection and loss of RIAKI transcriptomic signature suggest the therapeutic potential of C3 inhibition. Indeed, if C5 inhibition is the gold standard for complement inhibition, there is growing interest for C3 targeted therapies in diseases such as Paroxysmal Nocturnal Hemoglobinuria and many other conditions.[49]

In conclusion, our study demonstrates that complement activation, promoted by renal ischemia and heme overload, plays a key role in RIAKI in both mice and humans, independent from the initial cause of muscle damage. Therefore, drugs targeting complement activation and/or heme overload would represent promising therapeutics in critically ill patients.

Materials and Methods

The complete Materials and Methods are given in Supplement.

Collection of human kidney biopsies, urines and sera.

Patients. Kidney biopsies and clinical data from 10 patients with RIAKI were retrieved. All biopsies were performed to eliminate an alternative cause of AKI, or as part of the autopsy in one patient who died from rhabdomyolysis (RIAKI 6). All patients gave informed consent for the use of part of the biopsy for scientific purposes. Urine was collected from 3 and plasma from 11 RIAKI patients and leftover samples from the routine diagnostics were used for this study. All procedures were performed according to national ethical guidelines and were in accordance with the Declaration of Helsinki. Staining was performed for C3c, C3d, Lamp1, C4d, C1q, C5b-9, Collectin-11,[50] Factor H and CD31 on the kidney material (**Table S2)**; C3 and sC5b-9 were measured in plasma and western blot for C3 was performed in plasma and urine.

Animal experimentation

C57BL/6 WT, C3-/- and C4-/- and hepatoFH-/- mice[19] at the same genetic background were used for this study. Experimental protocols were approved by the Charles Darwin ethical committee (Paris, France) and by the French Ministry of Agriculture (Paris, France), APAFIS#2148 2019091015099240v1. Rhabdomyolysis was induced by intramuscular injection of 7.5ml/kg 50% glycerol.

Transcriptomic analysis.

mRNA was extracted and retrotranscribed in cDNA. Gene markers of kidney injury (**Table S3**) were analyzed by RTqPCR and RNAseq.

Immunofluorescence (IF) and immunochemistry (IHC) in mice

Frozen kidney sections were used for IF and IHC are summarized in **Table S1**.

Complement activation on proximal tubular cells in vitro.

RPTEC were exposed to skeletal muscle myoglobin or oxidized species of heme (heme-ox), followed by human serum. Staining for C3 fragments was analyzed by flow cytometry.

Evaluation of the myeloid infiltrate in mouse kidneys

Eight or 24h after injection of PBS or glycerol, mice were sacrificed, and the kidneys were dilacerated, and cell suspension was stained as described in **Table S3**.

Acknowledgments: The cytometric and microscopy analyses were performed at the Centre d'Histologie, d'Imagerie et de Cytométrie (CHIC) and the Centre de Recherche des Cordeliers UMRS1138 (Paris, France). We are grateful to the CHIC team for the excellent technical assistance. CHIC is a member of the Université Pierre et Marie Curie Flow Cytometry network (RECYF). We are grateful for excellent technical assistance from the Centre d'Expérimentations Fonctionnelles team of the Centre de Recherche des Cordeliers and for their support with animal experimentation. We are greatful for the team of the GenomIC plateform Cochin Institute INSERM U1016 headed by Dr. F. Letourner for the RNAseq analyses and the Biochemistry platform in Hospital Bichat Centre Recherche sur l'Inflammation-Paris for the evaluation of the renal function parameters in blood and urine of the mice.

This work was presented in the form of abstract at the 17th European Meeting on Complement in Human Disease" (EMCHD 2019), Madrid, Spain, 2019.

Funding: This work was supported by INSERM. IB received a fellowship from the Société Francophone de Néphrologie Dialyse et Transplantation (SFNDT).

Author contributions: Designed the research: LR, IB, MF. Performed the research: IB, VP, AG, CT, JL, MVD, FL. Provided patient samples and take care for the patients: KEK, AY, SC, PG, MLQ, RB, MLQ, MR, PL, CR, VG. Analyzed the data: LR, IB, VP, AG, MVD, SS, CF, VFB, MF. Provided vital reagents: PG. Wrote the manuscript: IB, VP, AG, MF, LR.

Conflict of interest: Dr. Roumenina reports grants from CSL Behring, outside the submitted work. The other authors have declared that no conflict of interest exists.

Supplementary information is available on Kidney International's website:

Complete Materials and Methods; Supplementary references; Supplementary Tables
Supplementary Figures

References

1. Bosch X, Poch E, Grau JM. Rhabdomyolysis and acute kidney injury. *N Engl J Med* 2009; **361:** 62-72.

2. Candela N, Silva S, Georges B, *et al.* Short- and long-term renal outcomes following severe rhabdomyolysis: a French multicenter retrospective study of 387 patients. *Ann Intensive Care* 2020; **10:** 27.

3. Huerta-Alardin AL, Varon J, Marik PE. Bench-to-bedside review: Rhabdomyolysis -- an overview for clinicians. *Crit Care* 2005; **9:** 158-169.

4. Kurtz TW, Maletz RM, Hsu CH. Renal cortical blood flow in glycerol-induced acute renal failure in the rat. *Circ Res* 1976; **38:** 30-35.

5. Boutaud O, Roberts LJ, 2nd. Mechanism-based therapeutic approaches to rhabdomyolysis-induced renal failure. *Free Radic Biol Med* 2011; **51:** 1062-1067.

6. Belliere J, Casemayou A, Ducasse L, *et al.* Specific macrophage subtypes influence the progression of rhabdomyolysis-induced kidney injury. *J Am Soc Nephrol* 2015; **26:** 1363-1377.

7. Okubo K, Kurosawa M, Kamiya M, *et al.* Macrophage extracellular trap formation promoted by platelet activation is a key mediator of rhabdomyolysis-induced acute kidney injury. *Nat Med* 2018; **24:** 232-238.

8. Rubio-Navarro A, Carril M, Padro D, *et al.* CD163-Macrophages Are Involved in Rhabdomyolysis-Induced Kidney Injury and May Be Detected by MRI with Targeted Gold-Coated Iron Oxide Nanoparticles. *Theranostics* 2016; **6:** 896-914.

9. Huang X, Zhao W, Zhang L, *et al.* The role of complement activation in rhabdomyolysis-induced acute kidney injury. *PLoS One* 2018; **13:** e0192361.

10. Merle NS, Church SE, Fremeaux-Bacchi V, *et al.* Complement System Part I - Molecular Mechanisms of Activation and Regulation. *Front Immunol* 2015; **6:** 262.

11. Merle NS, Grunenwald A, Rajaratnam H, *et al.* Intravascular hemolysis activates complement via cell-free heme and heme-loaded microvesicles. *JCI Insight* 2018; **3**.

12. Merle NS, Leon J, Poillerat V, *et al.* Circulating FH Protects Kidneys From Tubular Injury During Systemic Hemolysis. 2020; **11**.

13. Roumenina LT, Rayes J, Lacroix-Desmazes S, *et al.* Heme: Modulator of Plasma Systems in Hemolytic Diseases. *Trends Mol Med* 2016; **22:** 200-213.

14. Arumugam TV, Shiels IA, Woodruff TM, *et al.* The role of the complement system in ischemia-reperfusion injury. *Shock* 2004; **21:** 401-409.

15. Zhou W, Farrar CA, Abe K, *et al.* Predominant role for C5b-9 in renal ischemia/reperfusion injury. *J Clin Invest* 2000; **105:** 1363-1371.

16. Thurman JM, Ljubanovic D, Royer PA, *et al.* Altered renal tubular expression of the complement inhibitor Crry permits complement activation after ischemia/reperfusion. *J Clin Invest* 2006; **116:** 357-368.

17. Franzin R, Stasi A, Fiorentino M, *et al.* Inflammaging and Complement System: A Link Between Acute Kidney Injury and Chronic Graft Damage. *Front Immunol* 2020; **11:** 734.

18. Goutaudier V, Perrochia H, Mucha S, *et al.* C5b9 Deposition in Glomerular Capillaries Is Associated With Poor Kidney Allograft Survival in Antibody-Mediated Rejection. *Front Immunol* 2019; **10:** 235.

19. Vernon KA, Ruseva MM, Cook HT, *et al.* Partial Complement Factor H Deficiency Associates with C3 Glomerulopathy and Thrombotic Microangiopathy. *J Am Soc Nephrol* 2016; **27:** 1334-1342.

20. Farrar CA, Tran D, Li K, *et al.* Collectin-11 detects stress-induced L-fucose pattern to trigger renal epithelial injury. *J Clin Invest* 2016; **126:** 1911-1925.

21. Poillerat V, Gentinetta T, Leon J, et al. Hemopexin as an Inhibitor of Hemolysis-Induced Complement Activation. Front Immunol 2020; 11: 1684.

22. Komada T, Usui F, Kawashima A, *et al.* Role of NLRP3 Inflammasomes for Rhabdomyolysis-induced Acute Kidney Injury. *Sci Rep*, vol. 5, 2015.

23. Saku A, Hirose K, Ito T, *et al.* Fucosyltransferase 2 induces lung epithelial fucosylation and exacerbates house dust mite-induced airway inflammation. *J Allergy Clin Immunol* 2019; **144:** 698-709.e699.

24. Najafian B, Fogo AB, Lusco MA, *et al.* AJKD Atlas of Renal Pathology: Myoglobin Cast Nephropathy. *Am J Kidney Dis* 2017; **69:** e7-e8.

25. Schulze M, Pruchno CJ, Burns M, *et al.* Glomerular C3c localization indicates ongoing immune deposit formation and complement activation in experimental glomerulonephritis. *Am J Pathol* 1993; **142:** 179-187.

26. Wilson HR, Medjeral-Thomas NR, Gilmore AC, *et al.* Glomerular membrane attack complex is not a reliable marker of ongoing C5 activation in lupus nephritis. *Kidney Int* 2019; **95:** 655-665.

27. Passwell J, Schreiner GF, Nonaka M, *et al.* Local extrahepatic expression of complement genes C3, factor B, C2, and C4 is increased in murine lupus nephritis. *J Clin Invest* 1988; **82:** 1676-1684.

28. Biglarnia AR, Huber-Lang M, Mohlin C, *et al.* The multifaceted role of complement in kidney transplantation. *Nat Rev Nephrol* 2018; **14:** 767-781.

29. Pratt JR, Basheer SA, Sacks SH. Local synthesis of complement component C3 regulates acute renal transplant rejection. *Nat Med* 2002; **8:** 582-587.

30. Renner B, Ferreira VP, Cortes C, *et al.* Binding of factor H to tubular epithelial cells limits interstitial complement activation in ischemic injury. *Kidney Int* 2011; **80:** 165-173.

31. Xavier S, Sahu RK, Landes SG, *et al.* Pericytes and immune cells contribute to complement activation in tubulointerstitial fibrosis. *Am J Physiol Renal Physiol* 2017; **312:** F516-f532.

32. Xavier S, Sahu RK, Bontha SV, *et al.* Complement C1r serine protease contributes to kidney fibrosis. *Am J Physiol Renal Physiol* 2019; **317:** F1293-f1304.

33. Pedersen DV, Roumenina L, Jensen RK, *et al.* Functional and structural insight into properdin control of complement alternative pathway amplification. *Embo j* 2017; **36:** 1084-1099.

34. Chen JY, Galwankar NS, Emch HN, *et al.* Properdin Is a Key Player in Lysis of Red Blood Cells and Complement Activation on Endothelial Cells in Hemolytic Anemias Caused by Complement Dysregulation. *Front Immunol* 2020; **11:** 1460.

35. Dobo J, Pal G, Cervenak L, *et al.* The emerging roles of mannose-binding lectin-associated serine proteases (MASPs) in the lectin pathway of complement and beyond. *Immunol Rev* 2016; **274:** 98-111.

36. Asgari E, Farrar CA, Lynch N, *et al.* Mannan-binding lectin-associated serine protease 2 is critical for the development of renal ischemia reperfusion injury and mediates tissue injury in the absence of complement C4. *Faseb j* 2014; **28:** 3996-4003.

37. Yaseen S, Demopulos G, Dudler T, *et al.* Lectin pathway effector enzyme mannan-binding lectin-associated serine protease-2 can activate native complement C3 in absence of C4 and/or C2. *Faseb j* 2017; **31:** 2210-2219.

38. Shulman LM, Yuhas Y, Frolkis I, *et al.* Glycerol induced ARF in rats is mediated by tumor necrosis factor-alpha. *Kidney Int* 1993; **43:** 1397-1401.

39. Nishida K, Watanabe H, Ogaki S, *et al.* Renoprotective effect of long acting thioredoxin by modulating oxidative stress and macrophage migration inhibitory factor against rhabdomyolysis-associated acute kidney injury. *Sci Rep* 2015; **5:** 14471.

40. Kim JH, Lee SS, Jung MH, *et al.* N-acetylcysteine attenuates glycerol-induced acute kidney injury by regulating MAPKs and Bcl-2 family proteins. *Nephrol Dial Transplant* 2010; **25:** 1435-1443.

41. Homsi E, Janino P, de Faria JB. Role of caspases on cell death, inflammation, and cell cycle in glycerol-induced acute renal failure. *Kidney Int* 2006; **69:** 1385-1392.

42. Homsi E, Janino P, Amano M, *et al.* Endogenous hepatocyte growth factor attenuates inflammatory response in glycerol-induced acute kidney injury. *Am J Nephrol* 2009; **29:** 283-291.

43. Peng Q, Li K, Smyth LA, *et al.* C3a and C5a promote renal ischemia-reperfusion injury. *J Am Soc Nephrol* 2012; **23:** 1474-1485.

44. Peng Q, Wu W, Wu KY, *et al.* The C5a/C5aR1 axis promotes progression of renal tubulointerstitial fibrosis in a mouse model of renal ischemia/reperfusion injury. *Kidney Int* 2019; **96:** 117-128.

45. Schröppel B, Heeger PS, Thiessen-Philbrook H, *et al.* Donor Urinary C5a Levels Independently Correlate With Posttransplant Delayed Graft Function. *Transplantation* 2019; **103:** e29-e35.

46. Laudisi F, Spreafico R, Evrard M, *et al.* Cutting edge: the NLRP3 inflammasome links complement-mediated inflammation and IL-1beta release. *J Immunol* 2013; **191:** 1006-1010.

47. Suresh R, Chandrasekaran P, Sutterwala FS, *et al.* Complement-mediated 'bystander' damage initiates host NLRP3 inflammasome activation. *J Cell Sci* 2016; **129:** 1928-1939.

48. Cui J, Wu X, Song Y, *et al.* Complement C3 exacerbates renal interstitial fibrosis by facilitating the M1 macrophage phenotype in a mouse model of unilateral ureteral obstruction. *Am J Physiol Renal Physiol* 2019; **317:** F1171-f1182.

49. Mastellos DC, Ricklin D, Lambris JD. Clinical promise of next-generation complement therapeutics. *Nat Rev Drug Discov* 2019; **18:** 707-729.

50. Bayarri-Olmos R, Kirketerp-Moller N, Perez-Alos L, *et al.* Development of a Quantitative Assay for the Characterization of Human Collectin-11 (CL-11, CL-K1). *Front Immunol* 2018; **9:** 2238.

Figure Captions

Figure 1. C3d staining is positive in tubular cells of rhabdomyolysis (RIAKI) kidneys, independent of its cause. A) Masson Trichrome (left) and periodic acid Schiff stain (right) of a kidney section showing casts in the tubular lumen (*) and acute tubular necrosis with loss of the proximal tubule brush border (arrows). **B)** C3c staining in kidney sections from patients with acute tubular necrosis (ATN) caused by hypovolemia (left), rhabdomyolysis (RIAKI, middle) or from a renal allograft (48 hours post-transplant; ischemia-reperfusion, right) **C)** C3d staining kidney sections of patients with ATN caused by hypovolemia (left), Cisplatin toxicity (middle) and kidney allograft at 48 hours post-transplant (ischemia-reperfusion, right). RIAKI caused by autoimmune myositis: (RIAKI 1), crush syndrome (RIAKI 2), strenuous exercise (RIAKI 3), unknown cause (RIAKI 4), suspicion of Mac Ardle syndrome (RIAKI 5), LIPN1 deficiency (RIAKI 6), muscle compression (RIAKI 7-8), Dengue fever (RIAKI 9) and sepsis (RIAKI 10). *Original magnification x40.*

Figure 2. C3b/iC3b tubular deposits correlate with RIAKI severity. A) Hematoxylin-Eosin staining of paraffin embedded kidneys from PBS mice (left) and GLY mice (right), *original magnification x40*. **B)** CD31 (red) and C3b/iC3b (green) immuno-fluorescence on frozen kidneys from PBS mice(left), glycerol-treated mice (middle) and Cisplatin- injected mice (CIS, right), *original magnification x20*. **C)** Quantification of C3b/iC3b tubular deposits using Halo© Software (left, ****p< 0,0001, Mann-Whitney test) (left). **D)** Correlation between C3b/iC3b tubular deposits and blood urea nitrogen (BUN) (r^2 = 0,64; p<0,0001) (left) and creatinine (r^2=0,69; p<0,0001) (right). *BUN: blood urea nitrogen.*

Figure 3. Complement system activation in human and murine RIAKI: implication of classical and lectin pathway. A) Flow cytometry analysis of C3 deposits (left) and C4 deposits (right) on renal proximal tubular epithelial cells (RPTEC) incubated with increasing doses of myoglobin prior to addition of normal healthy serum. **B)** C4 staining on paraffin-embedded kidney in RIAKI (left) compared to lupus nephropathy (right) patients. **C)** Kidney injury measured by blood urea nitrogen (BUN) in WT mice injected with PBS (blue) or glycerol (GLY) (red) and C4-/- (purple) mice injected with glycerol (C4-/- GLY). **D)** Vascular aggression measured by mRNA expression of P-Selectin and VCAM-1 in WT-PBS (blue), WT-GLY (red) and C4-/- GLY (purple) mice. **E)** Tubular aggression measured by Lcn2 (NGAL) and Havcr1 (KIM-1) mRNA expression in WT-PBS (blue), WT-GLY (red) and C4-/- GLY (purple) mice. **F)** CD31 (red) and C3b/iC3b (green) immunofluorescence on frozen kidneys from C4-/- mice injected with PBS (C4-/- PBS) (left) and C4-/- mice injected with glycerol (C4-/- GLY) (right), *original magnification x20*. **G)** Representative immunofluorescence of renal cortex showing C3b/iC3b (green), CL-11 (purple), a merged image of C3b/iC3b and CL-11 in WT-PBS (up) and WT-GLY (down) mice. Kruskall Wallis test with Dunn's correction: *p<0,05; **p<0,01; ***p<0,001; ****p<0.0001. *BUN: blood urea nitrogen*

Figure 4. Hemopexin improves kidney function through vascular protection and decreases complement activation in murine RIAKI. A) Kidney mRNA expression of Heme Oxygenase-1 (HO-1) in GLY and PBS mice. **B)** FACS analysis of C3d deposits on RPTEC with increasing concentration of Heme (Fe3+). **C)** Kidney injury measured by BUN in GLY mice (red) and WT mice injected with Hemopexin (IV) prior to glycerol (black). **D)**

Tubular aggression measured by Lcn2 (NGAL) and Havcr (KIM-1) mRNA expression in GLY mice (red) and WT mice injected with Hemopexin (IV) prior to glycerol (black). **E)** Vascular aggression measured by mRNA expression in kidneys of P-Selectin, E-Selectin, VCAM-1 and ICAM-1 from GLY mice (red) and WT mice injected with Hemopexin (IV) prior to glycerol injection (Hx/GLY) (black). **F)** Immunofluorescence on frozen kidneys: C3b/iC3b (green) and CD31 (red) in PBS mice (left) GLY mice (middle) and Hemopexin-injected GLY mice (Hx/GLY) (right). **G)** Quantification of tubular C3 deposits by HALO Software from GLY (red) and WT mice injected with Hemopexin (IV) prior to glycerol (black). (right). *Dotted line represents the mean value of each marker for PBS mice. BUN: Blood urea nitrogen. RPTEC: renal proximal tubular epithelial cells.* Mann-Whitney test*: *p<0,05; **p<0,01; ***p<0,001; ****p<0.0001*

Figure 5. C5a Receptor 1 is upregulated on tubular cells and on macrophages in kidneys after glycerol injection. A) Kidney mRNA expression for C3aR1 and C5aR1 in PBS (blue) and GLY-treated mice (red). **B)** C5aR1 (red) immunofluorescence on frozen kidneys from PBS (left) and GLY (right) mice, white arrows are indicating interstitial staining, *original magnification x20.* **C)** Cell count for macrophages and neutrophils 8 hours (left) and 24 hours (right) after PBS (blue) or glycerol (GLY) (red) injection. **D)** Flow cytometry on whole kidneys 24 hours after PBS (up) and glycerol (down) injection. Gating on macrophages CD45+ Ly6G- CD68+. Analysis of HLA class II molecule (Iab), C5aR1 and Cd11b reveals the emergence of macrophages $CD68^{+}$ Iab^{-} $C5aR1^{hi}$ $Cd11b^{hi}$ **E)** C3b/iC3b (green) and Cd11b (red) immunofluorescence on frozen kidneys in GLY mice, *original magnification x20.*

Figure 6. C3-/- mice are protected from RIAKI. A) Kidney injury (renal function) measured by BUN in WT-PBS mice (PBS) (blue), WT-GLY mice (GLY) (red) and C3-/- GLY mice (left) (green). **B)** Correlation between BUN and Creatine Kinase in WT-GLY mice (r^2=0,56, p=0,0329) and C3-/- GLY mice (non-significant) (right). **C)** Volcano plot of WT-GLY versus WT-PBS mice. Genes with a fold change >2 and an adjusted p-value of less than 0,05 (red) are differentially expressed between the two groups. **D)** Heatmap of normalized counts (RSEM) in each mouse for the top 50 most differentially expressed genes (25 upregulated and 25 downregulated), defining the RIAKI signature. A row normalization is applied. (upper panel). Gene ontology analysis of biological pathways modulated in WT-GLY versus WT-PBS mice (lower panel). **E)** Heat map of normalized counts (RSEM) in each mouse (n=4 mice/group), for the top 50 most differentially expressed genes (25 upregulated and 25 downregulated) in the WT-PBS, WT-GLY and C3-/- GLY mice. A row normalization is applied. (upper panel). on the right column, in red are the genes of the RIAKI signature, which are completely normalized in the C3-/- (p value for the comparison of WT-GLY vs C3-/- GLY < 0.05 + a p value for C3-/- PBS vs WT-GLY > 0.05). In yellow are the genes which are partially normalized in the C3-/- mice (p value for the comparison of WT-GLY vs C3-/- GLY < 0.05 + a p value for C3-/- PBS vs WT-GLY < 0.05). In green are the genes which are not affected by C3 deficiency (p value for the comparison of WT-GLY vs C3-/- GLY > 0.05 + a p value for C3-/- PBS vs WT-GLY > 0.05). Gene ontology analysis of biological pathways modulated in WT-GLY versus C3-/- GLY mice. (lower panel). *BUN: blood urea nitrogen*

“	Age	Etiology	Other medical conditions	Treatments	Genetic exploration	Maximum CK level during hospitalization (U/L)	Hemo-dialysis at diagnostic	Creatinine at the biopsy (µmole/L)	Delay between diagnosis-biopsy	Basal blood creatinine (µmole/L)	Optic microscopy	Immuno-fluorescence	C3c deposits
1	69	Auto-immune myositis	No	*na*	No	461400	No	412	<1 week	88	ATN/ATIN	No deposits	No
2	38	Car accident (crush syndrome)	No	No	No	2500	Yes	800	<1 week	*na*	*na*	*na*	*na*
3	21	Strenuous Exercise	No	No	yes, negative	10100	No	132	<1 week	96	two cylinders	No deposits	No
4	13	Unknown	Atopic dermatitis	*na*	yes, negative	20 000	No	373	> 1 month	40.4	Tip lesion	Focal IgM, C1q and C3	Yes
5	41	Suspicion of Mac Ardle disease	Appendicectomy, proteinuria	No	yes, ongoing	10 000	Yes	1615 (on dialysis)	<1 week	70	ATN, eosinophilic cylinder, mesangial thickening, no fibrosis	IgA and C3 +++, IgM+, kappa+, lambda+ in mesangium	Yes
6	5	Lpin 1 deficiency	No	No	yes, heterozygous LPIN 1 mutation c1011C-G et c.1230C-T	20 000	No	anuria (previous episode with 373 µmol/L requiring dialysis)	<1 week	*na*	ATN	*na*	*na*
7	62	Muscle compression	D2 hypertension	No	No	1200	No	238	< 1 month	70.4	ATN+chronic injuries	No deposits	No
8	88	Muscle compression	*na*	No	No	1200	No	150	< 1 month	*na*	ATIN	No deposits	No
9	63	Sepsis	No	No	No	100 000	Yes	363	< 1 month	*na*	ATIN/ATN with cylinder	No deposits	No
10	14	Dengue fever	No	no	No	>100 000	Yes	674 (on dialysis)	<1 week	na	ATN and cylinder	No deposits	No

Table 1. Clinical and biological characteristics (ATN: acute tubular necrosis, ATIN: acute tubulo-interstitial nephritis, D2: Type 2 Diabetes Mellitus, na: not available)

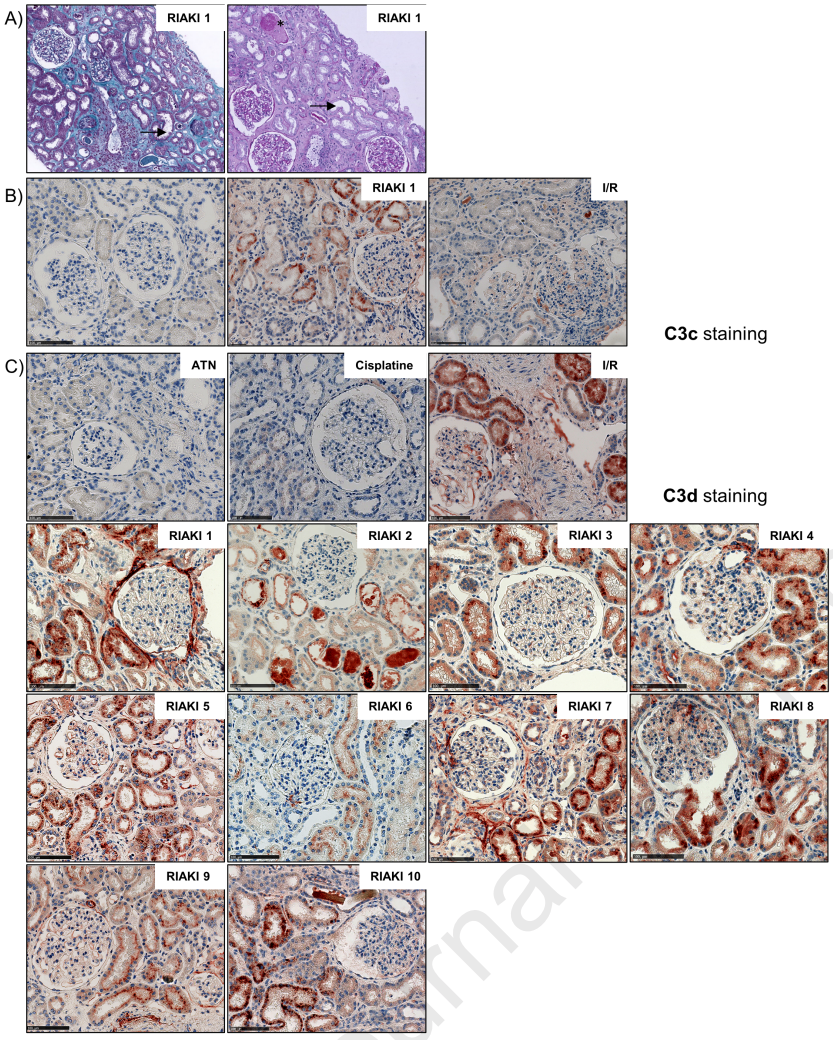

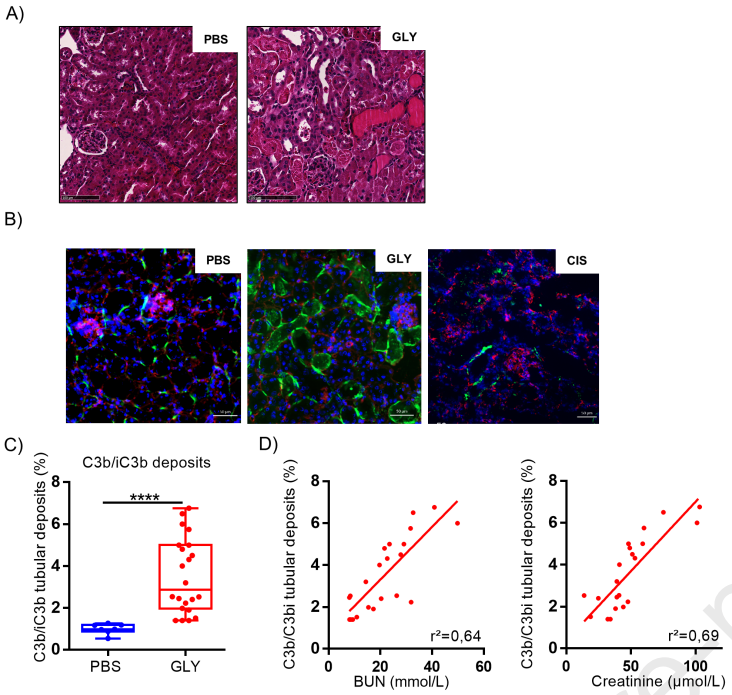

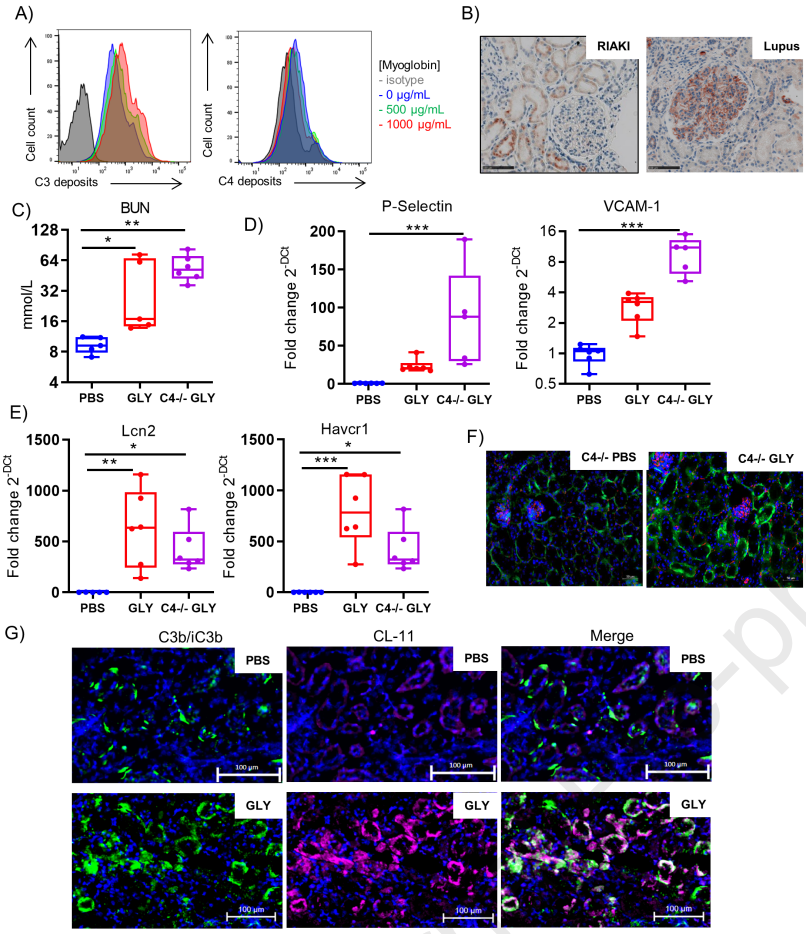

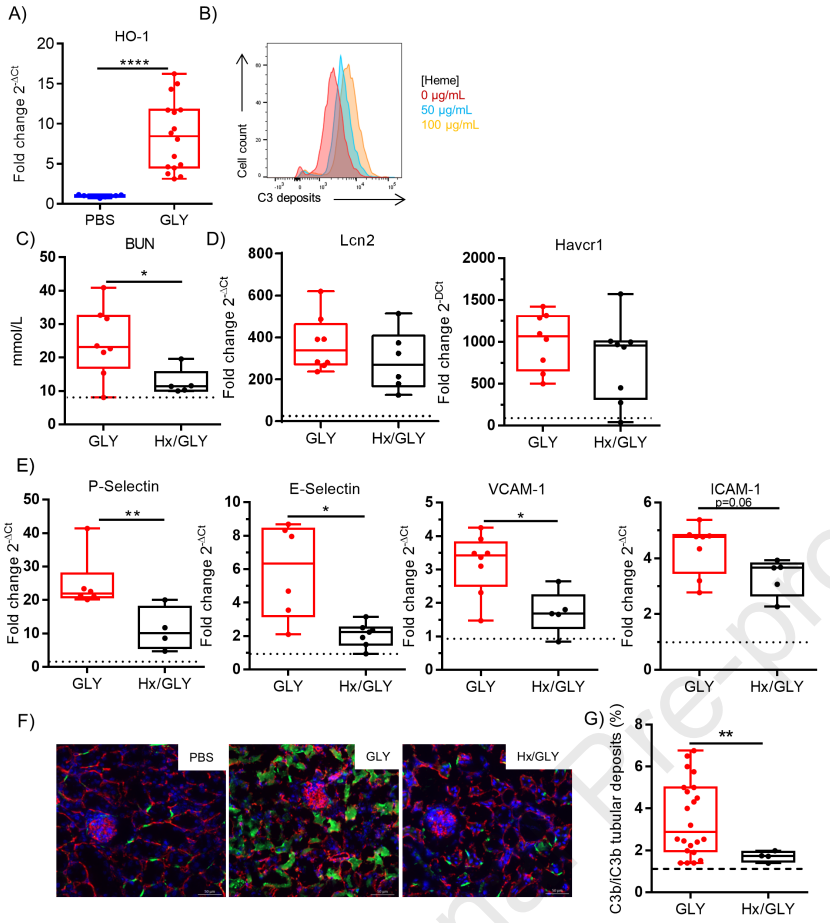

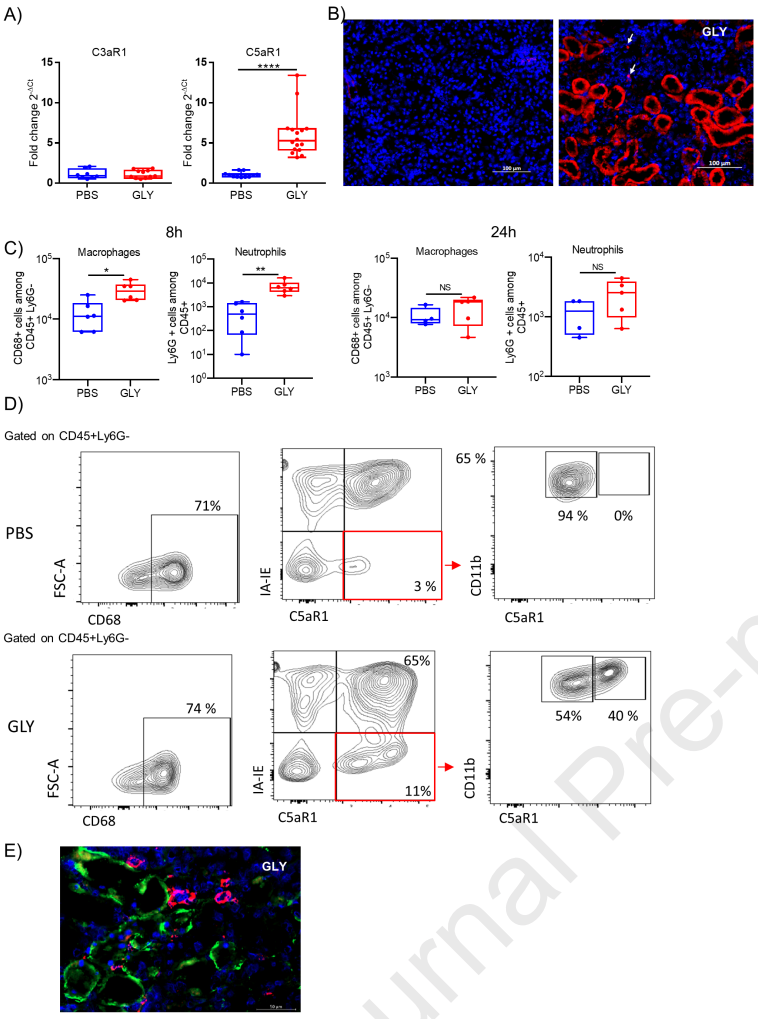

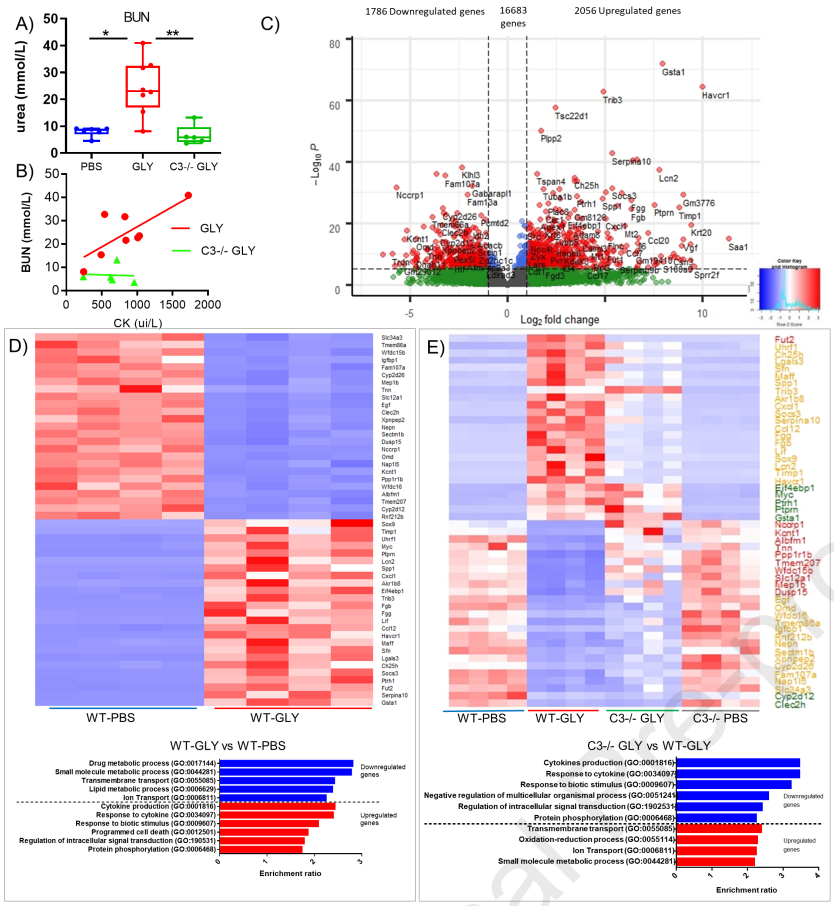

Received: 23 February 2018 | Revised: 4 September 2018 | Accepted: 9 September 2018

DOI: 10.1111/acel.12850

ORIGINAL PAPER

WILEY Aging Cell

Knockout of receptor for advanced glycation end-products attenuates age-related renal lesions

Thibault Teissier[1,*] | Valentine Quersin[1,2,*] | Viviane Gnemmi[3] | Maité Daroux[1] | Mike Howsam[1] | Florian Delguste[1] | Cécile Lemoine[1] | Chantal Fradin[1] | Ann-Marie Schmidt[4] | Christelle Cauffiez[5] | Thierry Brousseau[6] | François Glowacki[2,5] | Frédéric J. Tessier[1] | Eric Boulanger[1,7,†] | Marie Frimat[1,2,†]

[1]U995 - Lille Inflammation Research International Center, INSERM, CHU Lille, University of Lille, Lille, France

[2]Department of Nephrology, CHU Lille, Lille, France

[3]Department of Pathology, U1172 - Jean-Pierre Aubert Research Center, INSERM, CHU Lille, University of Lille, Lille, France

[4]Department of Medicine, Diabetes Research Center, NYU Langone Medical Center, New York, New York

[5]EA4483 IMPECS-IMPact of Environmental ChemicalS on Human Health, CHU Lille, University of Lille, Lille, France

[6]UF8832 - Biochimie Automatisée,Pôle de Biologie Pathologie Génétique, CHU Lille, Lille, France

[7]Department of Geriatrics, CHU Lille, Lille, France

Correspondence
Marie Frimat, INSERM U995/Team "Glycation: From Inflammation to Aging", Lille Inflammation Research International Center, Lille, France.
Email: marie.frimat@chru-lille.fr

Funding information
Institut National de la Santé et de la Recherche Médicale; Digest Science foundation

Abstract

Pro-aging effects of endogenous advanced glycation end-products (AGEs) have been reported, and there is increasing interest in the pro-inflammatory and -fibrotic effects of their binding to RAGE (the main AGE receptor). The role of dietary AGEs in aging remains ill-defined, but the predominantly renal accumulation of dietary carboxymethyllysine (CML) suggests the kidneys may be particularly affected. We studied the impact of RAGE invalidation and a CML-enriched diet on renal aging. Two-month-old male, wild-type (WT) and RAGE$^{-/-}$ C57Bl/6 mice were fed a control or a CML-enriched diet (200 μg CML/g_{food}) for 18 months. Compared to controls, we observed higher CML levels in the kidneys of both CML WT and CML RAGE$^{-/-}$ mice, with a predominantly tubular localization. The CML-rich diet had no significant impact on the studied renal parameters, whereby only a trend to worsening glomerular sclerosis was detected. Irrespective of diet, RAGE$^{-/-}$ mice were significantly protected against nephrosclerosis lesions (hyalinosis, tubular atrophy, fibrosis and glomerular sclerosis) and renal senile apolipoprotein A-II (ApoA-II) amyloidosis ($p < 0.001$). A positive linear correlation between sclerosis score and ApoA-II amyloidosis score ($r = 0.92$) was observed. Compared with old WT mice, old RAGE$^{-/-}$ mice exhibited lower expression of inflammation markers and activation of AKT, and greater expression of *Sod2* and SIRT1. Overall, nephrosclerosis lesions and senile amyloidosis were significantly reduced in RAGE$^{-/-}$ mice, indicating a protective effect of RAGE deletion with respect to renal aging. This could be due to reduced inflammation and oxidative stress in RAGE$^{-/-}$ mice, suggesting RAGE is an important receptor in so-called inflamm-aging.

KEYWORDS
advanced glycation end-products, amyloidosis, chronic kidney disease, nephrosclerosis, receptor for AGEs, renal aging

*These authors contributed equally to this study.
†These authors co-directed this study.

1 | INTRODUCTION

Kidney function declines with age (Bolignano, Mattace-Raso, Sijbrands, & Zoccali, 2014; Glassock, Warnock, & Delanaye, 2017), resulting in elderly people being particularly susceptible to developing chronic kidney disease (CKD). The prevalence of CKD—defined as a glomerular filtration rate (GFR) inferior to 60 ml/min/1.73 m^2—was thus more than 30% in a European cohort of patients over 70 years old (Ebert et al., 2016; Glassock et al., 2017). Nonspecific morphologic changes are associated with aging kidneys and designated by the generic term "nephrosclerosis." Histologically, this is characterized by nephron loss, global glomerulosclerosis (GS > 10%), arteriosclerosis, tubular atrophy, and interstitial fibrosis (>5%) (Denic, Glassock, & Rule, 2016; O'Sullivan, Hughes, & Ferenbach, 2017).

Consequent to the rapid growth in the proportion of elderly people throughout the world ("European Commission: The 2015 ageing report. Eur Econ 3:424," European Commission, 2015; GA, Atlanta, 2013), an increase in the number of CKD diagnoses would appear to be inevitable. However, more than a third of people exhibit no change in GFR with age (Bolignano et al., 2014; Lindeman, Tobin, & Shock, 1985), suggesting that age-related renal impairment could be preventable. Gender, ethnicity, genetic factors, and comorbidities are known to influence renal outcomes (Choudhury & Levi, 2011; Smyth, Duffy, Maxwell, & McKnight, 2014), but other factors remain to be clarified.

The impact of advanced glycation end-products (AGEs) on CKD, especially through binding to their main receptor RAGE (receptor for AGEs), has received significant research attention (Clarke, Dordevic, Tan, Ryan, & Coughlan, 2016; Stinghen, Massy, Vlassara, Striker, & Boullier, 2016). The AGEs form a heterogeneous group of molecules resulting from permanent binding of reducing sugars to a range of amino-compounds. Their endogenous formation occurs under various conditions such as hyperglycemia and oxidative stress, but also aging. Their presence is moreover clearly identified in foods: Daily intake of *N*ε-carboxymethyllysine (CML, the most studied AGE) can be as high as 252 μg/kg body weight in a typical European diet (Tessier & Birlouez-Aragon, 2012). Evidence has recently accumulated incriminating the endogenous AGE/RAGE axis in age-related diseases. RAGE is a multiligand, transmembrane receptor activating major pro-inflammatory and pro-oxidative signaling pathways. Its expression in numerous cell types increases with aging and pathological conditions such as diabetes, but a role for this receptor has been postulated in the premature dysfunction of several organs, even in the absence of diabetes (Frimat et al., 2017; Ramasamy, Shekhtman, & Schmidt, 2016). The impact of chronic exposure to dietary AGEs on aging remains poorly studied, however.

Considering the preferential accumulation of CML in the kidneys under a CML-enriched diet (Li et al., 2015; Tessier et al., 2016) and studies linking dietary AGEs and kidney damage (Feng et al., 2007; Zheng et al., 2002), we hypothesized that kidneys are target organs for accelerated aging induced by AGE/RAGE interactions. In order to study this question, histologic markers of renal aging were analyzed in 2-month-old male wild-type (WT) and $RAGE^{-/-}$ C57Bl/6 mice fed a control or a CML-enriched diet over 18 months.

2 | RESULTS

2.1 | Prolonged intake of a CML-enriched diet results in renal accumulation of glycation products

A diffuse antibody-mediated CML staining was observed in the kidneys of all WT mice but was more intense in mice fed a CML-enriched diet compared with control mice. CML staining predominated in the proximal tubular cells and along the internal wall of arteries. We found similar results in the kidneys of $RAGE^{-/-}$ mice suggesting that CML accumulation from the CML-enriched diet is governed by RAGE-independent mechanisms (Figure 1a). These results were confirmed using liquid chromatography with tandem mass spectrometric (HPLC-MS/MS) detection in kidney samples. The mean levels of free CML were higher among the mice fed the CML-enriched diet, both in WT (0.05 ± 0.02 and 0.45 ± 0.2 μmol/g of dry matter for control and CML diet, respectively: $p = 0.15$) and $RAGE^{-/-}$ mice (0.03 ± 0.02 and 0.85 ± 0.3 μmol/g of dry matter for control and CML diet, respectively: $p < 0.01$). These differences between groups were also observed for concentrations of protein-bound CML (275 ± 145 and 1,331 ± 740 μmol/mol lysine for control and CML WT mice, respectively: $p = 0.07$; 190 ± 47 and 1,486 ± 947 μmol/mol lysine for control and CML $RAGE^{-/-}$ mice, respectively: $p < 0.05$), thereby suggesting a RAGE-independent mechanism of CML formation (Figure 1b-c).

2.2 | Prolonged intake of a CML-enriched diet does not significantly affect renal aging

Prior to assessing the effects of a CML-enriched diet and RAGE invalidation on renal aging, we first ensured that weight, glycaemia, cholesterolemia, and triglyceridemia were comparable between mice fed the control and CML-enriched diets. None of the WT or $RAGE^{-/-}$ mice became diabetic, dyslipidemic, or obese under the influence of a CML-enriched diet (Supporting Information Table S1). Renal parameters were then studied, and lesions of arteriolar hyalinosis, tubular atrophy, interstitial fibrosis, and GS (histological markers of nephrosclerosis, Figure 2a) were all assessed "blind.".

Renal weight, plasma creatinine, and urea were not statistically different between control and CML groups, in either WT or $RAGE^{-/-}$ mice (data not shown). We analyzed the expression of *Kim-1* and *Ngal* as sensitive markers of kidney injury associated with CKD progression in humans (Alderson et al., 2016): The expression of these genes was also unaffected by the CML-rich diet (Supporting Information Figure S1a-b).

The assessment of nephrosclerosis markers at 20 months of age gave similar results: The CML-rich diet had no significant effect on arteriolar hyalinosis, tubular atrophy, or fibrosis score (Supporting Information Figure S1c-e). There was a minor worsening of GS under the influence of the CML-rich diet in WT mice (Supporting Information Figure S1f-h): Only 6.5% glomeruli lacked any sign of sclerosis in CML WT mice against 31%, 61% and 67% in control WT, control $RAGE^{-/-}$ and CML $RAGE^{-/-}$, respectively; the median GS score and percentage of global GS—the end-stage of glomerular lesion—also

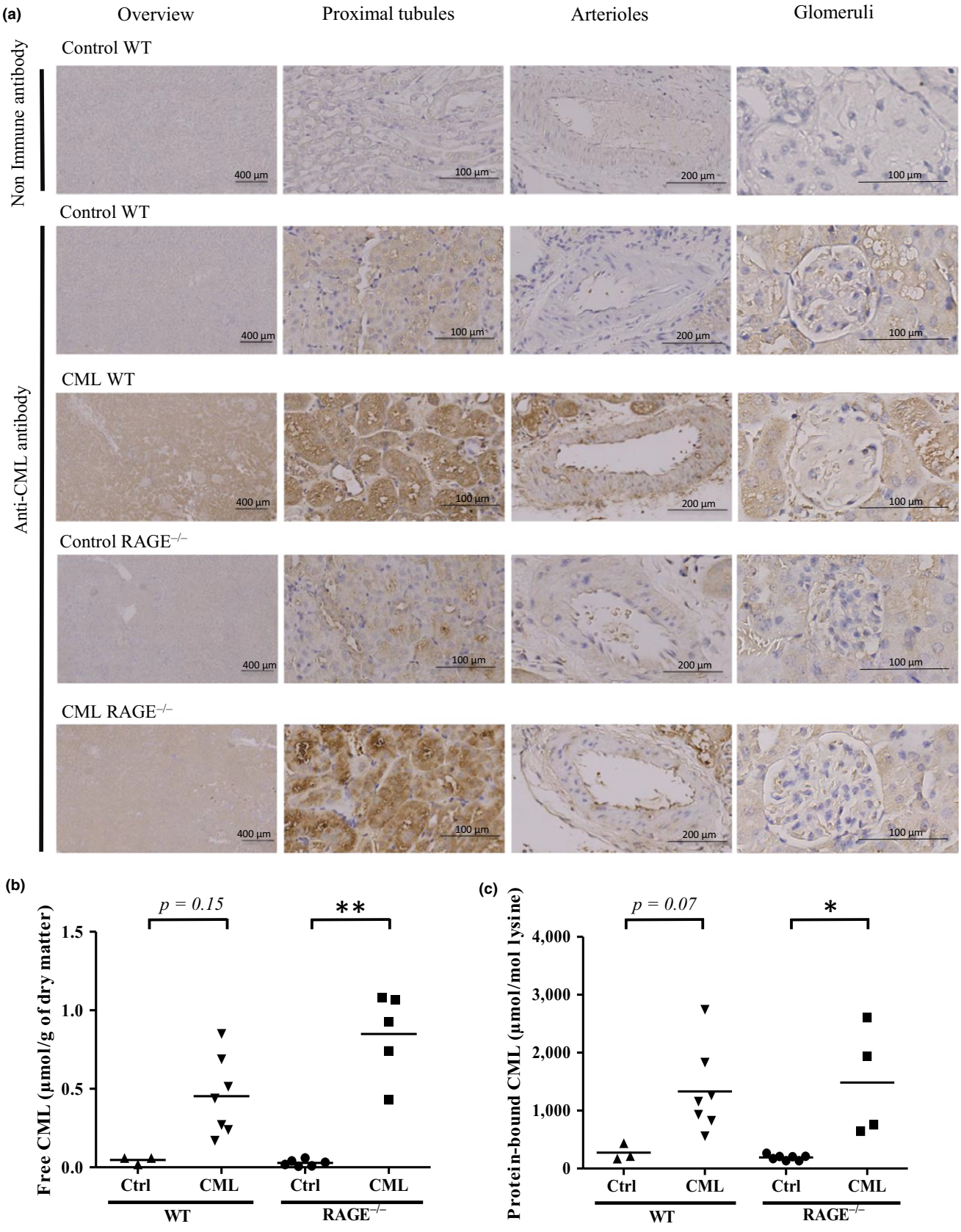

FIGURE 1 CML accumulation in the kidneys of WT and RAGE$^{-/-}$ mice was diet-dependant. (a) Representative localization of protein-bound CML studied by IHC on kidney sections showed that mice fed a CML-enriched diet exhibited predominantly tubular staining. From left to right: low magnification, high magnification on proximal tubules, arterioles and glomeruli. (b-c) Quantification by HPLC-MS/MS of (b) free and (c) protein-bound CML in kidneys. *$p < 0.05$, **$p < 0.01$, Kruskal–Wallis test

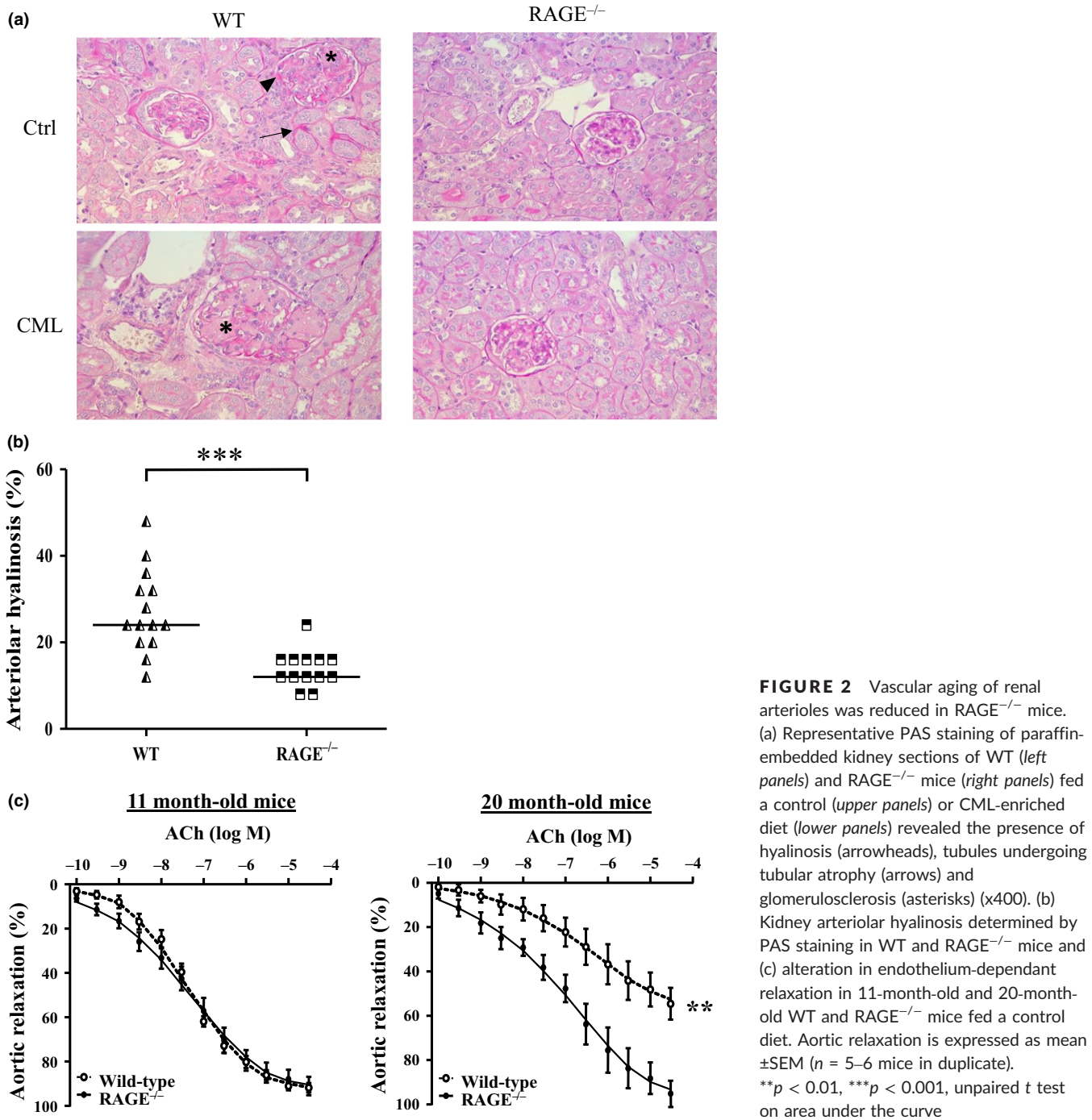

FIGURE 2 Vascular aging of renal arterioles was reduced in RAGE$^{-/-}$ mice. (a) Representative PAS staining of paraffin-embedded kidney sections of WT (*left panels*) and RAGE$^{-/-}$ mice (*right panels*) fed a control (*upper panels*) or CML-enriched diet (*lower panels*) revealed the presence of hyalinosis (arrowheads), tubules undergoing tubular atrophy (arrows) and glomerulosclerosis (asterisks) (x400). (b) Kidney arteriolar hyalinosis determined by PAS staining in WT and RAGE$^{-/-}$ mice and (c) alteration in endothelium-dependant relaxation in 11-month-old and 20-month-old WT and RAGE$^{-/-}$ mice fed a control diet. Aortic relaxation is expressed as mean ±SEM (n = 5–6 mice in duplicate). $^{**}p < 0.01$, $^{***}p < 0.001$, unpaired t test on area under the curve

followed this trend (CML WT>control WT>control and CML RAGE$^{-/-}$). These differences were not significant, however, in contrast to the results observed when we compared WT with RAGE$^{-/-}$ mice. In order to analyze the impact of the RAGE invalidation on renal aging, we thus focused on differences between WT and RAGE$^{-/-}$ mice, irrespective of diet.

2.3 | RAGE knockout mice are protected against nephrosclerosis lesions

All mice had hyaline deposits on the arteriole walls (10% to 48% of studied vessels), but the median percentage of vessels with hyaline deposits was higher in WT than in RAGE$^{-/-}$ mice (24% vs. 12%, respectively, $p < 0.001$) (Figure 2b). In order to study the evolution of endothelial function with age, we measured the percentage of aortic relaxation mediated by different concentrations of acetylcholine (Ach) in middle-aged (11-month-old) or old (20-month-old) WT and RAGE$^{-/-}$ mice. No difference was observed between 11-month-old WT and RAGE$^{-/-}$ mice (92 ± 7 and 91% ± 2% of max relaxation, respectively). At 20 months old, however, WT mice exhibited reduced responsiveness to Ach (55% ± 2% of max. relaxation vs. 11-month-old WT mice, $p < 0.001$) in contrast to RAGE$^{-/-}$ mice with conserved endothelial function (95% ± 1% of max. relaxation) (Figure 2c).

Both tubular atrophy and interstitial fibrosis lesions were also more present in WT than in RAGE$^{-/-}$ mice. The median percentage of tubular atrophy was 18% and 14% ($p < 0.01$), and the median fibrosis scores were 3 and 1 A.U. ($p < 0.001$) in WT and RAGE$^{-/-}$ mice, respectively (Figure 3a-b). Fibrosis was identified in renal interstitium of all WT mice, but was often mild to absent in RAGE$^{-/-}$ mice (Figure 3c). The *Ngal* expression, more specifically associated with tubulointerstitial damage (Rysz, Gluba-Brzózka, Franczyk, Jabłonowski, & Ciałkowska-Rysz, 2017), was significantly higher in WT mice (~15.5 ± 6.6) than RAGE$^{-/-}$ mice (~6.4 ± 5.6, $p < 0.05$). Comparing old WT with old RAGE$^{-/-}$ mice, there was no difference in the *Kim-1* expression (Figure 3d-e).

The median GS score at 20 months of age, calculated after histological evaluation of sclerosis intensity of 60 glomeruli per mouse, was higher in WT mice (49.3 A.U.) than in RAGE$^{-/-}$ mice (10 A.U., $p < 0.001$). Only 13% of the glomeruli lacked any sign of sclerosis in WT mice against 63% in RAGE$^{-/-}$ mice ($p < 0.001$). The mean percentage of global GS (glomeruli with a GS score of 100) was 14.6% in WT mice, while no global GS was observed in RAGE$^{-/-}$ mice (Figure 4a-c).

2.4 | RAGE knockout prevents senile amyloidosis

The GS appeared nodular with developing hypertrophic glomeruli. The mean size of the glomeruli was significantly larger in WT than in RAGE$^{-/-}$ mice (1.0 ± 0.3 and 0.6 ± 0.1 A.U., respectively: $p < 0.001$, Figure 4d). Birefringence under polarized light, obtained after Congo Red staining, suggested that this nodular sclerosis was at least partly caused by amyloidosis. This was confirmed by the presence of serum amyloid protein (SAP) in immunohistochemistry assays, and the identification of 5–10 nm fibrils by electron microscopy (Figure 4e-h). Thus, 8 of the 14 (57%) WT mice were amyloidosis positive against only 1 of the 13 (8%) RAGE$^{-/-}$ mice (7 of the 9 amyloid mice were fed the CML-rich diet, Supporting Information Figure S2a).

A positive ApoA-II protein staining occurred in the same locations as the amyloid deposits, suggesting an ApoA-II amyloidosis (AApoA-II) thought to be related to aging processes in mice (Kitagawa et al., 2003). The ApoA-II deposition was mainly localized in glomeruli, with various intensities according to the glomeruli and individual mice (Figure 5a). Interstitial AApoA-II was also observed when the vast majority of glomeruli showed extensive deposits, suggesting a more advanced

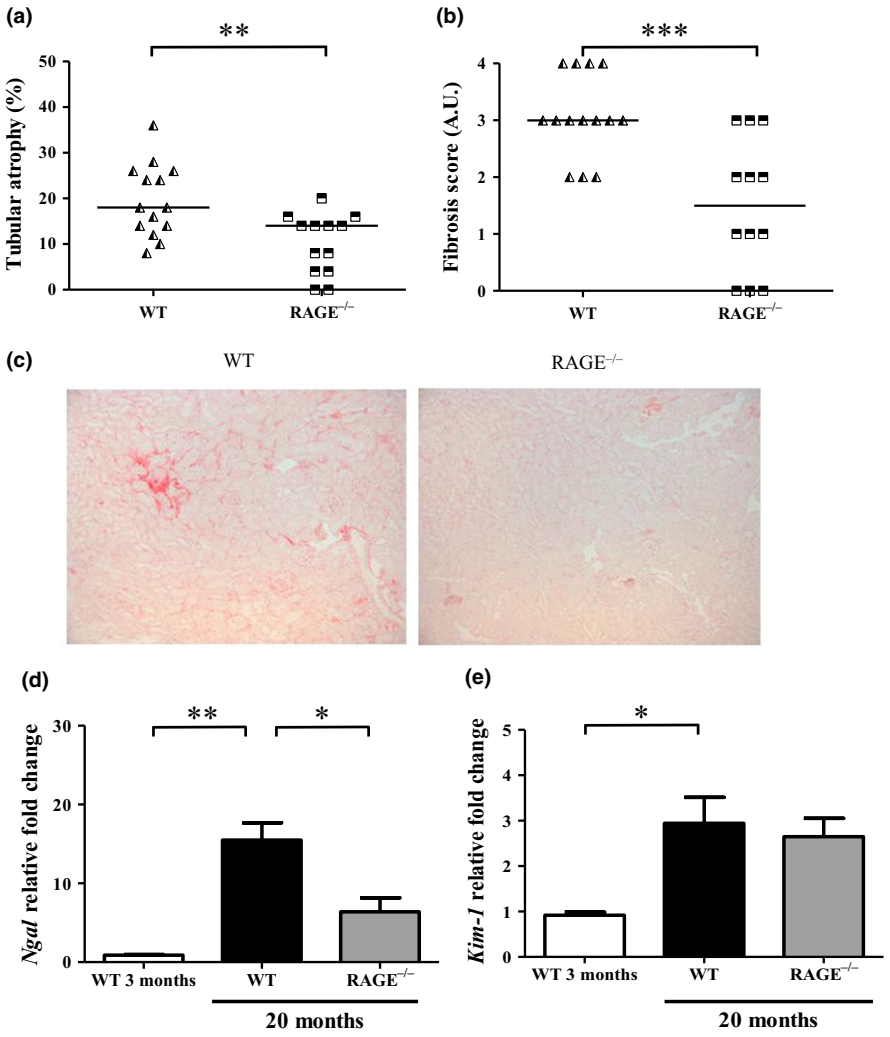

FIGURE 3 RAGE$^{-/-}$ mice were protected against tubulo-interstitial aging. Quantification of (a) tubular atrophy was determined by PAS staining and (b) interstitial fibrosis by Sirius red staining. (c) Representative Sirius red staining of control and CML WT and RAGE$^{-/-}$ mice at low magnification (x 100). (d-e) Expression of kidney injury markers *Ngal* (d) and *Kim-1* (e) in renal tissue from 3- or 20-month-old WT and RAGE$^{-/-}$ mice (mean ±SEM, $n = 3$ for 3-month-old mice and $n = 10$ for 20-month-old mice). $^{*}p < 0.05$, $^{**}p < 0.01$, $^{***}p < 0.001$, unpaired *t* test or Kruskal–Wallis test for multiple comparisons

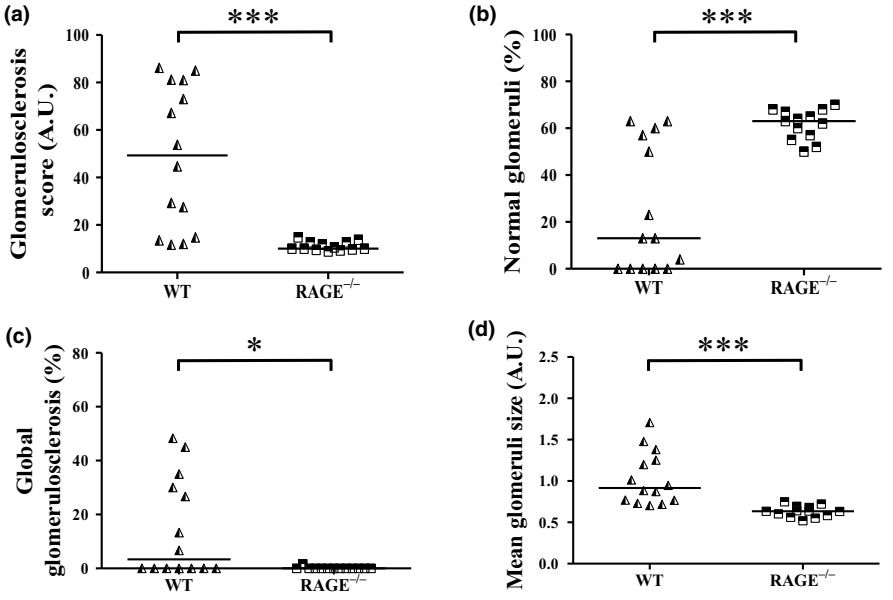

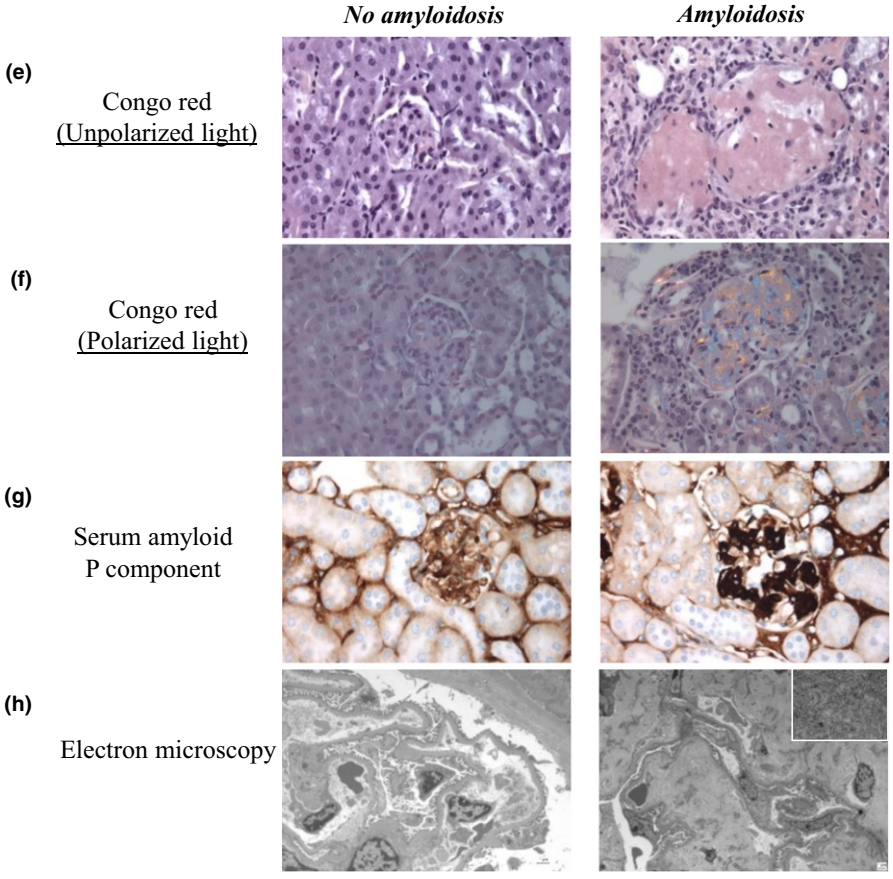

FIGURE 4 Amyloidosis-linked glomerulosclerosis was largely prevented in RAGE$^{-/-}$ mice. Quantification of GS in paraffin-embedded kidney sections indicated (a) the GS score (60 glomeruli/mouse) which was used to determine (b) the percentage of normal glomeruli (glomeruli with GS score of 0) and of (c) global GS (glomeruli with a GS score of 100). (d) Mean glomeruli size (30 glomeruli/mouse). Determination of amyloidosis-positive lesions in paraffin-embedded kidney sections after (e) Congo red staining under nonpolarized light (x 400) and (f) polarized light showing birefringence (x400), (g) Immunohistochemistry of Serum Amyloid P component (SAP, x 400) and (h) electron microscopy showing the absence in control WT mouse (*left panel*, x 1,000) and the presence in CML WT mouse (*right panel*, x 1670 low magnification, x 21,560 high magnification in the frame) of amyloid fibrils. *$p < 0.05$, ***p <0.001, Mann–Whitney test, representative images

stage of amyloidosis. Other proteins known to be amyloidogenic were tested (serum amyloid A, involved in chronic inflammatory diseases, and peptides β1–40 and β1–42, responsible for amyloid plaques in Alzheimer's disease), but none were correlated with the identification of amyloidosis (data not shown). The WT mice had a median AApoA-II score significantly higher than RAGE$^{-/-}$ mice which had no or very few deposits (2.5 ± 1.3 vs. 1.1 ± 0.2 A.U., respectively: $p < 0.01$; Figure 5b). A trend also suggested greater AApoA-II deposition in CML WT than in control WT mice (1.2 A.U.), but this trend was not observed when RAGE$^{-/-}$ groups were compared (Supporting Information Figure S2b). The GS intensity was correlated with AApoA-II score ($r = 0.92$, $p < 0.0001$, Figure 5c).

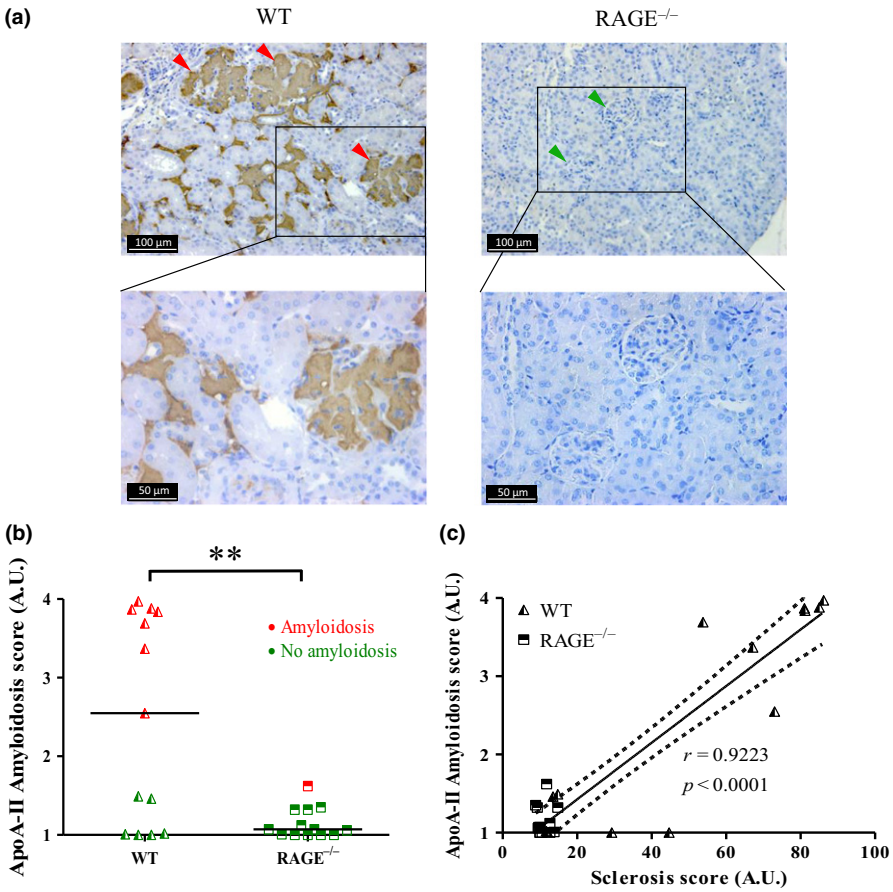

FIGURE 5 AApoA-II was largely absent in RAGE$^{-/-}$ mice. AApoA-II in kidney tissue sections from 20-month-old WT mice (*left panel*) and RAGE$^{-/-}$ mice (*right panel*) were immunostained using an anti-ApoA-II antibody (a) green arrowheads, no deposits; red arrowheads, extensive deposits (representative image). (b) Scoring of ApoA-II amyloid deposits obtained from IHC and calculated from the grading of 100 glomeruli per mouse, where 1 = no deposit, 2 = small, 3 = moderate and 4 = extensive deposits. Red dots, amyloidosis-positive mice; green dots, amyloidosis-negative mice. (c) Linear regression analysis between AApoA-II and sclerosis scores obtained for all four conditions, y = 0.036 x + 0.70, r = 0.9223, dotted line: 95% confidence intervals (C). $^{**}p < 0.01$, unpaired *t* test

2.5 | RAGE knockout mice exhibited less inflammation and were better protected against oxidative stress

Compared to 3-month-old WT mice, the mRNA levels of *Il-6*, *Tnf-α* and *Vcam-1* increased, respectively, ~15.8-, 10.6- and 4.5-fold in 20-month WT mice and ~5.6-, 3.4- and 2.1-fold in RAGE$^{-/-}$ mice (Figure 6a-c). The increase in these markers was significant in old WT mice but not in old RAGE$^{-/-}$ mice, suggesting a similar pro-inflammatory profile in young WT and old RAGE$^{-/-}$ mice. Expression of the antioxidant genes, *Sod2* (a mitochondrial manganese-dependent superoxide dismutase), *Cat* (a peroxide hydrogen detoxifier) and *Hmox* (known to increase under influence of oxidative stress and recently described as ameliorating the oxidative stress-induced endothelial senescence (Luo et al., 2018)), was also analyzed. While *Cat* expression did not change with age or genotype, *Sod2* expression was significantly lower in old WT mice when compared with young WT (0.56 ± 0.1, $p < 0.01$) and old RAGE$^{-/-}$ mice (0.75 ± 0.1, $p < 0.05$). An important decrease in *Hmox* was also observed in both old WT (0.38 ± 0.2) and RAGE$^{-/-}$ (0.49 ± 0.1) mice but was only significant in the former ($p < 0.01$) (Figure 6d-f).

As a first step to elucidate the mechanisms underlying this potential protective effect of RAGE knockout, and in light of our results on inflammation and oxidation markers, we focused on SIRT1 (associated with longevity and known to decrease with age (Yuan et al., 2016)) and the AKT/mTor pathway [involved in kidney disease (Kajiwara and Masuda, 2016)]. SIRT1 was higher in RAGE$^{-/-}$ than WT mice (1.6-fold ±0.8, $p = 0.056$, Figure 6g). Conversely, the S6 subunit of the 40S ribosome (pS6RP or S235/236), a mTORC1 activity indicator and, more significantly, pAkt (S473, a mTORC2 activity indicator) were lower in old RAGE$^{-/-}$ than WT mice (0.1 ± 0.11 and 0.42 ± 0.15, respectively, $p < 0.05$) (Figure 6h-i).

3 | DISCUSSION

Although the small sample sizes necessitate caution in interpreting our results, we here report that RAGE knockout mice developed significantly less nephrosclerosis and senile amyloid lesions than WT mice, suggesting a key role for this receptor in the renal aging process. Prolonged exposure to a CML-enriched diet was associated with CML accumulation in kidneys, but there was no evident relationship between these deposits and renal injuries; CML accumulation was RAGE-independent and thus could not explain the differences between WT and RAGE$^{-/-}$ mice in kidney function/structure. We found lower levels of inflammation and oxidative stress in RAGE$^{-/-}$ mice, which may contribute to our proposed protective effect of RAGE invalidation through modulation of SIRT1 expression and the AKT/mTOR pathway.

In accordance with other studies, CML accumulated in kidneys of animals fed a CML-enriched diet (Li et al., 2015; Tessier et al., 2016).

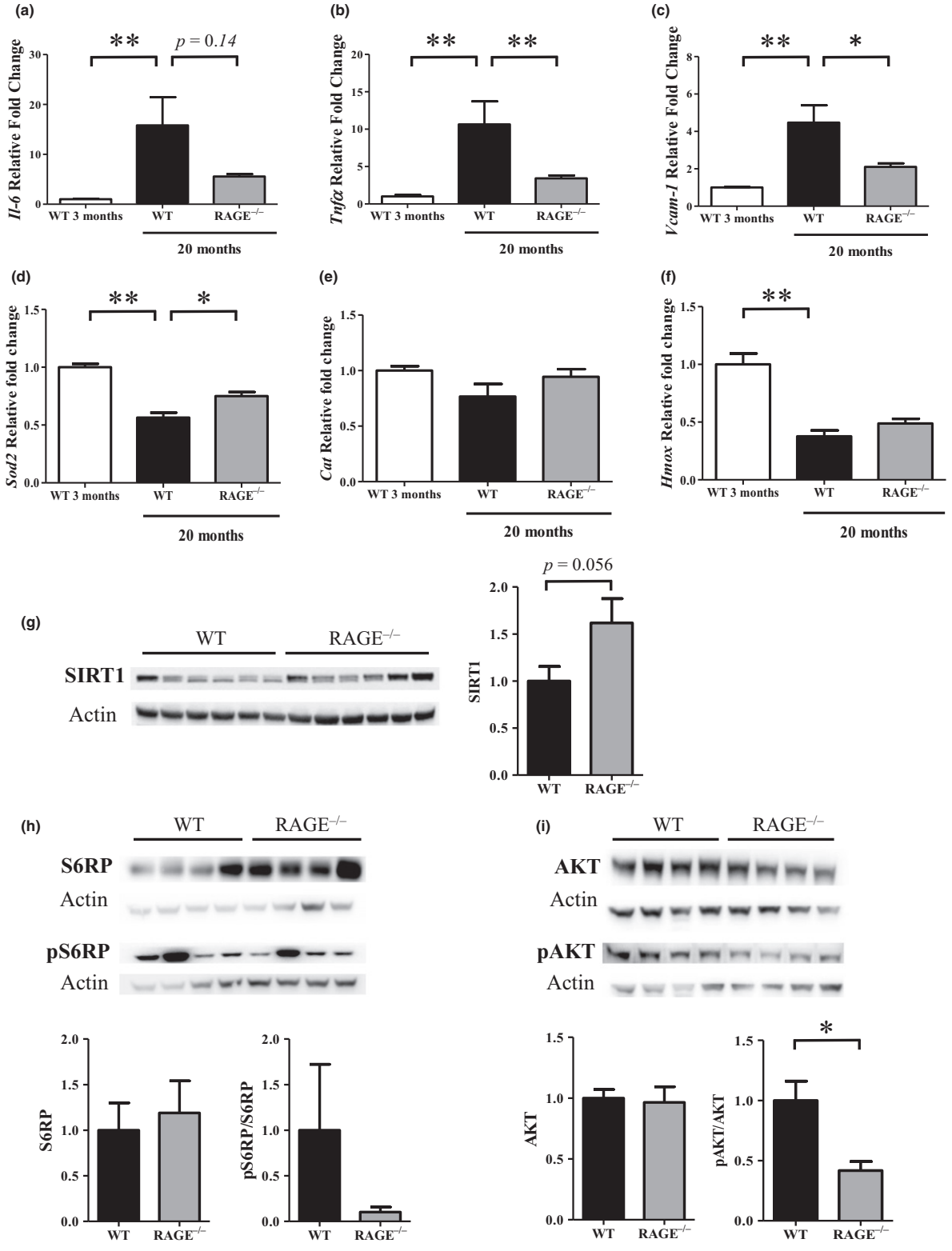

FIGURE 6 Inflammation and oxidation markers were decreased in RAGE$^{-/-}$ mice. Inflammation markers (a) *Il-6*, (b) *Tnfα* and (c) *Vcam-1* and oxidation markers (d) *Sod2*, (e) *Cat* and (f) *Hmox* mRNA expression were measured in renal tissue from 3- or 20-month-old WT and RAGE$^{-/-}$ mice (mean ±SEM, n = 3 for 3-month-old mice and n = 10 for 20-month-old mice). Representative western blot and quantification of protein levels of (g) SIRT1 (mean ±SEM, n = 10), (h) pS6RP (Ser235/236)/S6RP and (i) pAKT (Ser473)/AKT in kidney extracts of 22- to 26-month-old mice (mean ±SEM, n = 4). *$p < 0.05$, **$p < 0.01$, Mann–Whitney test or Kruskal–Wallis test for multiple comparisons

We confirmed the RAGE-independent nature of this accumulation (Tessier et al., 2016), and also separately quantified both free/dipeptide CML and protein-bound CML. Since dietary CML cannot enter the circulation in protein-bound form (Alamir et al., 2013), protein-bound CML must result from endogenous formation. This could be the consequence of oxidative stress, a condition thought to favor CML production from dicarbonyl compounds and known to occur in aging and CKD (Roca, Grossin, Chassagne, Puisieux, & Boulanger, 2014; Stinghen et al., 2016). Thus, ingested CML could activate other, RAGE-independent oxidative stress pathways, such as the epidermal growth factor receptor pathway (Chen et al., 2010), and/or participate in protein synthesis as described with noncanonical amino acids in artificial systems (Calve, Witten, Ocken, & Kinzer-Ursem, 2016). Surprisingly, we did not observe a significant negative effect of a CML-enriched diet on nephrosclerosis lesions in comparison with the significant positive impact of RAGE invalidation. Only GS and ApoAII amyloid deposits were higher (but not significantly so) in the CML WT versus control WT mice. While there is no published study establishing a direct link between AGE accumulation and renal aging, these results nevertheless seem to run counter to a body of related evidence. A potential deleterious effect of AGE accumulation can be inferred from diabetic nephropathy (Choudhury & Levi, 2011; Vlassara et al., 1994), in which CML deposits are, however, more pronounced. Moreover, an AGE-rich diet has been associated with proteinuria and structural changes in the kidneys of rodent models, whereas an AGE-poor diet induced fewer histological lesions and conserved renal function (Feng et al., 2007; Zheng et al., 2002). We hypothesize that any effect of dietary AGEs could be obscured by the relatively advanced age of our mice. Indeed, the majority of old control WT mice presented significant lesions of all renal structures and a third exhibited AApoA-II, suggesting that aging is important in this regard.

Among the age-related renal lesions that we reported, this observation of a link between nodular GS and AApoA-II is interesting. While AApoA-II is very uncommon in humans, it is described as a senile renal marker in mice and its prevalence varies according to genotype (Kitagawa et al., 2003). This age-related susceptibility to AApoA-II in mice may be explained by two characteristics of this protein. First, human ApoA-II is dimerized while the murine ApoA-II is monomeric and hence less stable. Second, ApoA-II has a higher methionine content in mice than humans and methionine is an amino acid known to be prone to oxidation (Gursky, 2014). It has been shown that the lipid peroxidation of high-density lipoproteins (HDLs, of which ApoA-II is a major constituent) induced oxidation of methionine components (Anantharamaiah et al., 1988); consequently, the 3D structure of ApoA-II could change and alter its affinity for HDLs. With subsequent dissociation from HDLs, ApoA-II could unfold until its aggregation and subsequent nucleation, the first step in amyloid fibrils formation (Wong, Binger, Howlett, & Griffin, 2010). Promoting oxidation and lipid peroxidation, aging, and RAGE expression together could thus favor structural changes and the deposition of ApoA-II in the kidneys, causing amyloidosis followed by GS. In a susceptible model such as C57BL6 mice, AApoA-II appears to be a useful marker of aging that is highly reduced when RAGE is knocked-out, and would further appear to be accelerated by prolonged intake of a CML-enriched diet.

Not only AApoA-II, but all the nephrosclerosis lesions assessed here were reduced in RAGE$^{-/-}$ mice. The involvement of this receptor has already been reported in different kidney diseases, especially diabetic nephropathy. Indeed, genetic deletion or pharmacologic blockage of RAGE was associated with a decrease of renal lesions in different animal models of diabetes (Kaida et al., 2013; Myint et al., 2006; Vlassara et al., 1994). Independent of the underlying etiology, RAGE has been also implicated in CKD and its attendant cardiovascular complications through the formation of AGEs and the promotion of oxidative stress induced by renal failure itself (Stinghen et al., 2016). Our work here has illustrated that, even in the absence of prior kidney disease, RAGE could be involved in "normal" renal aging. The pro-aging mechanisms induced by RAGE are multiple and especially include the perpetuation of a pro-inflammatory phenotype and ROS generation; in accordance with this, RAGE$^{-/-}$ mice here presented less inflammation and were better protected against oxidative stress. Previous studies have shown that a deficiency in SOD2 results in oxidative stress, interstitial inflammation, and accelerated renal senescence in a murine model (Rodriguez-Iturbe et al., 2007). Thus, the smaller decrease of *Sod2* expression in RAGE$^{-/-}$ mice with age could suggest enhanced protection against renal aging. Concurrently, and in accordance with previous studies showing that knockout or inhibition of RAGE prevented CML- or LPS-induced reduction in SIRT1 expression (Grossin et al., 2015; Huang et al., 2015), SIRT1 expression was here downregulated in old WT compared with old RAGE$^{-/-}$ mice. Interestingly, reduced renal inflammation and fibrosis have been reported in genetic or pharmacological boosting of SIRT1 models (Hong et al., 2018; Morigi, Perico, & Benigni, 2018); on the other hand, its deletion was associated with an aggravation of kidney injuries such as GS (Chuang et al., 2017). Together, these results suggest a potentially major role for SIRT1 in renal aging. Moreover, our observation of decreased levels of phosphorylated AKT and S6RP in RAGE$^{-/-}$ mice could indicate a role for RAGE invalidation in a pro-longevity phenotype and renoprotection. Indeed, mTOR inhibition is the only therapeutic intervention that leads to enhanced health and life span in all studied models (Johnson, Rabinovitch, & Kaeberlein, 2013; Weichhart, 2018), and downregulation or inhibition of mTORC1 prevents GS, glomerular hypertrophy macrophage infiltration, and other lesions in murine models of diabetic nephropathy (Kajiwara and Masuda, 2016). We thus suggest that the greater inflammation we observed in old WT mice compared with old RAGE$^{-/-}$ mice could be the result of AKT- and/or SIRT1-dependant NF-κB pathway activation (Kane, Shapiro, Stokoe, & Weiss, 1999; Kauppinen, Suuronen, Ojala, Kaarniranta, & Salminen, 2013).

Taken together, our results point to a role for the RAGE receptor and its attendant signaling pathways in regulating inflammation, elevation of which is a recognized hallmark of aging (López-Otín, Blasco, Partridge, Serrano, & Kroemer, 2013) and central to so-called inflamm-aging (Franceschi et al., 2000). They also suggest that RAGE$^{-/-}$ mice present a pro-longevity phenotype, as evidenced by

their apparently attenuated renal aging. Further studies, in particular using tissue culture techniques, will be helpful not only in determining the mechanisms governing the pathways involved in this phenotype, but also in determining the potential utility of RAGE inhibitors in reducing renal aging in particular, and perhaps other age-related phenomena.

4 | EXPERIMENTAL PROCEDURES

4.1 | Animal experimentation

All animals were housed in the experimental research department of Lille University (Agreement number: C59–35010). They were maintained at constant temperature and humidity in a room with a 12-hr light cycle. All experiments were conducted in accordance with institutional guidelines and French Ministry of Agriculture recommendations for the care and use of laboratory animals, and with the approval of the Charles Darwin Ethics Committee for animal experimentation (number #00822.01). The male WT (Janvier Laboratories, Le Genest-St-Isle, France) and RAGE$^{-/-}$ (from Pr. A.M. Schmidt, New York University) C57Bl/6 mice (6–10/group) received either a control diet incorporating unglycated bovine serum albumin (control-BSA), or an isocaloric diet enriched with glycated BSA rich in CML (CML-BSA). Mice were fed ad libitum for 18 months (2 months old at beginning of protocol). Three- or 11-month-old mice fed control-BSA were used as controls to analyze baseline renal and endothelial function. Old 22- to 26-months-old WT and RAGE$^{-/-}$ mice fed a standard diet were used for western blot analysis.

CML-BSA was prepared as previously (Grossin et al., 2015). After glycation (16 hr, 37°C), 37%–40% of the lysine moieties were found to be modified, 80%–99% of which (on a molar basis) had been modified to CML. The control-BSA was prepared under the same conditions, but glyoxylic acid was omitted. The control-BSA and CML-BSA preparations (diluted in water) were added to mouse powdered standard diet (A04, Safe, Augy, France) at 200 μg CML/g_{food}. The concentration of protein, fatty acids, fiber, and carbohydrate did not differ between control-BSA and CML-BSA diets. A basal concentration of 17.5 ± 0.7 μg CML/g_{food} was determined in control-BSA diet. Diets were renewed every 7 days, and remaining food was weighed to assess mean daily CML intake. Mice were weighed every 3 months. At 20 months, surviving mice (6 control WT, 8 CML WT, 8 control RAGE$^{-/-}$ and 5 CML RAGE$^{-/-}$) were culled and blood samples collected by inferior vena cava puncture. Kidneys were halved longitudinally and immediately frozen for biochemical and chemical analyses, or preserved in FAA (Formaldehyde, Alcohol, Acetic acid), RNA later and glutaraldehyde for electron microscopic analyses.

4.2 | Immunohistochemistry

Four micrometer kidneys sections were deparaffinized and rehydrated by successive 3-min washes in xylene then ethanol (100% and 95%, respectively). Standard procedures were followed up for antigen retrieval (Target Retrieval Solution, Dako) and blockage steps (kit Vectastain ABC Elite Peroxydase), except for ApoA-II. Antigen retrieval was performed as previously (Kai et al., 2012): briefly, sections were first treated with proteinase K for 3 min. (Dako, ready-to-use) followed by an ethylenediaminetetraacetic acid (EDTA) bath (0.01 M, pH6 at 121°C for 10 min.) then a formic acid bath (70% for 5 min. at room temp.). Nonspecific fixation sites were blocked with rabbit or goat serum 5% (Sigma, R1933, G9023), while for ApoA-II assays, endogenous peroxydases were blocked using a Dual Endogenous Enzyme Block (Dako, S200380) and endogenous biotins with an Endogenous Avidin/Biotin Blocking Kit (Abcam, ab64212).

Primary antibodies (18 hr, 4°C) were as follows: anti-CML (rabbit Ig; 1:1000; Abcam ab27684), anti-SAP (rabbit Ig, Biocare PP132AA), and anti-ApoA-II (goat, 2 μg/ml, Santa Cruz sc-23609). Corresponding nonimmune Igs served as negative controls. After incubation (1 hr, room temp.) with Streptavidin HRP Conjugate (ImmunoReagents, Ba-103-HRPX), sections were stained using DAB Substrate (Cell Signaling, Kit #8059P) and counterstained using hematoxylin solution (Sigma Aldrich, GHS316) before mounting under coverslips.

4.3 | HPLC-MS/MS

A high-pressure liquid chromatography (HPLC)-triple quadrupole mass spectrometer (MS/MS) was used to quantify CML and lysine by isotope dilution in kidney extracts (Vantage LC-MS/MS, ThermoFisher Scientific). Frozen kidneys were lyophilized (Alpha 1–2 LD plus, Bioblock scientific) for 24 hr at −40°C and −0.1 mbar. Twenty mg of kidney was suspended in 10% trichloroacetic acid (Sigma Aldrich) for 30 min. on ice. After centrifugation at 21 000 G for 10 min. at 4°C, the supernatant (free CML) and the pellet (protein-bound CML) were separately incubated in $NaBH_4$ (83 mM) for 2 hr at room temp. The reaction was stopped by adding HCl 37% (1:1). The samples were then incubated at 110°C for 21 hr and a 200μl aliquot evaporated using a SpeedVac Concentrator (Thermo Scientific). Isotope-labeled internal standards were added to the final volume of 200μl of aqueous nonafluoropentanoic acid (NFPA, 5 mM, Sodipro), as follows: CML-d_2 0.05 mM (Polypeptide Group) or Lysine-$^{15}N_2$ 50 mM (Cortecnet). The samples were then filtered through 0.45 μm nylon filters (Sodipro). Separation was performed on a Hypercarb column (100 × 2.1 mm, 5 μm particle size; ThermoFisher Scientific) equipped with a guard column (10 × 2.1 mm, 5 μm particle size). Injection volume was 10μl, column temp. 10°C, and compounds were eluted with a binary mobile phase at 0.2 ml/min: Mobile phase A was a 10 mM aqueous solution of the ion-pairing agent NFPA, while mobile phase B was LC-MS grade acetonitrile (Sigma Aldrich). The elution gradient was as follows: 0–9 min 100%–75% A; 9–11 min 40% A; 11–13 min 40%–100% A; 13–21 min 100% A. The heated electrospray interface was operated in positive ionization mode (3,500 V, 250°C, sheath and auxiliary gas flows at 50 and 20 arbitrary units, respectively). The MS/MS transitions monitored were as follows: *m/z* 205-130 and *m/z* 207-130 for CML and CML-d_2, and *m/z* 147-130 and *m/z* 149-131 for lysine and Lysine-$^{15}N_2$, respectively. Quantification was performed using the ratio of responses for the unlabeled molecules and their respective

isotope-labeled internal standards in a 9-point calibration covering the concentration ranges 0–0.2 mM (CML) and 0–20 mM (Lysine).

4.4 | Histological analyses

Two sections were stained (3 or 5 µm according to purpose, at an interval of 200 µm) from the halves of paraffin-embedded kidneys retained for histological analyses: by Periodic Acid Schiff (PAS) to assess GS, tubular atrophy and arteriolar hyalinosis; by Sirius red to evaluate interstitial fibrosis under polarized light; and by Congo red to detect amyloid deposits under optical and polarized light. Samples were labeled without reference to treatment group, and all parameters (defined below) were analyzed "blind" by a qualified anatomopathologist and nephrologist using an optical microscope (Leica DM5500 B).

4.4.1 | Definitions

Arteriolar hyalinosis appeared as a pink hyaline material in arteriolar walls after PAS staining. For each mouse, 25 arterioles (10–15/section) were analyzed and described as positive or negative.

Tubular atrophy was defined by an attrition of the brush border of the tubular epithelium, a reduced tubular size and a thickening of the tubular basement membrane. For each mouse, 50 tubules (25/section) were analyzed and described as positive or negative.

Interstitial fibrosis was defined by a red-signal in Sirius red staining in the cortex (excepting the physiological staining in the border of the vessels). For each mouse, this parameter was graded thus: grade 0, no fibrosis; grade 1, at least 1 focal fibrosis lesion; grade 2, at least 2 focal or fibrosis lesions. The scores attributed by the two examiners were summed.

Glomerulosclerosis (GS), identified as an increased mesangial matrix, was assessed on 60 superficial and juxtamedullary glomeruli (30/section) for each mouse. This parameter was scored between 0% and 100% (intervals of 10%) for each glomerulus. A GS score was expressed as the mean for each mouse. Normal glomeruli yielded a GS score of 0 while global GS was defined by the maximum possible score of 100, indicating glomeruli were completely sclerotic.

To assess the size of glomeruli, 6 fields/section were studied for each mouse. The area of each glomerulus was measured using ImageJ.

Amyloidosis was defined by positive Congo red staining. Amyloid deposits in glomeruli were graded thus: grade 1, no deposit; grade 2, small amount; grade 3, moderate amount; grade 4, extensive deposits. An amyloidosis score was adapted from the literature and represented the mean score of a section for 100 glomeruli analyzed (Luo et al., 2015).

4.5 | Endothelial dysfunction: aortic reactivity

Aortic ring relaxation was investigated in 11- and 20-month-old WT and $RAGE^{-/-}$ mice fed the control diet. Aortic ring responsiveness was tested as previously (Grossin et al., 2015) in an automated dual small-vessel myograph (ADInstruments, Chalgrove, UK). Briefly, aortas were contracted by adding 3×10^{-6} M phenylephrine (Sigma) to standard Krebs solution in an organ bath (37°C, 5% CO_2 in O_2). Once the contraction phase had stabilized, the endothelium-dependent relaxation (EDR) was tested by the cumulative addition of acetylcholine (ACh, $10^{-10} \times 10^{-4}$ M; Sigma). Relaxation responses were expressed as a percentage of the maximal phenylephrine-induced contraction.

4.6 | RT-qPCR

RNA extraction from half-kidneys was performed with a commercial kit (Qiagen). ARN was quantified by spectrophotometry at 260 nm (Biotech Spec-nano, Shimadzu Biotech) and quality analyzed by RNA Standard Sens kit (BIO-RAD). For RT-qPCR, amplification of cDNA was performed with the following probe mixes (ThermoFisher): *Kim-1* (Mm00506686), *Ngal* (Mm01324470), *Il-6* (Mm00446190_m1), *Tnfα* (Mm00443258_m1), *Vcam-1* (Mm01320970_m1), *Sod2* (Mm01313000_m1), *Cat* (Mm00437992_m1), and *Hmox* (Mm00516005_m1). The mean cycle threshold (CT) values for both the target and internal control (*Ppia*, Mm02342430_g1) were determined for each sample. The fold change in the target gene, normalized to *Ppia* and relative to the expression of WT mice fed the control diet, was calculated as $2^{-\Delta\Delta CT}$.

4.7 | Western blot

Kidney tissues were homogenized in RIPA buffer in the presence of protease and phosphatase inhibitors in 1.5% β-mercaptoethanol using a precellys homogenizer. After centrifugation (19,000 g for 10 min at 4°C), supernatants were collected for protein analysis. Protein concentration was determined by the Bradford method (Bio-Rad protein assay dye, Bio-Rad): 20 µg of protein was separated using bolt 4%–12% Bis-Tris plus (Invitrogen) gels, or NuPAGE 7% Tris-Acetate gels (ThermoFisher) for larger molecular weights and was transferred to a polyvinylidene difluoride membrane (Bio-Rad). Nonspecific binding sites were blocked for 1 hr at 20°C with 5% milk or BSA, according to the antibody, in Tris-buffered Saline with 0.05% Tween 20 (TBS-T). Membranes were incubated with anti-SIRT1 (ab7343, Abcam, 1:900), anti-FoxO3A (12829, Cell Signaling, 1:1000), anti-pFoxO3A (Ser253, Ab47287, Abcam, 1:750), anti-S6RP (2317, Cell Signaling, 1:1000), anti-pS6RP (Ser235/236, 4858, Cell Signaling, 1:2000), anti-Akt (4691, Cell Signaling, 1:1000), anti-pAkt (Ser473, 9271, Cell Signaling 1:1000), or anti-Actin (A2066, Sigma Aldrich, 1:2000) overnight at 4°C followed by washing and incubation with horseradish peroxidase- (HRP-) conjugated anti-rabbit (7074, Cell Signaling, 1:5000) or anti-mouse (7076, Cell Signaling, 1:2000). After washing, chemiluminescent reaction was induced using Clarity Western ECL Substrate (Bio-Rad) and detection performed using a Fusion FX Spectra imager (Vilber). Bands were normalized to Actin levels using ImageJ.

4.8 | Biologic parameters

Cholesterol, triglycerides, urea, and fasting glucose serum levels were measured with a biochemistry analyzer VetTest® (IDEXX laboratory) according to manufacturer's instructions. Serum creatinine levels were measured by an enzymatic colorimetric assay with an autoanalyzer (COBAS 8000 modular analyzer series; kits #CREP2–05168589190).

4.9 | Statistical analysis

Statistical analysis was performed using GraphPad Prism 5.0 (La Jolla, CA, USA). A Kruskal–Wallis test followed by a Dunn's multiple comparison test was applied for multiple comparisons; otherwise, a two-tailed, unpaired *t* test was performed for samples with n∼10 and a Mann–Whitney test was performed for smaller samples. A p-value < 0.05 was considered as significant in either case ($\alpha = 0.05$).

ACKNOWLEDGMENTS

This work was supported by grants from Digest Science foundation and INSERM. The microscopy analyses were performed at the Bio Imaging Center, Lille University. We are grateful to the DHURE (experimental research department), Cécile Vignal and Madjid Djouina for their support with the animal experimentation. We thank Charles Paul-Constant, Steve Lancel and Nicolas Grossin for their practical assistance and advice.

CONFLICT OF INTEREST

The authors declare no conflict of interest.

AUTHORS' CONTRIBUTION

Study design: MF and EB. Provided RAGE-KO mice: AMS. Performed research: TT, VQ, MD, MH, FD, CL and TB. Histological data analyses: VQ, VG and MF. Statistical analyses: TT and FG. MH provided English proofreading assistance. All authors discussed the data and approved the submission.

REFERENCES

Alamir, I., Niquet-Leridon, C., Jacolot, P., Rodriguez, C., Orosco, M., Anton, P. M., & Tessier, F. J. (2013). Digestibility of extruded proteins and metabolic transit of N ε -carboxymethyllysine in rats. *Amino Acids*, *44*(6), 1441–1449. https://doi.org/10.1007/s00726-012-1427-3

Alderson, H. V., Ritchie, J. P., Pagano, S., Middleton, R. J., Pruijm, M., Vuilleumier, N., & Kalra, P. A. (2016). The associations of blood kidney injury molecule-1 and neutrophil gelatinase-associated lipocalin with progression from CKD to ESRD. *Clinical Journal of the American Society of Nephrology*, *11*(12), 2141–2149. https://doi.org/10.2215/CJN.02670316

Anantharamaiah, G. M., Hughes, T. A., Iqbal, M., Gawish, A., Neame, P. J., Medley, M. F., & Segrest, J. P. (1988). Effect of oxidation on the properties of apolipoproteins A-I and A-II. *Journal of Lipid Research*, *29*(3), 309–318.

Bolignano, D., Mattace-Raso, F., Sijbrands, E. J. G., & Zoccali, C. (2014). The aging kidney revisited: A systematic review. *Ageing Research Reviews*, *14*, 65–80. https://doi.org/10.1016/j.arr.2014.02.003

Calve, S., Witten, A. J., Ocken, A. R., & Kinzer-Ursem, T. L. (2016). Incorporation of non-canonical amino acids into the developing murine proteome. *Scientific Reports*, *6*, 32377. https://doi.org/10.1038/srep32377

Chen, S.-C., Guh, J.-Y., Hwang, C.-C., Chiou, S.-J., Lin, T.-D., Ko, Y.-M., … Chuang, L.-Y. (2010). Advanced glycation end-products activate extracellular signal-regulated kinase via the oxidative stress-EGF receptor pathway in renal fibroblasts. *Journal of Cellular Biochemistry*, *109*(1), 38–48. https://doi.org/10.1002/jcb.22376

Choudhury, D., & Levi, M. (2011). Kidney aging—inevitable or preventable? *Nature Reviews Nephrology*, *7*(12), 706–717. https://doi.org/10.1038/nrneph.2011.104

Chuang, P. Y., Cai, W., Li, X., Fang, L., Xu, J., Yacoub, R., … Lee, K. (2017). Reduction in podocyte SIRT1 accelerates kidney injury in aging mice. *American Journal of Physiology-Renal Physiology*, *313*(3), F621–F628. https://doi.org/10.1152/ajprenal.00255.2017

Clarke, R. E., Dordevic, A. L., Tan, S. M., Ryan, L., & Coughlan, M. T. (2016). Dietary advanced glycation end products and risk factors for chronic disease: A systematic review of randomised controlled trials. *Nutrients*, *8*(3), 125. https://doi.org/10.3390/nu8030125

European Commission (2015). The 2015 ageing report. *European Econonomics*, *3*, 424.

Denic, A., Glassock, R. J., & Rule, A. D. (2016). Structural and Functional Changes With the Aging Kidney. *Advances in Chronic Kidney Disease*, *23*(1), 19–28. https://doi.org/10.1053/j.ackd.2015.08.004

Ebert, N., Jakob, O., Gaedeke, J., van der Giet, M., Kuhlmann, M. K., Martus, P., … Schaeffner, E. S. (2016). Prevalence of reduced kidney function and albuminuria in older adults: The Berlin Initiative Study. *Nephrology Dialysis Transplantation*, *32*, 997–1005. 10.1093/ndt/gfw079

Feng, J. X., Hou, F. F., Liang, M., Wang, G. B., Zhang, X., Li, H. Y., … Liu, Z. Q. (2007). Restricted intake of dietary advanced glycation end products retards renal progression in the remnant kidney model. *Kidney International*, *71*(9), 901–911. https://doi.org/10.1038/sj.ki.5002162

Franceschi, C., Bonafè, M., Valensin, S., Olivieri, F., De Luca, M., Ottaviani, E., & De Benedictis, G. (2000). Inflamm-aging. An evolutionary perspective on immunosenescence. *Annals of the New York Academy of Sciences*, *908*, 244–254.

Frimat, M., Daroux, M., Litke, R., Nevière, R., Tessier, F. J., & Boulanger, E. (2017). Kidney, heart and brain: Three organs targeted by ageing and glycation. *Clinical Science (London, England: 1979)*, *131*(11), 1069–1092. https://doi.org/10.1042/CS20160823

GA, Atlanta, (2013). *Centers for Disease Control and Prevention: The State of Aging and Healthy in America*. Atlanta, GA: Createspace Independent Publisher.

Glassock, R. J., Warnock, D. G., & Delanaye, P. (2017). The global burden of chronic kidney disease: Estimates, variability and pitfalls. *Nature Reviews Nephrology*, *13*(2), 104–114. https://doi.org/10.1038/nrneph.2016.163

Grossin, N., Auger, F., Niquet-Leridon, C., Durieux, N., Montaigne, D., Schmidt, A. M., … Boulanger, E. (2015). Dietary CML-enriched protein induces functional arterial aging in a RAGE-dependent manner in mice. *Molecular Nutrition and Food Research*, *59*(5), 927–938. https://doi.org/10.1002/mnfr.201400643

Gursky, O. (2014). Hot spots in apolipoprotein A-II misfolding and amyloidosis in mice and men. *FEBS Letters*, *588*(6), 845–850. https://doi.org/10.1016/j.febslet.2014.01.066

Hong, Q., Zhang, L., Das, B., Li, Z., Liu, B., Cai, G., … Lee, K. (2018). Increased podocyte Sirtuin-1 function attenuates diabetic kidney injury. *Kidney International*, *93*(6), 1330–1343. https://doi.org/10.1016/j.kint.2017.12.008

Huang, K.-P., Chen, C., Hao, J., Huang, J.-Y., Liu, P.-Q., & Huang, H.-Q. (2015). AGEs-RAGE system down-regulates Sirt1 through the ubiquitin-proteasome pathway to promote FN and TGF-β1 expression in

male rat glomerular mesangial cells. *Endocrinology*, *156*(1), 268–279. https://doi.org/10.1210/en.2014-1381

Johnson, S. C., Rabinovitch, P. S., & Kaeberlein, M. (2013). mTOR is a key modulator of ageing and age-related disease. *Nature*, *493*(7432), 338–345. https://doi.org/10.1038/nature11861

Kai, H., Shin, R.-W., Ogino, K., Hatsuta, H., Murayama, S., & Kitamoto, T. (2012). Enhanced antigen retrieval of amyloid β immunohistochemistry: Re-evaluation of amyloid β pathology in Alzheimer disease and its mouse model. *The Journal of Histochemistry and Cytochemistry*, *60*(10), 761–769. https://doi.org/10.1369/0022155412456379

Kaida, Y., Fukami, K., Matsui, T., Higashimoto, Y., Nishino, Y., Obara, N., … Yamagishi, S. (2013). DNA aptamer raised against AGEs blocks the progression of experimental diabetic nephropathy. *Diabetes*, *62*(9), 3241–3250. https://doi.org/10.2337/db12-1608

Kajiwara, M., & Masuda, S. (2016). Role of mTOR inhibitors in kidney disease. *International Journal of Molecular Sciences*, *17*(6), 975. https://doi.org/10.3390/ijms17060975

Kane, L. P., Shapiro, V. S., Stokoe, D., & Weiss, A. (1999). Induction of NF-kappaB by the Akt/PKB kinase. *Current Biology: CB*, *9*(11), 601–604.

Kauppinen, A., Suuronen, T., Ojala, J., Kaarniranta, K., & Salminen, A. (2013). Antagonistic crosstalk between NF-κB and SIRT1 in the regulation of inflammation and metabolic disorders. *Cellular Signalling*, *25*(10), 1939–1948. https://doi.org/10.1016/j.cellsig.2013.06.007

Kitagawa, K., Wang, J., Mastushita, T., Kogishi, K., Hosokawa, M., Fu, X., … Higuchi, K. (2003). Polymorphisms of mouse apolipoprotein A-II: Seven alleles found among 41 inbred strains of mice. *Amyloid: The International Journal of Experimental and Clinical Investigation: The Official Journal of the International Society of Amyloidosis*, *10*(4), 207–214.

Li, M., Zeng, M., He, Z., Zheng, Z., Qin, F., Tao, G., … Chen, J. (2015). Increased accumulation of protein-bound N(ε)-(carboxymethyl)lysine in tissues of healthy rats after chronic oral N(ε)-(carboxymethyl)lysine. *Journal of Agricultural and Food Chemistry*, *63*(5), 1658–1663. https://doi.org/10.1021/jf505063t

Lindeman, R. D., Tobin, J., & Shock, N. W. (1985). Longitudinal studies on the rate of decline in renal function with age. *Journal of the American Geriatrics Society*, *33*(4), 278–285. https://doi.org/10.1111/j.1532-5415.1985.tb07117.x

López-Otín, C., Blasco, M. A., Partridge, L., Serrano, M., & Kroemer, G. (2013). The hallmarks of aging. *Cell*, *153*(6), 1194–1217. https://doi.org/10.1016/j.cell.2013.05.039

Luo, H., Sawashita, J., Tian, G., Liu, Y., Li, L., Ding, X., … Higuchi, K. (2015). Extracellular deposition of mouse senile AApoAII amyloid fibrils induced different unfolded protein responses in the liver, kidney, and heart. *Laboratory Investigation*, *95*(3), 320–333. https://doi.org/10.1038/labinvest.2014.158

Luo, W., Wang, Y., Yang, H., Dai, C., Hong, H., Li, J., … Li, Z. (2018). Heme oxygenase-1 ameliorates oxidative stress-induced endothelial senescence via regulating endothelial nitric oxide synthase activation and coupling. *Aging*. https://doi.org/10.18632/aging.101506

Morigi, M., Perico, L., & Benigni, A. (2018). Sirtuins in renal health and disease. *Journal of the American Society of Nephrology*, *29*(7), 1799–1809. https://doi.org/10.1681/ASN.2017111218

Myint, K.-M., Yamamoto, Y., Doi, T., Kato, I., Harashima, A., Yonekura, H., … Yamamoto, H. (2006). RAGE control of diabetic nephropathy in a mouse model: Effects of RAGE gene disruption and administration of low-molecular weight heparin. *Diabetes*, *55*(9), 2510–2522. https://doi.org/10.2337/db06-0221

O'Sullivan, E. D., Hughes, J., & Ferenbach, D. A. (2017). Renal aging: Causes and consequences. *Journal of the American Society of Nephrology*, *28*(2), 407–420. https://doi.org/10.1681/ASN.2015121308

Ramasamy, R., Shekhtman, A., & Schmidt, A. M. (2016). The multiple faces of RAGE – Opportunities for therapeutic intervention in aging and chronic disease. *Expert Opinion on Therapeutic Targets*, *20*(4), 431–446. https://doi.org/10.1517/14728222.2016.1111873

Roca, F., Grossin, N., Chassagne, P., Puisieux, F., & Boulanger, E. (2014). Glycation: The angiogenic paradox in aging and age-related disorders and diseases. *Ageing Research Reviews*, *15*, 146–160. https://doi.org/10.1016/j.arr.2014.03.009

Rodriguez-Iturbe, B., Sepassi, L., Quiroz, Y., Ni, Z., Wallace, D. C., & Vaziri, N. D. (2007). Association of mitochondrial SOD deficiency with salt-sensitive hypertension and accelerated renal senescence. *Journal of Applied Physiology*, *102*(1), 255–260. https://doi.org/10.1152/japplphysiol.00513.2006

Rysz, J., Gluba-Brzózka, A., Franczyk, B., Jabłonowski, Z., & Ciałkowska-Rysz, A. (2017). Novel Biomarkers in the Diagnosis of Chronic Kidney Disease and the Prediction of Its Outcome. *International Journal of Molecular Sciences*, *18*(8), 1702. https://doi.org/10.3390/ijms18081702

Smyth, L. J., Duffy, S., Maxwell, A. P., & McKnight, A. J. (2014). Genetic and epigenetic factors influencing chronic kidney disease. *American Journal of Physiology-Renal Physiology*, *307*(7), F757–F776. https://doi.org/10.1152/ajprenal.00306.2014

Stinghen, A. E. M., Massy, Z. A., Vlassara, H., Striker, G. E., & Boullier, A. (2016). Uremic toxicity of advanced glycation end products in CKD. *Journal of the American Society of Nephrology*, *27*(2), 354–370. https://doi.org/10.1681/ASN.2014101047

Tessier, F. J., & Birlouez-Aragon, I. (2012). Health effects of dietary Maillard reaction products: The results of ICARE and other studies. *Amino Acids*, *42*(4), 1119–1131. https://doi.org/10.1007/s00726-010-0776-z

Tessier, F. J., Niquet-Léridon, C., Jacolot, P., Jouquand, C., Genin, M., Schmidt, A.-M., … Boulanger, E. (2016). Quantitative assessment of organ distribution of dietary protein-bound (13) C-labeled N(ε) -carboxymethyllysine after a chronic oral exposure in mice. *Molecular Nutrition and Food Research*, *60*(11), 2446–2456. https://doi.org/10.1002/mnfr.201600140

Vlassara, H., Striker, L. J., Teichberg, S., Fuh, H., Li, Y. M., & Steffes, M. (1994). Advanced glycation end products induce glomerular sclerosis and albuminuria in normal rats. *Proceedings of the National Academy of Sciences of the United States of America*, *91*(24), 11704–11708. https://doi.org/10.1073/pnas.91.24.11704

Weichhart, T. (2018). mTOR as regulator of lifespan, aging, and cellular senescence: A mini-review. *Gerontology*, *64*(2), 127–134. https://doi.org/10.1159/000484629

Wong, Y. Q., Binger, K. J., Howlett, G. J., & Griffin, M. D. W. (2010). Methionine oxidation induces amyloid fibril formation by full-length apolipoprotein A-I. *Proceedings of the National Academy of Sciences of the United States of America*, *107*(5), 1977–1982. https://doi.org/10.1073/pnas.0910136107

Yuan, Y., Cruzat, V. F., Newsholme, P., Cheng, J., Chen, Y., & Lu, Y. (2016). Regulation of SIRT1 in aging: Roles in mitochondrial function and biogenesis. *Mechanisms of Ageing and Development*, *155*, 10–21. https://doi.org/10.1016/j.mad.2016.02.003

Zheng, F., He, C., Cai, W., Hattori, M., Steffes, M., & Vlassara, H. (2002). Prevention of diabetic nephropathy in mice by a diet low in glycoxidation products. *Diabetes/Metabolism Research and Reviews*, *18*(3), 224–237. https://doi.org/10.1002/dmrr.283

SUPPORTING INFORMATION

Additional supporting information may be found online in the Supporting Information section at the end of the article.

How to cite this article: Teissier T, Quersin V, Gnemmi V, et al. Knockout of receptor for advanced glycation end-products attenuates age-related renal lesions. *Aging Cell*. 2019;e12850. https://doi.org/10.1111/acel.12850

frontiers in Immunology

ORIGINAL RESEARCH
published: 20 December 2018
doi: 10.3389/fimmu.2018.03008

Heme Drives Susceptibility of Glomerular Endothelium to Complement Overactivation Due to Inefficient Upregulation of Heme Oxygenase-1

Olivia May[1,2,3†], Nicolas S. Merle[1,4,5†], Anne Grunenwald[1,3,6], Viviane Gnemmi[6], Juliette Leon[1,5], Cloé Payet[1,4], Tania Robe-Rybkine[1,4,5], Romain Paule[1], Florian Delguste[2], Simon C. Satchell[7], Peter W. Mathieson[8], Marc Hazzan[2,3], Eric Boulanger[2], Jordan D. Dimitrov[1,4,5], Veronique Fremeaux-Bacchi[1,9], Marie Frimat[2,3†] and Lubka T. Roumenina[1,4,5*†]*

[1] INSERM, UMR_S 1138, Centre de Recherche des Cordeliers, Paris, France, [2] INSERM, UMR 995, Lille, France, [3] University of Lille, CHU Lille, Nephrology Department, Lille, France, [4] Sorbonne Universités, UPMC Univ Paris 06, Paris, France, [5] Université Paris Descartes, Sorbonne Paris Cité, Paris, France, [6] University of Lille, INSERM, CHU Lille, Department of Pathology, UMR-S 1172 - Jean-Pierre Aubert Research Center, Lille, France, [7] Bristol Renal, University of Bristol, Bristol, United Kingdom, [8] University Lodge, University of Hong Kong, Hong Kong, Hong Kong, [9] Assistance Publique – Hôpitaux de Paris, Service d'Immunologie Biologique, Hôpital Européen Georges Pompidou, Paris, France

Atypical hemolytic uremic syndrome (aHUS) is a severe disease characterized by microvascular endothelial cell (EC) lesions leading to thrombi formation, mechanical hemolysis and organ failure, predominantly renal. Complement system overactivation is a hallmark of aHUS. To investigate this selective susceptibility of the microvascular renal endothelium to complement attack and thrombotic microangiopathic lesions, we compared complement and cyto-protection markers on EC, from different vascular beds, in *in vitro* and *in vivo* models as well as in patients. No difference was observed for complement deposits or expression of complement and coagulation regulators between macrovascular and microvascular EC, either at resting state or after inflammatory challenge. After prolonged exposure to hemolysis-derived heme, higher C3 deposits were found on glomerular EC, *in vitro* and *in vivo*, compared with other EC in culture and in mice organs (liver, skin, brain, lungs and heart). This could be explained by a reduced complement regulation capacity due to weaker binding of Factor H and inefficient upregulation of thrombomodulin (TM). Microvascular EC also failed to upregulate the cytoprotective heme-degrading enzyme heme-oxygenase 1 (HO-1), normally induced by hemolysis products. Only HUVEC (Human Umbilical Vein EC) developed adaptation to heme, which was lost after inhibition of HO-1 activity. Interestingly, the expression of KLF2 and KLF4—known transcription factors of TM, also described as possible transcription modulators of HO-1- was weaker in micro than macrovascular EC under hemolytic conditions. Our results show that the microvascular EC, and especially glomerular EC, fail to adapt to the stress imposed by hemolysis and acquire a pro-coagulant and

OPEN ACCESS

Edited by:
Nicole Thielens,
UMR5075 Institut de Biologie Structurale (IBS), France

Reviewed by:
Viviana P. Ferreira,
University of Toledo, United States
Mariusz Z. Ratajczak,
University of Louisville Physicians, United States

***Correspondence:**
Marie Frimat
marie.frimat@chru-lille.fr
Lubka T. Roumenina
lubka.roumenina@crc.jussieu.fr

[†]These authors have contributed equally to this work

Specialty section:
This article was submitted to Molecular Innate Immunity, a section of the journal Frontiers in Immunology

Received: 29 June 2018
Accepted: 05 December 2018
Published: 20 December 2018

Citation:
May O, Merle NS, Grunenwald A, Gnemmi V, Leon J, Payet C, Robe-Rybkine T, Paule R, Delguste F, Satchell SC, Mathieson PW, Hazzan M, Boulanger E, Dimitrov JD, Fremeaux-Bacchi V, Frimat M and Roumenina LT (2018) Heme Drives Susceptibility of Glomerular Endothelium to Complement Overactivation Due to Inefficient Upregulation of Heme Oxygenase-1. Front. Immunol. 9:3008. doi: 10.3389/fimmu.2018.03008

complement-activating phenotype. Together, these findings indicate that the vulnerability of glomerular EC to hemolysis is a key factor in aHUS, amplifying complement overactivation and thrombotic microangiopathic lesions.

Keywords: atypical hemolytic uremic syndrome, complement system, endothelial cells, heme, heme oxygenase-1, thrombomodulin

INTRODUCTION

The atypical hemolytic uremic syndrome (aHUS) is a rare, kidney-predominant, thrombotic microangiopathy (TMA) associated with the formation of fibrin-platelet clots in microvessels which trigger mechanical hemolysis (1). A dysregulated complement alternative pathway (AP) plays a key role in aHUS, as suggested by genetic abnormalities in AP proteins found in up to 60% of patients (2, 3) and the efficacy of anti-C5 therapy (4). Although the complement overactivation is systemic, a particular renal tropism of the TMA lesions exists, and injury of others organs is unusual in aHUS (5–10% of patients) (2, 5).

This susceptibility of renal endothelial cells (EC) to complement overactivation remains poorly understood. Despite the morphologic and functional differences between glomerular EC and other microvascular EC, no major differences were observed in the basal expression of complement regulators or complement component C3 deposits in resting state (6–10). The high expression of complement proteins in kidneys could explain the greater susceptibility of glomerular EC to complement attack. The EC-derived C3 and Factor B are, however, present at lower concentrations in kidney compared to the liver-derived C3 and FB in blood, to which endothelium is exposed *in vivo*. Additional factors are necessary to fully explain the vulnerability of the glomerular endothelium to complement-mediated injury and TMA in aHUS.

Cell-free hemoglobin and heme, released during hemolysis, are potent promoters of pro-inflammatory and pro-oxidant effects (11–13) and can induce EC phenotypical changes, affording them complement activating properties (8, 14, 15). Under hemolytic conditions EC also up-regulate the cytoprotective heme-degrading enzyme heme oxygenase 1 (HO-1) (15), and this overexpression was associated with increased resistance to complement activation in HUVEC (16). Nevertheless, the implication of HO-1 in the protection of glomerular endothelium has not, to our knowledge, been studied.

We here show that endothelial heterogeneity is apparent under hemolytic conditions: the microvascular EC, and particularly the glomerular EC, become vulnerable to injury through differences in their C3 regulation and heme degradation compared with macrovascular EC. These results might explain, at least in part, the renal tropism of complement-mediated TMA lesions in aHUS.

MATERIALS AND METHODS

Reagents

The oxidized form of heme (hemin, ferriprotoporphyrin IX), designated as heme, (Sigma or Frontier Scientific) and Sn(IV) mesoporphyrin IX (SnMPIX) (Frontier Scientific) were suspended at 10 mM in 50 mM NaOH, 145 mM NaCl, and therafter diluted in the appropriate vehicle (medium for culture cells, PBS for animal experimentation).

Animal Experimentation

All experiments were conducted in accordance with the recommendations for care and use of laboratory animals of the French Ministry of Agriculture and with the approval of the Charles Darwin Ethics Committee for animal experimentation (Paris, France) number APAFIS#3764-201601121739330v3. Six to eight-week-old female C57Bl/6 mice from Charles River Laboratories (L'Arbresle, France) were treated with intraperitoneal injection of 200 μL phosphate buffer saline (PBS, Dulbeco) or freshly prepared heme (40 μmol/kg corresponding to 27 μg/g body weight) at day 0 and 1. At day 2 mice were culled and the organs were then recovered: kidneys, lungs, heart and skin (1 cm^2) were preserved directly in plastic molds containing optimal cutting temperature (OCT) compound, placed on dry ice and frozen. Brains were otherwise frozen in isopentane at −70°C to preserve the tissue architecture before being placed in OCT and frozen.

Immunohistochemistry (IHC) and Immunofluorescence (IF)

Frozen organs sections (6 μm) were fixed in acetone. The primary antibodies were: Heme Oxygenase-1 (HO-1; rabbit anti-mouse, Abcam Ab13243, 5 μg/ml), C3b/iC3b (rat anti-mouse, Hycult biotech, HM1065, 1 μg/ml), Thrombomodulin (TM; rabbit anti-mouse, R&D systems, MAB3894, 20 μg/ml), CD31 (rat anti-mouse, Abcam Ab7388, 2 μg/mL), von Willebrand Factor (vWF; sheep anti-mouse, Abcam, Ab11713, 1/100). Staining was revealed by goat anti-rabbit AF647 (Thermoscientific, A21244, 5 μg/mL) or goat anti-rat AF555 (Thermoscientific, A21434, 5 μg/mL). Slides were scanned by Nanozoomer (Hamamatsu) and AxioScan (Zeiss) for IHC and IF, respectively.

Endothelial Cells Assays

Cells Culture

Human umbilical vein endothelial cells (HUVEC—a model of macrovascular EC), a human dermal EC line (HMEC—a microvascular EC model), conditionally immortalized (GENC) and human primary (HRGEC) glomerular EC were compared. HUVEC ($n = 7$ donors) were obtained from CHU Lille (France), HMEC were from ATCC (17) (US), GENC were from Dr. Satchell (Bristol, UK) (18) and HRGEC ($n = 3$) were from iCelltis (Toulouse, France). Cells were cultured as previously described (9, 10, 18): briefly, the growth medium was M199 20% fetal calf serum and 20% EGM2-MV (Lonza) for HUVEC, and EGM2-MV for the other cell types. HUVEC and HRGEC were used for

experiments until passage 4, HMEC between passages 2–7 and GENC between passages 23 and 30. Cells were exposed to heme at indicated doses overnight or for 30 min in serum-free medium OPTI (Thermo Fisher), or overnight to the pro-inflammatory cytokines TNFα and IFNγ (PeproTech) at 10 ng/ml and 10^3 U/ml in complete medium, respectively. Alternatively, HUVEC were exposed to heme or SnMPIX overnight before being re-challenged, or not, with 50 μM of heme. Dead cells were removed by washing. Normal human serum (NHS) was used as a source of complement.

Flow Cytometry

Cells were washed, detached, labeled and analyzed by flow cytometry (BD LSR II), and the data assessed using FCS Express software (*De Novo* software). Antibodies were diluted in PBA (PBS, BSA 0.5%, Azide 0.1%): anti-C3c (Quidel, A205, 10 μg/ml), anti-FH (antiFH#1, Quidel, A229, 55 μg/ml), anti-MCP-PE (Bio Rad, MCA2113, 10 μg/ml), anti-DAF (Bio Rad, MCA1614, 10 μg/ml). Staining was revealed by goat anti-mouse IgG PE (Beckman Coulter, IM0551). Cell viability was followed by annexin V-APC/DAPI staining (BD Bioscience).

RTqPCR

RNA extraction from cells was performed with a Qiagen kit. Quality and quantity of RNA were measured by an Agilent 2100 Bioanalyzer (Agilent Techonologies). RNA Integrity Number was considered acceptable if >9. After standard RT-PCR, amplification of cDNA was proceeded with following probes: actin-4332645, TM-hs00264920-s1, HO-1-hs01110250_m1, KLF2-Hs00360439_g1, KLF4-Hs00358836_m1, NRF2-Hs00975961_g1, BACH1-Hs00230917_m1. Data were analyzed by SDS2.3 and RQ manager software. The mean cycle threshold (CT) values for both the target and internal control (*β-actin*) were determined for each sample. The fold change in the target gene, normalized to *β-actin* and relative to the expression of untreated HUVEC, was calculated as 2–ΔΔCT (19).

Western Blot (WB)

Cells were lysed in RadioImmunoPrecipitation Assay (RIPA) buffer and deposited at 10 μg/ml on 10% pre-casted gels (Life Technology). After transfer, the HO-1 and actin were probed by a rat anti-human HO-1 IgG2b (R&D systems, MAB3776, 2 μg/ml) and a rabbit anti-actin (Sigma Aldrich, A2066, 1/10000). Secondary antibodies were goat anti-rat IgG-HRP (R&D systems, HAF005, 1/5000) and goat anti-rabbit IgG-HRP (Santa Cruz Technology, sc-2004, 1/10000). Blots were revealed by chemiluminescence (Super Signal West, Extended Duration Substrate, Thermoscientific myECL).

Study of C3b Cleavage

To study the contribution of TM to the cleavage of C3b by Factor I (FI) in the presence of Factor H (FH) as a cofactor, purified C3b (Calbiochem), diluted in Tris buffer (10 mM, NaCl 40 mM, pH7.4) at 20 μg/ml (300 μl), was incubated with human albumin (CSL Behring, 10 μg/ml), TM (R&D Systems, 10 μg/ml, 10 μl), or without protein for 10 min on ice. FH (20 μg/ml, 10 μl) was added on ice for 10 min. Each sample was separated into 4 tubes, and 4 μl of FI (10 μg/ml) was added per tube. DTT-Blue Reducing sample buffer (13 μL) was added at $t = 0$, 30 s, 2 min or 10 min to stop cleavage of C3b. Samples were denatured, resolved on a 10% gel and transferred onto a nitrocellulose membrane. The antibodies used for visualization by WB were an anti-C3 polyclonal goat antiserum (Merck Millipore, 204869, 1/5000) and a goat anti-rabbit antibody IgG-HRP (Santa Cruz, sc-2004, 1/5000).

Patients' Kidney Biopsies

Biopsies from two aHUS patients - P1 carrying C3 p.R161W [C3 gain of function (9)] and P2, having homozygous FH mutation p.C564F (FH deficiency)—were retrieved from the archive of the Pathology Institute of CHU Lille, France. P1 had a hemolytic anemia and histological analysis described typical lesions of glomerular and arteriolar TMA. Hemolysis was corrected at the moment of P2 biopsy, which reported predominant chronic TMA lesions, characterized by vessel wall thickening and thrombotic occlusion of many arterioles. Perls' Prussian blue staining identified hemosiderin deposits. Immunohistochemical analysis for HO-1 (rabbit anti-HO-1, Abcam) was performed on deparaffinized slides using Ventana XT autostainer (Ventana Medical systems). Immunofluorescence with rabbit anti-C3c (Dako) was performed on frozen slides. Secondary antibodies were coupled to Fluorescein IsoThioCyanate—FITC (Sigma Aldrich). A normal protocol, kidney allograft biopsy performed 3 months after transplant was used as a negative control and biopsies of two patients with chronic hemolysis (hemolysis associated with prosthetic heart valve) were used as positive controls for hemosiderin detection and tubular staining of HO-1 (20). Whole slides were scanned or analyzed by an Olympus microscope (Life Sciences Solutions) or Nanozoomer (Hamamatsu).

Statistics

Statistical analysis was performed with R software (21). The ggplot2 package (22) was used for graphical representations. Data are presented as medians and interquartile ranges. After a Kruskal-Wallis test, a Dunn's test was used for multiple pairwise comparisons. A p-value <0.05 was considered significant.

RESULTS

Heme-Induced C3 Fragment Deposition With a Particular Renal Tropism *in vivo*

We performed a comparative analysis of the deposition of C3 activation fragments in mouse organs under control conditions (injection of PBS) and after administration of heme using IF (**Figure 1**) and IHC (**Supplementary Figure 1**). No structural differences were detected in the kidneys or livers of heme-injected mice (Periodic Acid Schiff (PAS) and hematoxylin, eosin, saffron (HES) staining), in agreement with previous observations (13).

IHC staining for C3 activation fragments revealed minimal/absent staining in the three tested organs: kidney, heart and liver of PBS-injected mice. In heme-injected mice,

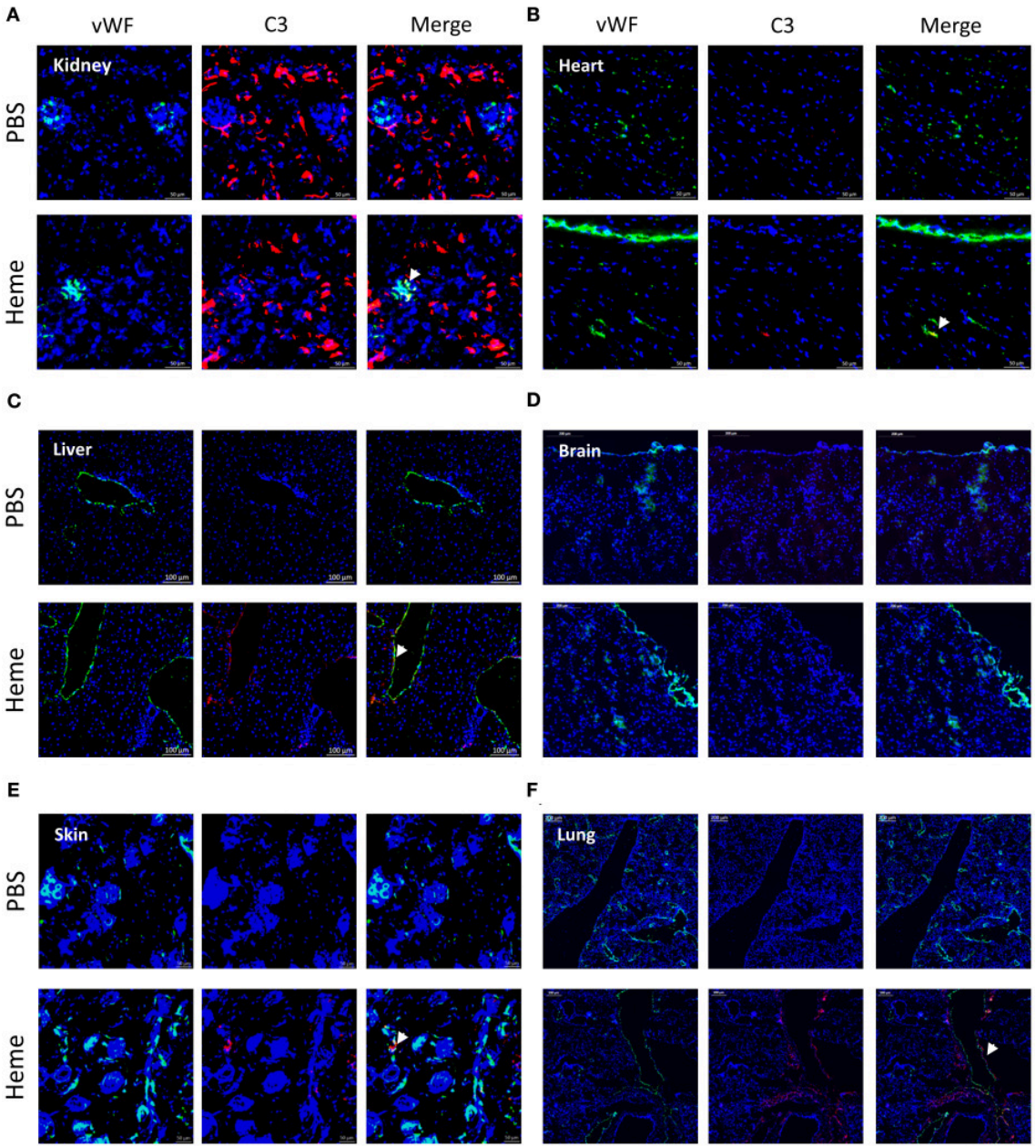

FIGURE 1 | Heme-induced complement C3 fragment deposition with a particular renal tropism *in vivo*. **(A-F)** C3b/iC3b staining (red), wWF staining (green) and colocalization vWF—C3b of frozen kidney x15 **(A),** heart x15 **(B),** liver x8 **(C)** brain x8 **(D),** skin x15 **(E)**, and lung x5 **(F)**; sections of mice treated with PBS (negative control, upper panel) or heme (lower panel) studied by immunofluorescence. Representative images of 3 independent experiments with 3 or 5 mice per group.

significant deposits were observed in kidney glomeruli, while only minimal effects were observed in heart or liver using this technique (**Supplementary Figures 1A–C**). We also studied the C3 fragment deposition using the more sensitive IF method. C3 staining was detected in kidneys of PBS-injected mice, located along the tubular basement membrane and in the Bowman's capsule (**Figure 1A**); it was minimal/absent in heart, liver, brain, skin and lungs of these mice (**Figures 1B–F**). In the presence of heme, strong C3b/iC3b staining was detected in kidneys (**Figure 1A**, **Supplementary Figure 1D**) contrary to heart and brain (**Figures 1B,D**). To a lesser extent, deposits were also revealed in liver, skin and lungs (**Figures 1C,E,F**). In the heme-exposed kidneys themselves, C3 fragment deposits were observed in vessels, intra-glomeruli, along the tubular basement membrane and in the Bowman's capsule. C3 deposits were detected on the glomerular EC, as seen by double staining for C3b/iC3b and vWF (**Supplementary Figure 1D**).

Long-Term Exposure to Heme Rendered Glomerular Endothelial Cells Susceptible to Complement Activation *in vitro*

We then tested whether the particular susceptibility of the glomerular endothelium to C3 activation fragment deposition could be reproduced *in vitro*, using cultured human EC from different vascular beds (**Figure 2A**). We compared human primary (HRGEC) and conditionally immortalized (GENC) glomerular cells with HUVEC (as a macrovascular EC model) and human microvascular EC line (HMEC), for their capacity to activate complement after exposure to heme. In accordance with the *in vivo* data, C3 deposits were significantly higher on glomerular EC (GENC and HRGEC) than on HUVEC and HMEC ($p < 0.05$). Overnight exposure to 50μM heme increased C3 deposition on average ∼2.6 fold on HUVEC, ∼4 fold on HMEC, ∼7.5 fold on GENC and ∼6 fold on HRGEC compared with the baseline. No significant difference was observed in terms of C3 fragment deposition at resting state on the tested EC (**Figures 2B,C**).

Others TMA-related stimuli were tested, such as exposure to pro-inflammatory cytokines TNFα and IFNγ (deemed pertinent as the primary trigger for aHUS could be an infection) or brief exposure (30 min) to heme [since hemolysis has been proposed as a secondary hit for aHUS (8)]. In both cases HUVEC and GENC showed a similar response profile, with increased C3 fragment deposition from NHS, but without significant difference between the cell types in either the resting state or in the 30 min heme-exposed cells, while GENC had lower levels of C3 deposition compared to HUVEC after activation by the pro-inflammatory cytokines ($p < 0.0001$) (**Figure 2D**).

The Increase of C3 Deposition on Glomerular EC Correlates With a Weaker FH Binding

Most cells adapt over the long term to resist to heme overload. Therefore, we compared the binding/expression of complement regulators after overnight exposure to heme (**Figure 3**). We detected a heme-concentration-dependent increase of FH binding from NHS, significantly higher on HUVEC, compared with the glomerular EC ($p < 0.05$) (**Figures 3A,B**). The expression of MCP and DAF did not differ among the four tested EC types at resting state (**Supplementary Figures 2A,B**), while under hemolytic conditions MCP decreased to a similar level for the four cell types and DAF displayed a heterogeneous behavior (**Figures 3C**,**D**).

TM Is Inefficiently Upregulated on Heme-Exposed Microvascular EC *in vivo* and *in vitro*

The susceptibility of microvasculature to TMA could be related not only to lower resistance to complement but also to inefficient thromboresistance or regulation of the coagulation cascade. TM is a key factor in reducing blood coagulation, but may serve also as complement regulator (23). Here, TM accelerated the cleavage of C3b to iC3b by FI, leading to the appearance of the α43 fragment at 30 s with a time-dependent increase; this band was invisible in the presence of albumin (irrelevant protein) or buffer at 30 s, appearing later (2 min) with a time-dependent increase (**Figure 4A**).

In vitro, the expression of TM did not differ among the four tested EC types at resting state (**Supplementary Figure 3**). After prolonged exposure to heme, *TM* gene expression (**Figure 4B**) increased in HUVEC (gene expression ∼6.1 fold at 50 μM heme, compared to baseline), while it was significantly lower in HMEC, GENC, and HRGEC ($p < 0.05$) compared with HUVEC. The TM level was also evaluated in different organs of heme-injected mice (**Figure 4C**). No difference was detected in glomeruli (strong basal staining) nor in heart or brain of heme- vs. PBS-injected mice. In contrast, a tendency toward an increase of TM was detected in skin, and a significant 18-fold increase of TM staining was found in the large vessels of the livers from heme-injected mice compared with PBS controls ($p < 0.05$). Surprisingly, an over 30-fold decrease of TM was seen in the lungs' microvasculature of heme-injected mice compared with controls ($p < 0.0001$) (**Figure 4C**).

Heme Oxygenase-1 (HO-1) Is Inefficiently Upregulated on Microvascular and Particularly on Glomerular Endothelium by Heme *in vitro* and *in vivo*

The susceptibility of the kidney to TMA lesions could be also related to a reduced resistance to oxidative stress and inefficient heme-degradation. HO-1 is the major heme-degrading enzyme and its expression is inducible after cell stress (15).

In mice, at basal condition (PBS), HO-1 staining was negative in the kidney (**Figure 5A**) as well as in others studied organs (**Figures 5B–F**). After heme injection, HO-1 staining was intense in the proximal tubules, but remained negative in glomeruli (**Figure 5A**, **Supplementary Figures 4A,B**). The same results were observed by IHC. Only minimal HO-1 staining was detected in some cases in heme-exposed glomeruli, corresponding to the glomerular epithelial cells and not endothelial cells in agreement with previous reports for human glomeruli (24); HO-1 expression was not detected in the brains of the heme-treated mice either. HO-1 labeling was positive in heart, liver, skin and lungs of heme-treated animals (**Figures 5B–F**), and visual colocalization with blood vessels was observed. In the skin, the HO-1 expression was particularly strong in the vessels of the hair follicles.

In vitro, heme-treatment induced ∼92.3 fold increased *HO-1* gene expression on HUVEC, compared to baseline (**Figure 6C**).This increase was weaker in the other cell types: ∼5.9 fold on HMEC ($p < 0.05$), ∼26.6 fold on GENC ($p < 0.05$) and ∼17 fold on HRGEC ($p < 0.05$). HO-1 protein expression level in HUVEC, and to a lesser extent HMEC, increased with increasing heme concentration (**Figures 6A,B**—note that HMEC are derived from cells isolated from human foreskins and lack hair follicles). Meanwhile, HO-1 expression on both glomerular EC types was only weakly detected.

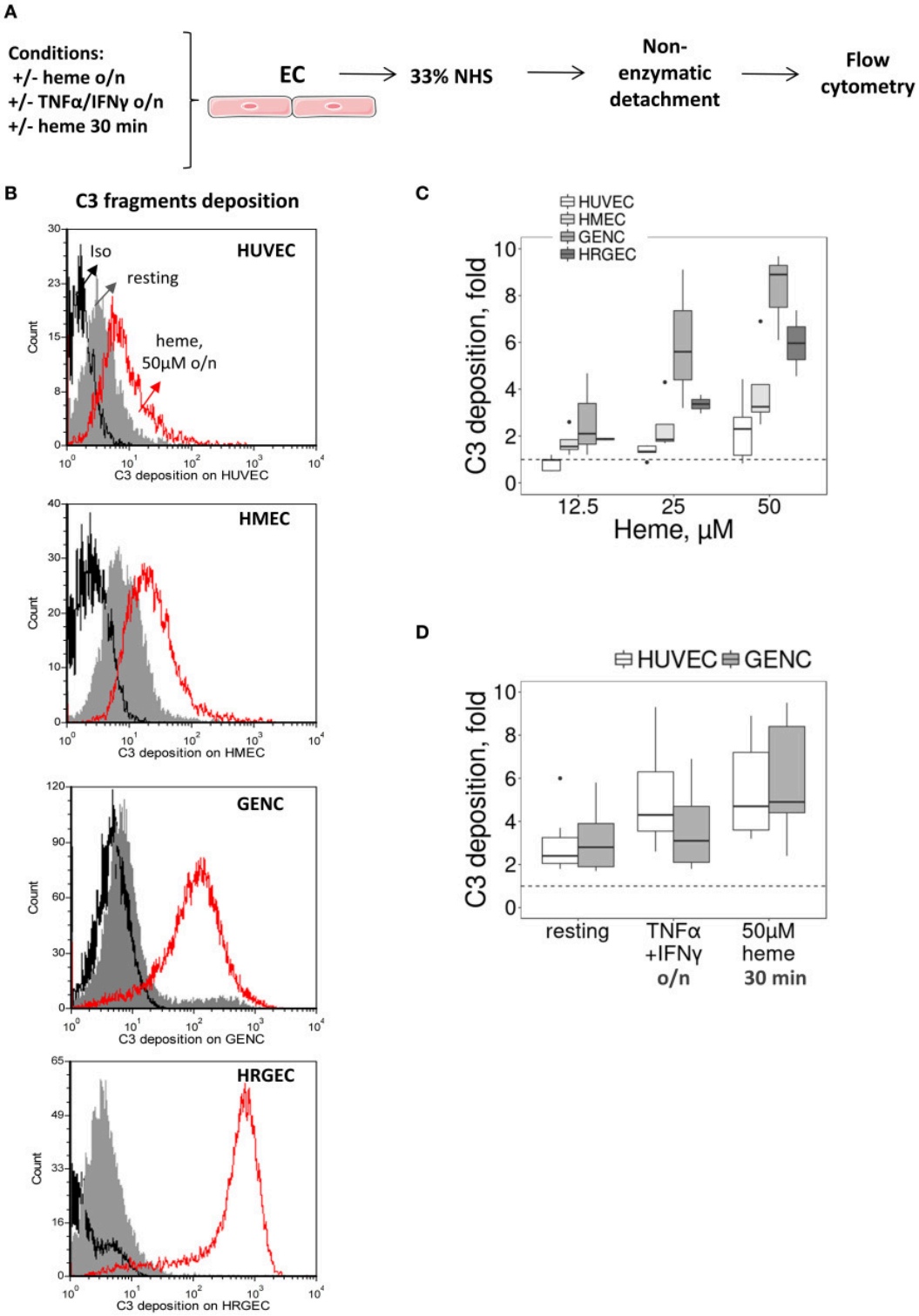

FIGURE 2 | Influence of heme and cytokines on C3 fragment deposits on cultured human EC. **(A)** Experimental settings of figures **(B–D)** study by flow cytometry of C3b/iC3b deposition on cultured human EC (HUVEC, HMEC, GENC, HREGC), pretreated with medium only, TNFα/IFNγ overnight, or 50 μM of heme (30 min or overnight) before incubation with 33% NHS diluted in M199 culture medium and non-enzymatic detachment. **(B)** C3b/iC3b fragment deposits on resting EC (gray histograms) or EC treated overnight with 50 μM of heme (red histograms). Isotype control IgG1 appears as a black histogram (Iso). Representative histograms of 3 independent experiments. **(C)** Quantification of C3b/iC3b fragments deposition on the four EC types, studied as a function of the dose of heme overnight ($n = 3–5$). **(D)** Quantification of C3b/iC3b fragments deposition on HUVEC and GENC pretreated with medium only, TNFα/IFNγ overnight, or 50 μM of heme (30 min) ($n = 3–5$).

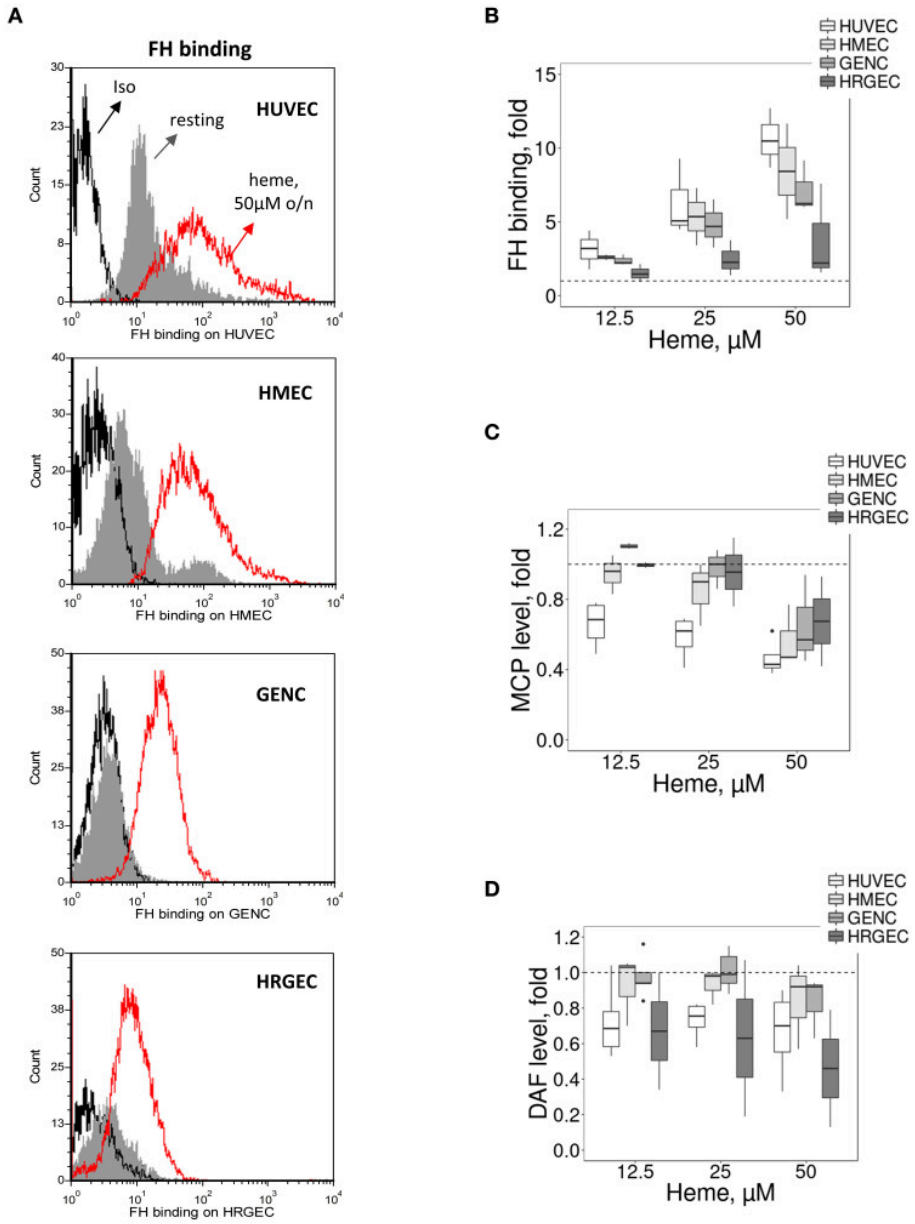

FIGURE 3 | Influence of heme on C3 convertase regulators on cultured human EC. Experimental settings are similar with **Figure 2**. **(A)** Binding of FH on resting EC (gray histograms) or EC treated overnight with 50 µM of heme (red histograms) before incubation with sera. FH binding was analyzed by flow cytometry. Isotype control IgG1 appears as a black histogram (Iso). Representative histograms of 3 independent experiments. Quantification of the **(B)** FH, **(C)** MCP, and **(D)** DAF staining, studied as a function of the dose of heme ($n = 3$–5).

HO-1 Is Inefficiently Upregulated in Patients' Glomerular Endothelium

In kidney biopsies of patients with hemolysis—aHUS or with prosthetic cardiac valve—IHC with anti-HO-1 revealed a tubular staining proportional to the degree of hemolysis observed by hemosiderin deposition by Perls' Prussian blue staining (**Figure 6D**). Glomerular endothelium HO-1 staining was negative (**Figure 6E**). No hemosiderin deposition, HO-1 mesangial or tubular stainings were detected in negative controls. It should be noted that all biopsies, even negative controls, displayed non-specific staining due to capture of the antibody by erythrocytes. Positive staining was nevertheless detected on podocytes, in agreement with previous observations (25). Similar to the mouse results, weak positive C3 staining was detected in some glomeruli of cardiac valve patients, while intense deposits were observed in the patients with complement abnormalities (**Figure 6F**).

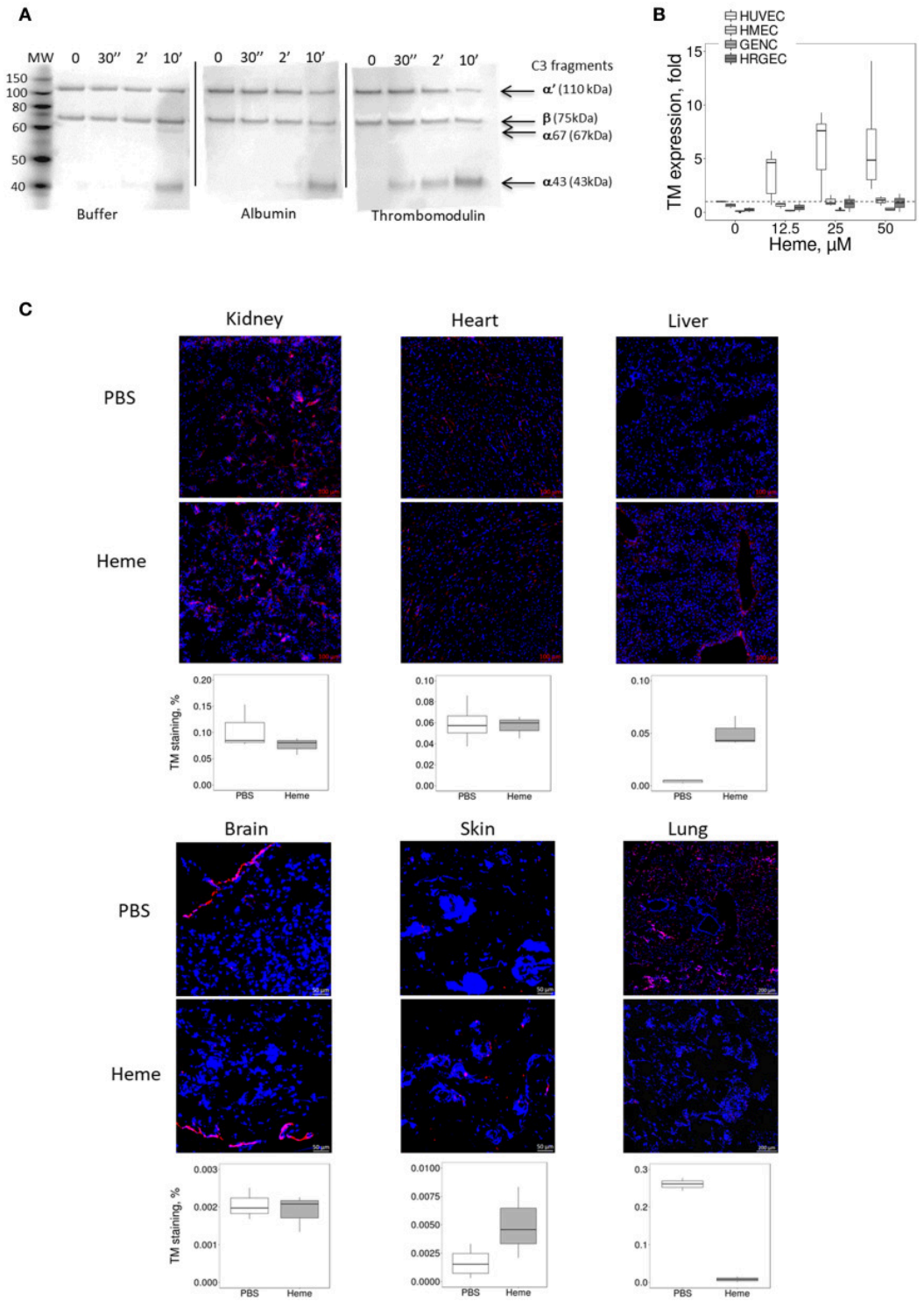

FIGURE 4 | Influence of heme on the TM expression *in vitro* on cultured human EC and in mice. **(A)** Functional activity of TM as complement regulator, studied using purified protein by western blot. C3b is composed of 2 chains, α and β, visible by WB as 2 bands. The α chain is cleaved by FI to give two new bands: α67 and α43. The intensity of these bands reflects the level of C3b conversion to iC3b. Incubation of C3b with FH and FI led to cleavage of C3b to iC3b in a time-dependent manner. Addition of TM accelerates the cleavage of C3b compared to albumin and buffer controls. **(B,C)** HUVEC, HMEC, GENC, and HRGEC were incubated with increasing concentrations of heme overnight and mRNA was extracted. Gene expression of **(B)** TM was measured by RTqPCR, ($n = 3$). **(C)** TM staining (in red) was studied by IF in frozen kidney (x15), heart (x15), liver (x8), brain (x8), skin (x15), and lung (x5) sections of mice treated with PBS (negative control) or heme. Representative images of 5 mice per group. Lower panels: quantification of TM staining in organs sections of PBS (white) and heme-injected mice (gray).

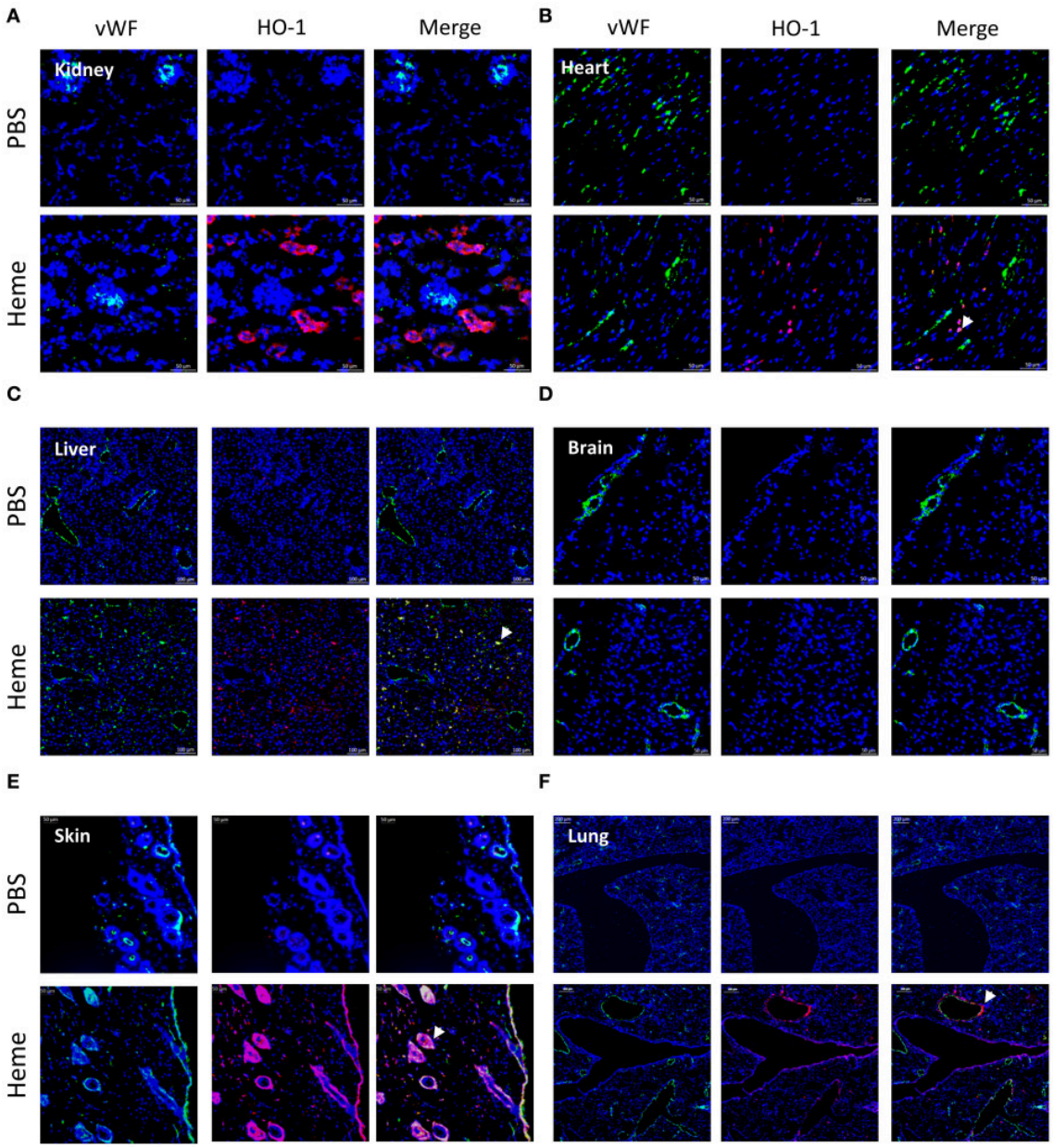

FIGURE 5 | Comparison of HO-1 expression in different organs after heme injection in mice. **(A-F)** vWF (green) staining, HO-1 (red) staining and colocalization on frozen kidney (x15), heart (x15) liver (x8), brain (x8), skin (x15), and lung (x15) sections of mice, injected with PBS (upper panel) or heme (lower panel), studied by IF. Representative results of 3 independent experiments with 3 or 5 mice per group.

Glomerular EC Fail to Accommodate a Second Challenge With Heme and Show Enhanced C3 Deposition

The HO-1 up-regulation is accompanied by accommodation and a gain in complement resistance in HUVEC (16). We here compared the C3 deposition on the four EC types after incubation overnight with different doses of heme (to induce HO-1 upregulation), followed by a second challenge with 50 μM of heme for 30 min and exposure to serum (**Figure 7A**). The 30 min heme-exposure caused about a 2-fold increase of the C3 deposition on EC not receiving heme overnight (not shown). Exposure to heme overnight followed by 50 μM heme for 30 min produced a dose-dependent decrease in C3 deposition on HUVEC, but an increase on glomerular EC (**Figure 7B**). C3 deposits decreased by ∼50% on HUVEC, while they significantly increased by ∼8 fold on GENC and ∼3 fold on HRGEC ($p < 0.05$) compared with HUVEC. HMEC showed an intermediate phenotype with C3 deposition comparable to baseline.

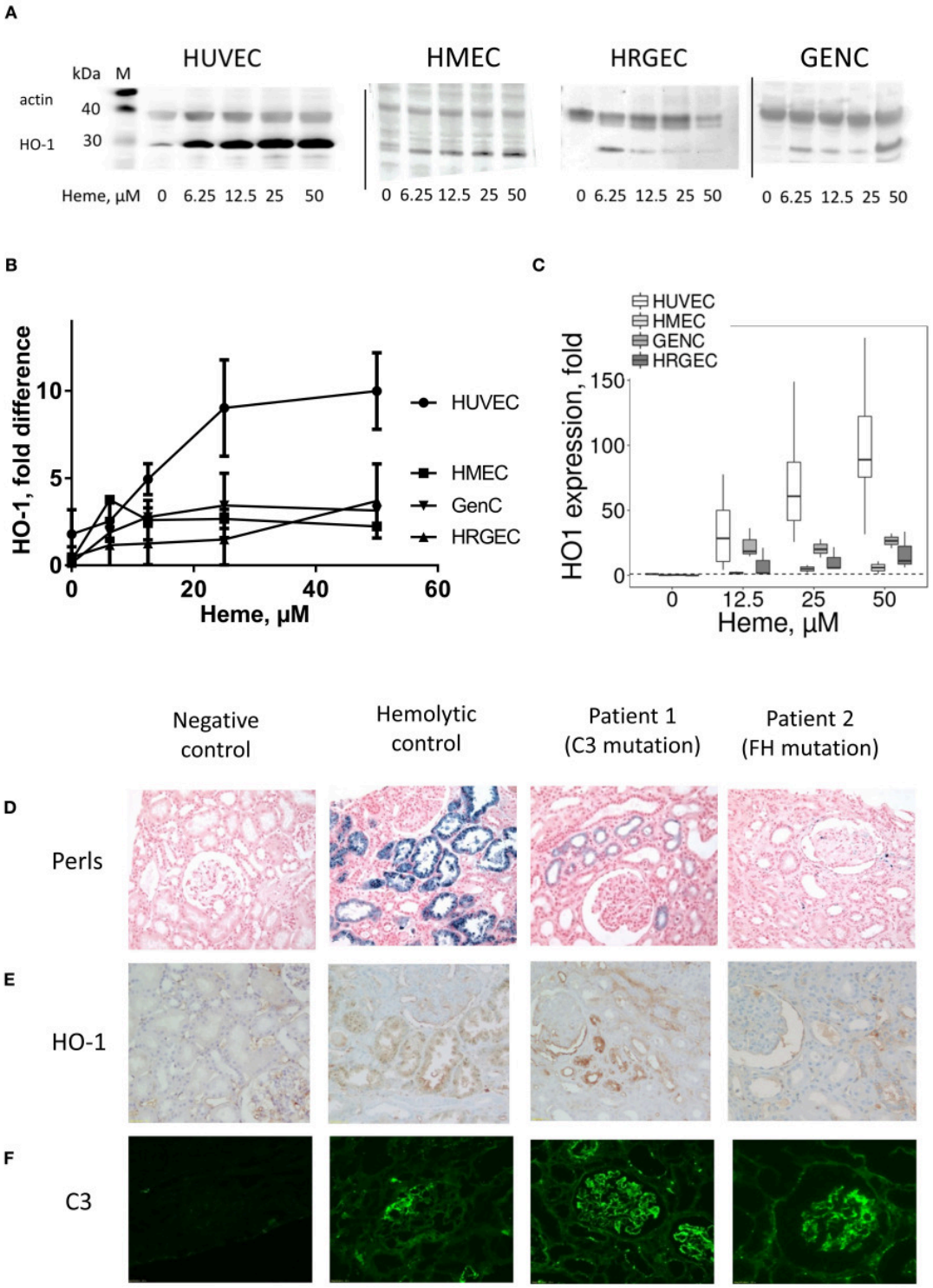

FIGURE 6 | Influence of heme on the HO-1 expression *in vitro* in cultured human EC and HO-1 expression and C3b deposition in human kidney biopsies under hemolysis **(A–C)** HUVEC, HMEC, GENC, and HRGEC were stimulated with increasing concentrations of heme overnight. **(A)** HO-1 protein level studied by western blot ($n = 2$–5). **(B)** Quantification of the western blots ($n = 2$–5), ratio of the band of HO-1, relative to the band of actin. **(C)** *HO-1* gene expression measured by RTqPCR ($n = 3$). **(D)** Hemolysis level on human kidney biopsies was evaluated by the hemosiderin deposits, revealed by Perls' coloration. **(E)** HO-1 (brown) and **(F)** C3 (green) staining were performed by IHC and IF, respectively. A normal protocol, kidney allograft biopsy performed 3 months after transplant was used as a negative control. Biopsies of a patient with chronic hemolysis (hemolysis associated with prosthetic heart valve) were used as a positive control. Two patients with aHUS carrying complement mutations were tested.

To find out to what extent this protective effect in HUVEC was HO-1 dependent, the HO-1 expression was induced by pre-incubation with another porphyrin of similar structure to heme (SnMPIX) but which blocks its activity (26–28). Overnight exposure of the cells to SnMPIX caused HO-1 expression, albeit 2–3 fold weaker than that induced by exposure to heme, and no increase of C3 deposition (data not shown). After a second challenge with heme, no protective effect against complement of the pre-incubation with SnMPIX was detected at any of the tested doses (up to 50 μM), contrary to heme which produced a protective effect after cells were exposed at 12.5 μM heme ($p < 0.05$) (**Figure 7C**).

TM and HO-1 Expression May Be Parallel Phenomena, Dependent on the Transcription Activity of KLF2 and KLF4

HO-1 expression is mainly dependent of the transcription factors *NRF2* and *BACH1*, but no major differences were found for their expression between the four EC types (**Figures 7D,E**), except for a slightly lower expression of *NRF2* at resting state for the glomerular HRGEC ($p < 0.05$).

We then studied transcription factors *KLF2 and KLF4* because they control the expression of TM (29), and KLF4 could also modulate HO-1 expression (30). For *KLF2*, a strong dose-dependent effect was noted in HUVEC with ∼9.8-fold increase compared with untreated cells after exposure to 50 μM of heme (**Figure 7F**). The increase in the other cell types was lower compared to HUVEC, with only ∼2, ∼3.3, and ∼3.8-fold after exposure to 50 μM heme for HMEC, GENC, and HRGEC, respectively. Strong *KLF4* gene expression was also observed with increases in heme concentration (**Figure 7G**). Exposure to 50 μM heme induced ∼25-fold increase of *KLF4* level in HUVEC, but only ∼1.26, ∼1.1, and ∼1.48-fold in the microvascular HMEC, GENC, and HRGEC, respectively. These results may be explained, at least in part, by the shared profile of TM and HO-1 expressions in microvascular EC.

DISCUSSION

In this study, we discovered a dichotomy in the phenotypic adaptation to hemolysis of macro- vs. microvascular endothelium. Macrovascular EC adapted to heme-overload by up-regulating the heme-degrading HO-1 and the coagulation and complement regulator TM, as well as exhibiting enhanced binding of the complement regulator FH. On the contrary, the microvascular EC, and in particular glomerular EC, were less efficient at each of these processes (**Figure 8A**), which resulted in a susceptibility of glomerular endothelium to heme-driven complement overactivation. These observations may help to explain the microvascular and renal tropism of the complement-mediated TMA lesions of aHUS (**Figure 8B**).

The tropism of TMA lesions for small vessels is a defining feature of this group of syndromes, but the mechanisms remain poorly described. Our results and data from the literature suggest that resting microvascular EC express similar or even higher levels of complement regulators and TM (6, 31, 32), failing thus to explain their susceptibility to TMA lesions. It is well-established that the presence of shiga toxin in typical HUS, complement abnormalities in aHUS, or ADAMTS13 deficiency in thrombotic thrombocytopenic purpura (TTP) are necessary but not sufficient in themselves to trigger TMA (1, 33). Inflammatory insult is a frequently described TMA-trigger. Nevertheless, our results showed that inflammatory mediators increased complement activation and decreased TM expression in both micro- and macrovasular EC, in accordance with previous studies (6, 33–35). Secondary hits are needed to overcome the tolerable EC stress and to promote overt endothelial injury and disease manifestation. Since hemolysis is a hallmark of TMA, it is tempting to speculate that oxidative stress and cell activation will be particularly noxious for the microvessels, in the kidney as well as other organs, amplifying cell damage, complement activation and thrombosis, contrary to macrovessels.

Hemolysis alone also does not induce renal TMA lesions (13) but may present a secondary challenge in the presence of deregulated complement, as in the case of aHUS (7, 8); indeed, heme activates complement AP directly in serum and this contributes to the C3 deposits found on EC (8, 11, 36–39). In support of this hypothesis, injection of heme resulted in a marked renal C3 deposition in mice, localized predominantly in the glomeruli, and similar to what has been observed for intravascular hemolysis and injection of cell-free hemoglobin (39). In contrast to kidneys, our examination of the heart, liver, brain, skin and lungs showed them to be largely unaffected by injection of heme, or to have exhibited only small increases in C3 deposits after injection (summary in the **Supplementary Table 1**). In agreement with these *in vivo* data, overnight exposure to heme induced stronger C3 deposition on glomerular EC compared with the macrovascular (HUVEC) and microvascular (HMEC) cell models. Together, these *in vivo* and *in vitro* observations point toward a vulnerability of the glomerular endothelium to complement deposition in the presence of heme. However, the inefficient adaptation to hemolysis in terms of HO-1 expression and TM up-regulation was also observed in other microvascular EC, both *in vitro* and *in vivo*, while only glomerular EC were subject to deposition of very high levels of C3 activation fragments upon exposure to heme.

These particularly elevated complement deposits in kidneys and glomerular cells may be explained by reduced binding of FH, the main regulator of the AP of complement (3), which is the most frequently affected among aHUS patients [genetic or acquired abnormalities found in >40% of patients (2, 40, 41)]. Moreover, we confirmed that FH is assisted by TM in the inactivation of C3b (23, 42, 43) and that the lower level of TM can further aggravate the inefficient complement regulation. The underlying mechanism(s) behind this reduced FH binding require further investigation, but the combination of decreased FH binding to glomerular EC under hemolytic conditions with FH mutations or autoantibodies could contribute to the susceptibility of glomerular EC to TMA lesions. Interestingly, a recent study also showed that renin, an enzyme produced specifically in the kidney, could cleave C3 and exacerbate the complement activation (44). The hemolysis-mediated complement activation could be an additional key

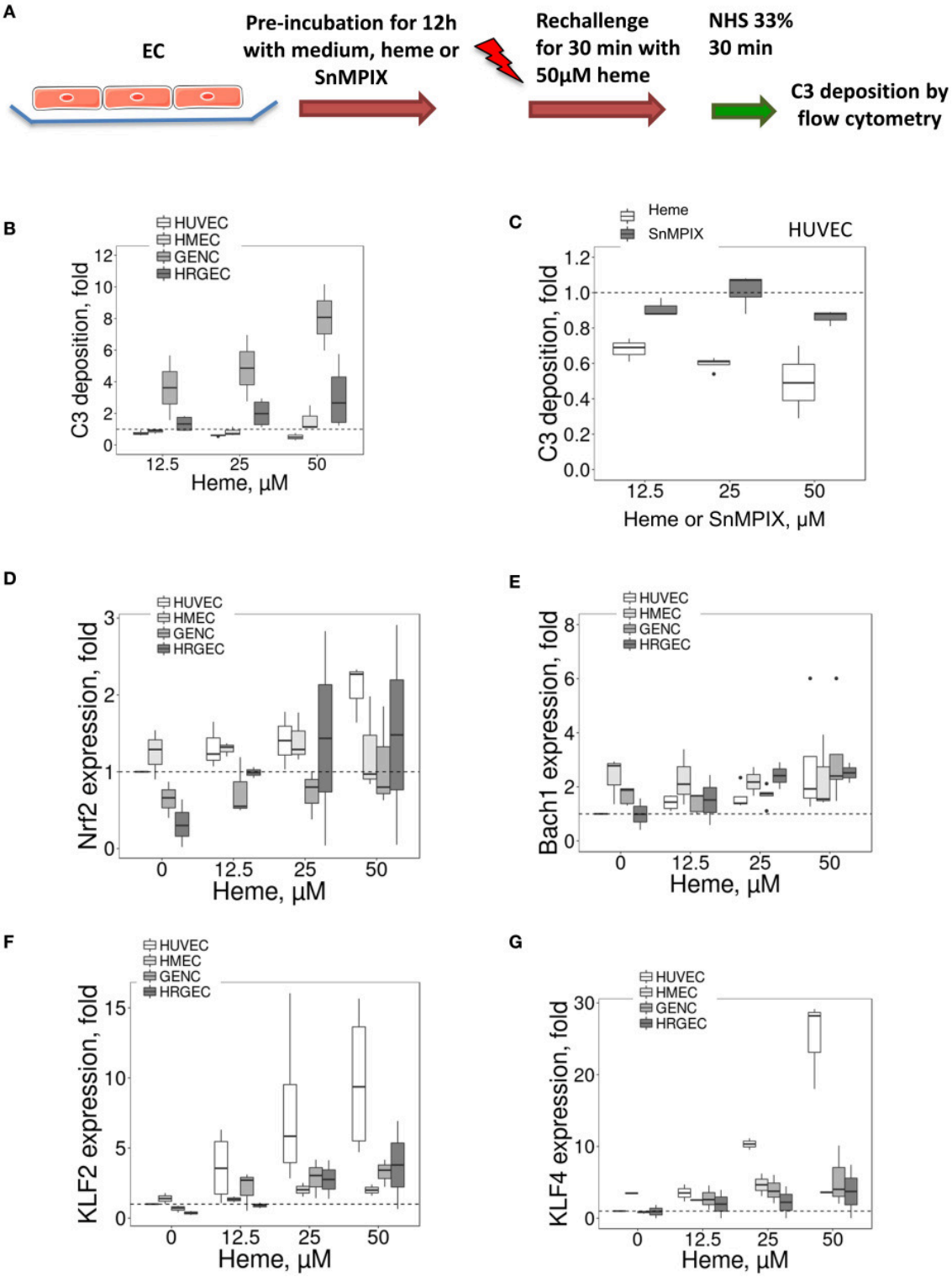

FIGURE 7 | Influence of porphyrin pre-incubation on C3 fragments deposition on EC and expression of HO-1 and TM transcription factors **(A)** Experimental settings of **B** and **C**: C3 fragments deposition study, on cultured human EC pretreated overnight with medium only or pre-incubated with porphyrin (heme or SnMPIX) and then rechallenged by 50 µM of heme during 30 min, followed by incubation with 33% NHS. C3b/iC3b staining was analyzed by flow cytometry. **(B,C)** C3 fragments deposition under the experimental conditions described above as a function of the dose of heme during the pre-incubation step **(B)** on EC, and as a function of the dose of heme or SnMPIX **(C)** during the pre-incubation step on HUVEC ($n = 3$). **(D–G)** HUVEC, HMEC, GENC, and HRGEC were stimulated with increasing concentrations of heme overnight. **(D)** *NRF2*, **(E)** *BACH1*, **(F)** *KLF2,* and **(G)** *KLF4* gene expression measured by RTqPCR ($n = 3$).

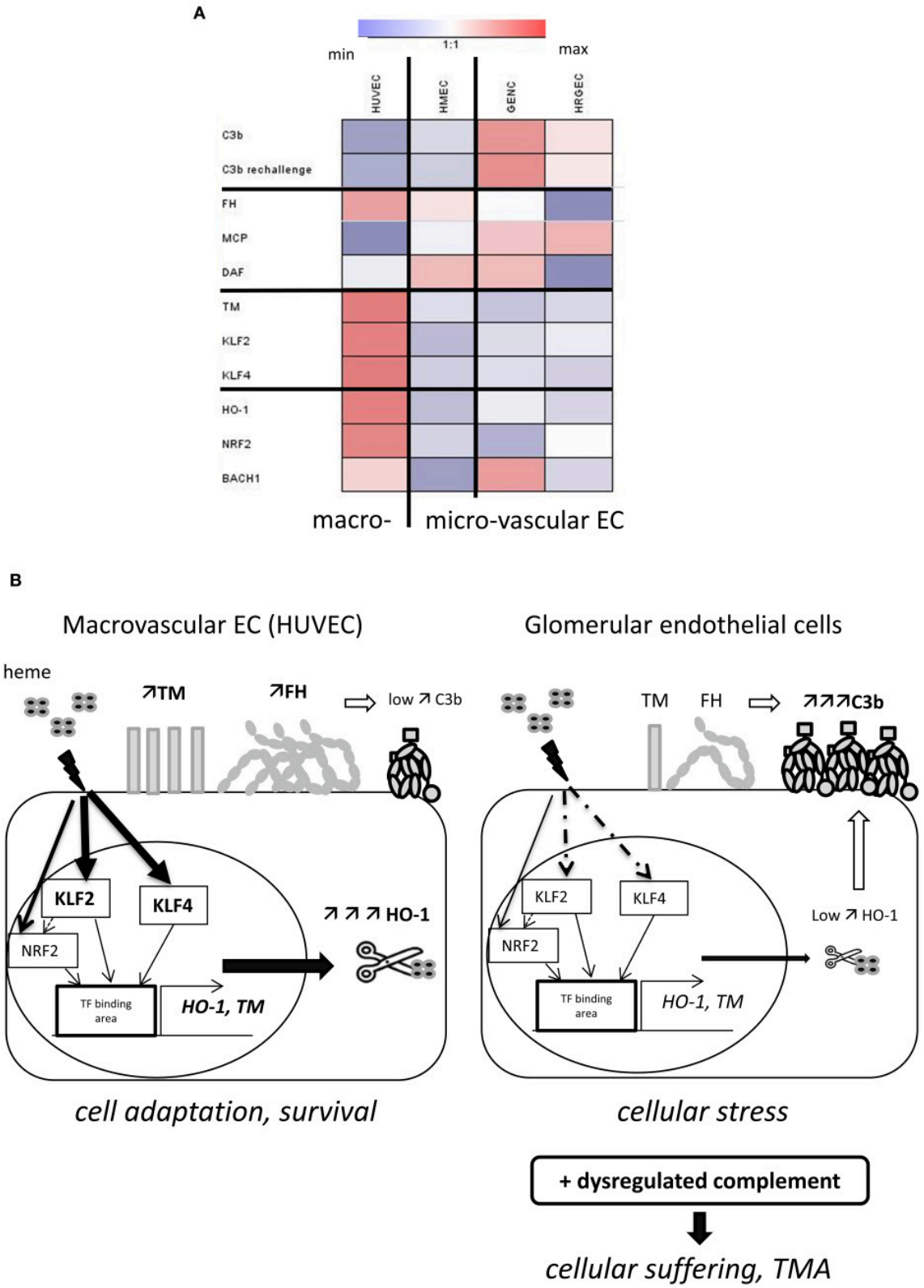

FIGURE 8 | Schematic representation of our model to explain the glomerular vulnerability to complement-mediated TMA. **(A)** Heat map, illustrating the variations of the studied parameters between the four EC types. Results of the fold difference of gene or protein expression or binding with exposure to 50μM heme were analyzed using Genesis software. White color indicates no difference (fold change 1), blue indicates reduction and red an increased expression/binding. **(B)** Proposed model to

(Continued)

FIGURE 8 | explain the microvascular/glomerular cell susceptibility of TMA lesions. Our results suggest that hemolysis is a key factor in the vulnerability of the glomerular EC complement overactivation and TMA. The glomerular EC have a weaker capacity to adapt to hemolysis and to up-regulate cytoprotective and stress-response genes, such as HO-1 and TM, compared to EC from other organs. This could be related to the lower levels of the transcription factors *KLF2* and *KLF4*. The inefficient degradation of heme due to the lack of HO-1 will result in stronger heme-mediated complement activation on the endothelium. The weaker expression of TM will on the one hand contribute to the pro-coagulant phenotype of the EC, and on the other hand contribute to inefficient degradation of the anaphylatoxins C3a and C5a and assist FH and FI in degradation of C3b. Finally, FH will bind less to heme-exposed glomerular EC compared to EC of other organs. This will be further exacerbated in case of complement overactivation, as in aHUS, leading to EC suffering and TMA.

element in this vicious circle, linking renin secretion, vascular damage and renal failure. Thus, the C3 deposits described in aHUS kidney biopsies, which are generally considered non-specific (45, 46), could reflect the complement activation due to hemolysis and deregulated complement, this last condition explaining why the C3 deposits are greater in aHUS patients than in cases of isolated hemolysis (cardiac valve).

The cells' capacity to express HO-1, to degrade heme and then detoxify it to cytoprotective metabolites biliverdin and CO, plays a key role in vascular protection (15, 47). *In vitro* studies have shown heme-mediated HO-1 expression in HUVEC (48, 49), and there is clear evidence for endothelial HO-1 expression in large vessels of patients with sickle cell disease (50), as well as in animal models of hemolysis or other stress inducers (51–55). In contrast, we found only HO-1 upregulation to be minimal or absent in glomerular EC (*in vitro* or *in vivo*), in aHUS and hemolytic patients, as well as in heme-injected mice. This observation is in agreement with published images of aHUS and under other hemolytic conditions (20, 24, 25, 56, 57) and indicates that glomerular endothelium does not have the capacity to efficiently up-regulate HO-1 in presence of heme. HO-1 production is, however, indispensable to the glomerular protection, as suggested by reported early damages of glomeruli in case of HO-1deficiency in murine model or in human (47, 58, 59). Mesangial proliferation and thickening of the capillary wall in accordance with endothelial swelling and detachment were indeed described in a HO-1 deficient young boy. This early aspect of mesangioproliferative glomerulonephritis was confirmed from sequential kidney samples (at 2, 5 and 6 year-old), while tubulo-interstitial damages advanced more progressively. This could to be related to the fact that the production of HO-1 within kidneys would be mainly tubular, while in the glomeruli the major HO-1 source would be the infiltrating macrophages, not the intrinsic glomerular cells (60). Further studies are needed to extend our knowledge on the different ways, that the EC from different vascular beds manage heme homeostasis, based on their specific ability to accumulate it, to transport it within the cell by FLVCR1, to express ferritin, store iron and to produce reactive oxygen species. Some of these parameters have been studied for HUVEC and HMEC, especially in the context of deficiency of the heme transporter FLVCR1a, but data on glomerular EC are lacking (61). Moreover, a recent study in the context of leukemia demonstrated that C3a and C5a trigger phosphorylation of MAPK, followed by downregulation of HO-1 expression in malignant cells (62). If such phenomenon operates in HO-1 expressing endothelium, complement activation by intravascular hemolysis and heme release may weaken the endothelial resistance. In such context, inhibitors of MAPK (such as SB203580) will result in upregulation of HO-1 and enhance resistance to hemolysis-derived products as well as to complement.

A protective role of HO-1 against immune complexes-mediated complement overactivation has also been described on HUVEC (16). Here, our results demonstrated a complement-protective effect of pre-incubation with heme in HUVEC. Ideally, this phenomenon should be confirmed after HO-1 silencing. In contrast, the glomerular EC showed a marked increase in C3 deposition. These results, together with the loss of this protective effect upon HO-1 inhibition in HUVEC, suggest that HO-1 activity for heme degradation contributes to protection against complement activation in this cell type—a phenomenon which is not operational in the glomerular endothelium. It is important to note that glomerular EC were able to upregulate HO-1 after incubation with a very potent inducer, such as CoPPIX (data not shown), suggesting that the machinery needed for its synthesis is present and can be triggered after potent stimulation. Nevertheless, induction of massive hemolysis *in vivo* was not strong enough to mediate HO-1 staining in glomerular EC, contrary to tubuli and podocytes [(13) and data not shown]. Our *in vivo* experiments also showed that the brain endothelium failed to upregulate HO-1 after heme injection, but this was not associated with concomitant deposition of C3 fragments. Sartain et al. recently demonstrated that brain microvascular EC express higher levels of complement regulators, compared to glomerular EC, and had a better capacity for suppressing the alternative pathway *in vitro* (32). These findings may help to explain the occurrence of lower levels of cerebral vessels' complement deposits and the fact that in aHUS, as well as in shiga toxin HUS, brain manifestations were found in only a small fraction of patients (63). On the other hand, the inefficient upregulation of HO-1 in the brain vasculature may contribute to the cerebral manifestations of TTP (also a TMA disease). The possible role of HO-1 expression in TTP pathophysiology requires further studies.

Interestingly, *KLF2* (64, 65), and *KLF4* (66), which are known transcription factors of TM, have also been shown to serve as modulators of *HO-1* expression (30). Therefore, the weaker up-regulation of TM and HO-1 we observed in microvascular EC could at least in part be related to differences in transcription regulation. Consistent with these data, other workers have reported that *KLF2* and *KLF4* were not significantly upregulated in glomeruli of aHUS patients compared with controls (67).

The observed differences in gene expression and phenotype among the tested EC here confirm the utility of HUVEC and HMEC as model EC types for macro- and microvascular endothelial, but highlight unique features and responses to activation in glomerular EC, which could perhaps be better modeled by glomerular (primary or cell line) EC in culture. A

limitation of our work is that, although we observed correlations, we do not provide direct evidence linking HO-1 and complement deposits *in vitro*, for which the knock out/knock in strategy would have been useful. Also, providing *in vivo* evidence that up-regulation of HO-1 could prevent complement activation and TMA lesions in a mouse model of aHUS was outside the scope of this study.

In conclusion, we have shown that when compared with macrovascular EC, microvascular EC, and glomerular EC in particular, are vulnerable to complement-mediated TMA at least in part because of their failure to adapt to hemolysis, to up-regulate cytoprotective and stress-response genes such as HO-1 and TM, and to bind FH (**Figure 8B**). We hypothesize that local, subclinical microthrombosis due to a primary triggering event (infection, pregnancy) will cause mechanical hemolysis in the kidney. By amplifying complement activation and pro-thrombogenic traits, heme will exacerbate endothelial activation. Once the threshold of tolerance is reached, this heme-induced endothelial and complement overactivation could sustain and perpetuate the TMA lesions. Together, our results indicate that the vulnerability of the glomerular EC to hemolysis is a key factor, predisposing them to complement overactivation and TMA, as seen in aHUS. The heme scavenger protein hemopexin has been efficient in preventing hemolysis-mediated C3 deposition in kidneys in a mouse model of intravascular hemolysis and on endothelial cells *in vitro* (39), as well as in models of stasis in sickle cell disease (68) or other hemolytic conditions (69). Therefore, heme-blocking agents may be explored as novel therapeutic strategies to prevent microvascular injury in TMA diseases.

AUTHOR CONTRIBUTIONS

LR, MF, and OM designed the study. OM, NM, AG, CP, TR-R, RP, VG, and FD performed research. SS and PM provided the GENC cell line. MH performed statistical analyses. LR, MF, OM, VF-B, JD, NM, AG, VG, and EB discussed the data. All authors wrote the manuscript and approved the submission.

ACKNOWLEDGMENTS

This work was supported by grants from Agence Nationale de la Recherche ANR JCJC—INFLACOMP 2015-2018 ANR-15-CE15-0001 to LR, ANR JCJC—COBIG ANR-13-JSV1-0006 to JD, Fondation du Rein under the aegis of the French Medical Research Foundation AMGEN 2014 FdR-SdN /FRM_FRIMAT and INSERM. The cytometric and microscopy analysis were performed at the Centre d'Histologie, d'Imagerie et de Cytométrie, (CHIC), Centre de Recherche des Cordeliers UMRS1138, (Paris, France) and we are grateful to the CHIC team for the excellent technical assistance. CHIC is a member of the UPMC Flow Cytometry network (RECYF). We are grateful for excellent technical assistance of the CEF team of the Centre de Recherche des Cordeliers for their support with the animal experimentation. The authors thank Dr. Michael HOWSAM (English proof-reader) for editorial assistance.

SUPPLEMENTARY MATERIAL

The Supplementary Material for this article can be found online at: https://www.frontiersin.org/articles/10.3389/fimmu.2018.03008/full#supplementary-material

REFERENCES

1. Fakhouri F, Zuber J, Frémeaux-Bacchi V, Loirat C. Haemolytic uraemic syndrome. *Lancet Lond Engl.* (2017) 390:681–96. doi: 10.1016/S0140-6736(17)30062-4
2. Fremeaux-Bacchi V, Fakhouri F, Garnier A, Bienaimé F, Dragon-Durey M-A, Ngo S, et al. Genetics and outcome of atypical hemolytic uremic syndrome: a nationwide French series comparing children and adults. *Clin J Am Soc Nephrol.* (2013) 8:554–62. doi: 10.2215/CJN.04760512
3. Merle NS, Church SE, Fremeaux-Bacchi V, Roumenina LT. Complement system part I - molecular mechanisms of activation and regulation. *Front Immunol* (2015) 6:262. doi: 10.3389/fimmu.2015.00262
4. Legendre CM, Licht C, Loirat C. Eculizumab in atypical hemolytic-uremic syndrome. *N Engl J Med.* (2013) 369:1379–80. doi: 10.1056/NEJMc1308826
5. Noris M, Remuzzi G. Genetics and genetic testing in hemolytic uremic syndrome/thrombotic thrombocytopenic purpura. *Semin Nephrol.* (2010) 30:395–408. doi: 10.1016/j.semnephrol.2010.06.006
6. Sartain SE, Turner NA, Moake JL. TNF regulates essential alternative complement pathway components and impairs activation of protein c in human glomerular endothelial cells. *J Immunol.* (2016) 196:832–45. doi: 10.4049/jimmunol.1500960
7. Roumenina LT, Rayes J, Frimat M, Fremeaux-Bacchi V. Endothelial cells: source, barrier, and target of defensive mediators. *Immunol Rev.* (2016) 274:307–29. doi: 10.1111/imr.12479
8. Frimat M, Tabarin F, Dimitrov JD, Poitou C, Halbwachs-Mecarelli L, Fremeaux-Bacchi V, et al. Complement activation by heme as a secondary hit for atypical hemolytic uremic syndrome. *Blood* (2013) 122:282–92. doi: 10.1182/blood-2013-03-489245
9. Roumenina LT, Frimat M, Miller EC, Provot F, Dragon-Durey M-A, Bordereau P, et al. A prevalent C3 mutation in aHUS patients causes a direct C3 convertase gain of function. *Blood* (2012) 119:4182–91. doi: 10.1182/blood-2011-10-383281
10. Roumenina LT, Jablonski M, Hue C, Blouin J, Dimitrov JD, Dragon-Durey M-A, et al. Hyperfunctional C3 convertase leads to complement deposition on endothelial cells and contributes to atypical hemolytic uremic syndrome. *Blood* (2009) 114:2837–45. doi: 10.1182/blood-2009-01-197640
11. Roumenina LT, Rayes J, Lacroix-Desmazes S, Dimitrov JD. Heme: modulator of plasma systems in hemolytic diseases. *Trends Mol Med.* (2016) 22:200–13. doi: 10.1016/j.molmed.2016.01.004
12. Belcher JD, Chen C, Nguyen J, Milbauer L, Abdulla F, Alayash AI, et al. Heme triggers TLR4 signaling leading to endothelial cell activation and vaso-occlusion in murine sickle cell disease. *Blood* (2014) 123:377–90. doi: 10.1182/blood-2013-04-495887
13. Merle NS, Grunenwald A, Figueres M-L, Chauvet S, Daugan M, Knockaert S, et al. Characterization of renal injury and inflammation in an experimental model of intravascular hemolysis. *Front Immunol.* (2018) 9:179. doi: 10.3389/fimmu.2018.00179
14. Dutra FF, Bozza MT. Heme on innate immunity and inflammation. *Front Pharmacol.* (2014) 5:115. doi: 10.3389/fphar.2014.00115
15. Gozzelino R, Jeney V, Soares MP. Mechanisms of cell protection by heme oxygenase-1. *Annu Rev Pharmacol Toxicol.* (2010) 50:323–54. doi: 10.1146/annurev.pharmtox.010909.105600

16. Kinderlerer AR, Gregoire IP, Hamdulay SS, Ali F, Steinberg R, Silva G, et al. Heme oxygenase-1 expression enhances vascular endothelial resistance to complement-mediated injury through induction of decay-accelerating factor: a role for increased bilirubin and ferritin. *Blood* (2009) 113:1598–607. doi: 10.1182/blood-2008-04-152934
17. Ades EW, Candal FJ, Swerlick RA, George VG, Summers S, Bosse DC, et al. HMEC-1: establishment of an immortalized human microvascular endothelial cell line. *J Invest Dermatol.* (1992) 99:683–90.
18. Satchell SC, Tasman CH, Singh A, Ni L, Geelen J, von Ruhland CJ, et al. Conditionally immortalized human glomerular endothelial cells expressing fenestrations in response to VEGF. *Kidney Int.* (2006) 69:1633–40. doi: 10.1038/sj.ki.5000277
19. Livak KJ, Schmittgen TD. Analysis of relative gene expression data using real-time quantitative PCR and the 2(-Delta Delta C(T)) Method. *Methods San Diego Calif.* (2001) 25:402–8. doi: 10.1006/meth.2001.1262
20. Morimoto K, Ohta K, Yachie A, Yang Y, Shimizu M, Goto C, et al. Cytoprotective role of heme oxygenase (HO)-1 in human kidney with various renal diseases. *Kidney Int.* (2001) 60:1858–66. doi: 10.1046/j.1523-1755.2001.01000.x
21. R Core Team. *R: A Language and Environment for Statistical Computing*. R Foundation for Statistical Computing, Vienna (2017).
22. Wickham H. *ggplot2: Elegant Graphics for Data Analysis*. New York, NY: Springer-Verlag (2009).
23. Delvaeye M, Noris M, De Vriese A, Esmon CT, Esmon NL, Ferrell G, et al. Thrombomodulin mutations in atypical hemolytic–uremic syndrome. *N Engl J Med.* (2009) 361:345–57. doi: 10.1056/NEJMoa0810739
24. Shimizu M, Ohta K, Yang Y, Nakai A, Toma T, Saikawa Y, et al. Glomerular proteinuria induces heme oxygenase-1 gene expression within renal epithelial cells. *Pediatr Res.* (2005) 58:666–71. doi: 10.1203/01.PDR.0000180557.68222.5A
25. Rubio-Navarro A, Sanchez-Niño MD, Guerrero-Hue M, García-Caballero C, Gutiérrez E, Yuste C, et al. Podocytes are new cellular targets of haemoglobin-mediated renal damage. *J Pathol.* (2018) 244:296–310. doi: 10.1002/path.5011
26. Maines MD, Trakshel GM. Tin-protoporphyrin: a potent inhibitor of hemoprotein-dependent steroidogenesis in rat adrenals and testes. *J Pharmacol Exp Ther* (1992) 260:909–16.
27. Soares MP, Lin Y, Anrather J, Csizmadia E, Takigami K, Sato K, et al. Expression of heme oxygenase-1 can determine cardiac xenograft survival. *Nat Med.* (1998) 4:1073–7. doi: 10.1038/2063
28. Silva G, Cunha A, Grégoire IP, Seldon MP, Soares MP. The antiapoptotic effect of heme oxygenase-1 in endothelial cells involves the degradation of p38 alpha MAPK isoform. *J Immunol.* (2006) 177:1894–903. doi: 10.4049/jimmunol.177.3.1894
29. Atkins GB, Jain MK. Role of Krüppel-like transcription factors in endothelial biology. *Circ Res.* (2007) 100:1686–95. doi: 10.1161/01.RES.0000267856.00713.0a
30. Ali F, Zakkar M, Karu K, Lidington EA, Hamdulay SS, Boyle JJ, et al. Induction of the cytoprotective enzyme heme oxygenase-1 by statins is enhanced in vascular endothelium exposed to laminar shear stress and impaired by disturbed flow. *J Biol Chem.* (2009) 284:18882–92. doi: 10.1074/jbc.M109.009886
31. Laszik Z, Mitro A, Taylor FB, Ferrell G, Esmon CT. Human protein C receptor is present primarily on endothelium of large blood vessels: implications for the control of the protein C pathway. *Circulation* (1997) 96:3633–40.
32. Sartain SE, Turner NA, Moake JL. Brain microvascular endothelial cells exhibit lower activation of the alternative complement pathway than glomerular microvascular endothelial cells. *J Biol Chem.* (2018) 293:7195–208. doi: 10.1074/jbc.RA118.002639
33. Sullivan M, Rybicki LA, Winter A, Hoffmann MM, Reiermann S, Linke H, et al. Age-related penetrance of hereditary atypical hemolytic uremic syndrome. *Ann Hum Genet.* (2011) 75:639–47. doi: 10.1111/j.1469-1809.2011.00671.x
34. Morigi M, Galbusera M, Gastoldi S, Locatelli M, Buelli S, Pezzotta A, et al. Alternative pathway activation of complement by Shiga Toxin promotes exuberant C3a formation that triggers microvascular thrombosis. *J Immunol.* (2011) 187:172–80. doi: 10.4049/jimmunol.1100491
35. Noris M, Galbusera M, Gastoldi S, Macor P, Banterla F, Bresin E, et al. Dynamics of complement activation in aHUS and how to monitor eculizumab therapy. *Blood* (2014) 124:1715–26. doi: 10.1182/blood-2014-02-558296
36. Pawluczkowycz AW, Lindorfer MA, Waitumbi JN, Taylor RP. Hematin promotes complement alternative pathway-mediated deposition of C3 activation fragments on human erythrocytes: potential implications for the pathogenesis of anemia in malaria. *J Immunol.* (2007) 179:5543–52. doi: 10.4049/jimmunol.179.8.5543
37. Lindorfer MA, Cook EM, Reis ES, Ricklin D, Risitano AM, Lambris JD, et al. Compstatin Cp40 blocks hematin-mediated deposition of C3b fragments on erythrocytes: Implications for treatment of malarial anemia. *Clin Immunol.* (2016) 171:32–5. doi: 10.1016/j.clim.2016.08.017
38. Roumenina LT, Radanova M, Atanasov BP, Popov KT, Kaveri SV, Lacroix-Desmazes S, et al. Heme interacts with c1q and inhibits the classical complement pathway. *J Biol Chem.* (2011) 286:16459–69. doi: 10.1074/jbc.M110.206136
39. Merle NS, Grunenwald A, Rajaratnam H, Gnemmi V, Frimat M, Figueres M-L, et al. Intravascular hemolysis activates complement via cell-free heme and heme-loaded microvesicles. *JCI Insight* (2018) 3:96910. doi: 10.1172/jci.insight.96910
40. Durey M-AD, Sinha A, Togarsimalemath SK, Bagga A. Anti-complement-factor H-associated glomerulopathies. *Nat Rev Nephrol.* (2016) 12:563–78. doi: 10.1038/nrneph.2016.99
41. Le Quintrec M, Roumenina L, Noris M, Frémeaux-Bacchi V. Atypical hemolytic uremic syndrome associated with mutations in complement regulator genes. *Semin Thromb Hemost.* (2010) 36:641–52. doi: 10.1055/s-0030-1262886
42. Heurich M, Preston RJS, O'Donnell VB, Morgan BP, Collins PW. Thrombomodulin enhances complement regulation through strong affinity interactions with factor H and C3b-Factor H complex. *Thromb Res.* (2016) 145:84–92. doi: 10.1016/j.thromres.2016.07.017
43. Tateishi K, Imaoka M, Matsushita M. Dual modulating functions of thrombomodulin in the alternative complement pathway. *Biosci Trends* (2016) 10:231–4. doi: 10.5582/bst.2016.01052
44. Békássy ZD, Kristoffersson A-C, Rebetz J, Tati R, Olin AI, Karpman D. Aliskiren inhibits renin-mediated complement activation. *Kidney Int.* (2018) 94:689–700. doi: 10.1016/j.kint.2018.04.004
45. Benz K, Amann K. Pathological aspects of membranoproliferative glomerulonephritis (MPGN) and haemolytic uraemic syndrome (HUS) / thrombocytic thrombopenic purpura (TTP). *Thromb Haemost.* (2009) 101:265–70. doi: 10.1160/TH07-12-0761
46. Lusco MA, Fogo AB, Najafian B, Alpers CE. AJKD Atlas of renal pathology: thrombotic microangiopathy. *Am J Kidney Dis.* (2016) 68:e33–4. doi: 10.1053/j.ajkd.2016.10.006
47. Yachie A, Niida Y, Wada T, Igarashi N, Kaneda H, Toma T, et al. Oxidative stress causes enhanced endothelial cell injury in human heme oxygenase-1 deficiency. *J Clin Invest.* (1999) 103:129–35. doi: 10.1172/JCI4165
48. Chen N, Shao W, Lv P, Zhang S, Chen Y, Zhu L, et al. Hemin-induced Erk1/2 activation and heme oxygenase-1 expression in human umbilical vein endothelial cells. *Free Radic Res.* (2007) 41:990–6. doi: 10.1080/10715760701468740
49. Wilson SJ, Keenan AK. Role of hemin in the modulation of H2O2-mediated endothelial cell injury. *Vascul Pharmacol.* (2003) 40:109–18. doi: 10.1016/S1537-1891(02)00340-3
50. Nath KA, Grande JP, Haggard JJ, Croatt AJ, Katusic ZS, Solovey A, et al. Oxidative stress and induction of heme oxygenase-1 in the kidney in sickle cell disease. *Am J Pathol.* (2001) 158:893–903. doi: 10.1016/S0002-9440(10)64037-0
51. Abraham NG, Rezzani R, Rodella L, Kruger A, Taller D, Li Volti G, et al. Overexpression of human heme oxygenase-1 attenuates endothelial cell sloughing in experimental diabetes. *Am J Physiol Heart Circ Physiol.* (2004) 287:H2468-77. doi: 10.1152/ajpheart.01187.2003
52. Li Z, Wang Y, Vanhoutte PM. Upregulation of heme oxygenase 1 by hemin impairs endothelium-dependent contractions in the aorta of the spontaneously hypertensive rat. *Hypertension* (2011) 58:926–34. doi: 10.1161/HYPERTENSIONAHA.111.173807

53. Zhang X, Bedard EL, Potter R, Zhong R, Alam J, Choi AMK, et al. Mitogen-activated protein kinases regulate HO-1 gene transcription after ischemia-reperfusion lung injury. *Am J Physiol Lung Cell Mol Physiol.* (2002) 283:L815–29. doi: 10.1152/ajplung.00485.2001
54. Lindenblatt N, Bordel R, Schareck W, Menger MD, Vollmar B. Vascular Heme Oxygenase-1 induction suppresses microvascular thrombus formation *in vivo*. *Arterioscler Thromb Vasc Biol.* (2004) 24:601–6. doi: 10.1161/01.ATV.0000118279.74056.8a
55. Kang L, Hillestad ML, Grande JP, Croatt AJ, Barry MA, Farrugia G, et al. Induction and functional significance of the heme oxygenase system in pathological shear stress *in vivo*. *Am J Physiol Heart Circ Physiol.* (2015) 308:H1402-13. doi: 10.1152/ajpheart.00882.2014
56. Shepard M, Dhulipala P, Kabaria S, Abraham NG, Lianos EA. Heme oxygenase-1 localization in the rat nephron. *Nephron* (2002) 92:660–4. doi: 10.1159/000064113
57. Yang Y, Ohta K, Shimizu M, Morimoto K, Goto C, Nakai A, et al. Selective protection of renal tubular epithelial cells by heme oxygenase (HO)-1 during stress-induced injury. *Kidney Int.* (2003) 64:1302–9. doi: 10.1046/j.1523-1755.2003.00231.x
58. Mosley K, Wembridge DE, Cattell V, Cook HT. Heme oxygenase is induced in nephrotoxic nephritis and hemin, a stimulator of heme oxygenase synthesis, ameliorates disease. *Kidney Int.* (1998) 53:672–8. doi: 10.1046/j.1523-1755.1998.00798.x
59. Kawashima A, Oda Y, Yachie A, Koizumi S, Nakanishi I. Heme oxygenase-1 deficiency: the first autopsy case. *Hum Pathol.* (2002) 33:125–30. doi: 10.1053/hupa.2002.30217
60. Ohta K, Yachie A, Fujimoto K, Kaneda H, Wada T, Toma T, et al. Tubular injury as a cardinal pathologic feature in human heme oxygenase-1 deficiency. *Am J Kidney Dis.* (2000) 35:863–70. doi: 10.1016/S0272-6386(00)70256-3
61. Petrillo S, Chiabrando D, Genova T, Fiorito V, Ingoglia G, Vinchi F, et al. Heme accumulation in endothelial cells impairs angiogenesis by triggering paraptosis. *Cell Death Differ.* (2018) 25:573–88. doi: 10.1038/s41418-017-0001-7
62. Abdelbaset-Ismail A, Borkowska-Rzeszotek S, Kubis E, Bujko K, Brzezniakiewicz-Janus K, Bolkun L, et al. Activation of the complement cascade enhances motility of leukemic cells by downregulating expression of HO-1. *Leukemia* (2017) 31:446–58. doi: 10.1038/leu.2016.198
63. Schaefer F, Ardissino G, Ariceta G, Fakhouri F, Scully M, Isbel N, et al. Clinical and genetic predictors of atypical hemolytic uremic syndrome phenotype and outcome. *Kidney Int.* (2018) 94:408–18. doi: 10.1016/j.kint.2018.02.029
64. Fledderus JO, Boon RA, Volger OL, Hurttila H, Ylä-Herttuala S, Pannekoek H, et al. KLF2 primes the antioxidant transcription factor Nrf2 for activation in endothelial cells. *Arterioscler Thromb Vasc Biol.* (2008) 28:1339–46. doi: 10.1161/ATVBAHA.108.165811
65. Wuestenberg A, Kah J, Singethan K, Sirma H, Keller AD, Rosal SRP, et al. Matrix conditions and KLF2-dependent induction of heme oxygenase-1 modulate inhibition of HCV replication by fluvastatin. *PloS ONE* (2014) 9:e96533. doi: 10.1371/journal.pone.0096533
66. Tsoyi K, Geldart AM, Christou H, Liu X, Chung SW, Perrella MA. Elk-3 is a KLF4-regulated gene that modulates the phagocytosis of bacteria by macrophages. *J Leukoc Biol.* (2015) 97:171–80. doi: 10.1189/jlb.4A0214-087R
67. Modde F, Agustian PA, Wittig J, Dämmrich ME, Forstmeier V, Vester U, et al. Comprehensive analysis of glomerular mRNA expression of pro- and antithrombotic genes in atypical haemolytic-uremic syndrome (aHUS). *Virchows Arch Int J Pathol.* (2013) 462:455–64. doi: 10.1007/s00428-013-1386-4
68. Belcher JD, Chen C, Nguyen J, Abdulla F, Zhang P, Nguyen H, et al. Haptoglobin and hemopexin inhibit vaso-occlusion and inflammation in murine sickle cell disease: Role of heme oxygenase-1 induction. *PLoS ONE* (2018) 13:e0196455. doi: 10.1371/journal.pone.0196455
69. Schaer DJ, Buehler PW, Alayash AI, Belcher JD, Vercellotti GM. Hemolysis and free hemoglobin revisited: exploring hemoglobin and hemin scavengers as a novel class of therapeutic proteins. *Blood* (2013) 121:1276–84. doi: 10.1182/blood-2012-11-451229

Conflict of Interest Statement: The authors declare that the research was conducted in the absence of any commercial or financial relationships that could be construed as a potential conflict of interest.

AJKD
Original Investigation

Renal Cortical Necrosis in Postpartum Hemorrhage: A Case Series

Marie Frimat, MD, PhD,[1,*] Melanie Decambron, MD,[2,*] Celine Lebas, MD,[3] Anissa Moktefi, MD,[4] Laurent Lemaitre, MD, PhD,[5] Viviane Gnemmi, MD, PhD,[6] Benedicte Sautenet, MD,[7] François Glowacki, MD, PhD,[1] Damien Subtil, MD, PhD,[8] Mercedes Jourdain, MD, PhD,[9] Agnes Rigouzzo, MD,[10] Isabelle Brocheriou, MD, PhD,[4] Jean-Michel Halimi, MD, PhD,[7] Eric Rondeau, MD, PhD,[11] Christian Noel, MD, PhD,[1] François Provôt, MD,[1] and Alexandre Hertig, MD, PhD[11]

Background: Pregnancy-related renal cortical necrosis may lead to end-stage renal disease. Although this obstetric complication had virtually disappeared in high-income countries, we have noted new cases in France over the past few years, all following postpartum hemorrhage.

Study Design: Case series.

Setting & Participants: We retrospectively identified 18 patients from 5 French nephrology departments who developed renal cortical necrosis following postpartum hemorrhage in 2009 to 2013.

Outcomes: Obstetric and renal features, therapeutic measures, and kidney disease outcome were studied.

Results: All patients had a severe postpartum hemorrhage (mean blood loss, 2.6 ± 1.1 [SD] L). Hemodynamic instability and disseminated intravascular coagulation were reported in 5 and 11 patients, respectively. All developed rapid onset of acute kidney injury and required hemodialysis. Diagnosis of renal cortical necrosis was performed 4 to 33 days following delivery. At 6 months postpartum, 8 patients remained dialysis dependent and none recovered normal kidney function. The length of exposure to tranexamic acid treatment was significantly more prolonged in women whose estimated glomerular filtration rate remained <15 mL/min/1.73 m^2 (7.1 ± 4.8 vs 2.9 ± 2.4 hours; $P = 0.03$).

Limitations: Retrospective study; small sample size.

Conclusions: In the setting of gravid endothelium, the conjunction of disseminated intravascular coagulation with the life-saving use of procoagulant and antifibrinolytic agents (recently implemented in France in a postpartum hemorrhage treatment algorithm) may give rise to a risk for uncontrolled clotting in the renal cortex and hence irreversible partial or diffuse cortical necrosis.

Am J Kidney Dis. 68(1):50-57. © *2016 by the National Kidney Foundation, Inc.*

INDEX WORDS: Renal cortical necrosis; postpartum hemorrhage; pregnancy; obstetric complication; acute kidney injury (AKI); tranexamic acid (TXA); TXA dosage; antifibrinolytic; end-stage renal disease (ESRD); France.

Pregnancy-related acute kidney injury (AKI) is a rare complication in high-income countries, with an estimated incidence from 1.5 to 4.5 per 10,000 deliveries.[1,2] Except for women with preexisting hypertension or chronic kidney disease, the long-term outcome of pregnancy-related AKI is usually favorable unless renal cortical necrosis (RCN) occurs.[3-5] RCN is defined as ischemic destruction of the renal cortex secondary to a prolonged decrease in renal arterial perfusion (vascular spasm, microvascular injury, or intravascular coagulation).[6] Obstetric RCN is especially associated with massive hemorrhage due to placenta previa, abruptio placentae, postpartum hemorrhage (PPH), or other severe complications such as amniotic fluid embolism and septic abortions.[7,8]

The incidence of pregnancy-related RCN is declining in developing countries, but it remains relatively high (5.2% and 30% of pregnancy-related AKI in Eastern India[9] and Pakistan,[10] respectively).

From the [1]Service de Néphrologie, Hôpital Claude Huriez, CHU Lille, Université de Lille, Lille; [2]Service de Néphrologie, Hôpital Victor Provo, Roubaix; [3]Service de Néphrologie, CH Valenciennes, Valenciennes; [4]Service d'Anatomie Pathologique, APHP, Hôpital Tenon, Paris; [5]Service de Radiologie, Hôpital Claude Huriez, CHU Lille, Université de Lille; [6]Centre de Biologie et Pathologie, CHU Lille, Université de Lille, Lille; [7]Service de Néphrologie, CHU Tours, Tours; [8]Pôle Femme Mère Nouveau-Né, Hôpital Jeanne de Flandre, EA 2694, PRES Université Lille Nord de France; [9]Pôle de Réanimation, CHU Lille, Université de Lille, Lille; [10]Anesthésie-Réanimation, APHP, Hôpital Trousseau; and [11]APHP, Hôpital Tenon, Urgences Néphrologiques et Transplantation Rénale, Paris, France.

[*]M.F. and M.D. contributed equally to this work.

Received June 4, 2015. Accepted in revised form November 29, 2015. Originally published online January 16, 2016.

Address correspondence to Marie Frimat, MD, PhD, Nephrology and Transplantation Department, Claude Huriez Hospital, CHU Lille, 2 avenue Oscar Lambret, Lille, France. E-mail: marie.frimat@chru-lille.fr

0272-6386
http://dx.doi.org/10.1053/j.ajkd.2015.11.022

However, in high-income countries, there are no recent reports of obstetric RCN, suggesting that this syndrome has virtually disappeared. In France, where most cases were triggered by puerperal sepsis due to *Clostridium perfringens*, the adoption in 1975 of the Veil Law authorizing abortion more or less eradicated this syndrome. Hence, the report of several cases of pregnancy-related RCN in Northern France during the past few years was noteworthy. In the Nord-Pas de Calais area (4 million inhabitants), only 2 cases of RCN were noted in 1988 to 2008, as opposed to 9 cases in 2009 to 2013, all of which occurred in the aftermath of PPH. This observation prompted us to study French cases of RCN following PPH, with the aim of describing these new events and highlighting the potential factors for inferior kidney disease outcome.

METHODS

Patients and Definitions

This is a retrospective series of 18 French adult cases of obstetric RCN from January 2009 to December 2013. Patient charts were obtained with help from the French Society of Nephrology by a call for clinical cases, and this study was approved by the relevant institutional ethics committee. Patients were included after informed consent according to the following criteria: (1) diffuse or patchy RCN, (2) subsequent PPH (estimated blood loss $>$ 500 mL following vaginal birth or $>$ 1,000 mL after caesarean section), and (3) requiring hemodialysis for 7 or more days.

Diagnosis of RCN was performed either by kidney biopsy or functional imaging, such as magnetic resonance imaging (MRI), contrast-enhanced ultrasonography (CEUS), or contrast-enhanced computed tomography (CECT). No signal intensity in T2- and gadolinium-enhanced T1-weighted MRI[11] or the lack of enhancement in CEUS[12] and CECT[13] within the cortex of both kidneys was considered as RCN. A central review (L.L.) of 12 MRIs was performed to characterize the lesions as diffuse or patchy: a continuous lack of enhancement along the renal cortex was defined as a diffuse RCN, whereas it was considered as patchy if lesions were discontinuous or limited to only part of the kidney. Gestational hypertension, proteinuria, and preeclampsia were defined as previously described.[14] Hemodynamic instability was defined as arterial systolic blood pressure $<$ 90 mm Hg and/or use of vasopressor therapies. Hemolysis was defined as the simultaneous measure of haptoglobin level $<$ 0.3 g/L and lactate dehydrogenase level $>$ 500 UI/L. Hepatic cytolysis was characterized by liver test results (serum aspartate and/or alanine aminotransferase) that were greater than 3 times the standard. Disseminated intravascular coagulation (DIC) was defined as a high D-dimer level associated with 1 major criterion (thrombocytopenia $<$ 50 g/L or prothrombin time $<$ 50%) or 2 minor criteria (platelet count ranging from 50-100 $\times 10^9$/L and/or prothrombin time from 50%-100% and/or fibrinogen $<$ 1 g/L). Oliguria and anuria were defined as urinary volume $\leq$ 500 or $\leq$ 50 mL/d, respectively. From 3 months postpartum, kidney function was evaluated by estimated glomerular filtration rate using the 4-variable MDRD (Modification of Diet in Renal Disease) Study equation.

Statistical Analysis

Quantitative variables were expressed as mean $\pm$ standard deviation, and qualitative variables were expressed as percentage. The normal distribution of quantitative variables was analyzed using Shapiro-Wilk test. Characteristics of patients who recovered partial kidney function (estimated glomerular filtration rate $\geq$ 15 mL/min/1.73 m^2 at 6 months postpartum) were compared with those of patients who did not by χ^2 or Fisher exact test for qualitative variables and *t* test or Mann-Whitney test for quantitative variables, as appropriate. Results were considered statistically significant for $P < 0.05$. All analyses were conducted using SPSS, version 15.0, statistical software (IBM).

RESULTS

Demographic and Obstetric Data

The main features of the 18 patients with RCN are detailed in Table 1. Mean age at diagnosis was 33.4 (range, 27-40) years. Eleven (61%) patients were primiparous and 7 (39%) had a twin pregnancy. The relevant previous obstetric histories were preeclampsia in patient 4 (P4) and P10 and 3 miscarriages in P17. None of the patients was known to have a nephropathy or other significant disease, except for P10 and P12, who had uncomplicated type 1 diabetes and factor XI deficiency, respectively. Gestational hypertension without proteinuria had occurred in 4 patients (P1, P2, P10, and P12), of whom 2 had required treatment.

Mean pregnancy term was 37.2 weeks. Labor was induced in 12 (67%) patients because of term pregnancy (n = 4), technical reasons (twin pregnancy or macrosomia; n = 3), or maternal rescue (sepsis due to chorioamnionitis, preeclampsia, or HELLP [hemolysis, elevated liver enzymes, low platelet count] syndrome; n = 5). A caesarean section was performed in 10 (56%) patients owing to unsuccessful vaginal delivery in 8 of them. All deliveries were complicated by severe PPH (blood loss $>$ 1,000 mL) mainly due to uterine atony (83%) or caused by DIC (P4), abruptio placentae (P12), and amniotic fluid embolism (P13) in the remaining cases. Average blood loss was 2.6 L $\pm$ 1.1 L. At admission to the intensive care unit (ICU), all patients had thrombocytopenia and 11 (61%) had DIC. Hemolysis and hepatic cytolysis were noted in 8 of 15 (53%) and 10 of 18 (56%) patients, respectively. These abnormalities followed delivery, except in P10, who had HELLP syndrome. Thrombocytopenia and hemolysis regressed spontaneously in 2 to 13 days.

With regard to the PPH treatment, mean volume of packed red blood cells was 1.45 $\pm$ 0.9 L and mean volume of resuscitation fluid was 3.4 $\pm$ 1.3 L as colloid solution (1.8 $\pm$ 1.4 L) and/or crystalloid solution (1.6 $\pm$ 1.2 L). Fibrinogen concentrates were given to 15 patients (mean, 5.4 $\pm$ 2 g). All patients received a loading dose of tranexamic acid (TXA) of 1 to 4 (mean, 1.8 $\pm$ 0.9) g, followed in 16 patients by a "maintenance dose" ranging from 0.5 to 1 g/h over 2 to 16 (mean, 5 $\pm$ 4.3) hours. Mean cumulative TXA dose varied from 2 to 11 (mean, 5.3 $\pm$ 2.8) g. In addition, 15 (83%)

Table 1. Characteristics of the 18 Patients

	1	2	3	4	5	6	7	8	9	10	11	12	13	14	15	16	17	18
Clinical features																		
Age, y	32	32	31	38	29	30	39	27	35	29	34	35	39	28	34	36	40	33
Gestational age, wk[a]	37	36	38	18	38	41	41	37	38	37	39	33	41	37	41	41	38	38
Peripartum data																		
Pregnancy disorders	PE	PE	—	Sepsis	—	—	—	—	—	HELLP	—	PE	—	—	—	—	—	—
Blood loss, L	3	1.7	1.9	1.3	2.6	1.5	2.1	4.2	1.7	2.6	2.2	1.8	2.5	3.5	2.1	1.9	5.6	4.6
Hemodynamic instability	−	−	−	+	−	−	−	+	−	−	−	−	+	+	−	+	−	−
First 24-h urinary volume, L	0.2	0.25	0	0.15	0.3	1.3	0.03	0.5	0.2	0.25	0.3	0.5	0.1	0	0.15	0.1	0	0.03
Laboratory data on ICU admission																		
Creatinine, mg/dL	1.9	2.6	3.7	2.5	1.4	2.9	2	1.5	2	3.2	4.1	1.9	1.8	1.9	2.1	1.9	3.3	1
Hemoglobin, g/dL	9.5	8.5	6.2	8.9	10.5	8.8	8.7	7.3	7.7	8.9	8.3	9.9	10.5	7.4	7.6	9.2	6.7	9.3
Haptoglobin, g/L	<0.07	<0.07	0.72	NA	0.31	1.28	<0.1	<0.07	0.55	<0.07	0.1	2.83	<0.2	0.08	0.37	1.31	<0.07	<0.07
LDH, UI/L	2,256	1,856	1,784	4,076	3,526	4,346	NA	2,318	2,125	4,726	3,222	659	NA	1,593	2,284	1,570	2,152	1,324
Platelet count, $\times 10^9$/L	39	23	93	48	53	43	75	30	51	58	86	63	79	79	55	37	58	57
Hepatic cytolysis	−	+	+	+	−	+	−	−	+	+	+	−	−	+	−	+	+	−
DIC	+	+	+	+	−	+	−	+	−	+	+	−	+	+	+	−	−	−
Postpartum hemorrhage treatment																		
Tranexamic acid treatment																		
Loading dose, g	4	2	1	2	2	4	2	2	1	1	2	1.5	1	1	1	1	2[b]	2.5[b]
Maintenance dose, g/h	1	0.5	1	0.5	1	1	1	0.5	0.5	0.5	0.5	0.5	0.5	1	1	1	0	0
Exposure duration, h	7	4	5	16	2	3	8	2	14	2	6	3	7	4	3	4	0	0
Other treatments																		
Red blood cells, L	2.1	0.9	0	1.2	1.5	1.2	1.2	2.1	0.6	1.2	0.9	0	2.4	1.5	2.1	3.6	1.8	1.8
Crystalloid, L	0	1	3	1.5	1.5	0	1	0	4	2	1.5	1	0.5	4	1	2.5	2.5	2.5
Colloid, L	2	2	1	2	4.5	5	2	3.5	1	1.5	3	0	1	0	1	1	1.5	0
Fibrinogen, g	9	6	3	6	6	4.5	3	7.5	4.5	6	0	0	9	6	0	3	4.5	3
Invasive procedures	L	−	−	H	L	EA	−	H	−	−	−	−	L	L/H	L/H	EA	L	L
RCN characteristics																		
Diagnostic tool used	MRI	MRI/B	MRI	MRI	MRI	MRI	CECT	MRI	MRI	MRI	MRI/B	MRI	MRI/B	MRI	MRI/B	B	CEUS/B	CEUS
Type	D	D	D	D	P	P	P	NA	NA	D	D	D	D	D	D		D	P
Kidney disease outcome																		
Follow-up, mo	36	28	22	34	36	28	55	27	21	12	12	26	16	14	36	21	12	12
Hemodialysis vintage, d	210	62	NR	NR	NR	7	66	23	NR	17	120	NR	NR	NR	60	13	46	19
eGFR at 6 mo postpartum	DD	22	DD	DD	DD	38	25	43	DD	48	12	DD	DD	DD	38	47	22	52
eGFR at last report	24	35	ESRD	ESRD	ESRD	51	46	70	ESRD	45	18	ESRD	ESRD	ESRD	46	45	49	74

Note: eGFRs expressed in mL/min/1.73 m^2. Conversion factor for serum creatinine in mg/dL to μmol/L, ×88.4.

Abbreviations: B, kidney biopsy; CECT, contrast-enhanced computed tomography; CEUS, contrast-enhanced ultrasonography; D, diffuse; DD, dialysis dependence; DIC, disseminated intravascular coagulation; EA, uterine artery embolization; eGFR, estimated glomerular filtration rate; ESRD, end-stage renal disease; H, hysterectomy; HELLP, hemolysis, elevated liver enzymes, low platelet count; ICU, intensive care unit; L, uterine artery ligation; LDH, lactate dehydrogenase; MRI, magnetic resonance imaging; NA, not available; NR, no recuperation; P, patchy; PE, preeclampsia; RCN, renal cortical necrosis.

[a]Weeks of amenorrhea.

[b]Loading dose administered twice at an interval of 30 minutes.

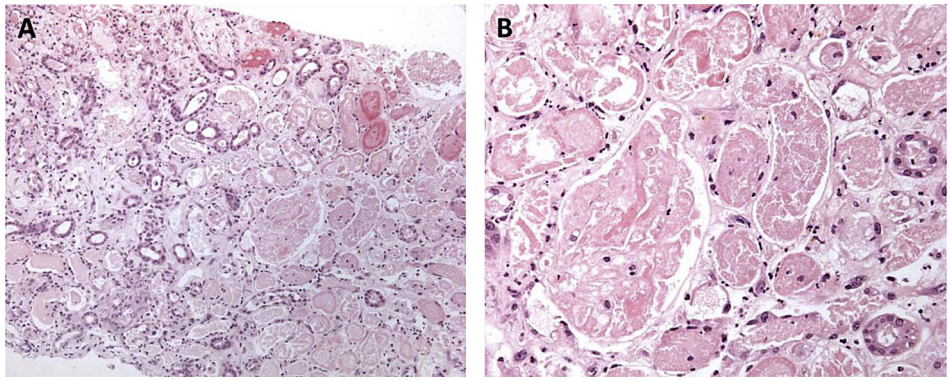

Figure 1. Histologic analysis of right kidney biopsy performed in patient 2 (13 days after postpartum hemorrhage). (A) Kidney biopsy specimen shows (right) deep cortical extensive necrosis, whereas the superficial cortex is spared from renal cortical necrosis (hematoxylin-eosin-saffron; original magnification, ×100). (B) An area of coagulation necrosis shows ghost outlines of tubules and glomeruli. Fibrin material is visible within the glomerular capillary lumina (hematoxylin-eosin-saffron; original magnification, ×200).

patients were treated with uterotonics and invasive procedures were required in 11 cases (61%), including 2 uterine artery embolizations, 5 uterine artery ligations, and 4 hysterectomies.

Renal Features

All patients were admitted to the ICU with AKI. Anuria and oliguria were reported in 7 (39%) and 10 (56%) of these patients, respectively. One patient (P6) had preserved urinary output of 1.3 L/d, but a serum creatinine level increase to 2.9 mg/dL. Mean serum creatinine level was 2.3 (range, 1-4.1) mg/dL. In addition to hypovolemia due to massive hemorrhage, other potential causes of AKI were identified: hemodynamic instability in 5 patients, of whom 2 had a superimposed amniotic fluid embolism (P13) or septic shock (P4), and vasopressor therapy was necessary in 2 of the 5 patients (P4 and P8); use of iodinated contrast medium in 8 patients; nonsteroidal anti-inflammatory drugs administered in the first 24 hours (P11). Hemodialysis was required for all patients, 11 of whom (61%) received this treatment in the first 24 hours because of persistent anuria with or without fluid overload.

In the setting of severe and persistent kidney failure, RCN was diagnosed 4 to 33 days postdelivery. Diagnosis was made via kidney biopsy in 6 (33%) patients. All had diffuse ischemic necrosis (>50%), and thrombosis of arterioles and/or glomerular capillaries was reported in 5 patients. In addition to necrosis of the cortical parenchyma, 1 patient (P2) also had identifiable lesions of fibrinoid necrosis in all arteriolar sections. Five of the 6 patients had compatible morphologic features on CEUS (n = 1) or MRI (n = 4), including patient P2, whose histologic and radiologic features are shown in Figs 1 and 2. In all other cases, RCN was diagnosed by MRI (n = 10), CEUS (n = 1), or CECT (n = 1) only. From a radiologic perspective, lesions were described as diffuse in 11 of 15 (73%) patients.

Kidney Disease Outcome

None of the patients had recovered normal kidney function at last follow-up (12-55 months); 11 were at CKD stage 2 (n = 2 [11%]), 3 (n = 7 [39%]), or 4 (n = 2 [11%]), and 7 (39%) had end-stage renal disease (ESRD). No significant difference was observed in terms of obstetric characteristics or clinical and biological features at ICU admission between women with estimated glomerular filtration rates < 15 mL/min/1.73 m^2 at 6 months postpartum and others. In particular, blood loss volume, hemodynamic parameters, hemoglobin level, DIC, and hemolysis features were similar between the groups (Table 2). Although RCN was more frequently characterized as diffuse (7 of 8 [88%] vs 4 of 7 [57%]), the difference was not statistically significant. One difference emerged relative to PPH management: in the lower eGFR group, the duration of the TXA maintenance dose was statistically longer (7.1 ± 4.8 vs 2.9 ± 2.4 hours; $P = 0.03$); mean loading and cumulative doses were similar (Table 2).

DISCUSSION

Although RCN has virtually disappeared in high-income countries, this report describes 18 cases that occurred recently in France, all in the aftermath of PPH. In addition to describing these new cases of obstetric RCN, this work brings to light the possible factors for poor kidney disease outcome.

Diagnosis of RCN was based on either gold-standard imaging (given their excellent contrast resolution without the toxicity of iodinated contrast, both the MRI and CEUS examinations are currently preferred[11,12,15]) or histologic findings from kidney biopsy samples. No discrepancy was noted in the 5 women who had both kidney biopsy and MRI or

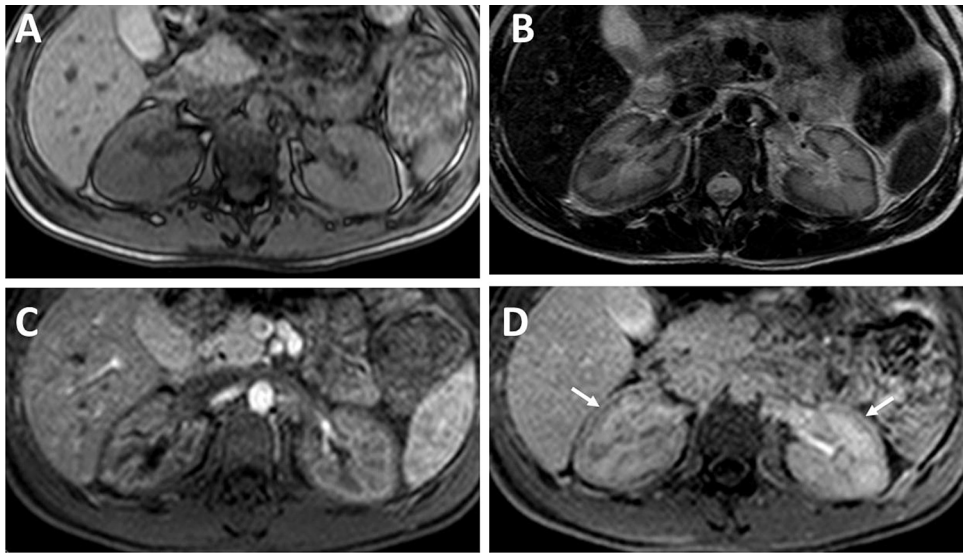

Figure 2. Magnetic resonance images of patient 2 (14 days after postpartum hemorrhage). (A) Axial T1-weighted image at the level of the left renal artery. (B) Axial T2-weighted image shows bilateral and diffuse cortical hypointensity. (C, D) Axial gadolinium-enhanced T1-weighted images at the (C) arterial phase and (D) excretory phase show a bilateral lack of cortical enhancement involving the inner cortex. At the later phase, capsular rim intensity is visible (arrows). Vascular opacification of the left kidney persists, which could explain the secondary partial renal recovery in this patient.

CEUS, suggesting that these procedures are similarly helpful in the diagnosis of RCN. However, imaging examinations are superior in establishing the diffuse or patchy nature of RCN lesions and may provide prognostic information.[15] Here, diffuse lesions were frequent among the patients with the worst kidney disease outcome, but they were not systematically associated with progression to ESRD, as shown by the outcome of 4 patients (P2, P10, P15, and P17). It is possible that early imaging examinations overestimate the extent of renal lesions, by analogy with myocardial stunning in ischemic cardiac disease. The best time at which to assess the prognosis of RCN using imaging techniques thus remains to be determined.

Unsurprisingly, the outcome of obstetric RCN appears poor. None of the patients recovered normal kidney function, and more than one-third (39%) eventually progressed to ESRD. This unfavorable outcome is consistent with recent reports, which describe the rate of progression to ESRD as 30% to 50% of all RCN.[9,16] Regarding the initial presentation, our patients shared several features: major blood loss (average, 2.6 L), oligoanuria (94%) indicating severe hypovolemia, and frequent DIC (61%) and/or hemolysis (53%), both suggesting an imbalance of endothelial homeostasis. Combined with the well-known pregnancy-related hypercoagulability state,[17] these factors might all have contributed to small renal artery constriction or obstruction and so facilitated the occurrence of RCN. Our study also questions the possible role of TXA. Prolonged exposure to this drug was associated here with poorer kidney disease outcome, whereas none of the other factors studied (blood loss volume, hemodynamic instability, DIC, and nephrotoxic exposition) appeared to increase the risk for severe RCN. A synthetic analogue of lysine, TXA inhibits the conversion of plasminogen to active plasmin, the enzyme responsible for fibrinolysis. This antifibrinolytic drug is widely prescribed to prevent or reduce blood loss in various surgical procedures (cardiac surgery,[18] for trauma patients,[19] and for combat injuries[20]), and its prophylactic use has also been proposed for preventing PPH without inducing AKI or thromboembolic events.[21,22] Only one randomized controlled trial has studied the use of TXA to treat PPH, and it did not report an increase of renal events at the 6-hour point (EXADELI [EXAcyl in the treatment of DELIvery haemorrhage] study).[23] Although some case reports have suggested an association between TXA treatment and RCN,[24,25] several studies observed no specific risk for kidney injury.

However, our patients differed from those in the main studies. The length of exposure to TXA was prolonged here, whereas there is generally no maintenance dose in most trials. Second, the initial presentation of our patients was obviously more severe: blood loss was 2.6 L on average, PPH management required a transfer to the ICU for 100% of patients, and mean resuscitation fluid volume was 3.4 L compared to 5% and ~1.5 L in the EXADELI study. Antepartum or early postpartum complications were also frequent (preeclampsia/HELLP

Table 2. Clinical Parameters and Management According to eGFR at 6 Months Postpartum

	eGFR < 15 (n = 9)	eGFR ≥ 15 (n = 9)	*P*
Obstetric parameters			
Age, y	33.4 ± 3.8	33.3 ± 4.4	0.9
BMI, kg/m^2	25.4 ± 3.6	23.2 ± 3.0	0.2
Twin pregnancy	4/9 (44.4)	3/9 (33.3)	0.5
Gestational hypertension	2/9 (22.2)	2/9 (22.2)	0.7
Gestational age, wk[a]	35.4 ± 6.9	38.9 ± 2.1	0.3
Predelivery disorders	3/9 (33.3)	2/9 (22.2)	0.5
Induction of labor	6/9 (66.7)	6/9 (66.7)	0.7
Cesarean delivery	3/9 (33.3)	7/9 (77.8)	0.08
Uterine atony	6/9 (66.7)	9/9 (100)	0.1
Blood loss, L	2.3 ± 0.7	2.9 ± 1.5	0.6
Hemodynamic instability	3/9 (33.3)	2/9 (22.2)	0.5
Biology			
Hemoglobin, g/dL	8.8 ± 1.5	8.3 ± 0.9	0.5
LDH, UI/L	2,405 ± 1,128	2,572 ± 1,264	0.8
Platelet count, ×10^9/L	65.7 ± 19.1	48.4 ± 16.4	0.06
Hemolysis	3/7 (42.8)	5/8 (62.5)	0.6
PT, %	56 ± 24	64 ± 19	0.4
Hepatic cytolysis	5/9 (55.6)	5/9 (55.6)	0.7
DIC	6/9 (66.7)	5/9 (55.6)	0.5
Renal presentation			
First 24-h urinary volume, mL	114 ± 105	290 ± 409	0.4
Anuria	4/9 (44.4)	3/9 (33.3)	0.5
Early hemodialysis	5/9 (55.6)	6/9 (66.7)	0.5
Creatinine, mg/dL	2.36 ± 0.9	2.28 ± 0.8	0.9
Diffuse cortical necrosis	7/8 (87.5)	4/7 (57.1)	0.3
Therapeutics			
Red blood cells, L	1.13 ± 0.8	1.77 ± 0.8	0.1
Crystalloid loading, L	1.9 ± 1.5	1.4 ± 1	0.4
Colloid loading, L	1.6 ± 1.5	1.9 ± 1.5	0.6
Total loading volume, L	3.5 ± 1.7	3.3 ± 0.9	0.8
Uterotonics	8/9 (88.9)	7/9 (77.8)	0.5
Invasive procedure	5/9 (55.6)	6/9 (66.7)	0.5
Iodinated contrast medium exposure	4/9 (44.4)	4/9 (44.4)	0.7
Fibrinogen, g	4.8 ± 3.3	4.2 ± 2.2	0.6
Tranexamic acid			
Loading dose, g	1.7 ± 1	1.9 ± 0.9	0.5
Cumulative dose, g	6.3 ± 2.8	4.4 ± 2.6	0.2
Treatment duration, h	7.1 ± 4.8	2.9 ± 2.4	0.03

Note: Values for categorical variables are given as number (percentage); for continuous variables, as mean ± standard deviation. eGFRs expressed in mL/min/1.73 m^2. Conversion factor for serum creatinine in mg/dL to μmol/L, ×88.4.

Abbreviations: BMI, body mass index; DIC, disseminated intravascular coagulation; eGFR, estimated glomerular filtration rate; LDH, lactate dehydrogenase; PT, prothrombin time.

[a]Weeks of amenorrhea.

syndrome and hemodynamic instability in 4 and 5 patients, respectively) and more than half developed DIC. In addition, all patients had AKI, suggested by the presence of oligoanuria and/or serum creatinine level increase. Because intravenous TXA is entirely eliminated by glomerular filtration, it accumulates if kidney function deteriorates: the half-life of the drug is thus increased 9-fold, from about 2 hours in healthy individuals to more than 18 hours in patients with serum creatinine levels > 5.6 mg/dL (>500 μmol/L).[26] The severity of RCN lesions depends on the duration of the cortical ischemia.[6] An overly prolonged inhibition of fibrinolysis might be deleterious in a setting that combines several factors threatening the endothelium: severe hypovolemia due to massive hemorrhage, concomitant use of fibrinogen concentrates, DIC, and the complex pregnancy-related coagulopathy. We should keep in mind that a gravid endothelium is particularly susceptible, as shown by Apitz,[27] who demonstrated that a single injection of endotoxin was sufficient to drive a Shwartzman reaction in kidneys from pregnant rabbits. In another experimental work studying glomerular fibrinolytic activity in the rat, the simultaneous

administration of thrombin and an antifibrinolytic (aminocaproic acid) was associated with persistent thrombi, presumably due to inhibition of the action of plasmin on fibrin.[28]

The rate of PPH has increased in the past 2 decades in several high-income countries, where it remains a major cause of maternal mortality (13% of maternal deaths).[29] This temporal increase seems associated with the increase in uterine atony.[30,31] Although the reasons for this are unclear, the roles of labor augmentation and prior caesarean section have been discussed.[32] Currently, TXA is the only available antifibrinolytic drug in clinical practice, and its early administration for treating PPH resistant to uterotonics has been recently recommended by an international expert panel.[33] Our aim is not to dispute these life-saving recommendations. Our observations simply highlight the possible effect of prolonged exposure in the setting of severe PPH and kidney failure and suggest that patients receiving a maintenance dose of TXA should be carefully monitored. The WOMAN (World Maternal Antifibrinolytic) trial should provide additional information. This international randomized trial, which plans to recruit 15,000 women, will investigate the impact of TXA administration in women with clinically diagnosed PPH.[34] Notably, in this trial, the maximum dose will be 2 g, corresponding to the dose range that has been shown to inhibit fibrinolysis and provide hemostatic benefit.[35]

ACKNOWLEDGEMENTS

We thank Carine Arlicot, Bernard Bailleux, Amaury Ben Henda, Serge Biausque, Marie Isabelle Bornes, Jean Luc Chagnon, Emmanuel Closset, Capucine Coulon, Morgane Commereuc, Christelle Denis, Pierre-François Dequin, Philippe Deruelle, Ahmed Hasib, Anais Ladaique, Corinne Lemoine, Fabrice Massoni, Emmanuelle Mercier, Eric Moxhon, Nathalie Perrotin, Jerome Phalippou, Patrick Thiriot, Nadia Tillouche, Laurent Tronchon, Anne Sylvie Valat, and Laurence Vrigneaud, who provided us with clinical data for the disease course of the patients; Eileen Boyle and Felicity Kay (professional proofreader) for English language proofreading; and Maite Daroux and Arnaud Lionet for the fruitful discussions.

Support: None.

Financial Disclosure: The authors declare that they have no relevant financial interests.

Contributions: Research idea and study design: MF, MD, FP, AH; providing of clinical information: CL, BS, FG, DS, MJ, AR, J-MH, ER, CN; data acquisition: MF, MD, CL; data analysis/interpretation: MF, FG, FP, AH, LL (imaging data), AM, VG, IB (histological data); statistical analysis: MF, FG; supervision or mentorship: FP, AH (who co-directed this study). Each author contributed important intellectual content during manuscript drafting or revision and accepts accountability for the overall work by ensuring that questions pertaining to the accuracy or integrity of any portion of the work are appropriately investigated and resolved. MF takes responsibility for ensuring that this study has been reported honestly, accurately, and transparently; that no important aspects of the study have been omitted; and that any discrepancies from the study as planned have been explained.

Peer Review: Evaluated by a 2 external peer reviewers, a pathologist, a Co-Editor, and the Editor-in-Chief.

REFERENCES

1. Callaghan WM, Creanga AA, Kuklina EV. Severe maternal morbidity among delivery and postpartum hospitalizations in the United States. *Obstet Gynecol*. 2012;120(5):1029-1036.

2. Mehrabadi A, Liu S, Bartholomew S, et al. Hypertensive disorders of pregnancy and the recent increase in obstetric acute renal failure in Canada: population based retrospective cohort study. *BMJ*. 2014;349:g4731.

3. Bouaziz M, Chaari A, Turki O, et al. Acute renal failure and pregnancy: a seventeen-year experience of a Tunisian intensive care unit. *Ren Fail*. 2013;35(9):1210-1215.

4. Gurrieri C, Garovic VD, Gullo A, et al. Kidney injury during pregnancy: associated comorbid conditions and outcomes. *Arch Gynecol Obstet*. 2012;286(3):567-573.

5. Fakhouri F, Vercel C, Fremeaux-Bacchi V. Obstetric nephrology: AKI and thrombotic microangiopathies in pregnancy. *Clin J Am Soc Nephrol*. 2012;7(12):2100-2106.

6. László FA. Renal cortical necrosis. Experimental induction by hormones. *Contrib Nephrol*. 1981;28:1-216.

7. Grünfeld JP, Ganeval D, Bournérias F. Acute renal failure in pregnancy. *Kidney Int*. 1980;18(2):179-191.

8. Kim HJ. Bilateral renal cortical necrosis with the changes in clinical features over the past 15 years (1980-1995). *J Korean Med Sci*. 1995;10(2):132-141.

9. Prakash J, Vohra R, Wani IA, et al. Decreasing incidence of renal cortical necrosis in patients with acute renal failure in developing countries: a single-centre experience of 22 years from Eastern India. *Nephrol Dial Transplant*. 2007;22(4):1213-1217.

10. Ali A, Ali MA, Ali MU, Mohammad S. Hospital outcomes of obstetrical-related acute renal failure in a tertiary care teaching hospital. *Ren Fail*. 2011;33(3):285-290.

11. Jeong JY, Kim SH, Sim JS, et al. MR findings of renal cortical necrosis. *J Comput Assist Tomogr*. 2002;26(2):232-236.

12. McKay H, Ducharlet K, Temple F, Sutherland T. Contrast enhanced ultrasound (CEUS) in the diagnosis of post-partum bilateral renal cortical necrosis: a case report and review of the literature. *Abdom Imaging*. 2014;39(3):550-553.

13. Catalano OA, Napolitano M, Leni D, Ticca C, Vanzulli A. Contrast enhanced computer tomography of two cases of bilateral acute cortical necrosis, one of which related to amphetamine abuse. *Emerg Radiol*. 2005;11(5):306-308.

14. Chaiworapongsa T, Chaemsaithong P, Yeo L, Romero R. Pre-eclampsia part 1: current understanding of its pathophysiology. *Nat Rev Nephrol*. 2014;10(8):466-480.

15. François M, Tostivint I, Mercadal L, Bellin MF, Izzedine H, Deray G. MR imaging features of acute bilateral renal cortical necrosis. *Am J Kidney Dis*. 2000;35(4):745-748.

16. Sahay M, Swarnalata Swain M, Padua M. Renal cortical necrosis in tropics. *Saudi J Kidney Dis Transplant*. 2013;24(4):725-730.

17. Hellgren M. Hemostasis during normal pregnancy and puerperium. *Semin Thromb Hemost*. 2003;29(2):125-130.

18. Fergusson DA, Hébert PC, Mazer CD, et al. A comparison of aprotinin and lysine analogues in high-risk cardiac surgery. *N Engl J Med*. 2008;358(22):2319-2331.

19. Shakur H, Roberts I, Bautista R. Effects of tranexamic acid on death, vascular occlusive events, and blood transfusion in trauma patients with significant haemorrhage (CRASH-2): a randomised, placebo-controlled trial. *Lancet*. 2010;376(9734):23-32.

20. Morrison JJ, Dubose JJ, Rasmussen TE, Midwinter MJ. Military Application of Tranexamic Acid in Trauma Emergency Resuscitation (MATTERs) Study. *Arch Surg*. 2012;147(2):113-119.

21. Ferrer P, Roberts I, Sydenham E, Blackhall K, Shakur H. Anti-fibrinolytic agents in post partum haemorrhage: a systematic review. *BMC Pregnancy Childbirth*. 2009;9(1):29.

22. Peitsidis P, Kadir RA. Antifibrinolytic therapy with tranexamic acid in pregnancy and postpartum. *Expert Opin Pharmacother*. 2011;12(4):503-516.

23. Ducloy-Bouthors A-S, Jude B, Duhamel A, et al. High-dose tranexamic acid reduces blood loss in postpartum haemorrhage. *Crit Care*. 2011;15(2):R117.

24. Koo JR, Lee YK, Kim YS, Cho WY, Kim HK, Won NH. Acute renal cortical necrosis caused by an antifibrinolytic drug (tranexamic acid). *Nephrol Dial Transplant*. 1999;14(3):750-752.

25. Odabaş AR, Cetinkaya R, Selçuk Y, Kaya H, Coşkun U. Tranexamic-acid-induced acute renal cortical necrosis in a patient with haemophilia A. *Nephrol Dial Transplant*. 2001;16(1):189-190.

26. Andersson L, Eriksson O, Hedlund PO, Kjellman H, Lindqvist B. Special considerations with regard to the dosage of tranexamic acid in patients with chronic renal diseases. *Urol Res*. 1978;6(2):83-88.

27. Apitz K. Die Wirkung bakterieller Kulturfiltrate nach Umstimmung des gesamten Endothels beim Kaninchen. *Virchows Arch Pathol Anat Physiol Klin Med*. 1934;293(1):1-33.

28. Sraer JD, Delarue F, Dard S, De Seigneux R, Morel-Maroger L, Kanfer A. Glomerular fibrinolytic activity after thrombin perfusion in the rat. *Lab Invest*. 1975;32(4):515-517.

29. Khan KS, Wojdyla D, Say L, Gülmezoglu AM, Van Look PFA. WHO analysis of causes of maternal death: a systematic review. *Lancet*. 2006;367(9516):1066-1074.

30. Dupont C, Occelli P, Deneux-Tharaux C, et al. Severe postpartum haemorrhage after vaginal delivery: a statistical process control chart to report seven years of continuous quality improvement. *Eur J Obstet Gynecol Reprod Biol*. 2014;178:169-175.

31. Joseph K, Rouleau J, Kramer M, et al. Investigation of an increase in postpartum haemorrhage in Canada. *BJOG*. 2007;114(6):751-759.

32. Kramer MS, Dahhou M, Vallerand D, Liston R, Joseph KS. Risk factors for postpartum hemorrhage: can we explain the recent temporal increase? *J Obstet Gynaecol*. 2011;33(8):810-819.

33. Abdul-Kadir R, McLintock C, Ducloy A-S, et al. Evaluation and management of postpartum hemorrhage: consensus from an international expert panel: Evaluation and Management of Severe PPH. *Transfusion*. 2014;54(7):1756-1768.

34. Shakur H, Elbourne D, Gülmezoglu M, et al. The WOMAN Trial (World Maternal Antifibrinolytic Trial): tranexamic acid for the treatment of postpartum haemorrhage: an international randomised, double blind placebo controlled trial. *Trials*. 2010;11:40.

35. Horrow JC, Van Riper DF, Strong MD, Grunewald KE, Parmet JL. The dose-response relationship of tranexamic acid. *Anesthesiology*. 1995;82(2):383-392.

Regular Article

VASCULAR BIOLOGY

Complement activation by heme as a secondary hit for atypical hemolytic uremic syndrome

Marie Frimat,[1-5] Fanny Tabarin,[1-4] Jordan D. Dimitrov,[1-3] Caroline Poitou,[2,4] Lise Halbwachs-Mecarelli,[1-4] Veronique Fremeaux-Bacchi,[1,6] and Lubka T. Roumenina[1-3]

[1]Institut National de la Santé et de la Recherche Médicale (INSERM) Unite Mixte de Recherche en Sante 872, Cordeliers Research Center, Paris, France; [2]Université Paris Descartes Sorbonne Paris-Cité, Paris, France; [3]Université Pierre et Marie Curie, Paris, France; [4]INSERM U845, Hôpital Necker, Paris, France; [5]Service de Néphrologie, Hôpital Claude Huriez, Centre Hospitalier Regional Universitaire, Lille, France; and [6]Hopital Européen Georges-Pompidou, Service d'Immunologie Biologique, Assistance Publique-Hôpitaux de Paris, Paris, France

Key Points

- Heme activates complement alternative pathway in serum and on endothelial cell surfaces.
- Heme-induced complement activation in the presence of complement mutations contributes as a secondary hit to the development of aHUS.

Atypical hemolytic uremic syndrome (aHUS) is characterized by genetic and acquired abnormalities of the complement system leading to alternative pathway (AP) overactivation and by glomerular endothelial damage, thrombosis, and mechanical hemolysis. Mutations per se are not sufficient to induce aHUS, and nonspecific primary triggers are required for disease manifestation. We investigated whether hemolysis-derived heme contributes to aHUS pathogenesis. We confirmed that heme activates complement AP in normal human serum, releasing C3a, C5a, and sC5b9. We demonstrated that heme-exposed endothelial cells also activate the AP, resulting in cell-bound C3 and C5b9. This was exacerbated in aHUS by genetic abnormalities associated with AP overactivation. Heme interacted with C3 close to the thioester bond, induced homophilic C3 complexes, and promoted formation of an overactive C3/C5 convertase. Heme induced decreased membrane cofactor protein (MCP) and decay-accelerating factor (DAF) expression on endothelial cells, giving Factor H (FH) a major role in complement regulation. Finally, heme promoted a rapid exocytosis of Weibel-Palade bodies, with membrane expression of P-selectin known to bind C3b and trigger the AP, and the release of the prothrombotic von Willebrand factor. These results strongly suggest that hemolysis-derived heme represents a common secondary hit amplifying endothelial damage and thrombosis in aHUS. (*Blood*. 2013;122(2):282-292)

Introduction

Atypical hemolytic uremic syndrome (aHUS) is a rare kidney-predominant thrombotic microangiopathy (TMA) associated with formation of fibrin-platelet clots in the glomerular microvasculature leading to mechanical hemolysis.[1] This disease is related to a dysregulation of the complement alternative pathway (AP), as shown by the identification of genetic or acquired abnormalities in AP regulators or activators in more than 60% of patients.[2] aHUS has an incomplete penetrance among mutation carriers, and a triggering event is presumably required for the disease manifestation. This primary hit can be an infection, pregnancy, drug, or other cell-activating event. Sera from aHUS patients carrying mutations deposit complement on endothelial cells activated by inflammatory cytokines,[3] suggesting continuous aggression on the endothelium. However, not all infections trigger aHUS in patients. It is frequently the second pregnancy postpartum period that is associated with the disease.[4] Therefore, other factors appear to be necessary to exceed the threshold of tolerable endothelial stress leading to severe TMA lesions.

In acute phase TMA, mechanical hemolysis induces the release of hemoglobin into the bloodstream.[5] This hemoglobin is readily oxidized to ferric hemoglobin (methemoglobin) which, in turn, liberates heme. In physiological conditions, cell-free hemoglobin and heme are promptly scavenged by haptoglobin and hemopexin, respectively, which prevent their accumulation and limit their toxicity.[6] However, at high concentrations of circulating hemoglobin, as in hemolytic diseases, these detoxification systems are overwhelmed,[7] causing undesirable cell, tissue, and organ injury. The effects of heme exposure on the vascular system have been widely reported and include, in particular, heme iron–induced oxidative stress, vascular inflammation with recruitment of leukocytes, hemolysis,[8-10] and thrombosis.[11,12] Nevertheless, the participation of hemolysis in the development of TMA, as in aHUS, is not well studied.

Heme has been shown to activate the complement AP and to promote the deposition of C3 activation products on erythrocytes, as in malaria.[13,14] Complement AP activation has also been reported during the acute phase of other hemolytic disorders, such as sickle-cell disease,[15] β thalassemia major,[16] and thrombotic thrombocytopenic purpura,[17] but the participation of hemoglobin or its breakdown products in complement activation has not been investigated.

Here, we studied the effect of heme on complement activation and endothelial damage in the context of TMA in aHUS and potentially in other hemolysis-related diseases.

Submitted March 12, 2013; accepted May 14, 2013. Prepublished online as *Blood* First Edition paper, May 21, 2013; DOI 10.1182/blood-2013-03-489245.

The publication costs of this article were defrayed in part by page charge payment. Therefore, and solely to indicate this fact, this article is hereby marked "advertisement" in accordance with 18 USC section 1734.

Methods

Reagents

The oxidized form of heme (hemin [ferriprotoporphyrin IX], designated as heme), hematoporphyrin IX, and hemoglobin were from Sigma. Stock solutions of 10 mM hemin and hematoporphyrin in 50 mM NaOH and 145 mM NaCl, stored at 4°C in the dark, were diluted just before use in phosphate-buffered saline (PBS) or M199 medium. All purified complement proteins and complement immunodepleted sera were from Complement Technologies. C3 from Calbiochem and Factor B (FB) from Quidel were also used. Recombinant FB was expressed in HEK293T cells as described.[18] Complement enzyme-linked immunosorbent assay (ELISA) kits were from Quidel and HyCult.

aHUS patient sera

Serum samples were obtained from healthy blood donors or from aHUS patients from the French aHUS cohort.[19] Approval was obtained from the Institut National de la Santé et de la Recherche Médicale (INSERM) institutional review board for these studies. Informed consent was provided according to the Declaration of Helsinki. Samples harboring six different mutations have been tested: three C3 mutations[3,20] (5 patients) and three Factor H (FH) mutations.[19] An AB blood group serum obtained from the French blood transfusion center Etablissement Français du Sang was used as a common standard in all experiments (normal human serum [NHS]).

Endothelial cell assays

Primary human umbilical vein endothelial cells (HUVECs) and conditionally immortalized glomerular endothelial cells (GEnCs)[18,21] were cultured as described previously.[3] They were incubated with heme and then serum, as described in the Figure 2, 3 and 6 legends. Cells in 24-well plates were detached, labeled, and analyzed by flow cytometry (FACSCalibur). Cells grown in 96-well plates were fixed with paraformaldehyde and analyzed by ELISA. Each condition was assayed in sixplicate wells (3 wells for the ELISA and 3 wells treated with crystal violet and analyzed by colorimetry to normalize the results with cell numbers). For fluorescence microscopy, HUVECs were grown in endothelial growth medium 2 (EGM2; Lonza) on gelatin-coated slides, stimulated, then fixed with paraformaldehyde and labeled as described in the Figure 2C legend. They were then analyzed with a Zeiss LSM700 confocal microscope, and photographs were processed with Image J64 software. Cell-free supernatants, centrifuged twice at 350*g* to remove residual cells, were assayed for von Willebrand factor (vWF) with a home-made sandwich ELISA.[22]

Surface plasmon resonance (SPR). C3, C3b, C3a, C3d, FH, Factor D (FD), or FB were immobilized on the GLC sensor chips of ProteOn XPR36 equipment according to the manufacturer (BioRad). Six different concentrations of heme (starting with 300 nM) or heme-exposed proteins (C3, C3b, FB, or FH) were injected as analytes.

The C3/C5 convertase formation was followed by consecutive injections of native C3 (80 μg/mL), then FB (50 μg/mL) with FD (0.1 μg/mL), C3 again, and C5 (20 μg/mL) last on heme-exposed immobilized C3 and C3b. Alternatively, C3, C3b, FH, FB, or FB + FD were exposed to heme of different molar excess, diluted in cascade, and injected on a protein-coated chip.

Absorbance spectroscopy. Absorbance spectra of hemin were recorded by using a Unicam Helios b UV-vis spectrophotometer, as described previously.[23] Human C3, C3b, or C3a (Calbiochem; CompTech) was diluted to 500 nM in PBS. Aliquots of heme resulting in final concentrations of 0.01 to 20 μM were added to the optical cell–containing proteins and to a reference optical cell containing PBS only. The absorbance spectra in the wavelength range of 350 to 700 nm were recorded (300 nm/min).

Size exclusion chromatography. The molecular composition of native and 10-fold molar excess heme-exposed C3 was analyzed by using the fast protein liquid chromatography Akta Purifier 10 system with a 30-mL Superose-6 column equilibrated with PBS. Detection was set at dual wavelengths: 280 nm for proteins and 400 nm for heme.

Molecular docking. The atomic coordinates of C3 (PDB 2A73[24]) were used for the molecular docking. HexServer (http://hexserver.loria.fr/) was used to accommodate the heme molecule to C3, as described previously for C1q.[23] Criteria for final C3-heme complex selection were based on the total energy of binding. Visualization was done by PyMol (www.pymol.org).

Results

Heme activates complement AP

Heme induced fluid-phase complement activation in NHS, as shown by a dose-related increase of C3a, C5a, and sC5b9 levels, measured by ELISA (Figure 1). Similar levels of C3a, C5a, and C5b9 were measured in NHS, in NHS-EGTA-Mg^{2+}, and in C2-depleted serum. The latter two conditions allow AP activation only. No activation was observed in FB-depleted serum, which is deprived of AP activation. Adding back purified FB restored the heme-induced complement activation capacity. No complement activation was observed with an iron-devoid derivative of heme, hematoporphyrin, under the same conditions (data not shown).

Exposure of endothelial cells to heme results in complement activation on the cell surface

To mimic the situation of intravascular hemolysis, human endothelial cells, HUVECs, and GEnCs were pretreated with increasing heme concentrations, washed, and incubated with NHS. Cell-bound C3 fragments (markers of complement activation) were analyzed by flow cytometry after cell detachment or by ELISA and immunofluorescence on adherent cells. As shown in Figure 2A-C, the level of cell-bound C3 was minimal on resting cells when compared with the immunoglobulin G1 isotype control. Exposure to heme resulted in a concentration-dependent increase of C3 deposits on both HUVECs and GEnCs detected by flow cytometry (Figure 2A), ELISA (Figure 2B), and by immunofluorescence microscopy (Figure 2C). Complement deposits were still observed when heme-treated cells were submitted to up to 5 washes before the addition of complement (data not shown), revealing a cell-directed effect of heme. Complement activation by heme-treated cells occurred via the AP, since C3 deposits were persistent in the presence of EGTA-Mg^{2+} and in C2-depleted serum but strikingly diminished in FB-depleted serum (Figure 2D). The addition of purified FB to the FB-depleted serum restored C3 fragment deposition. These effects were observed with both HUVECs (Figure 2D) and GEnCs (data not shown). Importantly, C5b9 complexes were also detected by flow cytometry on heme-treated cells (Figure 2E), reflecting the formation of a C5 convertase. Exposure of endothelial cells to heme up to 200 μM for 1 hour did not induce apoptosis and necrosis as measured by Annexin V and propidium iodide labeling (data not shown).

Complement activation on endothelial cells is exacerbated in the presence of sera with aHUS-related complement mutations and aHUS-relevant model conditions

To test whether complement dysregulation or overactivation in sera induces modification in C3 deposition on heme-exposed endothelial cells, sera from normal controls or from aHUS patients with previously described FH mutations (FH-aHUS)[19] or C3 mutations (C3-aHUS)[3,20] were used. Exacerbation of the C3 deposition was observed by flow cytometry on GEnCs (Figure 3A) and on HUVECs (data not shown) in contact with patients' sera compared with normal controls (n = 30). C3 deposition on resting cells was

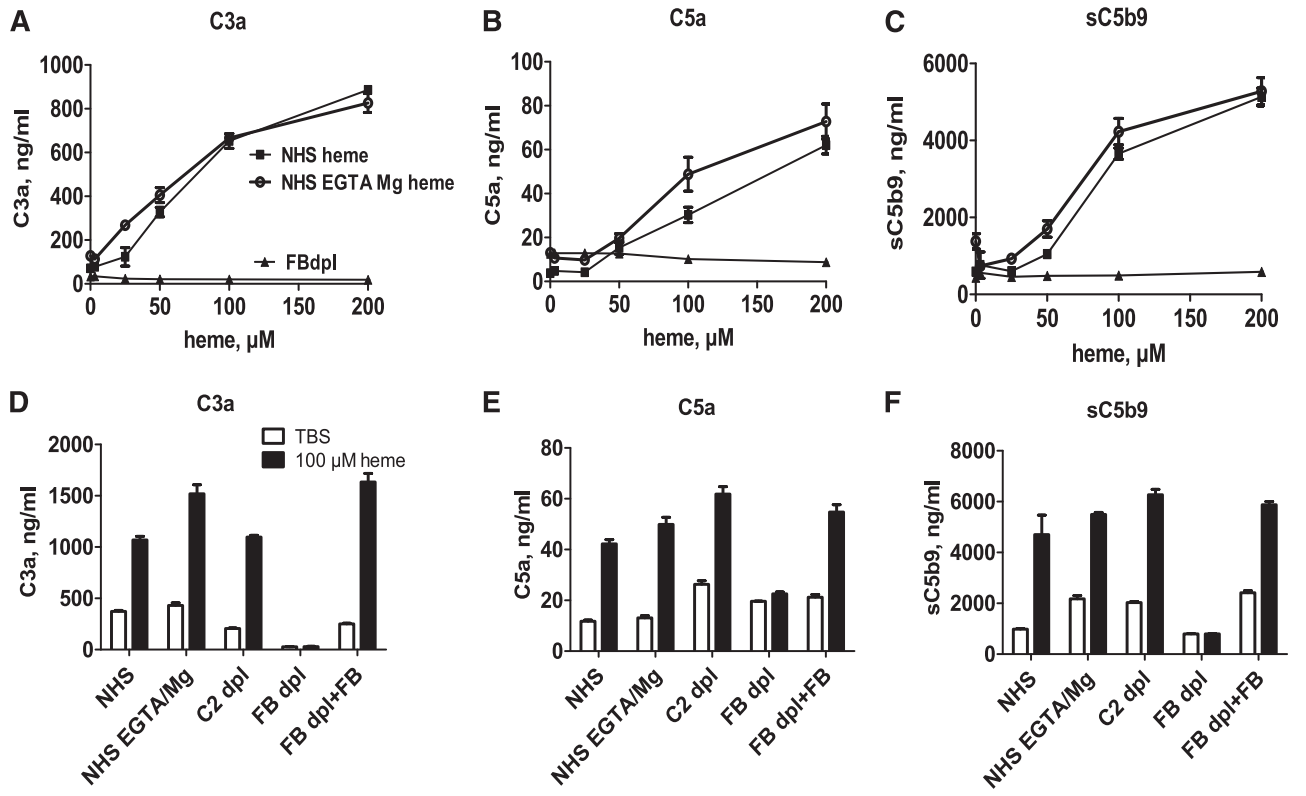

Figure 1. Heme activates the complement AP in serum. (A-C) Normal or FB-depleted sera was incubated v/v with twofold dilutions of heme in M199 medium, without or with 10 mM EGTA and 5 mM $MgCl_2$. After a 30-minute incubation at 37°C, the levels of released C3a, C5a, and sC5b9 were measured by ELISA. (D-F) To show the involvement of the AP, these complement components were measured after a similar incubation of NHS, without or with EGTA-Mg, C2-depleted (dpl) serum, or FB-depleted serum, reconstituted or not with 150 μg/mL purified FB, with 100 μM heme. Results are expressed as mean ± standard deviation (SD) of 2 experiments with triplicate measurements.

enhanced in sera from about half the patients, although on heme-exposed cells, it was significantly increased with sera from all of the patients when compared with 30 normal sera. Immunofluorescence microscopy observations of heme-exposed HUVECs incubated with sera from patients with C3 mutations showed increased C3 deposition, cell retraction, and/or detachment when compared with cells incubated with normal sera (Figure 3B). C3 deposition was similarly augmented on heme-treated HUVECs incubated in conditions mimicking aHUS sera, that is, with FB-depleted serum restored with a recombinant FB with aHUS gain-of-function mutation D254G[18] compared with the wild-type FB (Figure 3C); in the presence of FI-depleted (Figure 3D) or FH-depleted (Figure 3E) sera, as a model for FI and FH deficiency; or in the presence of blocking anti-FH antibody directed against the N- and C-termini of FH, as found in patients with autoimmune aHUS[25,26] (Figure 3F).

Heme binds to C3

To find out whether heme activation of AP was a result of its interaction with a particular complement protein, the binding of heme to C3, FB, FH, and FD was tested by SPR. Strong, specific, and dose-dependent binding to surface-immobilized C3 (hence C3b like $C3(H_2O)$[27]) and 50% less to FH and FB was detected (Figure 4A). No binding to FD was found. Further, heme was shown to bind the C3a fragment of C3 in contrast to C3b and C3d (Figure 4B). C3 (H_2O), C3b, and C3d were functionally active, since they bound FH (data not shown), excluding artifacts due to protein alterations.

To further examine the binding of heme to C3 and its fragments, C3, C3b, and C3a were exposed to heme, and alterations in the specific electronic configuration of heme were then studied by absorption spectroscopy. The absorbance spectrum of oxidized heme showed a ΔA increase in the molar extinction coefficient at the Soret band (around 400 nm) in the presence of C3 and C3a and a 4-nm and 8-nm red shift, respectively (Figure 4C). C3b showed only ΔA with no red shift. The titration of C3a and C3b with increasing concentrations of heme resulted in saturable ΔA (at about two- to sixfold heme excess), although titration of C3 did not reach saturation even at 20-fold molar excess of heme, suggesting C3 oligomer formation (Figure 4D).

To gain further insight into the possible location of the heme binding site(s) in the C3 molecule, molecular docking was performed. HexServer returned 14 top-scored models with total calculated energy of the system between −397.61 kJ/mol and −306.06 kJ/mol (Figure 4E). The first binding site (4 models) was located near the anaphylatoxin (ANA) domain (C3a after cleavage by the C3 convertase). The second site (8 models) was less than 10 Å from the thioester bond (Cys988-Gln991) in the thiol ester-containing domain (TED) at the interface with macroglobulin domain 2 (MG2) and macroglobulin domain 8 (MG8) (Figure 4F). The last site (2 models) is located in close proximity to the second one at the interface between the TED and MG2 domains.

Heme binding to C3 favors C3/C3 interactions

The possibility that heme induces homophilic C3 interactions was assessed by SPR. Heme-exposed C3 injected in the fluid phase was able to bind in a dose-dependent manner to C3 (Figure 4G), but not to C3b (data not shown) immobilized on the chip. Heme-exposed

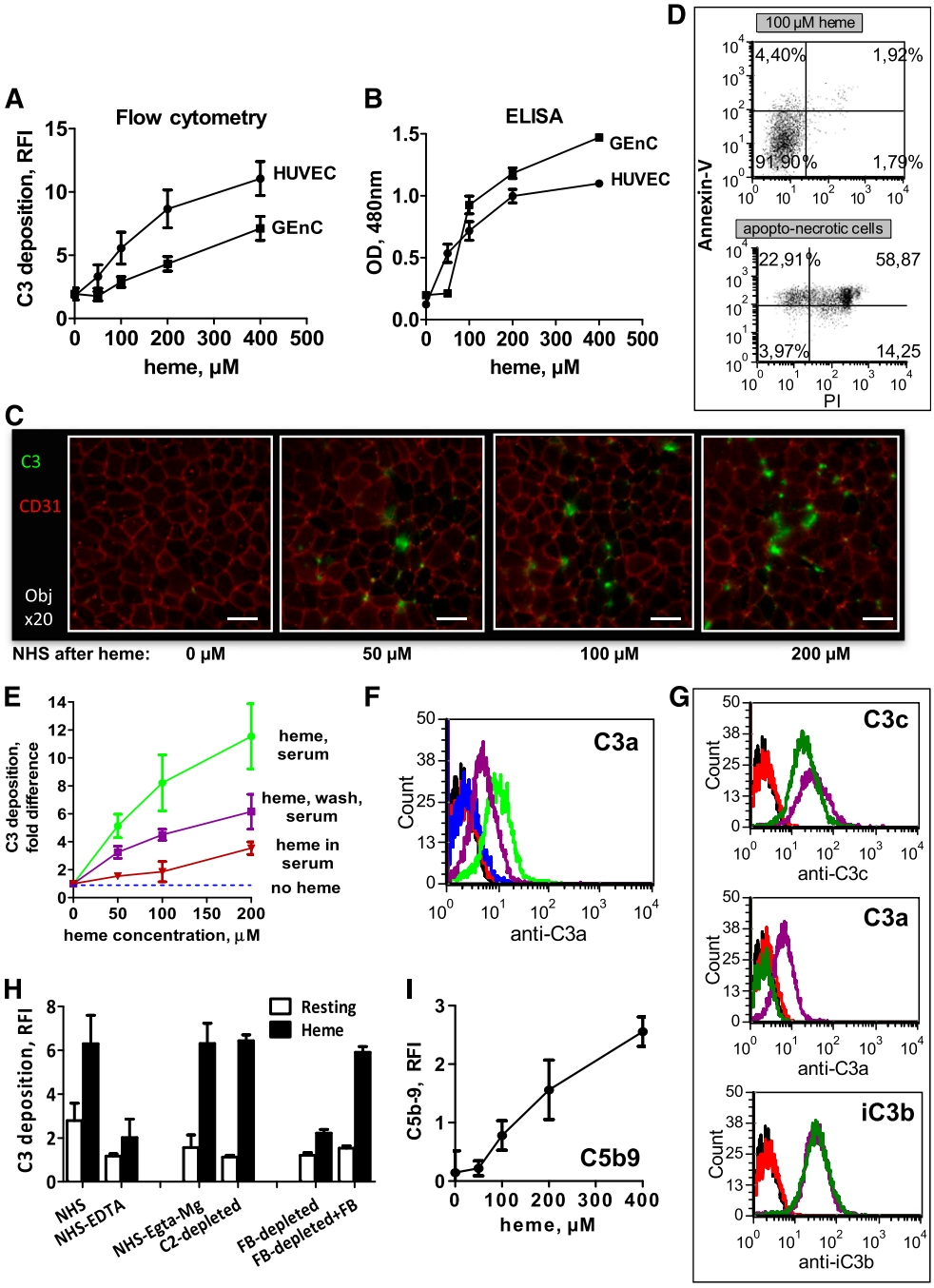

Figure 2. Complement activation on heme-treated endothelial cells results in cell-bound C3 fragments and C5b9. HUVECs or GEnCs were stimulated with increasing concentrations of heme in M199 medium for 20 minutes at 37°C. If not stated otherwise, cells washed with PBS with Ca^{2+}/Mg^{2+} (Gibco) were incubated for 30 minutes at 37°C in NHS diluted 1:4 in M199 medium. (A) Washed cells were detached with PBS, 1% bovine serum albumin, 10 mM EDTA, 0.1% sodium azide, without (HUVECs) or with 5 mg/mL lidocaine (GEnC) to be analyzed by flow cytometry after labeling with anti-C3c monoclonal antibody (mAb) (Quidel) and phycoerythrin-labeled secondary antibody (mean ± SD of mean fluorescent intensities relative to the mAb isotype control (RFI, n = 3). (B) Washed cells were fixed with 4% paraformaldehyde and 2% saccharose for 20 minutes at room temperature for analysis by cell-ELISA after labeling with biotin–anti-C3c (Quidel) in Tris-buffered saline–bovine serum albumin and peroxidase-extravidin (Sigma) revealed with 3,3′,5,5′-tetramethylbenzidine substrate (Pierce) (mean ± SD of triplicate wells from one of 3 similar experiments). (C) HUVECs were fixed with paraformaldehyde as in (B) to be analyzed by confocal microscopy after labeling with a mouse anti-CD31 mAb and a rabbit anti-C3 Ab revealed with Alexa555 (red)- and Alexa488 (green)-labeled secondary antibodies (Molecular Probes); scale bar, 50 µm. (D) Heme-exposure, under the experimental conditions used, did not induce cell death. HUVECs were exposed to 100 µM heme, quickly detached with trypsin, stained with Annexin V and propidium iodide, and analysed by flow cytometry. Apopto-necrotic HUVECs spontaneously detached overnight from a confluent monolayer served as a positive control for Annexin V and propidium iodide staining. Representative dot plots out of 3 independent experiments are shown. (E) Heme-induced C3 deposition on HUVECs were measured by flow cytometry with an anti-C3c mAb, under conditions favoring a fluid phase complement activation (heme added to the cells together with serum, "heme in serum"), direct effect on the cell surface (heme exposure as in panels [A], [B] and [C], "heme, wash, serum"); or both (cells pre-exposed to heme, then treated with serum with no washing step, "heme, serum") (mean ± SD of 3 independent experiments). (F) The presence of uncleaved C3 on the surface of heme-exposed HUVECs were tested by staining with anti-C3a mAb the cells exposed with 100 µM heme and NHS as in (E). Blue, resting cells; purple, "heme, wash, serum"; green, "heme, serum"; black, unstained cells; red, isotype control IgG1. (G) Acidic wash of the uncovalently bound C3 forms from the heme-exposed cells. HUVECs were exposed to 100 µM heme, washed and incubated with NHS. Subsequently, 3 washes with PBS (purple histogram) or with a pH 2.7 PBS-25 mM Glycine buffer (green line) were performed. The cells were stained with anti-C3c, anti-C3a or anti-iC3b neoepitope antibody (Quidel) and analyzed by flow cytometry. Signal from unstained cells is presented in black and the isotype control IgG1 is in red; representative histograms of 3 independent experiments. (H) Heme-induced C3 deposition is dependent on the alternative complement pathway. HUVECs treated as in (A), with or without 100 µM heme, were incubated with 1:4 diluted NHS, with or without 10 mM EDTA or 10 mM EGTA and 5 mM $MgCl_2$, C2-depleted or FB-depleted serum, with and without 150 mg/ml purified FB. C3 deposits were measured, as in (A), by flow cytometry (mean ± SD RFI, n = 4). (I) HUVECs treated as in (A) were labeled with a mouse anti-C5b-9 mAb kindly provided by Prof Paul Morgan (Cardiff, United Kingdom) (n=3).

C3b on the chip did not interact with either C3b or C3 (data not shown). C3 on the chip, exposed to increasing heme concentrations, bound native C3 injected in the fluid phase (first step of the SPR profile in Figure 5A) in a heme dose-dependent manner.

To assess the stability of heme-induced C3-C3 complexes, the molecular composition of C3 after exposure to heme was analyzed by size exclusion chromatography. A fraction of heme-exposed C3 was eluted earlier than native C3, corresponding to homophilic C3 interactions and formation of dimers and higher-order oligomers (Figure 4H). These oligomers showed stable heme binding, since some heme, detected by its specific absorbance at 400 nm, co-eluted with the oligomeric protein detected by the 280-nm absorbance. Free heme has a low molecular weight and is retained by the column.

Heme interaction with C3 favors the formation of a C3/C5 convertase

To explain the observed heme-induced AP activation and in view of the heme-induced homophilic C3 interaction described earlier, the effect of heme on the C3 convertase formation was investigated by SPR (Figure 5). C3 (Figure 5A) and C3b (Figure 5B) were immobilized on the sensor chip and exposed to increasing concentrations of heme. As in Figure 4, a dose-dependent binding of heme to C3, but not to C3b, was detected. A fixed amount of C3 was then injected, which bound strongly to heme-exposed C3 but only minimally to C3b. Further fixed concentrations of FB and FD were flowed onto the chip, to form the C3 convertase. A dose-dependent increase of the signal was detected on heme-exposed C3-coated flow cells but there was little or no effect on C3b-coated flow cells. Subsequent injections of fixed concentrations of C3 followed by C5 resulted again in a dose-dependent increase of binding to the heme-exposed C3 surface. Since a slight heme binding to FB was detected (as shown in Figure 4A), the effect of heme on the ability of FB to interact with C3 and to form a C3 convertase was tested. No difference in the interaction of FB with C3 and C3b in the presence of FD was detected after FB exposure to up to 10-fold molar excess of heme (Figure 5C-D).

Heme enhances FH binding to C3 and to endothelial cell surfaces

Since heme binding to FH was detected in Figure 4A, the influence of heme on the binding of FH to its C3 and C3b ligands was studied. Heme-exposed C3 bound FH more strongly compared with native C3, reaching more than a threefold increase at 10-fold molar excess of heme (Figure 6A). In contrast, heme-exposed C3b bound FH similarly to native C3b binding (data not shown). The increased C3-FH binding was a consequence of C3 exposure to heme, since FH exposure to up to 10-fold molar excess of heme did not alter its interaction with C3 and C3b (Figure 6B).

Heme treatment of HUVECs resulted in a dose-dependent increase of FH binding to the cell surface upon incubation with NHS (Figure 6C). Of note, no FH was detected on HUVECs in the absence of serum by using a mixture of three anti-FH monoclonal antibodies (mAbs) (data not shown). In order to test whether FH bound to heme-treated cells was functionally active and able to control C3 deposition, cells were incubated with PBS, with C3-depleted serum (as a source of FH without C3 deposition), or with FH-depleted serum (allowing C3 deposition with no FH), followed by a second step of NHS incubation (Figure 6D). Preincubation with FH contained in the C3-depleted serum resulted in a 40% lower C3 deposition than the control preincubated in PBS. By contrast, preincubation with FH-depleted serum resulted in 20% higher C3 deposition than with the NHS control. Moreover, inhibition of FH-mediated control by cell preincubation with an FH 19-20 construct able to interact with the cell membrane and to compete with FH[28] resulted in a dose-dependent decrease of FH binding and concomitant increase of C3 deposition on the cell surface (Figure 6E).

Heme decreases the membrane control of complement activation

Heme-induced complement activation on endothelial cells could be the result of either defective control or local overactivation or both. To study the role of complement regulators, expression levels of CD59, decay-accelerating factor (DAF), and membrane cofactor protein (MCP) were measured on resting or heme-treated HUVECs by flow cytometry. As shown in Figure 7A, heme treatment decreased the membrane expression of DAF and MCP in a dose-dependent manner, with no modification of CD59 levels. Heme at 50 μM resulted in about 50% loss of MCP and DAF when compared with untreated cells.

Heme induces the membrane expression of P-selectin on endothelial cells

P-selectin has been described as a C3b-binding protein, capable of initiating complement activation.[29] Thus, we analyzed the membrane expression of P-selectin on endothelial cells and observed a time-dependent increase of this expression during heme treatment (Figure 7B). The rapid expression, in less than 30 minutes, excluded a de novo synthesis but suggested a mobilization of Weibel-Palade bodies. Indeed, a secretion of vWF was observed, as measured by ELISA, in parallel with P-selectin membrane expression (Figure 7C).

Discussion

We report that heme activates complement in the fluid phase and on endothelial cells and induces a prothrombotic phenotype by a set of five probably co-existing mechanisms (summarized in Figure 7D). Our data allow us to propose a novel hypothesis in which hemolysis would serve as a secondary hit for aHUS manifestation. A triggering event preceding the acute phase of aHUS may lead to formation of an initial thrombus responsible for erythrocyte rupture and heme release. We suggest that heme amplifies complement activation and creates a positive feedback loop that sustains and perpetuates the histologic TMA lesions. Upon exceeding a threshold, this heme-induced complement overactivation becomes a second hit for the manifestation of a full-blown aHUS. This may shed new light on aHUS pathogenesis and explain, at least in part, the incomplete penetrance of the disease, which would develop only after such an amplification of primary pathogenic events. First, we found that the presence of heme in NHS is sufficient to trigger fluid phase complement AP activation with release of anaphylotoxins C3a and C5a, as well as sC5b9, in agreement with previous reports.[13,30] Heme has a dual role in complement, activating AP but inhibiting the binding of C1q to its ligands.[23] We investigated the mechanism of AP complement activation and showed that it results from the interaction of heme with the C3 molecule, which favors C3 homophilic interactions and leads to the formation of an active AP C3/C5 convertase.

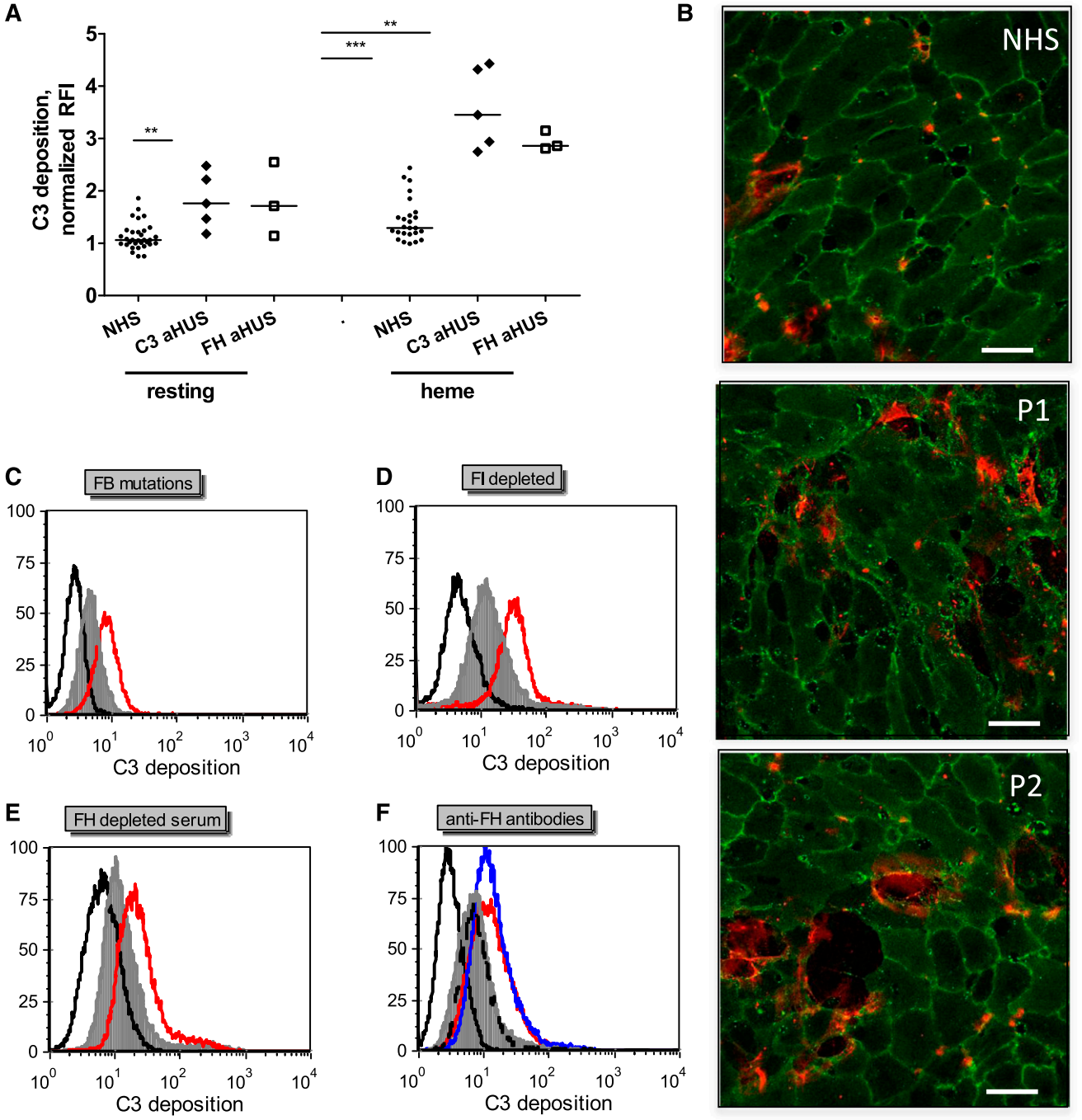

Figure 3. C3 deposits on heme-treated endothelial cells are increased with sera from aHUS patients compared with normal sera. Endothelial cells were treated as in Figure 2A with 100 μM heme and 1:4 dilutions of various sera representing aHUS relevant conditions. (A) Resting or heme-exposed GEnCs were incubated with NHS (n = 30) or sera from aHUS patients with FH (n = 3) or C3 (n = 5) mutations, and the level of C3 deposition was measured by fluorescence-activated cell sorter. (B) HUVECs were exposed to 100 μM heme and 1:4 dilutions of NHS and sera from two aHUS patients with C3 mutations (P1 and P2) and labeled with anti-CD31 (green) and anti-C3 (red) for immunofluorescence, as in Figure 2C. Scale bar = 50 μm. (C-E) Heme-exposed HUVECs were treated with normal sera (gray) or different model conditions for aHUS (red). (C) FB-depleted serum complemented with recombinant FB either wild-type or with aHUS-related mutation D254G, (D) FI-depleted serum, (E) FH-depleted serum, and (F) normal serum complemented with blocking anti-FH antibodies against the N-terminus (Ox24, AbD Serotec; blue) or C-terminus (C18, Santa Cruz; red) or nonblocking antibody (Ox23, dashed line). The isotype control is in black. A representative histogram from 1 of at least 3 independent experiments is presented. Statistical significance, $^{**}P < .01$, $^{***}P < .001$.

Molecular docking revealed that one of the most likely heme-binding sites on C3 is adjacent to the thioester bond. The insertion of the redox active heme at this site may favor the thioester bond hydrolysis and the transition of native C3 to hydrolyzed C3*. Importantly, hydrolyzed C3* is able to bind FB and form a C3 convertase, contrary to native C3. Therefore, heme-induced generation of C3* could explain the fluid phase AP activation in heme-treated serum (Figure 7D, step 1). Heme is known to mediate protein covalent cross-linking and oligomer formation[31] and indeed induces the formation of C3/C3 complexes. Those are particularly critical for the formation of a fluid phase C5 convertase, which requires C3b/C3b covalent linkage for an efficient affinity for C5.[32] Iron-devoid heme derivative hematoporphyrin did not activate complement, strongly suggesting that

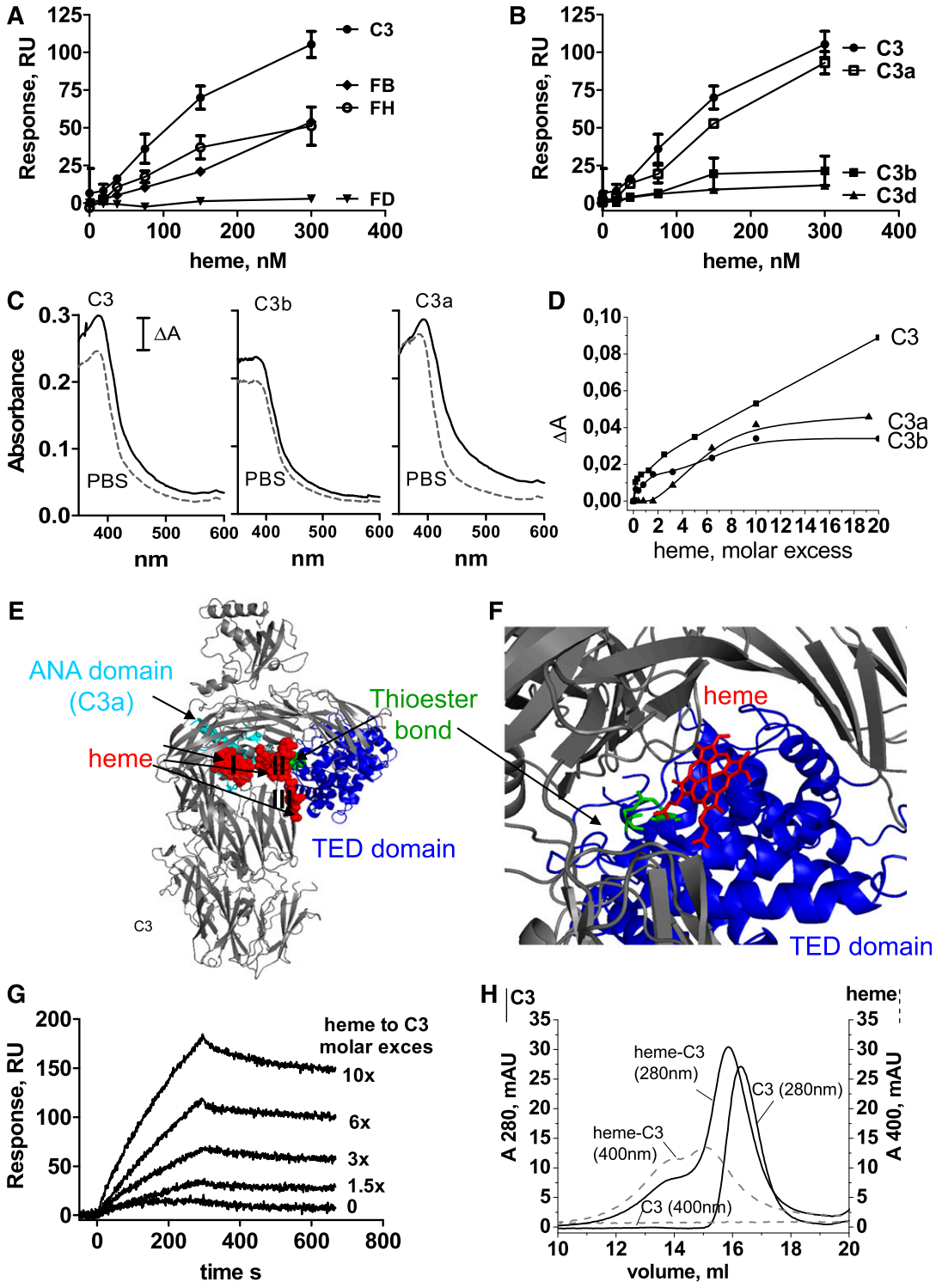

Figure 4. Binding of heme to C3. SPR analysis of the binding of different concentrations of heme to (A) AP proteins and (B) C3 fragments immobilized on the chip (mean ± SD from 3 experiments on 2 chips). The flow rate was 30 μL/min with N-2-hydroxyethylpiperazine-N′-2-ethanesulfonic acid (HEPES) running buffer (10 mM HEPES, 150 mM NaCl, Tween 0.005%; pH 7.3). Each interaction was tested on at least two different chips at least twice per chip. Data were double referenced and analyzed by using ProteOn manager software. (C) Absorption spectroscopy for the binding of heme at a 10-fold molar excess to C3, C3b, and C3a. Dashed gray line represents the spectrum of heme in PBS and the black line represents the spectrum of heme in the presence of protein. (D) Dose-dependence of the binding of heme to C3, C3b, and C3a. Heme was added to the protein solution and incubated for 2 minutes in the dark at 20°C before recording the spectrum. Absorbance differences between protein-bound hemin and hemin at absorbance maxima (λ = 395 nm) in the Soret region (ΔA) were used to build titration binding curves. (E) Molecular docking of heme to C3: heme (red spheres) in all 14 retrieved models docked to three regions of the molecule (I, II, and III), one being close to the ANA domain (cyan), the second being close to the thioester bond (green) in the TED domain (blue), and the third again being close to the TED domain. (F) Zoomed in view of the II cluster with the top-score heme molecule visualized using ball-and-stick art in red. The distance between the thioester bond (green) and heme is less than 10 Å. (G) SPR analysis of the binding of heme-exposed C3 to C3 immobilized on the chip. One experiment of 3 with similar results is presented. No interaction was detected in the absence of heme, although dose-dependent binding was found with increasing heme concentrations. (H) Size exclusion chromatography of native C3 and heme-exposed C3. Fast protein liquid chromatography with a Superose 6 column with dual wavelength was used (280 nm for C3, black line; 400 nm for heme, gray dashed line). C3 at 6.4 μM was incubated for 10 minutes on ice with PBS or 64 μM heme, giving 10-fold molar excess adjusted to a final volume of 1 mL and loaded to the column.

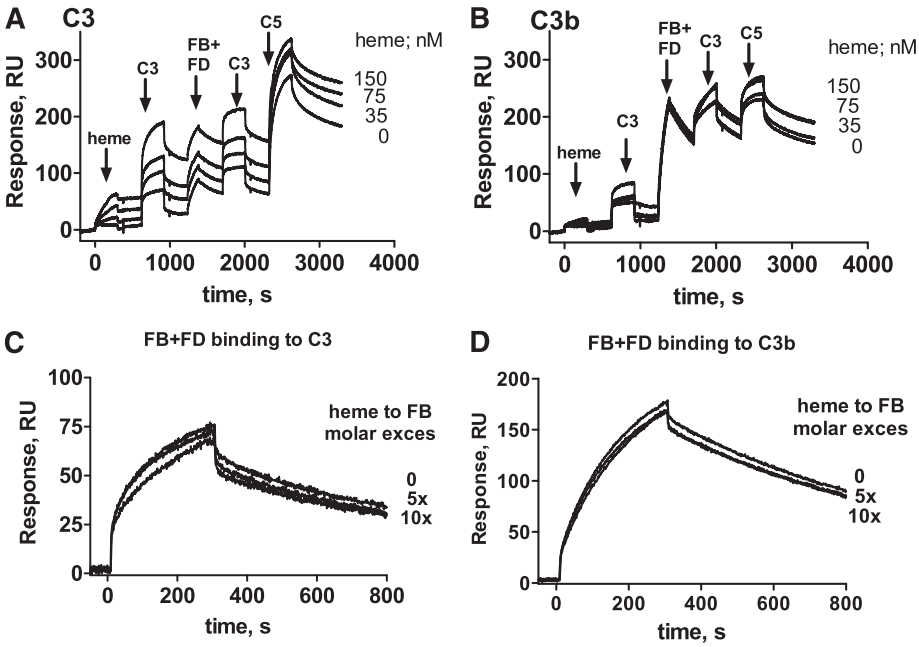

Figure 5. Heme interaction with C3 favors the formation of the AP C3/C5 convertases. C3 convertase was formed on an SPR chip coated with (A) C3 and (B) C3b. $MgCl_2$ (1 mM final) was added in HEPES running buffer for interactions involving FB. C3 or C3b on the chip was exposed to increasing concentrations of heme as indicated. Subsequently, a series of injections of C3, FB + FD, C3, and C5 allowed formation of a C3/C5 convertase on the chip. One representative experiment of 4 is shown. The influence of heme on the capacity of FB and FD to bind to (C) C3 and (D) C3b was measured by SPR. C3 and C3b were immobilized on the chip and FB and FD, either native or exposed to five- and 10-fold molar excess of heme, were injected. One representative sensorogram set of 3 experiments is shown. Each interaction was tested on at least two different chips at least twice per chip, and the data were double referenced and analyzed by using ProteOn manager software.

iron redox activity is involved.[5] This is reminiscent of previous data showing that H_2O_2 and neutrophil-derived oxidants trigger the complement AP and may also activate C5 directly.[33]

Circulating free heme concentrations are about 6 to 30 μM in sickle-cell disease and thalassemia[7] but have not been reported in aHUS. Mechanical hemolysis in the renal microvasculature in

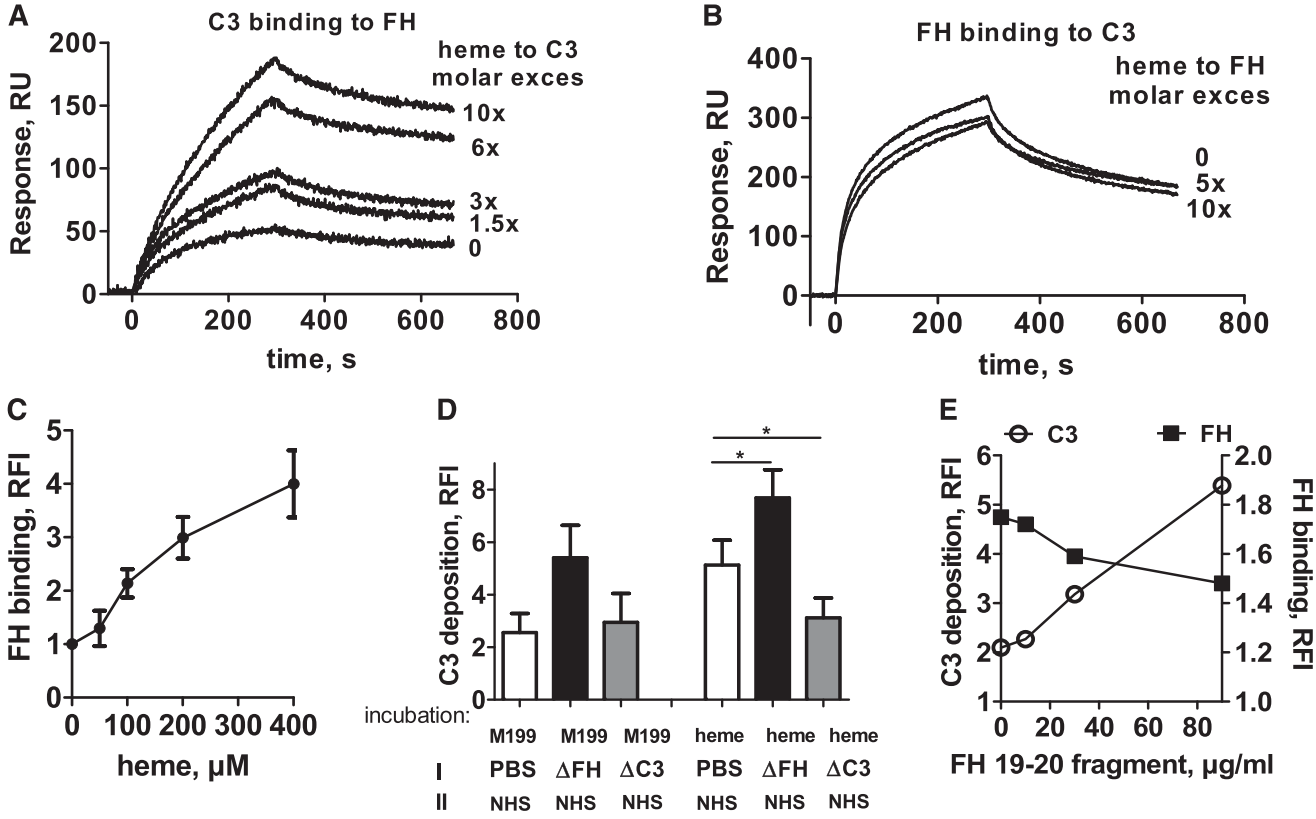

Figure 6. FH binds to heme-treated C3 and is the major serum factor regulating C3 deposition on heme-treated cells. (A) Heme-exposed C3 bound more strongly to immobilized FH, as measured by SPR but (B) heme-exposed FH bound immobilized C3 in the same manner as did native FH. (C) HUVECs were treated with increasing doses of heme and 1:4 NHS, detached as in Figure 2A, and labeled with anti-FH mAb Ox23. Results are expressed as RFI mean ± SD (n = 3). (D) Resting HUVECs and cells treated with 100 μM heme for 20 minutes, were sequentially incubated for 30 minutes at 37°C, first with either PBS, FH-depleted serum, or C3-depleted serum (source of FH), washed, and incubated as a second step with NHS (*$P < .05$, paired Student t test; n = 3). (E) HUVECs treated with 100 μM heme for 20 minutes were incubated with increasing concentrations of Short Consensus Repeat (SCR) 19-20 FH peptide for 15 minutes at 37°C, then with 1:4 NHS for 30 minutes. (D-E) C3 deposits were analyzed by flow cytometry and expressed as mean ± SD RFI (n = 3).

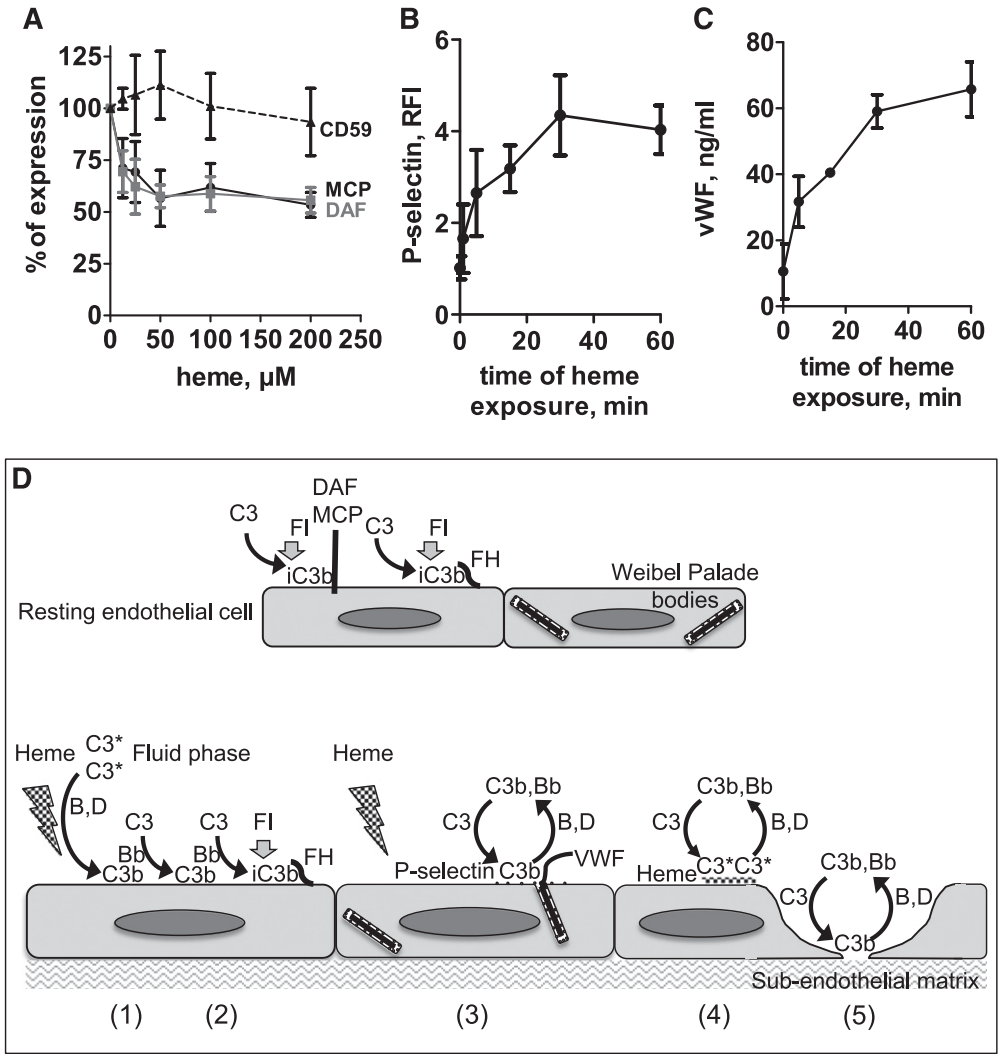

Figure 7. Effects of heme treatment of endothelial cells. (A) HUVECs treated with increasing doses of heme for 20 minutes and detached were labeled with anti-CD55, phycoerythrin-labeled anti-MCP, or anti-CD59 and analyzed by flow cytometry. Results are expressed as the percentage of the initial mean fluorescence intensity measured on untreated cells (mean ± SD; n = 3). (B) HUVECs treated with 100 µM heme for different times were detached at 4°C and labeled with anti–P-selectin (R&D Systems) (mean ± SD; n = 3). (C) Supernatants of cells were tested in a vWF-specific ELISA. Results are expressed as mean ± SD of triplicate wells from one of 3 similar experiments. (D) Schematic view of different nonexclusive mechanisms leading to complement activation on heme-treated cells. (1) Heme intercalates into the C3 molecule (C3*), activates complement in the fluid phase, and deposits C3b on nearby endothelial cells. (2) This C3b initiates the formation of a cell-bound C3 convertase, favored by the decrease of DAF and MCP membrane expressions on heme-treated cells, FH remaining as the major AP control protein. (3) Heme induces the mobilization of Weibel-Palade bodies with the secretion of vWF and the appearance of P-selectin able to bind C3b and to focus the AP amplification cycle. (4) Heme can also bind directly to the cell surface, where it activates complement as in the fluid phase. (5) Heme induces cell retraction, exposing the subendothelial matrix known to efficiently activate complement.

aHUS probably results in local heme concentration, at the site of hemolysis and before dilution in the blood flow, much higher than concentrations measured in the peripheral blood. The concentration-dependent effects of heme on complement and endothelium could, at least in part, explain why vascular lesions are mainly restricted to microvessels in TMA. The 100 µM heme concentration used in these in vitro experiments, which corresponds to the destruction of less than 0.05% of bloodstream erythrocytes,[13] thus seems physiologically reasonable.

This work is the first demonstration that free heme triggers complement AP activation on endothelial cells. Although little or no C3 deposits were observed on resting cells, they reached significant levels on heme-treated HUVECs and GEnCs. Moreover, cell-bound C5b9 was detected, reflecting the formation of a C5 convertase and the release of C5 fragments C5a and C5b9 known to activate endothelial cells and to promote endothelium permeability.[34]

Imbalance between complement activation and regulation may explain the observed AP activation on endothelial cells (Figure 7D, step 2). Indeed, a decrease of DAF (CD55) and MCP (CD46) expression was detected after exposure of HUVECs to heme, similar to previous observations of downregulated complement regulators on retinal epithelial cells submitted to brief oxidative stress.[35] DAF and MCP are responsible for the protection of endothelium against autologous complement attack. Their downregulation has been reported on apoptotic and necrotic cells,[36] but we did not detect significant increase of apoptosis with heme under the experimental conditions used.

In contrast to the decreased expression of MCP and DAF, exposure of endothelial cells to heme resulted in enhancement of FH binding to the cell membrane. FH thus appears to compensate for the loss of membrane-bound complement inhibitors DAF and MCP, as has been described on apoptotic cells.[37] Heme-treated cells would then be particularly sensitive to complement attack in the presence of

defective FH, as is found in more than 30% of aHUS patients presenting with FH mutations or anti-FH autoantibodies.[1,19,38] Indeed, levels of C3 deposits on heme-treated cells increased in FH-depleted serum or in the presence of the FH SCR 19-20 fragment known to compete with FH[28] or with anti-FH blocking antibodies.

FH enhanced binding to heme-treated cells could result from FH interaction with oxidized epitopes on the heme-exposed membrane[39] or with heme itself, bound to the lipid bilayer.[40,41] Indeed, a direct binding of heme to FH was detected by SPR in this study. Heme-exposed C3 also bound more strongly to FH compared with native C3. Heme-exposed FH interacted normally with C3 and C3b and, once bound to the cell membrane, it maintained its functional activity.

Complement activation on endothelial cells could also result from the expression of P-selectin (Figure 7D, step 3). Indeed, P-selectin has been identified as a C3b-binding protein, and on cells expressing P-selectin, this expression alone was sufficient to activate the complement system marked by C3b deposition, C3a generation, and C5b9 formation.[29] We observed that heme treatment of endothelial cells induced membrane expression of P-selectin concomitantly with the secretion of vWF. This probably results from iron-induced oxidative stress, since oxygen radicals were shown to induce exocytosis of Weibel-Palade bodies and membrane P-selectin.[42] The exposure of P-selectin could thus focus the AP activation on the surface of heme-challenged endothelial cells. Of note, the main function of P-selectin is the recruitment of leukocytes expressing its ligand PSGL-1, and heme treatment could thus favor inflammation at the surface of endothelial cells. vWF secretion could recruit platelets and contribute to a prothrombotic state of heme-exposed endothelial cells. The overall effects of heme reported here are reminiscent of those of Shiga toxin, a primary trigger of HUS, which induces P-selectin expression on endothelial cells, resulting in C3 binding and alternative pathway activation together with a vWF-mediated thrombus formation.[43]

Heme also binds directly to the cell membrane phospholipids,[40,44] where it could activate complement as in the fluid phase (Figure 7D, step 4). In addition, the endothelial cell retraction, which occurs after treatment with heme[45] and exposes the complement activating subendothelial matrix[46] may lead to heme-dependent C3 deposition on the endothelium (Figure 7D, step 5). We indeed observed a preferential localization of C3 deposits along intercellular junctions.

In HUS, we hypothesize that multiple potential triggers such as viral infection, pregnancy, or drugs lead to initial microthrombi formation. Erythrocyte fractionation on these microthrombi would result locally in microvessels in concentrations of heme sufficient to promote the release of vWF and the activation of complement and the release of C5a and C5b9, thus amplifying the initial thrombosis and inflammation. This amplification would normally be limited by the homeostatic control of complement and by the cleavage of vWF by the 13th member of a disintegrin-like and metalloprotease with thrombospondin type 1 motif, 13 (ADAMTS-13). Genetic or antibody-induced alterations of complement proteins in aHUS or of ADAMTS-13 in HUS would synergize with hemolysis, thus decreasing the threshold of the initial triggers to overcome homeostatic control and trigger an explosive endothelial injury and thrombosis. Moreover, heme-induced complement activation and endothelial injury may not be restricted to HUS and could contribute to the pathogenesis of thrombotic events observed in hemolytic episodes of different etiologies.

Acknowledgments

The authors thank Prof P. Mathieson and Dr S. Satchel (Bristol, United Kingdom) for providing the GEnC cell line, Prof Paul Morgan (Cardiff, United Kingdom) for his gift of the anti-C5b9 mAb, Dr Sakari Jokiranta (Helsinki, Finland) for giving us the FH SCR 19-20 construct, Dr Julie Rayes for her help with the vWF analysis, and Prof P. Lesavre (Paris, France) for the fruitful discussions. Part of the cytometric analysis was done at the Centre d'Imagerie Cellulaire et de Cytomètrie, Centre de Recherche des Cordeliers UMRS 872 (Paris, France). Centre d'Imagerie Cellulaire et de Cytomètrie is a member of the Université Pierre et Marie Curie Flow Cytometry network.

This work was supported by grants from Agence Nationale de la Recherche (ANR Genopath 2009-2012 09geno03101I), Assistance Publique-Hôpitaux de Paris (Programme Hospitalier de Recherche Clinique (AOM08198), European EU FP7 grant 2012-305608 (EURenOmics Consortium), by Association pour l'Information et la Recherche sur les maladies Rénales Génétiques France, and by INSERM.

Authorship

Contribution: L.T.R., L.H.-M., J.D.D., and V.F.-B. designed the project and initiated the research; M.F., L.T.R., L.H.-M., and J.D.D. designed and performed the experiments, did the analysis, and prepared the figures; F.T. and C.P. performed experiments; M.F., L.T.R., L.H.-M., J.D.D., and V.F.-B. wrote the manuscript.

Conflict-of-interest disclosure: The authors declare no competing financial interests.

Correspondence: Lubka T. Roumenina, Cordeliers Research Center, INSERM UMRS 872, team 13; 15 rue de l'Ecole de Medecine, entrance E, floor 3; 75006 Paris, France; e-mail: lubka.roumenina@crc.jussieu.fr.

References

1. Noris M, Remuzzi G. Atypical hemolytic-uremic syndrome. *N Engl J Med.* 2009;361(17):1676-1687.
2. Roumenina LT, Loirat C, Dragon-Durey MA, Halbwachs-Mecarelli L, Sautes-Fridman C, Fremeaux-Bacchi V. Alternative complement pathway assessment in patients with atypical HUS. *J Immunol Methods.* 2011;365(1-2):8-26.
3. Roumenina LT, Frimat M, Miller EC, et al. A prevalent C3 mutation in aHUS patients causes a direct C3 convertase gain of function. *Blood.* 2012;119(18):4182-4191.
4. Fakhouri F, Roumenina L, Provot F, et al. Pregnancy-associated hemolytic uremic syndrome revisited in the era of complement gene mutations. *J Am Soc Nephrol.* 2010;21(5):859-867.
5. Balla J, Vercellotti GM, Jeney V, et al. Heme, heme oxygenase, and ferritin: how the vascular endothelium survives (and dies) in an iron-rich environment. *Antioxid Redox Signal.* 2007;9(12):2119-2137.
6. Kumar S, Bandyopadhyay U. Free heme toxicity and its detoxification systems in human. *Toxicol Lett.* 2005;157(3):175-188.
7. Muller-Eberhard U, Javid J, Liem HH, Hanstein A, Hanna M. Plasma concentrations of hemopexin, haptoglobin and heme in patients with various hemolytic diseases. *Blood.* 1968;32(5):811-815.
8. Balla G, Vercellotti GM, Eaton JW, Jacob HS. Iron loading of endothelial cells augments oxidant damage. *J Lab Clin Med.* 1990;116(4):546-554.
9. Belcher JD, Beckman JD, Balla G, Balla J, Vercellotti G. Heme degradation and vascular injury. *Antioxid Redox Signal.* 2010;12(2):233-248.

10. Chiu D, Lubin B. Oxidative hemoglobin denaturation and RBC destruction: the effect of heme on red cell membranes. *Semin Hematol.* 1989;26(2):128-135.
11. Cappellini MD. Coagulation in the pathophysiology of hemolytic anemias. *Hematology (Am Soc Hematol Educ Program).* 2007;74-78.
12. Rother RP, Bell L, Hillmen P, Gladwin MT. The clinical sequelae of intravascular hemolysis and extracellular plasma hemoglobin: a novel mechanism of human disease. *JAMA.* 2005; 293(13):1653-1662.
13. Pawluczkowycz AW, Lindorfer MA, Waitumbi JN, Taylor RP. Hematin promotes complement alternative pathway-mediated deposition of C3 activation fragments on human erythrocytes: potential implications for the pathogenesis of anemia in malaria. *J Immunol.* 2007;179(8): 5543-5552.
14. Evans KJ, Hansen DS, van Rooijen N, Buckingham LA, Schofield L. Severe malarial anemia of low parasite burden in rodent models results from accelerated clearance of uninfected erythrocytes. *Blood.* 2006;107(3):1192-1199.
15. Mold C, Tamerius JD, Phillips G Jr. Complement activation during painful crisis in sickle cell anemia. *Clin Immunol Immunopathol.* 1995; 76(3 Pt 1):314-320.
16. deCiutiis AC, Peterson CM, Polley MJ, Metakis LJ. Alternative pathway activation in sickle cell disease and beta-thalassemia major. *J Natl Med Assoc.* 1978;70(7):503-506.
17. Ruiz-Torres MP, Casiraghi F, Galbusera M, et al. Complement activation: the missing link between ADAMTS-13 deficiency and microvascular thrombosis of thrombotic microangiopathies. *Thromb Haemost.* 2005;93(3):443-452.
18. Roumenina LT, Jablonski M, Hue C, et al. Hyperfunctional C3 convertase leads to complement deposition on endothelial cells and contributes to atypical hemolytic uremic syndrome. *Blood.* 2009;114(13):2837-2845.
19. Fremeaux-Bacchi V, Fakhouri F, Garnier A, et al. Genetics and outcome of atypical hemolytic uremic syndrome: a nationwide French series comparing children and adults. *Clin J Am Soc Nephrol.* 2013;8(4):554-562.
20. Frémeaux-Bacchi V, Miller EC, Liszewski MK, et al. Mutations in complement C3 predispose to development of atypical hemolytic uremic syndrome. *Blood.* 2008;112(13):4948-4952.
21. Satchell SC, Tasman CH, Singh A, et al. Conditionally immortalized human glomerular endothelial cells expressing fenestrations in response to VEGF. *Kidney Int.* 2006;69(9): 1633-1640.
22. Rayes J, Hollestelle MJ, Legendre P, et al. Mutation and ADAMTS13-dependent modulation of disease severity in a mouse model for von Willebrand disease type 2B. *Blood.* 2010;115(23): 4870-4877.
23. Roumenina LT, Radanova M, Atanasov BP, et al. Heme interacts with c1q and inhibits the classical complement pathway. *J Biol Chem.* 2011;286(18): 16459-16469.
24. Janssen BJ, Huizinga EG, Raaijmakers HC, et al. Structures of complement component C3 provide insights into the function and evolution of immunity. *Nature.* 2005;437(7058):505-511.
25. Józsi M, Strobel S, Dahse HM, et al. Anti factor H autoantibodies block C-terminal recognition function of factor H in hemolytic uremic syndrome. *Blood.* 2007;110(5):1516-1518.
26. Blanc C, Roumenina LT, Ashraf Y, et al. Overall neutralization of complement factor H by autoantibodies in the acute phase of the autoimmune form of atypical hemolytic uremic syndrome. *J Immunol.* 2012;189(7):3528-3537.
27. Andersson J, Ekdahl KN, Larsson R, Nilsson UR, Nilsson B. C3 adsorbed to a polymer surface can form an initiating alternative pathway convertase. *J Immunol.* 2002;168(11):5786-5791.
28. Lehtinen MJ, Rops AL, Isenman DE, van der Vlag J, Jokiranta TS. Mutations of factor H impair regulation of surface-bound C3b by three mechanisms in atypical hemolytic uremic syndrome. *J Biol Chem.* 2009;284(23):15650-15658.
29. Del Conde I, Crúz MA, Zhang H, López JA, Afshar-Kharghan V. Platelet activation leads to activation and propagation of the complement system. *J Exp Med.* 2005;201(6):871-879.
30. Smith DJ, Winslow RM. Effects of extraerythrocytic hemoglobin and its components on mononuclear cell procoagulant activity. *J Lab Clin Med.* 1992; 119(2):176-182.
31. Vincent SH. Oxidative effects of heme and porphyrins on proteins and lipids. *Semin Hematol.* 1989;26(2):105-113.
32. Rawal N, Pangburn MK. Structure/function of C5 convertases of complement. *Int Immunopharmacol.* 2001;1(3):415-422.
33. Shingu M, Nonaka S, Nishimukai H, Nobunaga M, Kitamura H, Tomo-Oka K. Activation of complement in normal serum by hydrogen peroxide and hydrogen peroxide-related oxygen radicals produced by activated neutrophils. *Clin Exp Immunol.* 1992;90(1):72-78.
34. Fischetti F, Tedesco F. Cross-talk between the complement system and endothelial cells in physiologic conditions and in vascular diseases. *Autoimmunity.* 2006;39(5):417-428.
35. Thurman JM, Renner B, Kunchithapautham K, et al. Oxidative stress renders retinal pigment epithelial cells susceptible to complement-mediated injury. *J Biol Chem.* 2009;284(25): 16939-16947.
36. Thurman JM, Renner B. Dynamic control of the complement system by modulated expression of regulatory proteins. *Lab Invest.* 2011;91(1):4-11.
37. Trouw LA, Bengtsson AA, Gelderman KA, Dahlbäck B, Sturfelt G, Blom AM. C4b-binding protein and factor H compensate for the loss of membrane-bound complement inhibitors to protect apoptotic cells against excessive complement attack. *J Biol Chem.* 2007;282(39): 28540-28548.
38. Dragon-Durey MA, Sethi SK, Bagga A, et al. Clinical features of anti-factor H autoantibody-associated hemolytic uremic syndrome. *J Am Soc Nephrol.* 2010;21(12):2180-2187.
39. Weismann D, Hartvigsen K, Lauer N, et al. Complement factor H binds malondialdehyde epitopes and protects from oxidative stress. *Nature.* 2011;478(7367):76-81.
40. Balla J, Jacob HS, Balla G, Nath K, Eaton JW, Vercellotti GM. Endothelial-cell heme uptake from heme proteins: induction of sensitization and desensitization to oxidant damage. *Proc Natl Acad Sci USA.* 1993;90(20):9285-9289.
41. Balla G, Vercellotti GM, Muller-Eberhard U, Eaton J, Jacob HS. Exposure of endothelial cells to free heme potentiates damage mediated by granulocytes and toxic oxygen species. *Lab Invest.* 1991;64(5):648-655.
42. Patel KD, Zimmerman GA, Prescott SM, McEver RP, McIntyre TM. Oxygen radicals induce human endothelial cells to express GMP-140 and bind neutrophils. *J Cell Biol.* 1991;112(4):749-759.
43. Morigi M, Galbusera M, Gastoldi S, et al. Alternative pathway activation of complement by Shiga toxin promotes exuberant C3a formation that triggers microvascular thrombosis. *J Immunol.* 2011;187(1):172-180.
44. Ginsburg H, Demel RA. Interactions of hemin, antimalarial drugs and hemin-antimalarial complexes with phospholipid monolayers. *Chem Phys Lipids.* 1984;35(4):331-347.
45. Neely SM, Gardner DV, Green D, Ts'ao CH. Effect of hematin on endothelial cells and endothelial cell-platelet interactions. *Am J Pathol.* 1984;115(3):390-396.
46. Hindmarsh EJ, Marks RM. Complement activation occurs on subendothelial extracellular matrix in vitro and is initiated by retraction or removal of overlying endothelial cells. *J Immunol.* 1998; 160(12):6128-6136.

2013 122: 282-292
doi:10.1182/blood-2013-03-489245 originally published online May 21, 2013

Complement activation by heme as a secondary hit for atypical hemolytic uremic syndrome

Marie Frimat, Fanny Tabarin, Jordan D. Dimitrov, Caroline Poitou, Lise Halbwachs-Mecarelli, Veronique Fremeaux-Bacchi and Lubka T. Roumenina

Blood (print ISSN 0006-4971, online ISSN 1528-0020), is published weekly by the American Society of Hematology, 2021 L St, NW, Suite 900, Washington DC 20036.

blood

2012 119: 4182-4191
Prepublished online January 13, 2012;
doi:10.1182/blood-2011-10-383281

A prevalent C3 mutation in aHUS patients causes a direct C3 convertase gain of function

Lubka T. Roumenina, Marie Frimat, Elizabeth C. Miller, Francois Provot, Marie-Agnes Dragon-Durey, Pauline Bordereau, Sylvain Bigot, Christophe Hue, Simon C. Satchell, Peter W. Mathieson, Christiane Mousson, Christian Noel, Catherine Sautes-Fridman, Lise Halbwachs-Mecarelli, John P. Atkinson, Arnaud Lionet and Veronique Fremeaux-Bacchi

Blood (print ISSN 0006-4971, online ISSN 1528-0020), is published weekly by the American Society of Hematology, 2021 L St, NW, Suite 900, Washington DC 20036.

A prevalent C3 mutation in aHUS patients causes a direct C3 convertase gain of function

*Lubka T. Roumenina,[1-3] *Marie Frimat,[3-5] Elizabeth C. Miller,[6] Francois Provot,[5] Marie-Agnes Dragon-Durey,[1,3,7] Pauline Bordereau,[1] Sylvain Bigot,[4] Christophe Hue,[1-3] Simon C. Satchell,[8] Peter W. Mathieson,[8] Christiane Mousson,[9] Christian Noel,[5] Catherine Sautes-Fridman,[1-3] Lise Halbwachs-Mecarelli,[3,4] John P. Atkinson,[6] Arnaud Lionet,[5] and Veronique Fremeaux-Bacchi[1,7]

[1]Cordeliers Research Center, Inserm Unité Mixte de Recherche en Santé (UMRS) 872, Paris, France; [2]Université Pierre et Marie Curie, Paris, France; [3]Université Paris Descartes, Paris, France; [4]Inserm U845, Hôpital Necker, Paris, France; [5]Service de Néphrologie, Hôpital Claude Huriez, Centre Hospitalier Universitaire, Lille, France; [6]Division of Rheumatology, Washington University School of Medicine, St Louis, MO; [7]Hopital Europeen Georges Pompidou, Service d'Immunologie Biologique, Assistance Publique–Hôpitaux de Paris, Paris, France; [8]Academic Renal Unit, University of Bristol, Southmead Hospital, Bristol, United Kingdom; and [9]Service de Néphrologie, Centre Hospitalier Universitaire, Dijon, France

Atypical hemolytic uremic syndrome (aHUS) is a rare renal thrombotic microangiopathy commonly associated with rare genetic variants in complement system genes, unique to each patient/family. Here, we report 14 sporadic aHUS patients carrying the same mutation, R139W, in the complement C3 gene. The clinical presentation was with a rapid progression to end-stage renal disease (6 of 14) and an unusually high frequency of cardiac (8 of 14) and/or neurologic (5 of 14) events. Although resting glomerular endothelial cells (GEnCs) remained unaffected by R139W-C3 sera, the incubation of those sera with GEnC preactivated with proinflammatory stimuli led to increased C3 deposition, C5a release, and procoagulant tissue-factor expression. This functional consequence of R139W-C3 resulted from the formation of a hyperactive C3 convertase. Mutant C3 showed an increased affinity for factor B and a reduced binding to membrane cofactor protein (MCP; CD46), but a normal regulation by factor H (FH). In addition, the frequency of at-risk FH and MCP haplotypes was significantly higher in the R139W-aHUS patients, compared with normal donors or to healthy carriers. These genetic background differences could explain the R139W-aHUS incomplete penetrance. These results demonstrate that this C3 mutation, especially when associated with an at-risk FH and/or MCP haplotypes, becomes pathogenic following an inflammatory endothelium-damaging event. (*Blood*. 2012;119(18):4182-4191)

Introduction

The atypical hemolytic uremic syndrome (aHUS) is a rare kidney predominant thrombotic microangiopathy, associated with genetic abnormalities in the regulators and activators of the alternative complement pathway.[1] A complement genetic abnormality has been identified in $>60\%$ of patients.[2] Most commonly, they correspond to rare distinct point mutation variants unique for each patient/family.[3] The small number of patients sharing a particular mutation often precludes investigations on the consequence of each particular mutation and on the influence of additional factors for the disease manifestation. Therefore, it is still unclear why aHUS has incomplete penetrance among the mutation carriers, despite the clear functional consequences of the mutations. Complement dysregulation is linked, by as yet not well-understood mechanisms, to the induction of a procoagulant phenotype on glomerular endothelial cells (GEnCs). Thrombi are formed in the kidney microvasculature, resulting in end-stage renal disease (ESRD) 1 year after the first flare in $\sim 50\%$ of the cases.[1]

Complement is an innate immune surveillance system, designed to fight infections and to handle damaged or apoptotic cells and debris.[4] It may be activated by 3 pathways, all leading to the cleavage of the central component C3 by an enzymatic complex called a C3 convertase. The C3 convertase of the alternative pathway, C3bBb, is composed of the active fragments of C3 and factor B (FB).

To avoid accidental host tissue injury, the complement system is tightly controlled on self-surfaces by regulators such as factor H (FH), factor I (FI) and membrane cofactor protein (MCP; CD46). In aHUS, these regulators are frequently mutated and unable to efficiently protect the endothelium from complement attack.[1] C3 mutations were recently discovered in aHUS and only few reports describe the clinical outcome of such patients.[5-8] Functional analysis of 9 of these C3 mutations revealed that most of them result in impaired regulation by MCP and hence in indirect, or secondary, gain of function of the C3 convertase.[5] It has also become evident that aHUS could be associated with an intrinsically hyperactive C3 convertase. Three such mutations have been reported in FB.[9,10] They resulted in the formation of a more potent C3 convertase, resistant to decay by complement regulators and leading to enhanced C3 deposition on resting GEnC. A particular hyperactive C3 convertase, formed with mutated C3, was described in patients with dense deposit disease because of in frame deletion of 2 amino acid residues.[11] To date, no C3 mutations in aHUS have been described that are able to directly enhance the function of the C3 convertase.

Submitted September 30, 2011; accepted January 3, 2012. Prepublished online as *Blood* First Edition paper, January 13, 2012; DOI 10.1182/blood-2011-10-383281.

*L.T.R. and M.F. contributed equally to this study.

The online version of this article contains a data supplement.

The publication costs of this article were defrayed in part by page charge payment. Therefore, and solely to indicate this fact, this article is hereby marked "advertisement" in accordance with 18 USC section 1734.

Table 1. Clinical presentation and outcome of the R139W-aHUS patients

Patient	1	2	3	4	5	6	7	8	9	10	11	12	13	14
Year of first episode	1981	2006	1992	1971	1989	1988	2003	2003	2005	2008	2010	2009	2008	2005
Sex	M	F	F	M	F	F	F	M	F	F	F	F	F	F
Age at onset, y	0.6	0.8	1.2	2	15.5	18.4	21.9	21.9	23.5	30.8	34	35	51	72.5
Initial diagnosis	HUS	HUS	HUS	nd	HUS	HUS	HUS	HUS	HUS	HUS	HUS	HUS	HUS	NA
(Trigger suspected)	(None)	(Infection)	(Infection)	(None)	(Infection)	(OC?)	(PP)	(Cocaine?)	(PP)	(OC?)	(OC?)	(PP)	(None)	(None)
First symptoms														
Diarrhea (bloody)	+(−)	−	na	na	+(−)	−	+ (−)	+(−)	−	+(−)	na	−	na	−
Oligoanuria/AHT	−/+	+/+	na	na	−/+	+/+	−/+	+/+	+/+	−/−	na	+/+	na	−/+
Laboratory presentation														
Creatinine, μmol/L	124	108	na	na	398	885	566	974	1451	487	na	889	na	204
Hemoglobin, g/dL	4.5	6.7	na	na	7.3	6.3	5.8	9.1	6.7	6.2	na	6.7	na	10
Haptoglobin, g/L	nd	< 0.1	na	na	< 0.1	< 0.1	< 0.1	< 0.1	< 0.1	< 0.1	na	< 0.1	na	< 0.1
Schizocytes, %	6	5	na	na	< 1	3-5	10	3-5	3-5	3-5	na	3-5	na	nd
Platelets counts, $\times 10^9$/L	142	16	na	na	113	60	79	86	112	67	na	226	na	280
Nephrotic syndrome	+	+	na	na	+	−	+	+	+	+	na	+	na	−
First flare treatment														
Acute hemodialysis	−	+	na	−	−	+	+	+	+	+	na	+	na	−
Plasmatherapy	+	+	−	−	+	+	+	+	−	+	+	+	+	−
(Details)	4ET/7 d	10PE/10 d			8PE/11 d	10PE/26 d	16PE/22 d	7PE/10 d		13PE/20 d	na	6PE/7 d	na	
Clinical course														
Extrarenal event	Cardiac	Cardiac neurologic		None	None	Neurologic	Cardiac neurologic	Cardiac neurologic	Neurologic	Cardiac	na	Cardiac	Cardiac	Cardiac
Relapse (numnber)	0	1	4	6	1	2	1	0	1	0		0	0	0
Renal outcome	ESRD	ESRD	CKD	ESRD	CKD	ESRD	ESRD	ESRD	ESRD	CKD	CKD	CKD	ESRD	ESRD
(Delay 1st HUS-ESRD or follow-up of CKD)	(11 y)	(7 mo)	(19 y)	(37 y)	(21 y)	(5 mo)	(4 mo)	(1 mo)	(1mo)	(2 y)	(6 mo)	(2 y)	(12 mo), diseased	(18 mo)
Renal transplantation	3	0*	0	0*	0*	2*	0	1	0*	0	0	0	0	1
Failure (HUS)	3 (1)					2 (2)								1 (1)
Others mutations									FH_{R341H}		FH_{F960S}			
Homozygous at-risk haplotypes	FH	FH+MCP	MCP	MCP		FH		MCP	H+MCP					

aHUS indicates atypical hemolytic uremic syndrome; F, female; M, male; HUS, hemolytic uremic syndrome; nd, not determined; na, not applicable; NA, nephroangiosclerosis; ESRD, end-stage renal disease; CKD, chronic kidney disease; AHT, arterial hypertension; FH, factor H; MCP, membrane cofactor protein; ET, exchange transfusion; PP, postpartum; OC, oral contraception; PE, plasma exchanges; and PI, plasma infusion.

+ indicates yes; and −, no.

*Project of renal transplantation.

Here, we report the first large series of aHUS patients carrying the same genetic abnormality in C3, R139W. This is the first description of a direct gain-of-function mutation in C3 that forms a hyperactive C3 convertase as well as being resistant to regulation by MCP, but not by FH. This C3 mutation, especially if associated with at-risk FH and MCP haplotypes, becomes pathogenic following an endothelium-damaging event.

Methods

Patients

Patients were recruited from the French aHUS cohort of patients (n = 343). Diagnosis of HUS was defined by the simultaneous and acute occurrence of at least 3 of the following 4 criteria: acute renal failure, microangiopathic hemolytic anemia, thrombocytopenia, and/or histologic thrombotic microangiopathy. Further definitions and the case reports are given in supplemental Methods (available on the *Blood* Web site; see the Supplemental Materials link at the top of the online article). The clinical history of patients P7 and P9 has been reported previously.[12] This study was approved by the Inserm ethical commission.

Structure analysis

The crystal structures of C3,[13] C3b,[14] C3b-FH1-4,[15] C3bBb,[16] C3bB[17] and MCP[18] are available in Protein Data Bank. Molecular graphic imaging and analysis were produced using the Pymol and UCSF Chimera package[19] (http://www.cgl.ucsf.edu/chimera/). Protein numbering throughout this study is according to the sequence of the mature protein, lacking the signal peptide. Wherever appropriate, the numbering will be according to the gene sequence (starting with c.) and to the protein with the 22-amino-acid-long leader peptide (starting with p.).

Endothelial cell assays

Conditionally immortalized GEnCs[10,20] (passage 29-35) and third-passage primary HUVECs were used for this study. Detailed of culturing conditions are given in supplemental Methods. Briefly, GEnCs and HUVECs, either resting or stimulated with TNFα/IFNγ, were exposed to normal human sera (NHS) from 50 donors or R139W sera or FH-depleted (FH-dpl) serum. Alternatively, blocking anti-FH (Ox24[21]) mAb was added to these sera or anti-MCP (GB24[22]). In addition, R139W sera were supplemented with different concentrations of purified FH (Comptech). Released C3a, C5a, and sC5b9 were measured in the supernatant using specific ELISAs (Quidel). Cells were incubated with a mouse anti–human C3c mAb (Quidel), followed by a secondary anti–mouse IgG-PE or an anti-tissue factor-PE Ab (BD Pharmingen) and analyzed by flow cytometry as described in supplemental Methods.

Recombinant C3 production

The R139W mutant C3 was produced from the wild-type (WT) C3 plasmid as described.[5] The expression level of the plasmids was compared after multiple transient transfections using Lipofectamine. The plasmid was introduced into CHO cells via stable transfection using selection with G418. The constructs were sequenced in their entirety to confirm that no additional mutations had been introduced. The synthesis of C3 was assessed by a sandwich ELISA, using immobilized anti–human C3 Ab for capture and biotinylated anti–human C3, followed by streptavidin-HRP (Amersham) for detection. The expression levels were similar between WT and mutant plasmids. Supernatants derived from stable transfected cells containing recombinant WT and R139W-C3 as well as supernatants of the mock-transformed cells (SN0), were used to purify C3 by ion exchange chromatography using DEAE Sepharose (GE Healthcare) and eluted with 0.2M NaCl.

Surface plasmon resonance

The interaction of wild-type and mutant C3 with FH, MCP, and FB was analyzed using surface plasmon resonance (SPR) technology with Biacore2000 equipment. In the first approach, FH and MCP were coupled to the CM5 biosensor chip (GE Healthcare) using standard amide-coupling technology, according to the manufacturer's instructions. Purified recombinant wild-type and mutant C3 were used as an analyte at concentrations of 1, 0.5, 0.25, 0.125, and 0.06nM. The flow rate was 10 μL/min in a HEPES buffer (10mM HEPES, 25mM NaCl, pH 7.4). An empty activated/deactivated flowcell served as a control.

Alternatively, the anti-C3d Ab (Quidel) was coupled to the 4 flowcells of the chip. Purified WT and R139W C3 and an equivalent purification fraction from the SN0 were loaded on 3 of the flowcells. No binding was detected in the case of SN0. WT and R139W C3 were always loaded to equivalent resonance units. FB was applied as an analyte at 0.06, 0.125, 0.25, 0.5, and 1nM in 1mM $MgCl_2$-containing HEPES buffer (without regeneration). The complex was allowed to decay spontaneously before the next concentration was injected.

Data were analyzed using BIAevaluation software and the RU from the blank flowcell was subtracted. Kinetic parameters were calculated by fitting the obtained sensorgrams into 1:1 interaction with a drifting baseline algorithm to give the lowest χ^2.

C3 convertase formation

Alternative pathway C3 convertase was assembled on a CM5 chip by preprogrammed injections of native and recombinant C3, FB, and FD. Native and recombinant C3 were mixed to mimic the heterozygous situation found in patient sera. In each case, 3 different samples were prepared: (1) purified recombinant WT (10 ng) or R139W C3 (10 ng) or equivalent volume of SN0 plus human C3 purified from plasma (Calbiochem; 10 ng), 3 μg of FB (Calbiochem) and 0.2 μg of FD (Calbiochem) were added in 10mM HEPES, 25mM NaCl, 1mM $MgCl_2$ running buffer to a final volume of 100 μL; (2) 7 μg of FB and 0.5 μg of FD in 200 μL of running buffer; and (3) purified recombinant WT (10 ng) or R139W C3 (10 ng) or equivalent volume of SN0 with human C3 purified from plasma (10 ng) in a final volume of 100 μL. Samples were injected as follows: sample 1, followed by sample 2, then sample 3 and, at the end, sample 2 again, followed by 100 s of running buffer only. Alternatively, 1mM $NiCl_2$ was used instead of $MgCl_2$ to stabilize the C3 convertase.

Results

Genetic analysis

Mutation screening. Direct sequencing of the C3 gene allowed identification of 14 patients (4% of the French aHUS cohort and ~ 50% of patients with C3 mutations) carrying the same heterozygous missense mutation: c.481C>T (Figure 1A), encoding for p.R161W substitution if the first Met was counted as 1 (ie, with a signal peptide of 22 residues, Figure 1B) or R139W of the mature protein (without the signal peptide). The affected R139 residue is partially exposed on the surface of C3 MG2 domain (Figure 1C). This mutation was absent in 550 healthy controls. Most of the patients and 150 of the normal controls came from the North of France. Two of the patients carried a second genetic abnormality in the FH gene (R341H for P9 and F960S for P11, Table 1). No missense or splice site mutations were present in the genes of FH, FI, MCP, C3, FB, and thrombomodulin. No complete deletion of CFHR1/3 was found. Eleven healthy R139W carriers were identified among 19 healthy individuals from the 6 families available for screening.

FH and MCP haplotypes analysis. The frequency of FH and MCP SNPs and haplotypes[23] was evaluated in the R139W-aHUS patients and their relatives and compared with healthy donors (Table 2). FH (FH_{TGTGT}) and MCP (MCP_{GGAAC}) at-risk haplotypes were significantly higher in R139W-aHUS compared with 190 normal donors. These 2 haplotypes were also more frequent in

Table 2. Frequencies of FH and MCP haplotypes in R139W-aHUS patients, their healthy relatives carriers of R139W and normal donors

	Promoter −322 C/T	c.184G>A; p.Val62Ile	c.1204T>C; p.Tyr402His	c.2016A>G; p.Gln672Gln	c.2808G>T; p.Glu936Asp	Controls	R139W healthy carrier (n = 11) vs controls			R139W aHUS (n = 14) vs controls			R139W healthy carrier (n = 11) vs R139W aHUS (n = 14)		
						Freq	Freq	OR	Int 95%	*P*	Freq	OR	Int 95%	*P*	OR	Int 95%	*P*
CFH						(n = 275)											
H1	C	G	C	A	G	0.34	0.16	0.32	0.11-0.95	.04	0.06	0.15*	0.04-0.64*	.01*			ns
H2	C	A	T	A	G	0.2	0			ns	0.07			ns			ns
H3	T	G	T	G	T	0.13	0.22			ns	0.46	5.75*	2.63-12.59*	< .0001*	3.99*	1.18-13.5*	.03*
H4	C	G	T	A	G	0.17	0.41	0.09*	0.05-0.18*	< .0001*	0.09			ns			ns
	−652 A>G (rs2796267)	−366 A>G (rs2796268)	IVS9-78 G>A (rs1962149)	IVS12+638 G>A (rs859705)	c.4070 T>C (rs7144)												
MCP						(n = 192)											
MCP1	A	A	G	G	T	0.5	0.31	0.33*	0.14-0.8*	.01*	0.23	0.27*	0.11-0.69*	.006*			ns
MCP2	G	G	A	A	C	0.25	0.43			ns	0.59	4.64*	2.1-10.24*	.0001*	3.26*	1.09-9.78*	.03*
MCP3	G	A	G	G	T	0.12	0.09			ns	0.05			ns			ns
MCP4	A	G	A	A	C	0.09	0.06			ns	0.08			ns			ns

ns indicates not significant. See Table 1 for expansion of other abbreviations.
*Lines where significant differences were found. H3 haplotype (CFH *tgtgt*) and MCP2 haplotype (MCP *ggaac*) were previously identified at-risk haplotypes for aHUS.

R139W-aHUS, compared with healthy R139W carriers. The presence of FH_{TGTGT} together with R139W gave a 4-fold higher chance for disease development compared with R139W alone. Similarly, the presence of MCP_{GGAAC} with R139W increased 3-fold the risk for development of R139W-aHUS. In addition, 69% of R139W-aHUS were homozygous for the minor TT genotype of the rs3753394 SNP in the promoter region of FH, while it occurred only in 6% of normal donors and was not observed in healthy R139W carriers.

Four of the patients carried homozygous FH risk haplotype TGTGT and 5 patients homozygous MCP risk haplotype GGAAC (Table 1). Two of the patients (P2 and P9) carried both risk haplotypes. If the presence of the FH or MCP at-risk haplotype is considered as 1 risk copy when in a heterozygous form and as 2 risk copies when in a homozygous form, the sum of at-risk haplotype copies in FH and MCP could be estimated in R139W-aHUS and R139W healthy carriers. We were able to assign the individual haplotype alleles for 11 patients and 10 healthy carriers. Eighty-two percent of patients had 2 or more at-risk copies in FH and/or MCP versus 30% of the healthy carriers.

aHUS presentation

The onset of the R139W-aHUS was in the pediatric population (under 18 years) in 5 cases and in adults in 9 cases. A triggering event was suspected in 10 of 14 patients including an infection in 3 of 5 pediatric cases, while the adults < 50 years of age developed the disease postpartum (3 of 7) or in relation to drugs or toxins (4 of 7). No triggering event was identified in the patients > 50 years of age (2 of 2). The pediatric cases had nearly equal distribution of male (2 of 5) and female (3 of 5) patients while in adults 90% of the patients (8 of 9) were female. Shiga toxin–producing *Escherichia coli* were not present in any patient.

Initial clinical symptoms and laboratory test results are detailed in Table 1. Treatment consisted in plasma therapy in 10 patients: plasma exchange (30-80 mL/kg per session) or exchange transfusions in one case (P1). Cardiac events were reported in 8 of 14 patients. Echocardiography demonstrated a dilated cardiomyopathy with a reduction in left ventricular function in 7 patients. One patient (P13) died in relation to a cardiovascular event but the myocardial process was not defined. Heart failure occurred mostly at the R139W-aHUS onset but 2 patients (P10 and P1) experienced a delayed cardiomyopathy 2 and 6 months, respectively, after the hematologic remission. Cardiac function slowly improved with medical treatment but a left ventricular dysfunction persisted. Neurologic events occurred in 5 of 14 patients, always during the acute phase of the illness. Four patients had seizures and one had brachioplegia. Cranial computed tomographic scans were abnormal in 2 patients, showing diffuse multiple small infarcts. Neurologic manifestations resolved except for one (patient P2), who developed recurrent seizures requiring chronic therapy. Altogether, 9 of 14 patients developed an ESRD, 6 before 1 year of follow-up. Seven kidney transplantations were performed in 4 patients. Four transplanted kidneys were lost after 1 to 23 months because of an aHUS relapse, one of them under preventive plasma therapy.

Complement component assessment. Low C3 at the acute phase of the disease was detected in 6 of 9 patients, for whom samples were available from the acute phase. In contrast, all screened healthy carriers (samples available for 8 individuals) had normal C3 levels. No patient had anti-factor H autoantibodies. FH and FI antigenic levels and MCP expression (assessed by flow cytometry) were normal in all tested patients.

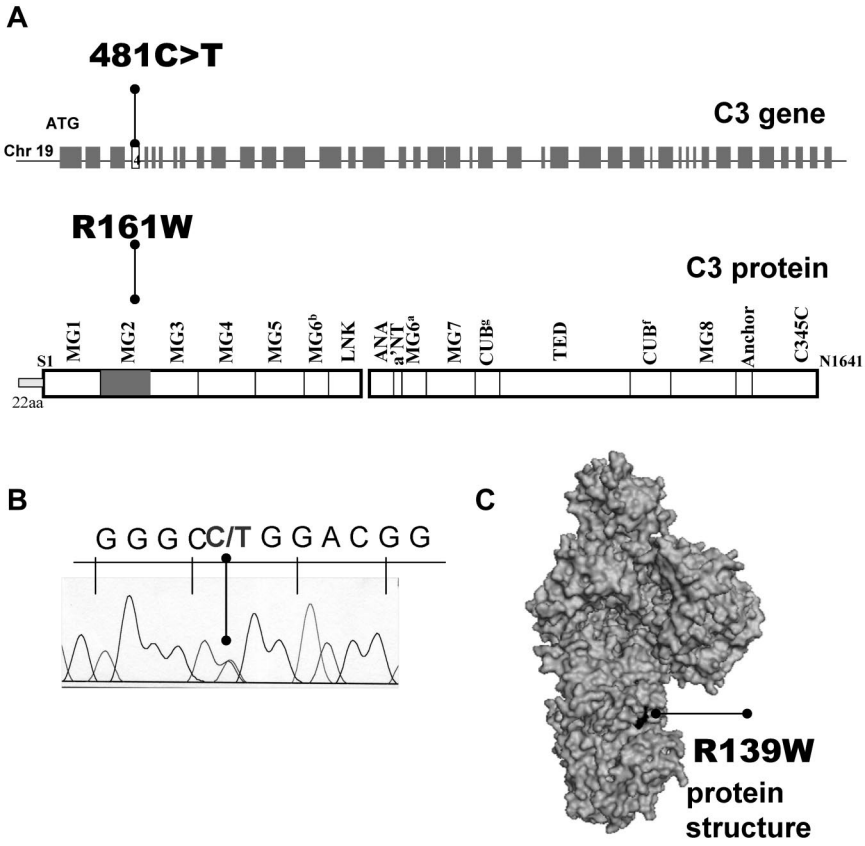

Figure 1. Localization of R139W C3 mutation. (A) Position within the C3 gene and the protein primary structure. (B) Representative histogram for the sequencing of a patient, carrier of R139W. (C) Mapping of R139W on the surface of C3 using Pymol software.

Functional characterization of the R139W mutation

Using R139W-C3–containing sera. *The R139W mutation led to complement activation on stimulated but not on resting endothelial cells.* Resting, adherent HUVECs or GEnCs were stimulated with proinflammatory cytokines (TNFα + IFNγ) and then incubated with sera from 3 patients with R139W-aHUS (P2, 5 and 14), 3 healthy carriers of the mutation from patient P5's family, 2 mutation-free members from the same family and compared with 50 different healthy donors (normal controls) and FH-depleted serum (FH-dpl, positive control; Figure 2). Minimal C3 deposition was observed on resting cells incubated with normal sera, aHUS patients' sera and all but 1 healthy carrier's sera (the second sister of patient P5-P5.S2; Figure 2A). FH-dpl led to increased deposition of C3 on the resting cell surface. The high C3 deposition observed P5.S2 serum, with GEnCs as well as with HUVECs from 5 different donors, is mainly alternative pathway dependent (persistent in presence of EGTA-Mg). The screening of FB and FH polymorphisms and CFHR1 copy numbers showed no peculiarity in this subject and, unfortunately, new serum samples were not available for further analysis. On cytokine-stimulated cells, C3 deposition from all tested R139W-HUS patients and healthy R139W carriers was increased, compared with healthy donors and was similar to the FH-dpl (Figure 2A). In the large family tested, the increase of C3 deposition perfectly correlated with the presence of the mutation (as could be seen from the genealogic tree in supplemental Figure 1). The augmented C3 deposition was accompanied by increased C3a and C5a release, sC5b-9 formation, and tissue-factor expression. These effects were observed both using HUVECs (supplemental Figure 1) and GEnCs (Figure 2A).

The C3 deposition from R139W serum on stimulated EC was controlled by FH but not by MCP. To determine whether the increase in C3 deposition from R139W serum was caused by defective regulation of the R139W C3 by FH or by MCP, function blocking Abs were used (Figure 3A). FH-dpl was used as a control for defective regulation by FH. If the blocking anti-FH OX24 Ab was applied to NHS, C3 deposition on resting cells was increased 2-fold compared with NHS and was equivalent to that of the FH-dpl. The same Ab caused a more than 4-fold increase in C3 deposition when applied to a serum containing R139W-C3. Similar experiments were performed using blocking anti-MCP GB24 Ab. Addition of this Ab to NHS caused a 2.5-fold increase in C3 deposition, similar to FH-dpl. When the anti-MCP Ab was applied to FH-dpl or to R139W serum, the C3 deposition exceeded control levels by 5-fold and 3-fold, respectively. Addition of purified FH to sera of R139W-aHUS patient or healthy relatives but carrying the same mutation resulted in a decreased C3 deposition on activated GEnC (Figure 3B). The C3 deposition reached levels obtained with NHS when the FH concentration was doubled.

Using recombinant proteins. *The R139W mutation affected C3 interaction with MCP, not with FH.* The affected residue R139 is in close proximity to the FH CCP3 binding site[15] and to the suggested MCP CCP3 binding site[18] (Figure 4A-B). ELISA (Figure 4C-D) and SPR (Figure 4E-F) revealed a normal interaction with FH, but the binding to MCP was decreased. Kinetic analysis indicated a statistically significant 2-fold decrease in the association rate (7.11×10^4 Ms^{-1} for the WT vs 2.97×10^4 Ms^{-1} for R139W, $P = .016$, n = 4, *t* test) and no difference in the dissociation rate, resulting in a 3-fold reduction in the apparent binding affinity

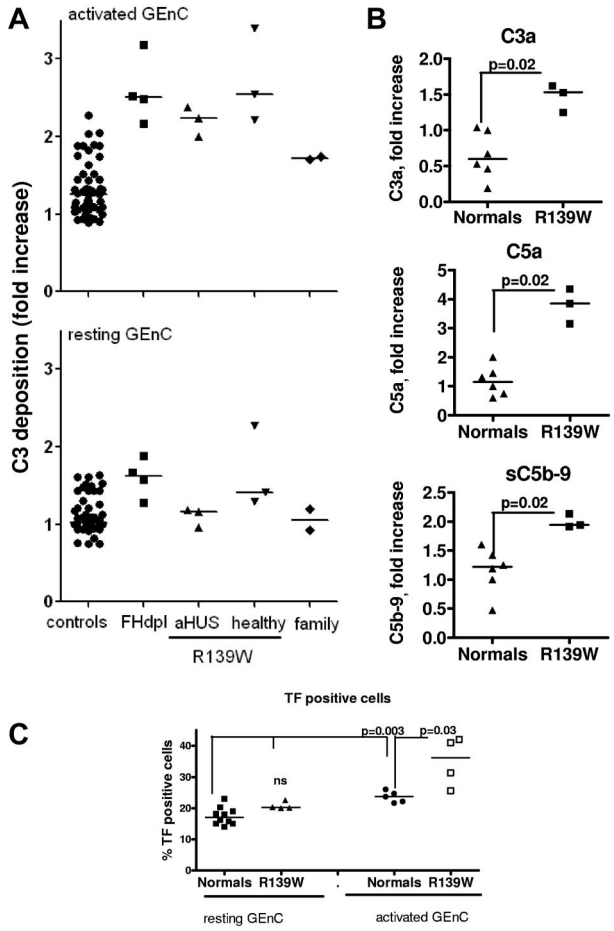

Figure 2. Complement activation on glomerular endothelial cells, incubated with sera from R139W-aHUS patients and their healthy relatives. (A) C3 deposition on resting or TNFα/IFNγ activated GEnCs in the presence of sera from 50 individual normal donors, FHdpl (4 different lots), R139W-aHUS patients (P2, P5, and P14), healthy relatives of patient P5 bearing the mutation (5.F indicates father; and 5.S1 and 5.S2, sisters) or mutation-free relatives of patient P5, indicated as family (5.M indicates mother; and 5.B, brother). C3 depositions (RFI) obtained with each patient or healthy donor were normalized by the C3 deposition from one normal human serum on resting cells, considered as a standard and run in each experiment to obtain the fold increase. Each point is a mean of 3-5 independent experiments. Statistical significance (***$P < .001$) was calculated by ANOVA. (B) Levels of C3a, C5a, and soluble C5b-9, released after incubation of the TNFα/IFNγ activated GEnCs with serum from normal donors (n = 6) or R139W sera (n = 3), were measured by ELISA. The level of C3a, C5a, or sC5b-9 in the supernatant (one-third diluted serum) from resting cells was subtracted from the corresponding levels on activated cells, to obtain the specific amount of C5a and sC5b-9 released because of complement activation. Results are expressed as fold increase, compared with a standard normal serum as in panel A. The statistical analysis was a Mann-Whitney test. (C) Tissue-factor expression on TNFα/IFNγ activated or resting GEnCs after overnight incubation with sera from normal donors (n = 6) or R139W-positive sera (n = 4). The percentage of TF-positive cells was measured by flow cytometry. The statistical analysis was the Mann-Whitney test.

(1.57×10^8 M^{-1} for the WT vs 5.15×10^7 Ms^{-1} for R139W, $P = .045$, n = 4, *t* test). No difference was observed for the kinetic parameters of the interaction with FH. The decay acceleration activity of FH was identical for the WT and R139W-C3 (supplemental Figure 2A). Both C3 forms were cleaved by factor I in presence of FH as a cofactor, but the cleavage of R139W was slightly delayed compared with the WT (supplemental Figure 2B).

R139W is a gain-of-function mutation leading to a hyperactive C3 convertase. Structural aspects of the formation of the alternative complement pathway C3 convertase C3bBb have been recently described.[16,17] R139W mapped far from FB in the closed structure of C3bB and C3bBb. However, it was in close proximity to the SP domain of FB in the so-called open form of C3bB, which is capable of binding FD and allows generation of the active convertase C3bBb (Figure 5A). Therefore, the influence of R139W on the interaction with FB was analyzed. Both ELISA (Figure 5B) and SPR (Figure 5C) demonstrated an increased binding of FB to R139W, specifically, a nearly 2-fold increase in the binding affinity secondary to enhanced association rate. No difference was observed in dissociation parameters. To determine whether this increased binding could lead to hyperfunctional C3 convertase, the formation of the C3 convertase was assessed by SPR. In the presence of R139W the convertase was more efficient, leading to increased C3b deposition on the chip (Figure 5D). This phenomenon was observed both in the presence of Mg (Figure 5D) and of Ni ions (not shown).

Discussion

Atypical HUS is a predominant renal thrombotic microangiopathy strongly associated with complement genetic abnormalities.

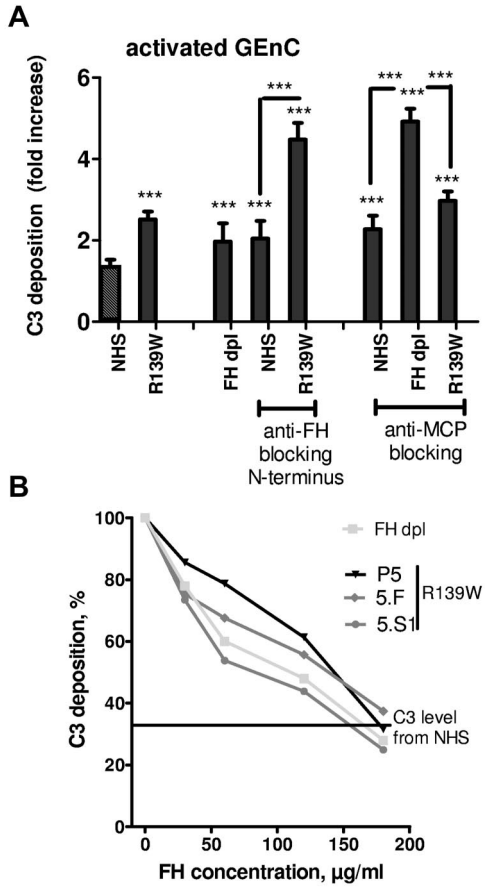

Figure 3. Effects of blocking FH and MCP on the regulation of C3 deposition from WT or R139W sera. (A) GEnCs preactivated with TNFα/IFNγ were incubated for 30 minutes with the standard normal human serum, FHdpl, or R139W sera, in the presence or absence of blocking mAbs against FH (Ox24) or MCP (GB24). The C3 deposition was evaluated by flow cytometry as in Figure 2A. ***$P < .0001$, unpaired *t* test. Unless specifically mentioned, the comparison was made with the NHS (the first bar with a black and white pattern). (B) GEnCs activated with TNFα/IFNγ were incubated for 30 minutes with normal human sera, FHdpl, or R139W sera in the presence of increasing doses of purified FH. C3 deposition in the absence of FH for the FHdpl or R139W-positive sera (from aHUS patient and healthy carriers) was taken as 100% and each C3 level percentage, in the presence of different doses of FH, was calculated. The starting FH concentration was in the normal range for P5, 5.F, and 5.S1. The level of C3 deposition from a normal serum is given as a straight line.

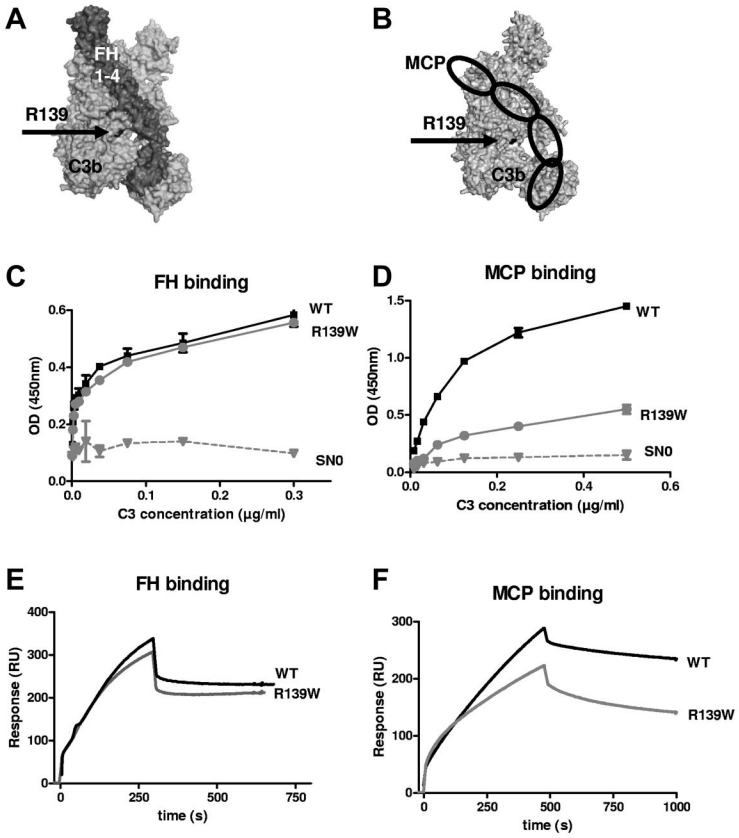

Figure 4. Interaction of R139W with MCP and FH. R139 position (A) on the structure of C3b in a complex with FH CCP1-4 or (B) in a model complex with MCP. R139 is close to CCP3 binding site of both FH and MCP. Direct binding of recombinant WT or mutant C3 to (C) FH or (D) MCP, studied by ELISA. FCS-free supernatant, containing recombinant WT or mutant C3 produced by stably transfected CHO cells, was used as a source of C3. SN0 is the supernatant of cells transfected with a plasmid not containing the C3 gene. The real-time binding of recombinant WT or mutant C3 to (E) FH or (F) MCP was studied by SPR, using recombinant C3 proteins purified from serum-free culture supernatants by DEAE-Sepharose column.

Nevertheless, the contributions of the complement system mutations to the expression of a procoagulant phenotype of the glomerular endothelium and to the disease manifestation remain elusive. Here, we report a large series of aHUS patients who carry the same genetic abnormality, R139W, in the central complement component C3. This mutation, found in 14 unrelated patients, accounted for half of the C3 mutations associated with aHUS in France. Most of the patients came from the north of France, but did not share a high level of polymorphisms in the vicinity of the C3 gene (data not shown). This suggests that, if there was a founder effect, it was ancient. R139W was not identified in normal controls, confirming it as a mutation and not a rare polymorphism. Given the high frequency of this genetic abnormality, it could be considered as a prototypical aHUS C3 mutation, similar to R1210C in FH.[24]

The functional consequences of R139W were analyzed using sera containing R139W-C3 and recombinant proteins. Incubation of resting endothelial cells (both HUVECs and GEnCs) with R139W positive sera did not result in increased C3 deposition, except in one case of a healthy carrier. These results are in contrast to what we observed previously for 2 mutations in FB, which caused increased C3 deposition even on resting cells.[10] No significant increase in TF expression was observed if resting GEnCs were cultured with R139W serum, compared with healthy controls. The fact that the presence of R139W-C3 is tolerated by healthy endothelium could explain why the disease associated with this mutation occurs at variable ages, in the majority of the cases after a triggering event, and has an incomplete penetrance. Atypical HUS flares are frequently preceded by a triggering event, as in 10 of the 14 patients reported here. Herein, we observed increased complement deposition on glomerular endothelial cells exposed to R139W sera, if cells had been stimulated by proinflammatory cytokines.

All tested R139W containing sera caused increased C3 deposition compared with normal donors and a perfect correlation was observed between this C3 deposition and the presence of the mutation in patient P5's family. This result was similar to our model conditions of complement dysregulation, using FH-depleted serum or blocking FH or MCP with an inhibitory Ab. The enhanced C3 deposition was accompanied by increased release of C3a, C5a, and formation of the soluble terminal complement complex C5b9 (sC5b9), indicating that complement activation on the cell surface proceeded to its final stages. C5a and sC5b9 are known to induce TF expression on HUVECs.[25,26] Stimulated GEnCs on culture with R139W sera also expressed higher TF levels, compared with the same cells cultured with normal human sera. Of note, R139W sera from patients and healthy carriers resulted in similar levels of deposited or released complement active fragments and of TF expression. Thus, we provide experimental evidence that complement hyperactivation in aHUS is indeed linked to the expression of a procoagulant phenotype of the GEnCs and therefore participates in the thrombotic process.

The functional consequences of this mutation were studied at the molecular level. Positioning of R139 on the structure of C3b in complex with 3 of its most important ligands revealed that this residue is in proximity to the binding site for CCP3 of FH,[15] the putative binding site for CCP3 of MCP[18] and the binding site of the FB's serine protease (SP) domain in the open conformations as part of the C3 proconvertase C3bB. Structural aspects of the C3 convertase formation have been extensively studied.[16,17,27-29] Binding of FB to C3b induces a dynamic equilibrium between a closed (loading) and open (activation) form. This conformational change is accompanied by a reorientation of FB catalytic SP domain, which comes into contact with the MG2 and the CUB domains of C3b in the open form. The activation form allows factor D binding and formation of the active convertase C3bBb. The R139 residue is far from the FB binding site in the loading form, but the SP domain comes close to this residue in the active form. Experimental results

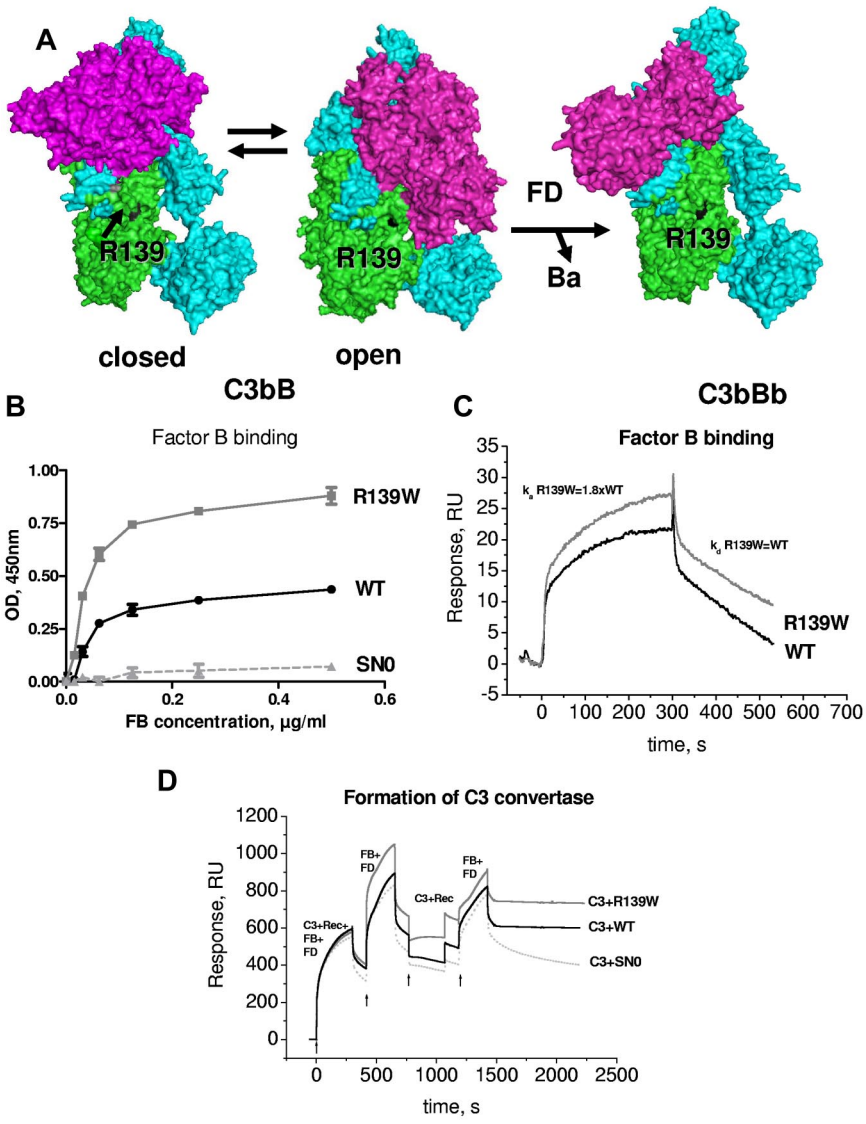

Figure 5. Interaction of R139W with factor B. (A) R139 position on the structures of C3b with FB in closed (refractory to cleavage by FD) and open (prone to cleavage by FD) conformations and on the structure of the C3bBb complex. The α and β chains of C3b are depicted in blue and green and FB is colored in magenta. (B) Binding of FB to WT or mutant recombinant C3, bound to an anti-C3d mAb, coated to the ELISA plate. Serum-free supernatant was used as a source of recombinant C3 molecules. (C) The binding of FB to recombinant WT or R139W C3, bound to an anti-C3d mAb on the CM5 biosensor chip, was studied by SPR using Biacore. Recombinant C3 proteins, purified from serum-free culture supernatants by DEAE-Sepharose column, were used. (D) Formation of a C3 convertase on the biosensor chip by subsequent injection of C3+FB+FD, followed by an injection of FB+FD. Purified WT or R139W recombinant C3 were mixed with native C3, purified from plasma. Proteins deposition on the chip was followed over time. For panels B through D, 1 representative experiment of 3, performed with 3 independent productions of C3, is presented.

here demonstrated a 2-fold increase in the binding of R139W to FB, because of a faster association rate. Furthermore, mutant C3 formed a hyperactive C3 convertase. These results are in agreement with the structural data and confirm the importance of the MG2 domain for binding of FB.

This is the first rigorously analyzed case of a direct gain of function of a C3 mutation. All mutations previously described[5] are indirect gain of function, resulting from ineffective regulation by MCP. Interestingly, the direct binding of R139W C3 to FH and its decay acceleration activity were undistinguishable from wild-type C3, both by ELISA and SPR, notwithstanding the close proximity of the mutated residue to the FH-binding site. The cofactor activity of FH toward R139W cleavage by factor I was only moderately decreased, compared with the wild type. The interaction with MCP was affected by the mutation, causing a strong decrease in binding (measured by ELISA) and a 3-fold decrease in binding affinity (studied by SPR), because of a slower association rate. Once formed, the complex had the same dissociation rate as the WT. These results demonstrate that the binding sites for FH and MCP are not identical and do not involve the same contact residues because R139W differentially influences the interaction with these 2 complement regulators.

The notion that R139W could be regulated by FH but not by MCP was confirmed by a different approach, using function blocking anti-FH and anti-MCP Abs in R139W containing serum. When anti-MCP blocking Ab was applied to R139W sera, C3 deposition was slightly increased, suggesting that in this experimental set-up MCP does not contribute much to the regulation of C3 deposition. In contrast, anti-FH blocking Ab in R139W sera raised C3 deposition to the levels observed in the absence of both MCP and FH. Also, addition of purified FH was able to control the C3 deposition in R139W positive sera in the normal range of healthy donors. These results confirm the capacity of FH to regulate R139W C3 and emphasize FH essential role in complement regulation in sera harboring this mutation.

Although a family history of aHUS was not found in all 14 patients, 11 R139W healthy carriers were identified in 6 families in which genetic analysis was performed. Two patients carried additional mutations in FH outside the hotspot region CCP19-20. To find out whether healthy carriers differed in their genetic background from the R139W-aHUS patients, the frequency of the aHUS at-risk haplotypes in FH (FH_{TGTGT}) and in MCP (MCP_{GGAAC}) were compared. The R139W-aHUS patients had significantly higher frequency of these at-risk haplotypes compared with healthy controls, as

previously reported in patients with aHUS.[30] In contrast, these frequencies were similar in healthy R139W carriers and in normal donors. The presence of R139W together with FH_{TGTGT} conferred 4-fold higher risk and with $MCP_{GGAAC,}$ 3-fold higher risk for development of aHUS, respectively, compared with R139W alone. Among the R139W-aHUS patients, 82% had 2 or more at-risk alleles in FH and/or MCP genes, compared with 30% of the healthy carriers. This clear distinction between healthy carriers and patients demonstrates the critical role of the FH and MCP genetic background for the development of aHUS in the presence of a mutant C3.

The R139W-aHUS had variable disease manifestations and both severe and milder renal phenotypes were found. Nevertheless, the R139W-aHUS was marked by a high frequency of extrarenal complications (> 60% of the patients). Particularly, 60% of the patients had cardiac events and 35% had neurologic events either during the acute phase or at distance from the aHUS episodes. Cardiac symptoms in HUS and aHUS are rarely mentioned, mostly in isolated case reports. A dilated cardiomyopathy (as in our R139W-aHUS patients) has been the most frequent observation.[31-34] In a series of 64 autopsied HUS cases, heart involvement was detected in 19 patients.[35] Only one study of aHUS pediatric cases reported a high frequency of cardiomyopathy, affecting 10 children (43% of the cohort). Nevertheless, no mutation screening was performed in these 2 patients' series.[36] Cardiac complications have been reported in patients with a FH mutations leading to haploinsufficiency[34]; in 1 of 7 children with autoimmune aHUS[37] and in 3 of 45 cases of the French autoimmune aHUS.[38] Further studies are needed to determine whether there exists a specific association of cardiac complications with R139W-aHUS. Nevertheless, results suggest that echocardiographic screening of patients with aHUS should be performed at admission and during the follow-up because cardiac complications could be more frequent than reported or associated with particular forms of aHUS, as is the case here.

Starting from the observation that R139W causes a hyperactivity of C3 and reduced binding to MCP, a rational therapeutic strategy could be suggested for these patients. An optimal situation would be an agent capable of controlling the mutant convertase or its consequences. We found that the addition of purified FH to the R139W-C3 of sera was capable of reducing C3 deposition on activated GEnCs in a dose-dependent manner. Therefore, purified FH, or FH regulatory domains containing constructs (as the FH-CR2 hybrid inhibitor TT30[38]), could be considered as a therapeutic option for R139W-aHUS. Experimental assessment for the susceptibility of a mutant convertase to control by FH should be considered as a mean to find potential putative responders to purified FH treatment. Some mutations such as the FB gain of function[10] appear to be resistant to regulation by FH. Independent of the localization of the mutation, the generation of adverse products of complement hyperactivation, such as C5a and C5b9, can be efficiency blocked by eculizumab, a mAb blocking the cleavage of the complement protein C5. This therapeutic agent has reduced the magnitude of the thrombotic microangiopathy, restored kidney function, and improved quality of life in a small number of aHUS patients.[39,40]

In summary, we describe the genotype-phenotype and structure-function relationships for a frequent direct gain-of-function mutation in C3. The number of patients and healthy carriers with the R139W form of C3 on different genetic backgrounds indicates that this mutation, particularly if associated with an at-risk FH and/or MCP haplotypes, becomes pathogenic in association with an endothelium-damaging event.

Acknowledgments

The authors are grateful to Stephane Bally, François Bouissou, Eric Boulanger, Michel Foulard, Jacques Fourcade, Jean Pierre Grunfeld, Bruno Hurault de Ligny, Nassim Kamar, Annie Lahoche-Manucci, Christophe Legendre, Evelyne Macnamara, and Lionel Rostaing who provided us clinical data for the disease course of the R139W-aHUS patients. They thank Julie Bloch and Dr François Glowacki for the help with establishing the normal donors' cohort from the north of France. They are grateful to Delphine Beury, Stephanie Ngo, Nelly Poulain, and Tania Rybkine for their excellent technical assistance. They are grateful also to Alain Bacchi for the help with the statistical analysis.

This work was supported by grants from Agence Nationale de la Recherche (ANR Genopath 2009-2012 09geno03101I and ANR Biotheque 2008-2011 R08086DS), Assistance Publique–Hôpitaux de Paris (Program Hospitalier de Recherche Clinique, AOM05130/P051065 and AOM08198), AIRG (Association pour l'information et la recherche sur les maladies rénales génétiques) France, Université Paris Descartes and Université Pierre et Marie Curie, by Inserm, the National Institutes of Health (NIH) GM9111, A1041592 and AR48335, and NIH/National Heart, Lung, and Blood Institute (NHLBI) T32 HL007317.

L.T.R. was a recipient of an European Molecular Biology Organization Long-Term Fellowship ALTF 444-2007.

Authorship

Contribution: L.T.R., M.F., E.C.M., L.H.-M, J.P.A., A.L., and V.F.-B. designed the research; L.T.R., M.F., and E.C.M. performed the research; L.T.R., M.F, E.C.M., M.-A.D.-D., C.S.-F., L.H.-M., J.P.A., A.L., and V.F.-B. analyzed and discussed the data; L.T.R., M.F., E.C.M., L.H.-M., J.P.A., and V.F.-B. wrote the manuscript; F.P., C.M., C.N., and A.L. provided clinical information and were in charge of the patients; P.B., S.B., and C.H. provided technical assistance; and S.C.S. and P.W.M. provided the GEnC cell line.

Conflict-of-interest disclosure: The authors declare no competing financial interests.

Correspondence: Dr Veronique Fremeaux-Bacchi, Service d'Immunologie Biologique, Hôpital Européen Georges Pompidou, 20-40 rue Leblanc, 75908 Paris cedex 15, France; e-mail: veronique.fremeaux-bacchi@egp.aphp.fr.

References

1. Noris M, Remuzzi G. Atypical hemolytic-uremic syndrome. *N Engl J Med.* 2009;361(17):1676-1687.
2. Le Quintrec M, Roumenina L, Noris M, Fremeaux-Bacchi V. Atypical hemolytic uremic syndrome associated with mutations in complement regulator genes. *Semin Thromb Hemost.* 2010;36(6):641-652.
3. Roumenina LT, Loirat C, Dragon-Durey MA, Halbwachs-Mecarelli L, Sautes-Fridman C, Fremeaux-Bacchi V. Alternative complement pathway assessment in patients with atypical HUS. *J Immunol Methods.* 2011;365(1-2):8-26.
4. Ricklin D, Hajishengallis G, Yang K, Lambris JD. Complement: a key system for immune surveillance and homeostasis. *Nat Immunol.* 2010;11(9):785-797.
5. Fremeaux-Bacchi V, Miller EC, Liszewski MK, et al. Mutations in complement C3 predispose to development of atypical hemolytic uremic syndrome. *Blood.* 2008;112(13):4948-4952.
6. Lhotta K, Janecke AR, Scheiring J, et al. A large

family with a gain-of-function mutation of complement C3 predisposing to atypical hemolytic uremic syndrome, microhematuria, hypertension and chronic renal failure. *Clin J Am Soc Nephrol.* 2009;4(8):1356-1362.

7. Maga TK, Nishimura CJ, Weaver AE, Frees KL, Smith RJ. Mutations in alternative pathway complement proteins in American patients with atypical hemolytic uremic syndrome. *Hum Mutat.* 2010;31(6):E1445-E1460.
8. Noris M, Caprioli J, Bresin E, et al. Relative role of genetic complement abnormalities in sporadic and familial aHUS and their impact on clinical phenotype. *Clin J Am Soc Nephrol.* 2010;5(10):1844-1859.
9. Goicoechea de Jorge E, Harris CL, Esparza-Gordillo J, et al. Gain-of-function mutations in complement factor B are associated with atypical hemolytic uremic syndrome. *Proc Natl Acad Sci U S A.* 2007;104(1):240-245.
10. Roumenina LT, Jablonski M, Hue C, et al. Hyperfunctional C3 convertase leads to complement deposition on endothelial cells and contributes to atypical hemolytic uremic syndrome. *Blood.* 2009;114(13):2837-2845.
11. Martinez-Barricarte R, Heurich M, Valdes-Canedo F, et al. Human C3 mutation reveals a mechanism of dense deposit disease pathogenesis and provides insights into complement activation and regulation. *J Clin Invest.* 2010;120(10):3702-3712.
12. Fakhouri F, Roumenina L, Provot F, et al. Pregnancy-associated hemolytic uremic syndrome revisited in the era of complement gene mutations. *J Am Soc Nephrol.* 2010;21(5):859-867.
13. Janssen BJ, Huizinga EG, Raaijmakers HC, et al. Structures of complement component C3 provide insights into the function and evolution of immunity. *Nature.* 2005;437(7058):505-511.
14. Janssen BJ, Christodoulidou A, McCarthy A, Lambris JD, Gros P. Structure of C3b reveals conformational changes that underlie complement activity. *Nature.* 2006;444(7116):213-216.
15. Wu J, Wu YQ, Ricklin D, Janssen BJ, Lambris JD, Gros P. Structure of complement fragment C3b-factor H and implications for host protection by complement regulators. *Nat Immunol.* 2009;10(7):728-733.
16. Rooijakkers SH, Wu J, Ruyken M, et al. Structural and functional implications of the alternative complement pathway C3 convertase stabilized by a staphylococcal inhibitor. *Nat Immunol.* 2009;10(7):721-727.
17. Forneris F, Ricklin D, Wu J, et al. Structures of C3b in complex with factors B and D give insight into complement convertase formation. *Science.* 2010;330(6012):1816-1820.
18. Persson BD, Schmitz NB, Santiago C, et al. Structure of the extracellular portion of CD46 provides insights into its interactions with complement proteins and pathogens. *PLoS Pathog.* 2011;6(9).
19. Pettersen EF, Goddard TD, Huang CC, et al. UCSF Chimera–a visualization system for exploratory research and analysis. *J Comput Chem.* 2004;25(13):1605-1612.
20. Satchell SC, Tasman CH, Singh A, et al. Conditionally immortalized human glomerular endothelial cells expressing fenestrations in response to VEGF. *Kidney Int.* 2006;69(9):1633-1640.
21. Sim E, Palmer MS, Puklavec M, Sim RB. Monoclonal antibodies against the complement control protein factor H (beta 1 H). *Biosci Rep.* 1983;3(12):1119-1131.
22. Cho SW, Oglesby TJ, Hsi BL, Adams EM, Atkinson JP. Characterization of three monoclonal antibodies to membrane co-factor protein (MCP) of the complement system and quantification of MCP by radioassay. *Clin Exp Immunol.* 1991;83(2):257-261.
23. Esparza-Gordillo J, Goicoechea de Jorge E, Buil A, et al. Predisposition to atypical hemolytic uremic syndrome involves the concurrence of different susceptibility alleles in the regulators of complement activation gene cluster in 1q32. *Hum Mol Genet.* 2005;14(5):703-712.
24. Martinez-Barricarte R, Pianetti G, Gautard R, et al. The complement factor H R1210C mutation is associated with atypical hemolytic uremic syndrome. *J Am Soc Nephrol.* 2008;19(3):639-646.
25. Tedesco F, Fischetti F, Pausa M, Dobrina A, Sim RB, Daha MR. Complement-endothelial cell interactions: pathophysiological implications. *Mol Immunol.* 2000;37(1-2):91.
26. Tedesco F, Pausa M, Nardon E, Introna M, Mantovani A, Dobrina A. The cytolytically inactive terminal complement complex activates endothelial cells to express adhesion molecules and tissue factor procoagulant activity. *J Exp Med.* 1997;185(9):1619-1627.
27. Janssen BJ, Gomes L, Koning RI, et al. Insights into complement convertase formation based on the structure of the factor B-cobra venom factor complex. *EMBO J.* 2009;28(16):2469-2478.
28. Torreira E, Tortajada A, Montes T, Rodriguez de Cordoba S, Llorca O. Coexistence of closed and open conformations of complement factor B in the alternative pathway C3bB(Mg2+) proconvertase. *J Immunol.* 2009;183(11):7347-7351.
29. Torreira E, Tortajada A, Montes T, Rodriguez de Cordoba S, Llorca O. 3D structure of the C3bB complex provides insights into the activation and regulation of the complement alternative pathway convertase. *Proc Natl Acad Sci U S A.* 2009;106(3):882-887.
30. de Cordoba SR, de Jorge EG. Translational mini-review series on complement factor H: genetics and disease associations of human complement factor H. *Clin Exp Immunol.* 2008;151(1):1-13.
31. Alexopoulou A, Dourakis SP, Zovoilis C, et al. Dilated cardiomyopathy during the course of hemolytic uremic syndrome. *Int J Hematol.* 2007;86(4):333-336.
32. Leray H, Mourad G, du Cailar G, Mion C. [Dilated cardiomyopathy during post-partum hemolytic and uremic syndrome (HUS)]. *Nephrologie.* 1991;12(5):237-240.
33. Prakash J, Gupta S, Kumar H, Rawat UB. Recurrent ventricular tachycardia complicating atypical haemolytic-uraemic syndrome. *Nephrol Dial Transplant.* 1998;13(9):2419-2420.
34. Sallee M, Daniel L, Piercecchi MD, et al. Myocardial infarction is a complication of factor H-associated atypical HUS. *Nephrol Dial Transplant.* 2010;25(6):2028-2032.
35. Gallo EG, Gianantonio CA. Extrarenal involvement in diarrhoea-associated haemolytic-uraemic syndrome. *Pediatr Nephrol.* 1995;9(1):117-119.
36. Neuhaus TJ, Calonder S, Leumann EP. Heterogeneity of atypical haemolytic uraemic syndromes. *Arch Dis Child.* 1997;76(6):518-521.
37. Abarrategui-Garrido C, Martinez-Barricarte R, Lopez-Trascasa M, de Cordoba SR, Sanchez-Corral P. Characterization of complement factor H-related (CFHR) proteins in plasma reveals novel genetic variations of CFHR1 associated with atypical hemolytic uremic syndrome. *Blood.* 2009;114(19):4261-4271.
38. Dragon-Durey MA, Sethi SK, Bagga A, et al. Clinical features of anti-factor H autoantibody-associated hemolytic uremic syndrome. *J Am Soc Nephrol.* 2010;21(12):2180-2187.
39. Mache CJ, Acham-Roschitz B, Fremeaux-Bacchi V, et al. Complement inhibitor eculizumab in atypical hemolytic uremic syndrome. *Clin J Am Soc Nephrol.* 2009;4(8):1312-1316.
40. Kose O, Zimmerhackl LB, Jungraithmayr T, Mache C, Nurnberger J. New treatment options for atypical hemolytic uremic syndrome with the complement inhibitor eculizumab. *Semin Thromb Hemost.* 2010;36(6):669-672.